

**Defining the role of phytoene synthase in
carotenoid accumulation of high provitamin A
bananas**

By

Bulukani Mlalazi

Bachelor of Biotechnology Innovation (Hons.)

A thesis submitted for the degree of Doctor of Philosophy

at the

Queensland University of Technology

Centre for Tropical Crops and Biocommodities

2010

Abstract:

Vitamin A deficiency (VAD) is a serious problem in developing countries, affecting approximately 127 million children of preschool age and 7.2 million pregnant women each year. However, this deficiency is readily treated and prevented through adequate nutrition. This can potentially be achieved through genetically engineered biofortification of staple food crops to enhance provitamin A (pVA) carotenoid content. Bananas are the fourth most important food crop with an annual production of 100 million tonnes and are widely consumed in areas affected by VAD. However, the fruit pVA content of most widely consumed banana cultivars is low (~ 0.2 to 0.5 µg/g dry weight). This includes cultivars such as the East African highland banana (EAHB), the staple crop in countries such as Uganda, where annual banana consumption is approximately 250 kg per person. This fact, in addition to the agronomic properties of staple banana cultivars such as vegetative reproduction and continuous cropping, make bananas an ideal target for pVA enhancement through genetic engineering.

Interestingly, there are banana varieties known with high fruit pVA content (up to 27.8 µg/g dry weight), although they are not widely consumed due to factors such as cultural preference and availability. The genes involved in carotenoid accumulation during banana fruit ripening have not been well studied and an understanding of the molecular basis for the differential capacity of bananas to accumulate carotenoids may impact on the effective production of genetically engineered high pVA bananas. The production of phytoene by the enzyme phytoene synthase (PSY) has been shown to be an important rate limiting determinant of pVA accumulation in crop systems such as maize and rice. Manipulation of this gene in rice has been used successfully to produce Golden Rice, which exhibits higher seed endosperm pVA levels than wild type plants. Therefore, it was hypothesised that differences between high and low pVA accumulating bananas could be due either to differences in PSY enzyme activity or factors regulating the expression of the *psy* gene. Therefore, the aim of this thesis was to investigate the role of PSY in accumulation of pVA in banana fruit of representative high (Asupina) and low (Cavendish) pVA banana cultivars by comparing the nucleic acid and encoded amino acid sequences of the banana *psy* genes, *in vivo* enzyme activity of PSY in rice callus and expression of PSY through analysis of promoter activity and mRNA levels.

Initially, partial sequences of the *psy* coding region from five banana cultivars were obtained using reverse transcriptase (RT)-PCR with degenerate primers designed to conserved amino

acids in the coding region of available *psy* sequences from other plants. Based on phylogenetic analysis and comparison to maize *psy* sequences, it was found that in banana, *psy* occurs as a gene family of at least three members (*psy1*, *psy2a* and *psy2b*). Subsequent analysis of the complete coding regions of these genes from Asupina and Cavendish suggested that they were all capable of producing functional proteins due to high conservation in the catalytic domain. However, inability to obtain the complete mRNA sequences of Cavendish *psy2a*, and isolation of two non-functional Cavendish *psy2a* coding region variants, suggested that *psy2a* expression may be impaired in Cavendish. Sequence analysis indicated that these Cavendish *psy2a* coding region variants may have resulted from alternate splicing. Evidence of alternate splicing was also observed in one Asupina *psy1* coding region variant, which was predicted to produce a functional PSY1 isoform. The complete mRNA sequence of the *psy2b* coding regions could not be isolated from either cultivar.

Interestingly, *psy1* was cloned predominantly from leaf while *psy2* was obtained preferentially from fruit, suggesting some level of tissue-specific expression. The Asupina and Cavendish *psy1* and *psy2a* coding regions were subsequently expressed in rice callus and the activity of the enzymes compared *in vivo* through visual observation and quantitative measurement of carotenoid accumulation. The maize B73 *psy1* coding region was included as a positive control. After several weeks on selection, regenerating calli showed a range of colours from white to dark orange representing various levels of carotenoid accumulation. These results confirmed that the banana *psy* coding regions were all capable of producing functional enzymes. No statistically significant differences in levels of activity were observed between banana PSYs, suggesting that differences in PSY activity were not responsible for differences in the fruit pVA content of Asupina and Cavendish.

The *psy1* and *psy2a* promoter sequences were isolated from Asupina and Cavendish gDNA using a PCR-based genome walking strategy. Interestingly, three Cavendish *psy2a* promoter clones of different sizes, representing possible allelic variants, were identified while only single promoter sequences were obtained for the other Asupina and Cavendish *psy* genes. Bioinformatic analysis of these sequences identified motifs that were previously characterised in the *Arabidopsis psy* promoter. Notably, an ATCTA motif associated with basal expression in *Arabidopsis* was identified in all promoters with the exception of two of the Cavendish *psy2a* promoter clones (*Cpsy2apr2* and *Cpsy2apr3*). G1 and G2 motifs, linked to light-regulated responses in *Arabidopsis*, appeared to be differentially distributed between *psy1* and *psy2a* promoters. In the untranscribed regulatory regions, the G1 motifs were found only in *psy1* promoters, while the G2 motifs were found only in *psy2a*. Interestingly, both

ATCTA and G2 motifs were identified in the 5' UTRs of Asupina and Cavendish *psy1*. Consistent with other monocot promoters, introns were present in the Asupina and Cavendish *psy1* 5' UTRs, while none were observed in the *psy2a* 5' UTRs. Promoters were cloned into expression constructs, driving the β -glucuronidase (GUS) reporter gene. Transient expression of the Asupina and Cavendish *psy1* and *psy2a* promoters in both Cavendish embryogenic cells and Cavendish fruit demonstrated that all promoters were active, except *Cpsy2apr2* and *Cpsy2apr3*. The functional Cavendish *psy2a* promoter (*Cpsy2apr1*) appeared to have activity similar to the Asupina *psy2a* promoter. The activities of the Asupina and Cavendish *psy1* promoters were similar to each other, and comparable to those of the functional *psy2a* promoters.

Semi-quantitative PCR analysis of Asupina and Cavendish *psy1* and *psy2a* transcripts showed that *psy2a* levels were high in green fruit and decreased during ripening, reinforcing the hypothesis that fruit pVA levels were largely dependent on levels of *psy2a* expression. Additionally, semi-quantitative PCR using intron-spanning primers indicated that high levels of unprocessed *psy2a* and *psy2b* mRNA were present in the ripe fruit of Cavendish but not in Asupina. This raised the possibility that differences in intron processing may influence pVA accumulation in Asupina and Cavendish.

In this study the role of PSY in banana pVA accumulation was analysed at a number of different levels. Both mRNA accumulation and promoter activity of *psy* genes studied were very similar between Asupina and Cavendish. However, in several experiments there was evidence of cryptic or alternate splicing that differed in Cavendish compared to Asupina, although these differences were not conclusively linked to the differences in fruit pVA accumulation between Asupina and Cavendish. Therefore, other carotenoid biosynthetic genes or regulatory mechanisms may be involved in determining pVA levels in these cultivars. This study has contributed to an increased understanding of the role of PSY in the production of pVA carotenoids in banana fruit, corroborating the importance of this enzyme in regulating carotenoid production. Ultimately, this work may serve to inform future research into pVA accumulation in important crop varieties such as the EAHB and the discovery of avenues to improve such crops through genetic modification.

Table of Contents:

Abstract:.....	ii
Table of Contents:.....	v
List of Figures:.....	ix
List of Tables:.....	xi
List of Abbreviations:.....	xii
Declaration:.....	xiv
Acknowledgements:.....	xv
Chapter 1: Introduction.....	1
1.1 General introduction.....	1
1.2 Banana.....	3
1.2.1 Taxonomy and genetics.....	3
1.2.2 Banana as a target for pVA enrichment.....	3
1.3 Carotenoid metabolism.....	4
1.3.1 Carotenoid biosynthesis.....	6
1.3.2 Carotenoid cleavage.....	9
1.3.3 Regulation of carotenoid metabolism.....	10
1.4 Phytoene synthase.....	13
1.4.1 Properties of <i>psy</i>	13
1.4.2 The <i>psy</i> gene as a target for pVA enhancement.....	15
1.5 Objectives of the program of research and investigation.....	17
Chapter 2: General methods.....	19
2.1 General methods for nucleic acid purification from plant cells.....	19
2.1.1 Purification of total RNA from banana tissue.....	19
2.1.2 mRNA purification.....	19
2.1.3 DNA extraction.....	19
2.2 General methods in nucleic acid amplification, cloning and sequencing.....	20
2.2.1 PCR amplification.....	20
2.2.2 Restriction enzyme digestion of DNA.....	21
2.2.3 Agarose gel electrophoresis.....	21
2.2.4 Purification of DNA from agarose gels.....	21
2.2.5 DNA ligation.....	22
2.2.6 Transformation of <i>Escherichia coli</i> with recombinant plasmids.....	22
2.2.7 Growth of bacteria in liquid cultures.....	22
2.2.8 Purification of plasmid DNA.....	22

2.2.9	Storage of bacterial cultures	23
2.2.10	DNA sequencing	23
2.3	Plant tissue culture media.....	24
Chapter 3:	Isolation and characterisation of phytoene synthase sequences from banana	25
3.1	Introduction	25
3.2	Materials and methods	27
3.2.1	Plant material.....	27
3.2.2	Nucleic acid isolation from plant tissue	27
3.2.3	Oligonucleotide primers	27
3.2.4	RT-PCR of partial <i>psy</i> coding region using degenerate primers	29
3.2.5	Sequence analysis.....	29
3.2.6	Isolation of banana <i>psy</i> mRNA sequences	30
3.2.7	Isolation of partial banana <i>psy</i> sequences from gDNA	32
3.2.8	Amplification of the complete <i>psy</i> coding region from mRNA and gDNA.....	34
3.3	Results	35
3.3.1	Initial characterisation of banana <i>psy</i>	35
3.3.1.1	Isolation of partial banana <i>psy</i> sequences.....	35
3.3.1.2	Phylogenetic analysis of partial banana <i>psy</i> sequences	37
3.3.2	Isolation of complete <i>psy</i> mRNA sequences	39
3.3.2.1	Isolation of <i>psy1</i> mRNA sequences.....	40
3.3.2.2	Isolation of <i>psy2</i> coding regions.....	42
3.3.3	Phylogenetic analysis of complete banana <i>psy</i> coding regions	47
3.3.4	Analysis of Asupina and Cavendish <i>psy</i> gene structure	49
3.3.5	Further analysis of <i>psy</i> coding region variants	51
3.4	Discussion	51
Chapter 4:	Characterisation of phytoene synthase enzymes	60
4.1	Introduction	60
4.2	Materials and methods	61
4.2.1	Bioinformatic analysis of banana PSY protein sequences	61
4.2.2	Cloning of <i>psy</i> coding regions into binary vectors	62
4.2.3	Functional analysis of <i>psy</i> genes in rice	65
4.2.3.1	Callus induction and maintenance.....	65
4.2.3.2	Transformation of <i>Agrobacterium</i> with binary vectors.....	65
4.2.3.3	Preparation of <i>Agrobacterium</i> for transformation of rice callus	66
4.2.3.4	Transformation of rice callus	66
4.2.4	Analysis of carotenoid accumulation in rice callus	67
4.3	Results	68

4.3.1	PSY protein sequence analysis	68
4.3.1.1	Primary sequence analysis	68
4.3.1.2	Secondary and tertiary sequence analysis	70
4.3.2	Functional analysis of banana PSYs	74
4.3.2.1	Rice callus induction and optimisation of transformation	74
4.3.2.2	Comparison of banana <i>psy</i> genes in rice	76
4.4	Discussion	81
Chapter 5:	Characterisation of factors affecting phytoene synthase expression.....	88
5.1	Introduction.....	88
5.2	Materials and methods	89
5.2.1	Oligonucleotide primers.....	89
5.2.2	<i>psy</i> promoter isolation.....	89
5.2.3	Cloning of <i>psy</i> promoters into <i>pGEM-4Z</i> vectors	91
5.2.4	Bioinformatic analysis of promoter sequences	92
5.2.5	Preparation of banana tissue for microprojectile bombardment	93
5.2.5.1	Banana embryogenic cell suspensions	93
5.2.5.2	Banana fruit tissue.....	93
5.2.6	Microprojectile bombardment of <i>psy</i> promoter GUS constructs	94
5.2.6.1	Microprojectile bombardment procedure.....	94
5.2.6.2	Histochemical GUS staining.....	94
5.2.6.3	Fluorimetric analysis of GUS activity	95
5.2.7	Analysis of Asupina and Cavendish banana fruit ripening.....	95
5.2.7.1	Plant materials.....	95
5.2.7.2	Ripening trial	96
5.2.8	Semi-quantitative RT-PCR	96
5.2.8.1	Preparation of mRNA	96
5.2.8.2	RT-PCR analysis.....	97
5.3	Results.....	97
5.3.1	PSY promoter isolation and analysis	97
5.3.1.1	Promoter isolation.....	97
5.3.1.2	Promoter analysis.....	98
5.3.2	Comparison of promoter activity	105
5.3.2.1	Microprojectile bombardment of banana ECS.....	105
5.3.2.2	Microprojectile bombardment of banana fruit.....	106
5.3.3	Analysis of mRNA transcript abundance.....	114
5.3.3.1	Ripening trial	114
5.3.3.2	Semi-quantitative PCR.....	117

5.4	Discussion	122
Chapter 6:	General discussion.....	129
References:	137

List of Figures:

Figure 1.1: Structure of carotene cyclic end groups	5
Figure 1.2: Summary of carotenoid biosynthesis.....	7
Figure 1.3: Organisation of carotenoid biosynthetic enzymes in plastids.....	9
Figure 1.4: Analysis of carotenoid accumulation in tomato fruit	12
Figure 1.5: General structure of plant PSY proteins.....	14
Figure 3.1: Summary of 5' and 3'RLM-RACE strategies	31
Figure 3.2: Summary of genome walking strategy	33
Figure 3.3: Representative agarose gel showing amplification of partial <i>psy</i> coding region.....	35
Figure 3.4: Phylogenetic analysis of the banana <i>psy</i> partial coding region	38
Figure 3.5: Putative structure of <i>psy1</i> mRNA.....	41
Figure 3.6: Summary of <i>psy2a</i> and <i>psy2b</i> sequences isolated from Asupina and Cavendish.....	43
Figure 3.7: Agarose gel electrophoresis of <i>psy2a</i> 5' and 3' RLM-RACE products from Cavendish fruit mRNA	44
Figure 3.8: Analysis of <i>psy2</i> 3'RLM-RACE clones	46
Figure 3.9: Phylogenetic analysis of the coding regions of Asupina and Cavendish <i>psy</i> genes	48
Figure 3.10: Analysis of genomic sequence of Asupina and Cavendish <i>psy</i> genes.....	50
Figure 3.11: Analysis of coding region variants of Asupina <i>psy1</i> and Cavendish <i>psy2a</i>	52
Figure 3.12: Analysis of Cavendish <i>psy2c</i> partial sequence structure	53
Figure 4.1: Construction of <i>psy</i> coding region binary vectors	64
Figure 4.2: Primary structure of banana PSY proteins	69
Figure 4.3: Analysis of secondary and tertiary structure of banana PSY proteins.....	72
Figure 4.4: Testing of GFP reporter genes in rice callus	75
Figure 4.5: Pilot experiment to confirm carotenoid accumulation in transgenic rice callus.....	78
Figure 4.6: Carotenoid accumulation in rice callus	79
Figure 4.7: Total carotenoids in <i>Zpsy1</i> transformed rice calli	80
Figure 4.8: Carotenoid accumulation in rice calli transformed with different <i>psy</i> genes	82
Figure 5.1: Strategy for the isolation of <i>psy</i> promoter sequences	91
Figure 5.2: Strategy for generation of <i>psy</i> promoter constructs in pGEM-4Z.....	93
Figure 5.3: Updated <i>psy1</i> and <i>psy2a</i> genomic sequence information.....	99
Figure 5.4: Analysis of <i>psy</i> promoter sequences.....	100
Figure 5.5: Alignment of selected regions of <i>psy2a</i> promoters	101
Figure 5.6: Repeat sequence analysis of <i>psy2a</i> promoters.....	102
Figure 5.7: Secondary structure analysis of repeat region in the <i>psy2a</i> promoters.....	103
Figure 5.8: Identification of putative DNA regulatory motifs in banana <i>psy</i> promoters	104

Figure 5.9: Analysis of banana <i>psy</i> promoter activity in banana ECS	108
Figure 5.10: Analysis of <i>psy</i> promoter activity in gassed green fruit.....	110
Figure 5.11: Analysis of <i>psy</i> promoter activity in ungassed green fruit.....	113
Figure 5.12: Ripening of Asupina green fruit	115
Figure 5.13: Analysis of Asupina and Cavendish mRNA.....	118
Figure 5.14: Semi-quantitative PCR analysis of banana <i>psy</i> expression.....	121
Figure 5.15: Comparison of putative ATCTA motifs in <i>psy2a</i> promoters.....	125

List of Tables:

Table 1.1: Examples of animal VA and plant pVA sources	1
Table 1.2: Summary of the β -carotene yields of a range of high pVA bananas	4
Table 2.1: Composition of plant tissue culture (PTC) media.....	24
Table 3.1: Properties of banana cultivars used in the current project	27
Table 3.2: PCR primers used in the isolation of banana <i>psy</i> sequences.....	28
Table 3.3: Conserved regions of PSY proteins used to design degenerate primers.....	29
Table 3.4: Partial <i>psy</i> clones obtained using degenerate primer RT-PCR.	37
Table 5.1: PCR primers used in banana <i>psy</i> promoter isolation and semi-quantitative PCR	90
Table 5.2: Analysis of the ripening of Asupina and Cavendish green fruit.....	116

List of Abbreviations:

× g	gravity
°C	degrees Celsius
bp	base pair(s)
BLASTn	nucleotide basic local alignment search tool
CaMV35S	<i>cauliflower mosaic virus 35S</i>
CDD	conserved domain database
cDNA	complementary deoxyribonucleic acid
CTAB	centyltriethylammonium bromide
DEPC	diethylpyrocarbonate
DNA	deoxyribonucleic acid
DTT	dithiothreitol
EAHB	East African highland banana
EDTA	ethylenediaminetetraacetic acid
g	gram(s)
gDNA	genomic DNA
GFP	green fluorescent protein
GUS	β-glucuronidase
hr	hour(s)
IPTG	isopropyl-β-d-thiogalactopyranoside
Kb	kilobase(s)
kDa	kilodalton(s)
LN ₂	liquid nitrogen
mg	milligram(s)
min	minute(s)
mL	millilitre(s)
mM	millimolar
M-MLV	Moloney murine leukaemia virus
mmol	millimole(s)
mqH ₂ O	Milli-Q water (18.2 MΩ·cm water quality)
mRNA	messenger RNA
MUG	4-methylumbelliferyl-β-D-glucuronide trihydrate
NCBI	National centre for biotechnology information
ng	nanogram(s)
NIH	National Institute of Health

nm	nanometre(s)
No(s).	number(s)
OD ₆₀₀	optical density at 600 nm
pDNA	plasmid DNA
pmol	picomole(s)
pVA	provitamin A
PVP	polyvinylpyrrolidone
RACE	rapid amplification of cDNA ends
RLM-RACE	RNA ligase mediated-rapid amplification of cDNA ends
rRNA	ribosomal RNA
RT	reverse transcriptase
RT-PCR	reverse transcriptase polymerase chain reaction
SDS	sodium dodecyl sulphate
sec	seconds
TAE	tris-acetate EDTA
Taq	<i>Thermus aquaticus</i>
TE	tris-EDTA
U	units of activity
UTR	untranslated region
UV	ultraviolet
V	volts
v	version
v/v	volume per volume
VA	vitamin A
VAD	vitamin A deficiency
W	watts
w/v	weight per volume
X-gal	5-bromo-4-chloro-indolyl- β -D-galactopyranoside
X-gluc	5-bromo-4-chloro-3-indolyl-beta-D-glucuronic acid
μ g	microgram(s)
μ L	microlitre(s)
μ M	micromolar

Declaration:

“The work contained within this thesis has not been previously submitted for a degree or diploma at any other higher education institution. To the best of my knowledge and belief, this thesis contains no material previously published or written by another person except where due reference is made.”

Signed:

Date:

Acknowledgements:

The successful completion of my thesis would not be possible without the tangible support of a significant number of people to whom I would like to express my thanks:

Firstly I would like to thank my principal supervisor, Dr Marion Bateson, for lending me her wealth of knowledge and expertise throughout the entire process and for being a compassionate mentor.

I would also like to thank my associate supervisors: Dr Doug Becker, Dr Mark Harrison, Dr Harjeet Khanna and Professor James Dale. The insight and instruction that they have all provided throughout my PhD has been invaluable.

Dr Jason Geijskes, for the additional insights generously provided during my PhD.

Professor James Dale, for seeing the potential in me and entrusting me with the honour of undertaking this project in his lab.

I would like to thank the Bill and Melinda Gates Foundation as well as the QIDS scholarship scheme for their material support in making my PhD project possible.

I would like to thank the QUT staff, particularly in the School of Life Sciences, whose various activities contributed to the smooth progress of my thesis.

To the students and staff of the Centre for Tropical Crops and Biocommodities, thank you all for making the time that I spent among you worthwhile, as your helpfulness and understanding enriched my working environment.

To all my friends who have stood by me and encouraged me ceaselessly along the way, thank you, there are too many of you to name! Thanks particularly to Priver, Mumbi, Inge and Washington (Jnr) for the fun times had in the quest for the thesis.

To my family: Mum, Dad and Amu. I owe you so much in ways too innumerable to count! Thank you for your love, prayers and support, without which I could not have ever hoped to achieve this dream.

To God, for giving me the opportunity to live and work with the exceptional group of people mentioned above, and giving me strength and peace when I needed them most.

Chapter 1: Introduction

1.1 General introduction

The term vitamin A (VA) describes any natural or synthetic compound able to perform the functions attributed to this vitamin, and includes the retinoids (retinol and its derivatives) and the provitamin A (pVA) carotenoids (Bender, 2003). Retinoids are obtained from animal sources including animal liver and dairy products (NIH, 2006; Palace *et al.*, 1999). However, the pVA carotenoids α -carotene, β -carotene and β -cryptoxanthin are obtained from certain fruits and vegetables (Amaya, 2001; NIH, 2006; Palace *et al.*, 1999), absorbed by the digestive system and converted into retinol (von Lintig *et al.*, 2005). Selected examples of recommended animal (retinol) and plant (β -carotene) sources of VA are shown in Table 1.1. VA is important due to its diverse biological functions. It is involved in vision through the signalling action of rhodopsin, a covalent complex of 11-cis-retinal with an apoprotein called opsin (Okada *et al.*, 2001), and is important in embryonic development (Chen *et al.*, 1995) and the function of organs including bone (Harada *et al.*, 1995), lungs (Malpel *et al.*, 2000), skin (Roos *et al.*, 1998) and the immune system (Chew, 1993). pVA carotenoids also play a critical role as antioxidants in the direct control of oxidative stress, caused by reactive oxygen species (Chew and Park, 2004; Halliwell, 1997).

Table 1.1: Examples of animal VA and plant pVA sources. The content of retinol or β -carotene is expressed as a proportion of the weight of the raw/fresh food source using data obtained from the USDA National Nutrient Database for Standard Reference (USDA, 2008).

Food Source	VA compound	Amount ($\mu\text{g/g}$)
Chicken liver	retinol	33
Whole eggs	retinol	1
Carrots	β -carotene	83
Spinach	β -carotene	56
Apricots	β -carotene	11

The human body is incapable of *de novo* VA synthesis, therefore it must be obtained exclusively from the diet and metabolised into its bioactive and storable forms (von Lintig *et al.*, 2005). Vitamin A deficiency (VAD) is caused by inadequate dietary intake of VA compounds due to malnutrition or diseases that affect intestinal absorption such as diarrhoea (NIH, 2006). As a result, treatment and prevention of VAD is only possible through adequate dietary intake of VA or pVA compounds through supplementation, food fortification or dietary intervention (Filteau and Tomkins, 1999). Supplementation normally involves the intake of retinol or β -carotene in pharmacological formulations, such as cod liver oil, palm

oil or tablets (Solomons and Orozco, 2003; West, 2000). Food fortification is achieved using purified VA compounds to boost the nutritional value of commercially available foods such as margarine and breakfast cereals during manufacturing (West, 2000). Dietary intervention involves the integration of naturally rich VA sources into the diet of the population (West, 2000). Interestingly, the use of crops with pVA content enhanced through genetic engineering may provide a means by which dietary intervention may be achieved (West *et al.*, 2002).

VAD is a serious problem in developing countries where it affects up to 127 million children of preschool age and 7.2 million pregnant women each year (West, 2002). Clinical VAD is associated with various developmental, organ and immune dysfunctions with the first sign being xerophthalmia or night blindness, which untreated leads to permanent blindness (Sommer and West, 1996). The prevalence of VAD is widespread across Africa, where it is estimated to affect 33 million preschool age children (SanJoaquin and Molyneux, 2009). Studies showed that this disorder accounted for approximately 35% of overall mortality in Mozambican children below 5 years old (Aguayo *et al.*, 2005), while the rate of VAD in Tanzanian children (aged 7 to 14) was approximately 31.9% and significantly linked with anaemia (Tatala *et al.*, 2008). Additionally, analysis of VA levels of HIV infected patients in Uganda found that 33% suffered from VAD and were at increased risk of mortality compared to those not exhibiting VAD (Langi *et al.*, 2003). Bananas have potential in the treatment of VAD due to their wide production and consumption in developing countries (Ammar-Khodja, 2000), particularly Eastern Africa (Uganda, Burundi and Rwanda), where VAD is a significant problem. Banana is grown in over 120 countries and consumed by 400 million people, making it the fourth most nutritionally important staple food crop after rice, wheat and maize. In banana growing regions, 90% of the harvested crop is consumed by the local population and in East Africa, as much as 250 kg per person of the East African Highland Banana (EAHB) is consumed annually (Ammar-Khodja, 2000). Although high pVA bananas exist (Englberger, 2003), they are not widely consumed in most countries, and staple banana cultivars such as the EAHB are relatively low in pVA. One approach currently being investigated is to increase the pVA content in banana through genetic manipulation of the carotenoid biosynthetic pathway, specifically through increased expression of the enzyme phytoene synthase (PSY), as has previously been demonstrated in rice (Paine *et al.*, 2005). However, to date, the carotenoid biosynthetic pathway and the gene(s) encoding PSY have not been characterised in banana. Additionally, there is no understanding of the mechanisms responsible for the high pVA accumulation in some banana cultivars or if PSY plays a role in this, factors that could impact significantly on the enhancement of pVA in banana.

1.2 Banana

1.2.1 Taxonomy and genetics

There are over 1000 varieties of banana which are subdivided into 50 groups (Ammar-Khodja, 2000). Taxonomically, wild banana species are classified into one of five groups within the genus *Musa*, being: *eumusa*, *rhodochlamys*, *callimusa*, *australimusa* and *incertae sedis*. Of these, *eumusa*, *australimusa* and their hybrids constitute the predominant proportion of cultivated varieties (Daniells *et al.*, 2001). The diploid number of banana genomes ranges between $2n = 20$ and $2n = 22$ and these can be segregated into four genomes *acuminata* (A), *balbisiana* (B), *schizocarpa* (S) and *textiles* (T) (Daniells *et al.*, 2001; Pillay *et al.*, 2004). The T genome is characteristic of *Australimusa*, which includes *Musa textilis* and the Fe'i bananas, found in Papua New Guinea and Polynesia, which are poorly characterised and whose genotype is typically represented simply as Fe'i. Banana genomes may contain multiple types and their ploidy varies between diploid and tetraploid. Triploid bananas include the popular commercial varieties Cavendish (AAA) and Ladyfinger (AAB) as well as important staples such as the EAHB (AAA; Daniells *et al.*, 2001; Pillay *et al.*, 2004). There have been a number of studies focussed on characterising the structure and organisation of the banana genome (Gowen, 1995), including distribution of repetitive DNA sequences (Valárik *et al.*, 2002), determination of nucleotide content and gene density (Aert *et al.*, 2004; Kamate *et al.*, 2001), and the relationship between genome size and ribosomal DNA distribution (Bartos *et al.*, 2005). Many banana genes with different roles have been characterised and include ripening-related enzymes such as polyphenol oxidase (Gooding *et al.*, 2001), pectate lyase (Marin-Rodriguez *et al.*, 2003) and 1-aminocyclopropane-1-carboxylate (ACC) oxidase (Huang *et al.*, 1997; Liu *et al.*, 1999). However, extensive review of the literature suggests that none of the genes known to directly influence carotenoid biosynthesis have been characterised in banana, with work mainly focused on other characteristics such as disease resistance (Atkinson *et al.*, 2004; Chakrabarti *et al.*, 2003; Gowen, 1995).

1.2.2 Banana as a target for pVA enrichment

Banana plants have a relatively short maturation time (9 to 12 months after planting) and high fruit yield (20 to 25 kg of fruit per bunch; Ammar-Khodja, 2000) and banana fruit is a high energy source containing vitamin C and B group vitamins such as niacin and riboflavin, as well as minerals such as potassium (Gowen, 1995). Further, some varieties of Fe'i bananas are very good calcium sources (Englberger *et al.*, 2003a). Bananas are not typically regarded as a high pVA crop. However, cultivars with β -carotene levels ranging from 3.3 $\mu\text{g/g}$ (yellow fruit) to 27.8 $\mu\text{g/g}$ (orange fruit), and high α -carotene levels exist in the

Federated States of Micronesia and other areas (Englberger *et al.*, 2003c; Table 1.2). Comparatively, these cultivars have between 16 and 132 times the β -carotene content of commercial varieties (approximately 0.21 $\mu\text{g/g}$; Holden *et al.*, 1999). However, these bananas are usually not consumed in regions where they do not naturally occur due to factors such as quarantine restrictions and cultural acceptability (Englberger *et al.*, 2003a).

Table 1.2: Summary of the β -carotene yields of a range of high pVA bananas. The banana cultivars are ranked according to β -carotene yield. The taxonomic classification and genome type data were reported by Daniells *et al.* (2001). However, the Fe'i type bananas were simply classified as Fe'i (Englberger *et al.*, 2003c). The β -carotene yields of banana cultivars marked ^(a), ^(b) and ^(c) were obtained from results reported by Englberger *et al.* (2003c), Englberger (2003) and Holden *et al.* (1999), respectively.

Banana Cultivar	Taxonomic Classification	Genome Type	β -carotene content ($\mu\text{g g}^{-1}$)
Uht en yap ^(a)	Fe'i	Fe'i	27.80
Lakatan ^(b)	<i>Eumusa</i>	AA	8.37
Usr kulasr ^(a)	Fe'i	Fe'i	6.6
Pisang Kelat ^(b)	<i>Eumusa</i>	AAB	4.90
Pisang Rajah ^(b)	<i>Eumusa</i>	AAB	4.15
Usr Lakatan ^(a)	<i>Eumusa</i>	AA	3.30
Cavendish ^(c)	<i>Eumusa</i>	AAA	0.21

Due to their excellent bioavailability, good cultural acceptance in target areas and high nutritional value, bananas make an excellent target for pVA biofortification. Further, the sterility of commercially important bananas reduces the risk of gene transfer to wild species or related plants. In banana, conventional breeding of staple cultivars with high pVA varieties is not feasible because cultivated bananas are sterile due to cytoplasmic and genetic factors (Gowen, 1995), making it difficult to obtain viable seed for breeding. Conversely, the genetic modification of banana is an established technology using both microprojectile bombardment (Hermann *et al.*, 2001) and *Agrobacterium*-mediated (Khanna *et al.*, 2004) transformation. These gene transfer methods are preferred over conventional breeding as they produce more plants with desired traits in a shorter time frame due to the direct nature of gene transfer, and the efficient selection and micropropagation of transgenic plants. The genetic modification of edible plant varieties to enhance pVA bioavailability requires a detailed understanding of carotenoid metabolism.

1.3 Carotenoid metabolism

Carotenoids are lipophilic pigments found in all photosynthetic organisms and are characterised by an unsaturated 40 carbon backbone with as many as 15 double bonds (Busch *et al.*, 2002; Hirschberg, 2001; Taylor and Ramsay, 2005). This family includes

carotenes, such as α -carotene and β -carotene, and their oxygenated derivatives the xanthophylls, such as zeaxanthin and violaxanthin. They are localised predominantly in the chloroplasts and chromoplasts in plants (Sinha, 2004). In chloroplasts, they have critical roles in photosynthesis where they form part of light harvesting complexes, serving as photosynthetic electron transfer molecules by reducing chlorophyll. They are also photoprotective agents that prevent chlorophyll damage by dissipating excess light energy and inhibiting free radical reactions (Sinha, 2004; Taiz and Zeiger, 2002). Carotenoids also function in fruits and flowers where they attract animals and insects for pollination and seed scattering, as well as in some grains, roots and tubers (Sinha, 2004; Taylor and Ramsay, 2005). In addition, the phytohormone abscisic acid, which has well characterised roles in stress response, is derived from carotenoid precursors (Cutler and Krochko, 1999).

The three naturally occurring carotenoids with pVA activity are β -carotene, α -carotene and β -cryptoxanthin, which are nutritionally active because they have an unsubstituted β -ionone ring at one or both ends of the molecule (Figure 1.1; Bender, 2003; Yeum and Russell, 2002). β -carotene has β -ionone rings at both ends of the molecule and is therefore most efficiently converted to retinol. However, α -carotene and β -cryptoxanthin are less efficiently converted to retinol because they also have ϵ -cyclic and hydroxylated β -cyclic rings,

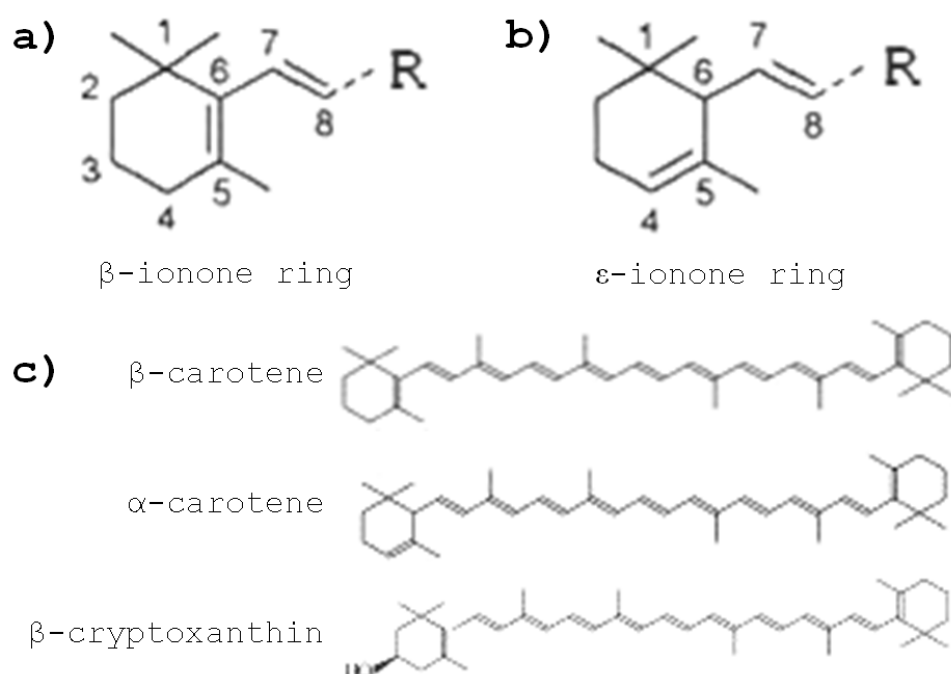


Figure 1.1: Structure of carotene cyclic end groups. The two basic ring structures a) β -ionone (β -cyclic) and b) ϵ -ionone (ϵ -cyclic) differ only in the position of the carbon-carbon double bond, which is between carbon 5 and 6 for β -ionone and between carbon 4 and 5 for ϵ -ionone. c) Summary of the structure of the pVA carotenoids [adapted from Cunningham and Gantt, 1998].

respectively (Cunningham and Gantt, 1998; West, 2000). The genes involved in carotenoid metabolism have been well characterised in both prokaryote and eukaryote systems, and have been reviewed extensively (Armstrong and Hearst, 1996; Cunningham and Gantt, 1998; Sinha, 2004). The regulation of these genes during fruit development has also been widely studied in systems such as tomato (Fraser *et al.*, 1994; Giuliano *et al.*, 1993; Pecker *et al.*, 1996; Ronen *et al.*, 1999) and citrus (Rodrigo *et al.*, 2004). This has resulted in a detailed understanding of the metabolic pathway, from which multiple molecular targets for the genetic improvement of pVA carotenoid biosynthesis have been identified (Cunningham and Gantt, 1998).

1.3.1 Carotenoid biosynthesis

The process of carotenoid biosynthesis is summarised in Figure 1.2 and begins with the conversion of isopentenyl diphosphate (IPP) to its isomer, dimethylallyl diphosphate (DMAPP). DMAPP is the initial substrate required to form the precursors for virtually all isoprenoid biosynthetic pathways (Cunningham and Gantt, 1998). The enzyme isopentenyl diphosphate isomerase (IPI) catalyses the conversion of IPP to DMAPP through a reversible allylic rearrangement that repositions the carbon-carbon double bond. Following isomerisation, the sequential addition of three IPP molecules to one DMAPP molecule (Figure 1.2a) by geranylgeranyl diphosphate synthase (GGPS), leads to the production of geranylgeranyl diphosphate (GGPP). The first committed step of carotenoid biosynthesis is the condensation of two GGPP molecules by the enzyme phytoene synthase (PSY) to produce the symmetrical phytoene molecule (Cunningham and Gantt, 1998). This is a two-step process involving the intermediate molecule prephytoene diphosphate (PPPP) and the removal of the diphosphate groups from the substrates, resulting in a linear hydrophobic product. The second step in carotenoid biosynthesis is the desaturation of phytoene to produce lycopene (Figure 1.2b), which is catalysed by two related enzymes, phytoene desaturase (PDS) and zeta (ζ)-carotene desaturase (ZDS). The process occurs via two desaturation steps where PDS converts phytoene to ζ -carotene via phytofluene, which is then transformed to lycopene by ZDS through the intermediate neurosporene (Cunningham and Gantt, 1998).

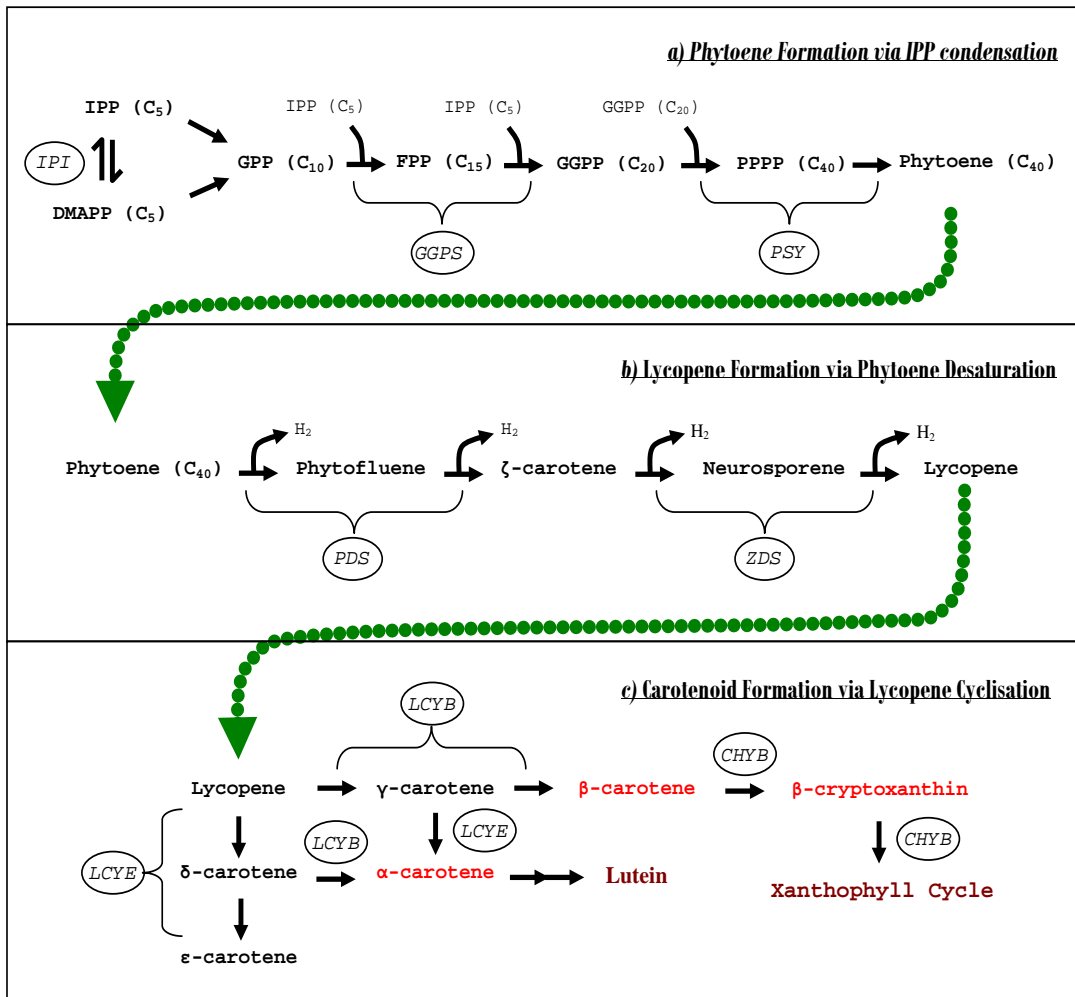


Figure 1.2: Summary of carotenoid biosynthesis illustrating the process by which short chain isoprenoids are biochemically converted into carotenoids and related compounds [adapted from Cunningham and Gantt, 1998]. Carotenoid biosynthesis can be considered to consist of three phases. The first stage **a)** is the condensation of isopentenyl diphosphate (IPP) and dimethylallyl diphosphate (DMAPP) into phytoene. The second part **b)** involves the desaturation of phytoene to lycopene, which is then converted into carotene compounds **c)** that are converted into lutein and xanthophylls. Although the precursors of phytoene production in **a)** are known to be involved in the synthesis of other isoprenoids, only their relevance to carotenoid biosynthesis has been highlighted. The dotted arrows show the transfer of carotenoid intermediates to subsequent phases of biosynthetic process. The circled text represents the different enzymes involved in carotenoid biosynthesis while the solid arrows (\rightarrow and \downarrow) represent substrate conversion events. The abbreviated enzyme names are: isopentenyl diphosphate isomerase (IPI), geranylgeranyl diphosphate synthase (GGPS), phytoene synthase (PSY), phytoene desaturase (PDS), ζ -carotene desaturase (ZDS), lycopene β -cyclase (LCYB), lycopene ϵ -cyclase (LCYE) and β -carotene hydroxylase (CHYB).

The linear lycopene molecule is converted to bicyclic carotene compounds such as α - and β -carotene through sequential cyclisation reactions catalysed by the lycopene β - and ϵ -cyclases (Figure 1.2c; Cunningham and Gantt, 1998). Lycopene β -cyclase (LCYB) catalyses the formation of β -carotene by forming two β -cyclic rings from both ends of the lycopene molecule in a process that produces the monocyclic γ -carotene intermediate. Similarly,

lycopene ϵ -cyclase (LCYE) creates δ -carotene, and then ϵ -carotene in two steps. However, ϵ,ϵ -carotenes are rare in plant systems and LCYE is normally involved in the synthesis of α -carotene, a β,ϵ -carotenoid, in concert with LCYB. The enzyme β -carotene hydroxylase (CHYB) sequentially adds hydroxyl groups to both β -ionone rings of the β -carotene molecule in two a step process, producing zeaxanthin via the intermediate β -cryptoxanthin (Figure 1.2c). This represents the first step in the conversion of carotenoids into xanthophylls and related compounds (Cunningham and Gantt, 1998).

Observation of the structural and functional properties of carotenoid biosynthetic enzymes resulted in the hypothesis that in plant and algal plastids, these enzymes function in three multi-enzyme complexes (Figure 1.3; Cunningham and Gantt, 1998). The first enzyme aggregate is a phytoene biosynthesis complex consisting of monomeric IPI and PSY complexed to a GGPP homodimer (Figure 1.3a). This complex is predicted to convert IPP into phytoene (Bonk *et al.*, 1997) and be soluble but membrane associated in its functional state due to PSY's lipid cofactor requirements (Fraser *et al.*, 2000; Schledz *et al.*, 1996) and the hydrophobic nature of isoprenoids (Cunningham and Gantt, 1998). This hypothesis is supported by evidence of organelle-specific functional segregation of GGPS family members (Okada *et al.*, 2000; Suire *et al.*, 2000). Analysis of cauliflower PDS provided further evidence of isoprenoid enzyme complex formation as this 55 kDa protein was associated with 350 kDa and 660 kDa complexes in the plastid membrane and stroma respectively (Lopez *et al.*, 2008b).

Phytoene is then transferred to adjacent membrane-bound β,β - and β,ϵ -complexes (Figure 1.3b and c) which ultimately produce β -carotene and α -carotene, respectively. The β,β -complex is thought to consist of an association of the homodimers of PDS, ZDS and LCYB, while β,ϵ -complexes differ only in the presence of a LCYB/LCYE heterodimer instead of the LCYB homodimer. The rarity of natural ϵ,ϵ compounds and questions over LCYE's ability to homodimerise suggest that ϵ,ϵ -complexes are not common (Cunningham and Gantt, 1998). Enzyme complex formation could help to explain the concurrent upregulation of endogenous PDS and ZDS in tomato lines transformed with prokaryotic PDS (Romer *et al.*, 2000), and changes in the α -carotene to β -carotene ratio in transgenic canola seeds modified with different combinations of isoprenoid biosynthetic enzymes (Ravanello *et al.*, 2003).

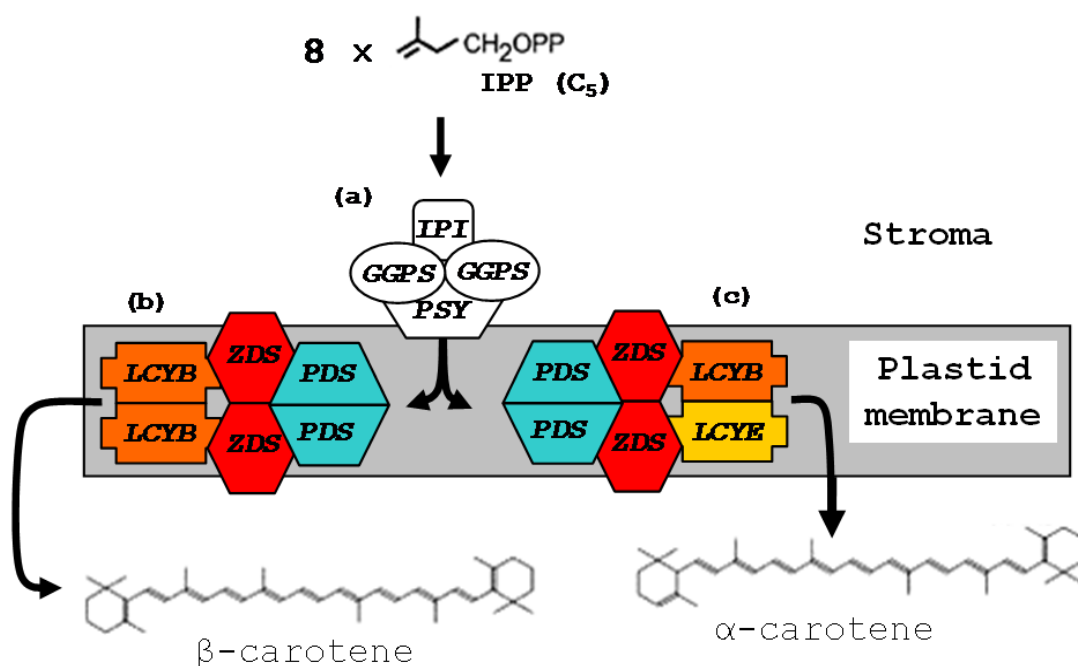


Figure 1.3: Organisation of carotenoid biosynthetic enzymes in plastids. At the start of carotenoid synthesis, eight IPP molecules are converted to phytoene by the stromal phytoene biosynthesis complex (a), which consists of monomeric IPI and PSY enzymes linked to a GGPS homodimer. This complex is linked to the plastid membrane by the membrane-associated PSY enzyme. Next, the lipophilic phytoene molecule is processed by the membrane-bound β,β- (b) and β,ε- (c) carotenoid synthesis complexes responsible for the production of α-carotene and β-carotene, respectively. [adapted from Cunningham and Gantt, 1998].

1.3.2 Carotenoid cleavage

Carotenoids are precursors for the biosynthesis of many secondary metabolites and some, such as abscisic acid (ABA), have signalling functions. Enzymes in the 9-cis-epocarotenoid cleavage dioxygenase (NCED) and carotenoid cleavage dioxygenase (CCD) protein families are involved in carotenoid catabolism (Tan *et al.*, 2001). NCEDs are involved in ABA biosynthesis and as such are not ideal targets for genetic improvement of pVA content due to the potential for abnormal phenotypes (Fray *et al.*, 1995). The function of NCEDs in relation to ABA metabolism has been reviewed elsewhere (Schwartz *et al.*, 2001; Tan *et al.*, 2001). The first member of the *ccd* gene family, *ccd1*, was characterised in *Arabidopsis* and appeared to function as a dimer that simultaneously cleaves both ends of its carotenoid substrates, which include β-carotene, zeaxanthin and lutein (Schwartz *et al.*, 2001). In tomato, CCD1 was also shown to cleave β-carotene precursors such as the monocyclic δ-carotene as well as the linear substrates phytoene, ζ-carotene and lycopene Simkin *et al.*, 2004. This enzyme has also been characterised in other plants including crocus (Bouvier *et al.*, 2003), grape (Mathieu *et al.*, 2005) and melon (Ibdah *et al.*, 2006). The various CCD1 cleavage products are volatile compounds involved in fruit maturation and flavour, microbial symbiosis and pathogen resistance, and light induced development of growing seedlings

(Mathieu *et al.*, 2005; Simkin *et al.*, 2004; Schwartz *et al.*, 2001). *ccd1* is part of a gene family that also includes *ccd4*, *ccd7* and *ccd8* and is distinct from the carotenoid cleavage enzymes involved in ABA synthesis (Tan *et al.*, 2003).

1.3.3 Regulation of carotenoid metabolism

Regulation of carotenoid metabolism occurs on multiple levels. Some major regulators of carotenoid metabolism include environmental factors such as ethylene production and light, which act through transcriptional and post-transcriptional mechanisms. Fruit ripening requires the coordinated expression of a variety of genes whose products facilitate the various fruit maturation processes, and ethylene biosynthesis plays a critical role in the regulation of such genes in climacteric fruit such as tomato (Moore *et al.*, 2002).

The effects of ethylene on the mRNA levels transcribed from the *psy*, *pds* and *zds* genes and their impact on phytoene, phytofluene and β -carotene accumulation were profiled in two cultivars of apricot, Moniqui and Goldrich, that produce white and orange fruit, respectively (Marty *et al.*, 2005). Expression profiles of these genes prior to ethylene-induced ripening were similar in both cultivars and correlated positively with increasing accumulation of phytoene, phytofluene and β -carotene. However, accumulation of these mRNAs and ethylene production was significantly greater in the white Moniqui fruit compared to Goldrich fruit, although in contrast, accumulation of phytoene and phytofluene was 2 fold higher in Goldrich fruit. Ethylene treatment of fruit from both cultivars doubled phytoene and phytofluene production and dramatically increased *psy* and *pds* expression. However, both β -carotene accumulation and *zds* expression were unaffected by ethylene treatment. The results showed that ethylene production regulated the production of the colourless carotenoids phytoene and phytofluene but not downstream β -carotene levels, suggesting that lycopene accumulation and *lcyb* expression are ethylene independent (Marty *et al.*, 2005).

Plant carotenoid biosynthesis is also known to be affected by light through the interactions of phytochromes with red and far-red light. The conformation of these proteins depends on the nature of the light they receive, and the modulation of plant maturation is activated by red light stimulation (Quail, 2002). Exposure to red-light was also found to increase total carotenoid accumulation by about 50% without altering total carotenoid composition in ripening tomato fruit (Schofield and Paliyath, 2005). Moreover, the catalytic activity of PSY was boosted by 40% and these effects were reversible upon exposure to far-red light. These results suggested that the observed increases in carotenoid metabolism were due to a phytochrome-mediated effect that occurred prior to peak PSY activity and mediated by

translational or post-translational factors. The *Arabidopsis psy* promoter has been characterised and found to be regulated by light (Welsch *et al.*, 2003), and this is discussed further in Chapter 5.

Carotenoid composition fluctuates during fruit development. This has been studied in a number of fruit including citrus (Kato *et al.*, 2004) and apricots (Marty *et al.*, 2005) and extensive studies have been undertaken in tomato, a model system in which the regulation of carotenoid composition during fruit development has been well characterised (Fraser *et al.*, 1994; Giuliano *et al.*, 1993; Giovannoni, 2004). In one study, *psy* mRNA was 18 and 52 fold greater than that of *pds* at the breaker (ripening triggered) and firm red (ripening complete) stages, respectively (Figure 1.4a; Giuliano *et al.*, 1993). In a subsequent study, the highest carotenoid concentration was reported to occur in ripened fruit (Figure 1.4b) while green fruit exhibited the highest activity of PSY, PDS and LCYB enzymes (Figure 1.4c; Fraser *et al.*, 1994). The *psy* and *pds* mRNA levels were also quantified and transcripts were only detected in breaker and post-breaker fruit, supporting previous observations by Giuliano *et al.* (1993). In addition, PSY activity at the immature green stage was approx 10 and 20 fold greater than PDS and LCYB, respectively (Fraser *et al.*, 1994). These studies demonstrate that the coordinated transcriptional regulation of carotenoid biosynthetic genes is a significant contributor to carotenoid accumulation during fruit development. The observed differential expression of *psy* and *pds* (Giuliano *et al.*, 1993; Fraser *et al.*, 1994) has led to the widely accepted hypothesis that this phenomenon is the predominant determinant of lycopene accumulation in tomato (Corona *et al.*, 1996; Hirschberg, 2001; Ronen *et al.*, 1999). The importance of transcriptional control in carotenoid biosynthesis was observed in the study of *lcyb* and *lcye*, which were found to have the same relative mRNA abundance as *psy* and *pds* at the immature green stage (Ronen *et al.*, 1999). However, during the transition to breaker fruit, *lcyb* and *lcye* mRNA decreased despite increasing expression of *psy* and *pds*. This suggested that lycopene accumulation in ripening tomato was due to down regulation of the genes that converted it to β -carotene. Further, the transcriptional control of multiple gene families appears to be significant in tissue-specific carotenoid accumulation during development. This hypothesis was supported by the detection of PSY proteins of different sizes in chloroplasts and chromoplasts (Fraser *et al.*, 1994) and the discovery of the leaf-associated *psy2* gene in tomato (Bartley and Scolnik, 1993).

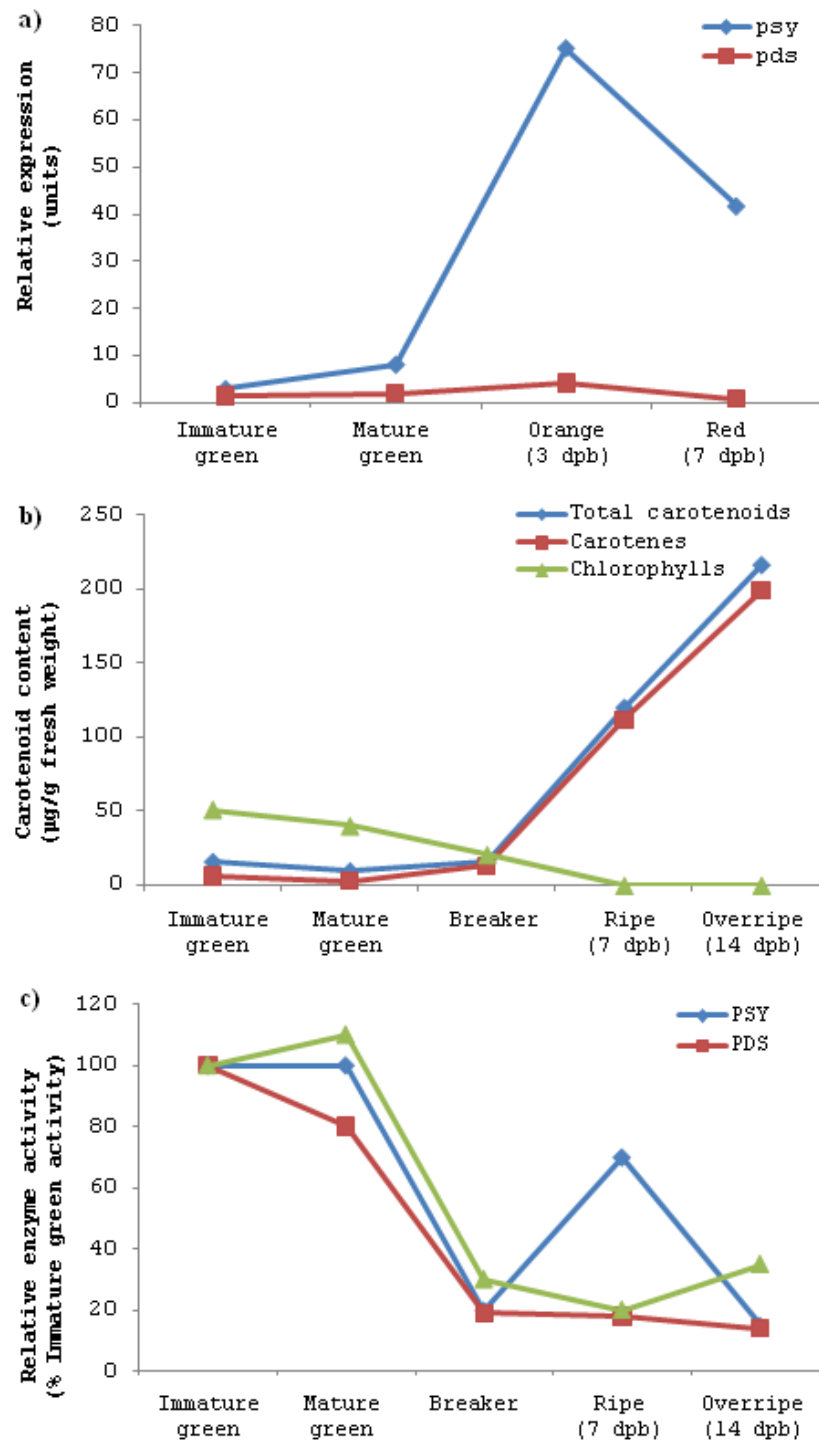


Figure 1.4: Analysis of carotenoid accumulation in tomato fruit. a) Accumulation of *psy* and *pds* mRNA over the first four stages of tomato fruit ripening [adapted from Giuliano *et al.* (1993)]. b) Changes in total carotenoid, carotene and chlorophyll content and c) carotenoid biosynthetic enzyme activity during the five stages of tomato fruit ripening [adapted from Fraser *et al.*, 1994]. Stages of fruit ripening: immature green and mature green - 2 weeks and 7 weeks post-fertilisation, respectively; breaker - marked by the first transition of fruit colour; firm red - 7 days post breaker (dpb); overripe - about 14 dpb (Fraser *et al.*, 1994; Lu *et al.*, 2001).

Carotenoids accumulate in the plastids where they are synthesised (Sinha, 2004). Chromoplasts store carotenoids in a number of ways including: crystals, oil bodies, lipid binding proteins, and membrane structures (Paine *et al.*, 2005; Vishnevetsky *et al.*, 1999). Significant work in this area has been done in the study of cauliflower *Or* mutants, which exhibited altered colour of the cauliflower curd due to β -carotene accumulation caused by a dominant single gene called the *Or* gene. Molecular analysis revealed no significant alterations in isoprenoid and carotenoid biosynthesis, and no linkage between carotenoid biosynthetic genes and the *Or* locus. This led to the hypothesis that the *Or* gene, may promote carotenoid accumulation through the creation of sheet-like structures that accumulated β -carotene (Li *et al.*, 2001). In subsequent studies, a detailed linkage map was constructed and markers associated with the *Or* gene locus were identified (Li and Garvin, 2003; Li *et al.*, 2003). Characterisation of this gene found that it encoded a protein that affects chromoplast formation and division (Lu *et al.*, 2006), and was capable of enhancing carotenoid production in tomato tubers (Lopez *et al.*, 2008a).

1.4 Phytoene synthase

1.4.1 Properties of *psy*

PSY is considered to be a major rate limiting step in carotenoid biosynthesis because it irreversibly channels GGDP towards carotenoid production and away from the production of many isoprenoids such as chlorophylls, tocopherols, gibberellins and quinones (Cunningham and Gantt, 1998). Consequently, PSY occupies a metabolic junction between multiple pathways and its activity may have a broad influence on isoprenoid production in plants. The importance of this enzyme makes it the logical starting point for investigating differential carotenoid accumulation in bananas.

The genes encoding PSY in higher plants, in many cases, have been found to exist as gene families with multiple members. While only one *psy* gene has been identified from *Arabidopsis* (Scolnik and Bartley, 1994) and daffodil (Schledz *et al.*, 1996), two distinct *psy* genes have been identified in plants such as tomato (Bartley *et al.*, 1992; Bartley and Scolnik, 1993), tobacco (Busch *et al.*, 2002), maize, rice (Gallagher *et al.*, 2004), and wheat (Cenci *et al.*, 2004; Pozniak *et al.*, 2007). Plant species with more than two *psy* genes may also exist. For example, the yellow gentian (*Gentiana lutea*) *psy* gene family (Zhu *et al.*, 2002) consists of four genes: *psy1*, *psy2*, *psy3* and *psy4* (GenBank accession numbers E15680, E15681, E15682 and E15683, respectively). Further, a third member of the maize and rice *psy* families, *psy3*, was recently identified (Li *et al.*, 2008a; Li *et al.*, 2008b). The complete gDNA sequence of a wheat *psy1* gene (*psy-A1*) was shown to be 4175 bp long and included six exons and five introns with an coding region of 1,284 bp (He *et al.*, 2008),

which was consistent with previous observations in maize and rice (Gallagher *et al.*, 2004). The PSY protein appears to be monomeric (Dogbo *et al.*, 1988) and is thought to interact with plastid membranes and other enzymes in carotenoid biosynthetic complexes (Chapter 1.3.1; Cunningham and Gantt, 1998). Analysis of *Arabidopsis* PSY, and the tomato PSY1 and PSY2 proteins (Figure 1.5) suggests that the plant PSY proteins include an N-terminal signal peptide that is subsequently cleaved (Bartley *et al.*, 1992; Bartley and Scolnik, 1993; Scolnik and Bartley, 1994). The mature protein has a single large prenyltransferase (Cunningham and Gantt, 1998) catalytic domain belonging to the trans-isoprenyl diphosphate synthases, head-to-head (1'-1) condensation reaction (Trans_IPPS_HH) family (NCBI CDD No. cd00683).

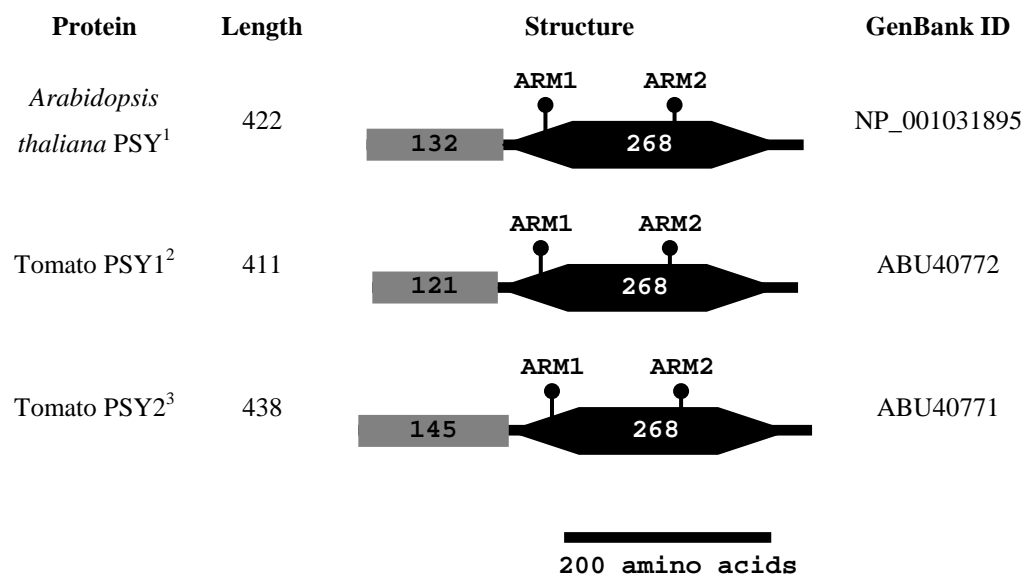


Figure 1.5: General structure of plant PSY proteins showing the signal peptides, catalytic domains and lengths of *Arabidopsis* PSY, tomato PSY1 and tomato PSY2. The lengths (black text) of the signal peptides (grey rectangle) was based on estimates by Scolnik and Bartley (1994)¹, Bartley *et al.* (1992)² and Bartley and Scolnik (1993)³. The catalytic domains (Trans_IPPS_HH; black hexagon) are indicated on each protein along with the positions of the first and second aspartic acid rich motifs (ARM1 and ARM2); the lengths (white text) of the mature proteins were obtained from the listed GenBank protein entries. All lengths are measured in amino acids.

Transcription of the *psy* genes has been reported in both leaf and fruit tissue of tomato (Bartley and Scolnik, 1993), with *psy1* expression associated with chromoplast-bearing tissues (fruit and petals) while *psy2* was more constitutively expressed (Giorio *et al.*, 2008). Semi-quantitative RT-PCR analysis of *psy1* and *psy2* expression in maize varieties with yellow endosperm (high carotenoid) or white endosperm (low carotenoid) colour implicated *psy1* in endosperm carotenoid accumulation. In leaf tissue of both maize varieties the *psy1* and *psy2* expression was similar. However, *psy1* expression was higher than *psy2* in yellow

endosperm maize, while only *psy2* was expressed in white endosperm maize. The *psy* expression in the leaf and endosperm of rice (white endosperm) was identical to that of white endosperm maize (Gallagher *et al.*, 2004). The recently identified *psy3* gene is thought to be involved in ABA-mediated stress tolerance in the roots of grasses such as maize and rice (Li *et al.*, 2008a).

Expression of *psy* during fruit development was influenced by ethylene production in apricot (Marty *et al.*, 2005), while in *Arabidopsis*, *psy* expression and enzymatic activity was shown to be regulated by light through phytochrome activity, and increased carotenoid content was only seen under light conditions that triggered chlorophyll synthesis (von Lintig *et al.*, 1997; Welsch *et al.*, 2000). Characterisation of the *Arabidopsis thaliana psy* promoter identified DNA regulatory motifs activated by different light conditions (Welsch *et al.*, 2003). Responses to red light were under the specific control of two adjacent G-box like elements roughly 200 bp upstream of the transcription start site. In contrast, constitutive promoter expression was linked to a pair of ATCTA motifs located approximately 840 bp from the transcription start site (Welsch *et al.*, 2003) and this motif was thought to coordinate the expression of genes involved in photosynthesis, and also carotenoid and tocopherol metabolism (Welsch *et al.*, 2003).

1.4.2 The *psy* gene as a target for pVA enhancement

The extensive knowledge of carotenoid metabolism in model systems has identified multiple targets for improvement of pVA content in nutritionally important crops. Considerable work has been undertaken towards the genetic manipulation of carotenoid biosynthesis in a number of plant systems and this area has been reviewed extensively (Sandmann, 2001a; Sandmann, 2001b; Taylor and Ramsay, 2005; Zimmermann and Hurrell, 2002). Significant work in enhancing pVA content in transgenic plants has been achieved through genetic manipulation of *psy* expression in tomato and rice.

Tomato is a commercially important crop known to naturally accumulate significant quantities of carotenoids, and has been used as a model to study the enhancement of carotenoid levels (Giuliano *et al.*, 1993; Fraser *et al.*, 1994). Early work involved the constitutive over-expression of the tomato *psy1* gene driven by the CaMV35S promoter (Fray *et al.*, 1995). Abnormal carotenoid accumulation was observed in numerous organs including the seed coat, immature fruit and abscission zones. Although lycopene and phytoene content was enhanced, the yields of β -carotene, total carotenoids and chlorophyll were unaffected. Interestingly, increased *psy1* mRNA levels produced dose dependent dwarfism in transgenic plants, due to a 30 fold reduction in gibberellin production that was

attributed to GGPP depletion. From this work it was apparent that constitutive carotenoid biosynthetic gene over-expression was inappropriate for genetic improvement of pVA content. Later, fruit-specific *psy* expression was achieved using the *Erwinia crtB* gene, encoding a PSY enzyme, which was chloroplast targeted using the tomato *psy1* transit peptide and regulated by the tomato polygalacturonase promoter (Fraser *et al.*, 2002). As a result, the concentrations of β -carotene, phytoene and lycopene increased by roughly two fold and total fruit carotenoid content was improved by between 200% and 400% without detriment to other isoprenoid pathways. β -carotene content of up to 200 $\mu\text{g/g}$ dry weight was reported.

The *psy* gene has also been used in the improvement of pVA content of rice endosperm. Genetically modified Golden Rice, with elevated endosperm pVA levels, represents one of the first concerted efforts to alleviate VAD through genetic engineering of a staple crop. Endosperm, the edible portion of the rice grain (Grusak, 2005), expresses *ggps* but not the enzymes required for conversion of GGPP into carotenoids, although these genes are present and expressed in other organs such as the leaf. Early work used *Agrobacterium*-mediated transformation to introduce the daffodil *psy* and *crtI* (a desaturase from *Erwinia uredovora* that has the function of both *pds* and *zds*) genes into rice endosperm in a single binary vector (Hoa *et al.*, 2003; Ye *et al.*, 2000). The expression of *psy* was driven by the rice endosperm glutelin (*gt1*) promoter and localised using its transit peptide, while *crtI* was constitutively expressed by the CaMV35S promoter and endosperm targeted using the pea RuBisCO small subunit signal peptide. These studies demonstrated that endogenous *lcyb* activity was sufficient to produce β -carotene upon addition of *psy* and the desaturase enzymes alone. However, the β -carotene yield of carotenogenic seeds, identified by their yellow colour, was only between 0.8 $\mu\text{g/g}$ and 1.6 $\mu\text{g/g}$ dry weight (Hoa *et al.*, 2003; Ye *et al.*, 2000).

Recent work succeeded in drastically improving the pVA content of rice and was conducted in three phases (Paine *et al.*, 2005). The activity of several *psy* genes from plants such as carrot, daffodil, maize and rice was compared by stably transforming them into maize callus and assessing the carotenoid content. The maize *psy* gene demonstrated the highest activity followed by the rice and carrot genes, respectively, which were each approximately 50% as active as maize *psy*. The daffodil *psy* gene was least active, consistent with the hypothesis that this gene was the limiting factor in pVA accumulation in the previous generation of Golden Rice. Selected *psy* genes were then used to create transgenic rice lines, using single expression cassettes containing a plastid targeted *psy* gene and a *crtI* gene (Ye *et al.*, 2000). Both were controlled by the rice *gt1* promoter with a catalase intron (Paine *et al.*, 2005). Selected transgenic rice lines exhibited yellow and even orange grain phenotypes that were

otherwise normal. The best performing genes were maize and rice *psy*, yielding 14 $\mu\text{g g}^{-1}$ and 18 $\mu\text{g g}^{-1}$ total carotenoids respectively with 80 to 90% β -carotene content compared with the low 1.2 $\mu\text{g g}^{-1}$ carotenoid yield of daffodil *psy* (Hoa *et al.*, 2003; Paine *et al.*, 2005). Interestingly, maize and rice *psy* genes had highest sequence similarity of 89% (Paine *et al.*, 2005), possibly explaining their high productivity as both gene sources are gramminaceous monocotyledonous plants. The last experiment involved the creation of a transgenic rice line, Golden Rice 2, using a construct expressing maize *psy* and *crtI*, both regulated by an intronless *gt1* promoter (Paine *et al.*, 2005). This produced a rice line yielding 37 $\mu\text{g g}^{-1}$ total endosperm carotenoid that accumulated 85% β -carotene, exceeding previously reported yields by 23 fold (Hoa *et al.*, 2003; Ye *et al.*, 2000). The authors hypothesised that the maize *psy* worked well due to the optimal nature of the rice endosperm environment and that despite this, PSY still limits further carotenoid yield (Paine *et al.*, 2005).

1.5 Objectives of the program of research and investigation

Following the development of Golden Rice, genetic engineering of staple banana cultivars to enhance pVA content is being undertaken in an attempt to combat VAD in regions where rice is not readily grown or consumed. At the start of this project little was known about carotenoid metabolism in banana, the sequences of the genes in the pathway or why the carotenoid content of fruit varies so much. A better understanding of the mechanisms enabling high pVA accumulation in banana varieties could prove valuable in the development of bananas with enhanced carotenoid content. Although there are many levels at which carotenoid biosynthesis can be regulated, there is considerable evidence that PSY plays a critical role directly linked to the capacity for pVA accumulation in a number of systems. Quantitative Trait Loci (QTL) analyses have demonstrated a putative association between the *psy1* locus and carotenoid content in maize (Wong *et al.*, 2004; Chander *et al.*, 2008) and with increased endosperm colour in durum wheat (*Triticum turgidum* var. durum; Pozniak *et al.*, 2007). This role is further supported by the results of genetically engineered tomato (Fraser *et al.*, 2002) and rice (Paine *et al.*, 2005) where overexpression of *psy* significantly increased pVA accumulation. Cumulatively, these studies demonstrate that PSY activity is an important rate limiting step in carotenoid biosynthesis, which is of great significance as the activity of this enzyme is the first irreversible step in this process (Cunningham and Gantt, 1998).

Therefore, the overall aim of this project was to investigate the role of PSY, at the level of protein function and gene expression, in the differential production of pVA carotenoids in bananas with both high and low pVA content. This was achieved by:

- i) isolation and characterisation of *psy* nucleotide sequences from high and low pVA bananas
- ii) analysis of banana PSY proteins using bioinformatics and expression in rice callus
- iii) comparison of the activity of banana *psy* gene promoters using reporter gene assays
- iv) investigation of *psy* mRNA levels in different tissues from high and low pVA bananas

Chapter 2: General methods

2.1 General methods for nucleic acid purification from plant cells

2.1.1 Purification of total RNA from banana tissue

Total RNA was obtained using the CTAB extraction method (Chang *et al.*, 1993) modified to include the CTAB RNA extraction buffer and polysaccharide removal procedure described by Asif *et al.* (2000). Essentially, plant tissue was ground in LN₂ and incubated with RNA extraction buffer (10 mL/g tissue) at 65 °C for 60 min. The mixture was extracted twice with chloroform and total RNA precipitated with $\frac{1}{3}$ volume of 10 M LiCl to the supernatant at 4 °C overnight. Total RNA was recovered by centrifugation at 17,000 × g for 20 min at 4 °C. The pellet was resuspended in DEPC-treated mqH₂O (100 µL per gram of starting plant material) and extracted again with an equal volume of chloroform. Polysaccharides were precipitated with $\frac{1}{30}$ volume of 3 M sodium acetate (pH 5.2) and 0.1 volume of 100% ethanol on ice for 30 min and removed by centrifugation at 10,000 × g for 25 min at 4 °C. RNA was precipitated from the supernatant with $\frac{1}{10}$ volume of 3 M sodium acetate (pH 5.2) and 3 volumes of 100% ethanol at –80 °C overnight and recovered by centrifugation at 10,000 × g for 20 min at 4 °C. The pellet was washed with 70% ethanol, dried under vacuum and resuspended in DEPC-treated mqH₂O as previously described. Total RNA was either used immediately or stored at –80 °C with or without prior DNase treatment.

2.1.2 mRNA purification

Banana mRNA was purified from total RNA (100 to 500 µg) using the GenElute™ mRNA Miniprep Kit (Sigma-Aldrich) according to the manufacturer's instructions.

2.1.3 DNA extraction

Banana leaf tissue (1 g) was ground in LN₂, added to 3 mL pre-warmed (65 °C) DNA extraction buffer (2% w/v CTAB; 2% w/v PVP; 100 mM Tris HCl, pH 8.0; 25 mM EDTA; 2 M NaCl; 1.4% v/v 2-mercaptoethanol) and incubated for 60 min at 65 °C with occasional mixing. Plant material was removed by centrifugation at 3880 × g for 10 min at room temperature and the supernatant extracted twice with an equal volume of chloroform under the same conditions. The aqueous phase was collected and 10 µL RNase A (1 mg/mL) was added before incubation at 37 °C for 60 min. The sample was extracted again with chloroform before precipitation of the DNA with an equal volume of isopropanol at –80 °C for 30 min. The DNA was collected by centrifugation at 3880 × g for 20 min at room

temperature and the pellet washed with 70% ethanol. The DNA pellet was dried under vacuum and resuspended in 50 μ L mqH₂O. The yield and quality of the DNA were assessed by spectrophotometry and agarose gel electrophoresis and either used immediately or stored at -20 °C.

When DNA of higher purity was required, the DNeasy Plant Mini Kit (Qiagen) was used. Banana leaf tissue (0.1 g) was ground in LN₂ and the DNA extracted as recommended by the manufacturer.

2.2 General methods in nucleic acid amplification, cloning and sequencing

2.2.1 PCR amplification

For all PCRs, thin walled 0.2 mL tubes were used to amplify products in a DNAEngine[®] thermocycler (Bio-Rad). Annealing temperatures were dependant on primers and are specified in individual chapters.

Standard DNA Amplification

PCR products were amplified from DNA template (~0.3 to 1 μ g) using either Taq DNA Polymerase (Roche Applied Science) or the GoTaq[®] Green Master Mix (Promega). Taq DNA Polymerase reactions included 1 \times PCR buffer, 300 μ M dNTP Mix (Roche Applied Science), 7.5 pmol of each PCR primer, 1 U Taq DNA polymerase, and mqH₂O to a final volume of 25 μ L. GoTaq Green[®] (Promega) PCRs included 1 \times GoTaq green master mix, 7.5 pmol of each primer, and mqH₂O to a total volume of 20 μ L. Templates were initially denatured at 94 °C for 3 min followed by 35 cycles of denaturation at 94 °C for 10 sec, annealing for 30 sec and extension at 72 °C for 1 min per Kb of expected product. A final extension step of 72 °C for 10 min was included.

Long Template Amplification

Amplification of long DNA templates was achieved using the Expand[™] Long Template PCR System (Roche Applied Science) as recommended by the manufacturer. The final reaction mix consisted of 500 μ M dNTP mix, 3.75 pmol of each primer, 0.5 μ L Expand Long Template Enzyme mix, 1 \times Expand PCR buffer 3, DNA template (~0.3 to 1 μ g) and mqH₂O to a final volume of 25 μ L. PCR conditions included an initial denaturation cycle of 94 °C for 3 min prior to 10 cycles of denaturation at 94 °C for 10 sec, annealing for 30 sec and extension at 68 °C for 1 min per Kb of expected product. This was followed by an additional identical 25 cycles with 10 sec added to each successive extension step. A final extension at 68 °C for 7 min was included.

RT-PCR

RNA template (amounts specified in each chapter) was used as template in RT-PCR using the Titan One Tube RT-PCR System (Roche Applied Science) as per the manufacturer's instructions. The final reaction contained 200 μ M dNTP mix, 5 mM DTT, 5 pmol of each primer, 5 U Protector RNase Inhibitor (Roche Applied Science), 0.5 μ L Titan Enzyme mix, 1 \times RT-PCR buffer, and mqH_2O to a final volume of 25 μ L. A single cycle of 50 $^{\circ}C$ for 30 min was included for cDNA synthesis and preceded PCR amplification. The reactions were denatured once at 94 $^{\circ}C$ for 2 min prior to 10 cycles of denaturation at 94 $^{\circ}C$ for 10 sec, annealing for 30 sec and extension at 68 $^{\circ}C$ for 1 min per Kb of expected product. This was followed by 25 cycles of 94 $^{\circ}C$ for 10 sec, annealing for 30 sec and 68 $^{\circ}C$ for 1 min per Kb of expected product with 5 sec added to each successive cycle. A final extension step of 68 $^{\circ}C$ for 7 min was included.

2.2.2 Restriction enzyme digestion of DNA

Up to 1 μ g of plasmid DNA (pDNA) or plant gDNA was incubated with 10 U of the appropriate restriction enzyme (Roche Applied Sciences) in compatible 1 \times reaction buffer at 37 $^{\circ}C$ for 1 to 16 hr.

2.2.3 Agarose gel electrophoresis

Unless otherwise specified, DNA fragments from PCR or restriction digestion analysis were mixed with 1 \times Agarose gel loading dye (0.04% bromophenol blue; 1.7 mM Tris-HCl, pH 8.0; 0.17 mM EDTA; 0.08% glycerol) and separated for 30 min in 1% agarose gels made with 1 \times TAE buffer (10 mM Tris-acetate; 0.5 mM EDTA, pH 7.8) containing 0.25 \times SYBR[®] Safe DNA Gel Stain (Invitrogen) at 4 V/cm on a B1 or B2 EasyCast Mini Gel System (Owl Separation Systems). Nucleic acids were visualized on a Safe Imager[™] blue light transilluminator (Invitrogen) and images recorded using a G-Box (Syngene) gel documentation system with GeneSnap v6.07 and GeneTools v3.07 software.

2.2.4 Purification of DNA from agarose gels

Bands were excised from agarose gels and the DNA purified using the Mobio UltraClean[™] GelSpin[™] DNA Purification Kit (Mobio Laboratories inc.) according to the manufacturer's instructions. All purified DNA was eluted in a final volume of 20 μ L of 10 mM Tris-HCl.

2.2.5 DNA ligation

Gel purified PCR products (3 μ L) were ligated to 50 ng of T-tailed pGEM-T Easy (Promega) vector, as recommended by the manufacturer, in 10 μ L reactions containing 1 U T4 DNA Ligase (Promega) and 1 \times Rapid Ligation Buffer for up to 16 hr at 4 $^{\circ}$ C. For all other ligations, the vector and insert DNA were linearised by restriction enzyme digestion and ligated in a 3:1 molar ratio (insert: vector) as described above.

2.2.6 Transformation of *Escherichia coli* with recombinant plasmids

Recombinant plasmids were transformed as previously described (Inoue *et al.*, 1990) into chemically competent *Escherichia coli* strain XL1-Blue (Stratagene) obtained from Don Catchpole (QUT). Chemically competent cells (50 μ l) were mixed with 5 μ l pDNA and incubated on ice for 30 min before heat shock at 42 $^{\circ}$ C for 45 sec. The cells were then incubated on ice for 2 min and then allowed to recover in 450 μ l of SOC liquid medium (2% w/v bacto-tryptone; 0.5% w/v bacto-yeast extract; 10 mM NaCl; 2.5 mM KCl; 0.94 M MgCl₂·6H₂O; 0.94 M MgSO₄·7H₂O; 20 mM glucose) for 1 hr at 37 $^{\circ}$ C. Transformed colonies were grown overnight at 37 $^{\circ}$ C on Luria-Bertani (LB) media (1% w/v bacto-tryptone; 0.5% w/v bacto-yeast extract; 170 mM sodium chloride) solidified with 1.5% w/v bacto-agar and containing 100 μ g/ μ l Ampicillin (unless otherwise specified). For blue/white selection, 250 μ L 2% (w/v) X-gal and 500 μ L 0.1 M IPTG were added per mL of LB solid medium.

2.2.7 Growth of bacteria in liquid cultures

Liquid cultures of *E. coli* were grown by inoculating single bacterial colonies into LB media and incubating overnight at 37 $^{\circ}$ C and 220 rpm. The culture volume depended upon the quantity of bacteria required for subsequent pDNA purification.

2.2.8 Purification of plasmid DNA

For most purposes, a standard alkaline lysis procedure (Sambrook and Russell, 2001) was used for isolation of pDNA from 1.5 mL *E. coli* cultures except that RNase A (~20 μ g) was added during the initial lysis step. The pDNA was resuspended in 50 μ L mqH₂O. For sequencing, pDNA was isolated using an UltraClean™ 6 Minute Mini Plasmid Prep Kit™ (Mobio Laboratories inc.), while for large scale plasmid purification (20 mL *E. coli* cultures) a Genopure Plasmid Midi Kit (Roche Applied Science) was used, both according to the manufacturer's instructions. The quality and quantity of pDNA was assessed by agarose gel electrophoresis and UV spectrophotometry.

2.2.9 Storage of bacterial cultures

Bacteria were stored at $-80\text{ }^{\circ}\text{C}$ as 1 mL glycerol cultures, prepared by mixing 500 μL overnight culture and 500 μL sterile 80% glycerol in cryovials and snap-freezing in LN_2 .

2.2.10 DNA sequencing

Plasmids were prepared for sequencing using the ABI Prism BigDye 3.1 Terminator (Applied Biosystems) system. The reaction mixtures (20 μL) consisted of up to 500 ng pDNA, 1 \times Big Dye Terminator Buffer, 1 μL Big Dye Terminator v3.1 Enzyme Mix (Applied Biosystems) and 3.2 pmol primer [either M13 forward (5'-GTAAAACGACGGCCAGT-3') or reverse (5'-CACACAGGAAACAGCTATGACCATG-3') universal sequencing primers or specific primers]. Sequence reactions were cycled in a DNAEngine® thermocycler (Bio-Rad) with an initial denaturation step of $94\text{ }^{\circ}\text{C}$ for 3 min followed by 35 cycles of $94\text{ }^{\circ}\text{C}$ for 10 sec, $60\text{ }^{\circ}\text{C}$ for 30 sec and $72\text{ }^{\circ}\text{C}$ for 1 min per Kb of expected product with 10 sec added to each successive cycle. A final extension step of $72\text{ }^{\circ}\text{C}$ for 10 min was included.

Sequencing reactions were purified by precipitation with 2 μL 125 mM EDTA, 2 μL 3 M sodium acetate and 50 μL 100% ethanol for 30 min at room temperature. Pellets were collected by centrifugation at $10,000 \times g$ for 15 min at room temperature, washed with 70% ethanol and dried under vacuum. Samples were analysed at Griffith University DNA Sequencing Facility (GUDSF) by capillary separation on a 3710xl DNA Analyser (Applied Biosystems).

2.3 Plant tissue culture media

The composition of all media used for plant tissue culture throughout this study is shown in Table 2.1.

Table 2.1: Composition of plant tissue culture (PTC) media used in this study

Media	Components
2N6 Media ¹	3% sucrose; 0.1% casein hydrolysate; 0.5 g/L proline; 0.5 g/L glutamine; 1× N6 Macronutrient solution; 1× N6 Micronutrient solution; 0.1 mM FeSO ₄ .7H ₂ O; 0.1 mM Na ₂ EDTA; 1× N6 Vitamins; 10 mg/mL 2,4-D; 0.25% phytigel, pH 5.8
1× N6 Macronutrient solution ¹	28 mM KNO ₃ ; 3.5 mM (NH ₄) ₂ SO ₄ ; 2.9 mM KH ₂ PO ₄ ; 0.75 mM MgSO ₄ .7H ₂ O; 1.13 mM CaCl ₂ .2H ₂ O
1× N6 Micronutrient solution ¹	19.7 mM MnSO ₄ .4H ₂ O; 25.9 mM H ₃ BO ₃ ; 5.2 mM ZnSO ₄ .7H ₂ O; 4.8 mM KI
1× N6 Vitamins ¹	555 μM myo-inositol; 26.6 μM glycine; 3.0 μM thiamine-HCl; 4.0 μM nicotinic acid; 2.4 μM pyridoxine-HCl
AAM media ³	AA salts and amino acids ⁵ ; 1× MS vitamins ⁴ ; 500 mg/L casein hydrolysate; 68.5 g/L sucrose; 36 g/L glucose; 100 μM acetosyringone; pH 5.2
BL ²	¹ / ₂ × MS Macronutrients ⁴ ; 1× MS Micronutrients ⁴ ; 0.4 mg/L thiamine; 0.5 mg/L nicotinic acid; 0.5 mg/L pyridoxine; 2.0 mg/L glycine; 10 mg/L ascorbic acid; 1.1 mg/L 2,4-D; 0.25 mg/L zeatin; 20 g/L sucrose; pH 5.7
BRM ²	¹ / ₁₀ × MS Macronutrients ⁴ ; ¹ / ₁₀ × MS Micronutrients ⁴ ; 1× MS vitamins ⁴ ; 0.4 g/L cysteine; 9.0 mg/L thiamine; 36 g/L glucose; 68.5 g/L sucrose; 100 μM acetosyringone; pH 5.2
CCM ²	¹ / ₁₀ × MS Macronutrients ⁴ ; ¹ / ₁₀ × MS Micronutrients ⁴ ; 1× MS vitamins ⁴ ; 0.4 g/L cysteine; 0.1 g/L glutamine; 0.1 g/L malt extract; 1.0 mg/L biotin; 10 g/L PVP; 10 mg/L ascorbic acid; 300 mg/L proline; 0.5 mg/L 2,4-D; 0.5 mg/L kinetin; 2.5 mg/L NAA; 30 g/L sucrose; 30 g/L maltose; 10 g/L glucose; 200 μM acetosyringone; 7.0 g/L agar; pH 5.3
Yeast-Mannitol (YM) ²	0.4 g/L yeast extract; 55 mM mannitol; 2.8 mM K ₂ HPO ₄ ; 800 μM MgSO ₄ .7H ₂ O; 1.7 mM NaCl; pH 7.0
YM Solid media	YM with 7 g/L bacto agar

¹ CAMBIA (2009); ² Khanna *et al.* (2004); ³ Hiei *et al.* (1994); ⁴ Murashige and Skoog (1962);

⁵ Toriyama and Hinata (1985)

Chapter 3: Isolation and characterisation of phytoene synthase sequences from banana

3.1 Introduction

Banana is a diverse group of plants with over a 1000 varieties that are morphologically variable and spread over a vast geographical area (Ammar-Khodja 2000). Four genome types (A, B, S, and T) have been identified in banana (Pillay *et al.*, 2004), and the A and B genomes are found in most cultivated bananas, such as Cavendish (AAA) and Ladyfinger (AAB). Conversely, the genotypes of few Polynesian Fe'i bananas, associated with the T-genome, have been characterised (Daniells *et al.*, 2001). However, the genotype of the Fe'i banana cultivar, Asupina, from Papua New Guinea is thought to be ATT (Sharrock and Frison, 1998). The pVA content in the edible portion of banana fruit varies among the different cultivars, and fruit colour ranges from yellow to dark orange (Englberger *et al.*, 2003b). However, the relationship between colour and genotype is not clear. Cultivars such as Asupina (Fe'i genome) and Lakatan (AA) have significantly higher pVA levels than bananas such as Cavendish (AAA; Englberger *et al.*, 2006).

The activity of the *psy* gene is a critical determinant of carotenoid accumulation as the production of phytoene leads irreversibly to carotenoid production (Cunningham and Gantt, 1998). Consequently, the *psy* gene has been the subject of extensive studies and has been isolated from various plants including the agronomically important tomato (Bartley *et al.*, 1992), maize (Palaisa *et al.*, 2003), rice (Paine *et al.*, 2005) and wheat (He *et al.*, 2008) crops. These studies support the theory that activity of this gene has a direct impact on carotenoid accumulation. As previously described (Chapter 1.4.1), the number of *psy* genes found in higher plants varies from one [e.g. *Arabidopsis* (Scolnik and Bartley, 1994); daffodil (Schledz *et al.*, 1996)] to as many as four [e.g. *Gentiana lutea* (Zhu *et al.*, 2002)]. At least two distinct *psy* genes have been identified in tomato (Bartley *et al.*, 1992; Bartley and Scolnik, 1993), tobacco (Busch *et al.*, 2002), maize (Gallagher *et al.*, 2004), rice (Gallagher *et al.*, 2004) and wheat (Cenci *et al.*, 2004; Pozniak *et al.*, 2007) and the recent characterisation of a third *psy* gene, *psy3*, (Li *et al.*, 2008a; Li *et al.*, 2008b) in maize and rice suggests that additional genes may also be present in other plants. In some cases, *psy* appears to be differentially expressed in plant tissues. In tomato, both *psy* genes function in leaf and fruit tissue (Bartley and Scolnik, 1993), although *psy1* has been predominantly associated with chromoplast bearing tissue (fruit and petals; Giorio *et al.*, 2008). Both *psy1* and *psy2*

were expressed in yellow endosperm maize, although *psy1* expression was higher (Gallagher *et al.*, 2004). Interestingly, only *psy2* was expressed in white endosperm maize mutants, although levels of both were similar in leaf tissue of both varieties. A similar expression profile was reported in leaf and endosperm of rice.

There have been numerous studies in maize investigating carotenoid accumulation in the endosperm. Sequence diversity of the *psy1* gene at the *y1* locus in yellow endosperm lines was 19 fold less than that of white endosperm lines, while sequence diversity at the leaf-associated *psy2* locus was similar for lines of both colours (Palaisa *et al.*, 2003). It was suggested that these differences were due to selection at the *y1* locus for the yellow endosperm phenotype. Recent QTL analyses have also supported the association between the *psy1* locus and phenotypic variation in carotenoid content of maize endosperm (Chander *et al.*, 2008). Similar QTL analysis in wheat also suggested that the *psy1* locus was associated with increased endosperm carotenoid content (Pozniak *et al.*, 2007). In wheat, which is triploid and consists of A and B genomes, *psy1* and *psy2* map to chromosomes 7 and 5, respectively (Cenci *et al.*, 2004; Pozniak *et al.*, 2007). Allelic variation of a co-dominant marker associated with a *psy1* gene (*psy-A1*) located on chromosome 7A in wheat accounted for between 20% and 28% of the phenotypic variance for yellow carotenoid content (He *et al.*, 2008). A subsequent study investigating the genetic effects of *psy1* allelic variation in Chinese winter wheat and spring wheat cultivars identified a third *psy-A1* allele and 5 alleles for *psy-B1* (chromosome 7B) and linked the *psy-B1* locus to yellow carotenoid content (He *et al.*, 2009). Taken together, these studies show that the *psy1* locus on chromosome 7 in both A and B genomes affects carotenoid accumulation in wheat endosperm. Whether similar associations between *psy* alleles and carotenoid accumulation occur in other plants, including banana is still unknown.

Various genes have been isolated from banana, particularly those encoding enzymes associated with fruit ripening such as polyphenol oxidases (Gooding *et al.*, 2001) and pectate lyases (Marin-Rodriguez *et al.*, 2003). However, despite the importance of this crop, there are no reports on characterisation of banana *psy* genes to date. This chapter describes the cloning, sequencing and comparative analysis of mRNA and genomic sequences of *psy* genes from selected high and low pVA banana cultivars to investigate their potential role in carotenoid accumulation.

3.2 Materials and methods

3.2.1 Plant material

Banana tissue and cultivars used in this investigation are listed in Table 3.1. The cultivars were selected based on material availability, fruit β -carotene content and genome composition. Leaf tissue for the five selected banana cultivars was obtained from tissue cultured plantlets maintained by Jen Kleidon (QUT) and originally obtained from the Queensland Department of Primary Industries (QDPI). Cavendish ripe fruit was purchased from a local supermarket and ungasped green fruit was obtained from the Brisbane Markets. A hand of Asupina fruit and field grown leaf tissue was obtained from Jeff Daniells (QDPI). One fruit was sampled at an early green stage while the remaining fruit was allowed to ripen before sampling. All plant material was stored at -80°C prior to use.

Table 3.1: Properties of banana cultivars used in the current project including the genotype, available tissue and pVA content of banana fruit, expressed as β -carotene equivalents. β -carotene equivalents^(a) were calculated as the sum of the total all-*trans* and *cis* β -carotene and half the α -carotene content (Englberger *et al.*, 2006).

Banana Cultivar	Genotype	Fruit β -carotene equivalents ($\mu\text{g/g}$) ^(a)	Available Tissue
Asupina	Fe'i	15.93	leaf / fruit
Cavendish	AAA	1.34	leaf / fruit
Ladyfinger	AAB	1.78	leaf
Lakatan	AA	3.54	leaf
Wain	Fe'i	5.32	leaf

3.2.2 Nucleic acid isolation from plant tissue

Total RNA was isolated from 5 to 10 g of leaf or fruit tissue as described in Chapter 2.1.1 and total mRNA was purified as per Chapter 2.1.2. DNA was isolated from Asupina and Cavendish leaf tissue using either the CTAB method or a DNeasy Plant Mini Kit (QIAGEN) depending on the required purity (Chapter 2.1.3).

3.2.3 Oligonucleotide primers

Oligonucleotide primers were obtained lyophilised from GeneWorks Pty Ltd and resuspended in mqH_2O to $1\ \mu\text{g}/\mu\text{L}$, or from Sigma-Proligo as a $100\ \mu\text{M}$ solution. Stock solutions were diluted to a working concentration of $10\ \mu\text{M}$ before use. The sequences of primers used in this chapter are given in Table 3.2.

Table 3.2: PCR primers used in the isolation of banana *psy* sequences

Primer name	Sequence (5'-3')	orientation ^a	Target sequence	Restriction site ^b
<i>psy-F01</i>	RTNTGGGCNATHAYGTNTGGTG	Forward	Banana <i>psy</i> gene coding region	None
<i>psy-R01</i>	RAARTYRTARTCRTTNGCYTCDAT	Reverse	Banana <i>psy</i> gene coding region	None
<i>5' Adapter-Out</i>	GCTGATGGCGATGAATGAACACTG	Forward	5'RACE adapter outer primer	None
<i>5' Adapter-In</i>	CGCGGATCCGAACACTGCGTTTGCTGGCTTTGATG	Forward	5'RACE adapter inner primer	None
<i>3' Adapter-Out</i>	GCGAGCACAGAATTAATACGACT	Reverse	3'RACE adapter outer primer	None
<i>3' Adapter-In</i>	CGCGGATCCGAATTAATACGACTCACTATAGG	Reverse	3'RACE adapter inner primer	None
<i>psy1-5' RACE-Out-01</i>	CGACTTCTTCAAGTCCATTCTCATTTCC	Reverse	Asupina and Cavendish <i>psy1</i>	None
<i>psy1-5' RACE-In-01</i>	ATTCTCATTTCC TTCGATCATGTCCCTG	Reverse	Asupina and Cavendish <i>psy1</i>	None
<i>psy2-5' RACE-Out01</i>	TTGTACCTCGATTTCCGCAGGTC	Reverse	Asupina and Cavendish <i>psy2</i>	None
<i>psy2-5' RACE-In-01</i>	TTCCGCAGGTCCATTCTCATTTCC	Reverse	Asupina and Cavendish <i>psy2</i>	None
<i>psy1-3' RACE-Out-01</i>	GCGGCAAGGTGACTGAGAAAATGG	Forward	Asupina and Cavendish <i>psy1</i>	None
<i>psy1-3' RACE-In-01</i>	AATGGAGGAGCTTCATGAAG	Forward	Asupina and Cavendish <i>psy1</i>	None
<i>psy2-3' RACE-Out01</i>	CATTAGCTCTTGCCATCGCGAATC	Forward	Asupina and Cavendish <i>psy2</i>	None
<i>psy2-3' RACE-In-01</i>	TCGCGAATCAACTCACCAACATAC	Forward	Asupina and Cavendish <i>psy2</i>	None
<i>AP1</i>	GTAATACGACTCACTATAGGGC	Forward	Genome Walking Adapter	None
<i>AP2</i>	ACTATAGGGCACGCGTGGT	forward	Genome Walking Adapter	None
<i>psy2-GW04</i>	GTACGCCGCGTCGAGTAG	Reverse	Cavendish <i>psy2a</i> gene	None
<i>psy2-GW05</i>	CAAGTAGAAAGTCTTGCCATACTC	Reverse	Cavendish <i>psy2a</i> gene	None
<i>psy2-GW06</i>	CCTCCACCATCTCCTCTTCA	Reverse	Cavendish <i>psy2a</i> gene	None
<i>psy2-GW07</i>	AACTGGCTGAACCCAGAGCTC	Reverse	Cavendish <i>psy2a</i> gene	None
<i>psy1-CR-F1</i>	ggatccATGGCGTGCCCTGTTGCTACGG	Forward	Asupina and Cavendish <i>psy1</i> exon 1	<i>BamHI</i>
<i>Apsy1-CR-R1</i>	tctagaTCATGTTTTAGCTAAACTTTGG	Reverse	Asupina <i>psy1</i> 3' Coding Region	<i>XbaI</i>
<i>Cpsy1-CR-R1</i>	tctagaTCATGTTTTTGCTAAGTTTGACTGGCTC	Reverse	Cavendish <i>psy1</i> 3' Coding Region	<i>XbaI</i>
<i>Apsy2a-CR-F1</i>	ggatccATGTCTGGCTCTATTGTTTTGG	Forward	Asupina <i>psy2a</i> 5' Coding Region	<i>BamHI</i>
<i>Apsy2a-CR-R1</i>	tctagaTTATAGTGTTCCCTGCAAATTTGG	Reverse	Asupina <i>psy2a</i> 3' Coding Region	<i>XbaI</i>
<i>Cpsy2a-CR-F1</i>	ccatggATGTCTGGCTCTGTTGTTTGGGTTGT	Forward	Cavendish <i>psy2a</i> Coding Region	<i>BamHI</i>
<i>Cpsy2a-CR-R1</i>	tctagaTTATAGTGTTCCCTGCAAATCTTGAAGG	Reverse	Cavendish <i>psy2a</i> Coding Region	<i>XbaI</i>
<i>Cpsy2b-CR-R1</i>	tctagaTTATGTCTTGTGCTCCTGTAAACC	Reverse	Cavendish <i>psy2b</i> Coding Region	<i>XbaI</i>

^(a) Primer orientation is indicated with respect to the mRNA sequence

^(b) Restriction enzyme sites are indicated in the primer sequence in lowercase

3.2.4 RT-PCR of partial *psy* coding region using degenerate primers

Partial fragments of the *psy* coding region were amplified by RT-PCR from mRNA of several banana varieties using degenerate forward and reverse primers, *psy-F01* and *psy-R01* (Table 3.2), designed to conserved regions shared by a number of plant PSYs (Table 3.3). Total mRNA (1 to 5 μ L, not quantitated as the concentration was too low for spectrophotometry) isolated from Asupina, Cavendish, Ladyfinger, Lakatan and Wain leaf tissue, and from Asupina and Cavendish fruit tissue, was used as template for RT-PCR using the Titan One Tube RT-PCR System (Roche Applied Science) as described in Chapter 2.2.1, with annealing temperature and extension time modified to 45 °C and 45 sec, respectively. The PCRs were analysed on a 1% agarose gel and the products gel purified and cloned into pGEM-T Easy (Chapter 2.2.3 to 2.2.8). Putative clones (10 to 12) were characterised by *Eco*RI restriction enzyme digestion and sequencing (Chapter 2.2.2 and 2.2.10).

Table 3.3: Conserved regions of PSY proteins used to design degenerate primers. A multiple sequence alignment was generated using Clustal W2. The regions from which degenerate primers were designed are shown in bold.

PSY source	GenBank No.	<i>psy-F01</i> region	<i>psy-R01</i> region
rice (PSY1)	AAS18307	RRRAI WAIYV WCRRT	LDE IEANDYNNF TKR
maize (PSY1)	NP_001108124.2	RRRAI WAIYV WCRRT	LDE IEANDYNNF TKR
<i>Arabidopsis</i>	NP_001031895	RRKAI WAIYV WCRRT	LDE IEANDYNNF TKR
grapefruit	AAD38051.2	RRRAI WAIYV WCRRT	LDE IEANDYNNF TKR
orange	AAF33237.1	RRRAI WAIYV WCRRT	LDE IEANDYNNF TKR
melon	CAA85775.1	RQKAI WAIYV WCRRT	LDE IEANDYDNF TKR
tomato	ABM45873	RRRAI WAIYV WCRRT	LDE IEANDYNNF TKR
capsicum	EU753855.1	RRKAI WAIYV WCRRT	LDE IEANDYNNF TKR
wolfberry	AAW88383	RRLAI WAIYV WCRRT	LDE IEANDYNNF TKR
marigold	AAM45379	RRKAI WAIYV WCRRT	LDE IEANDYNNF TKR
sunflower	AJ304825.1	RRKAI WAIYV WCRRT	LDE IEANDYNNH F'TKR
daffodil	CAA55391	RRRAI WAIYV WCRRT	LDE IEANDYNNF TKR
maize (PSY2)	NP_001108117.1	RRKAV WAIYV WCRRT	LDA IEANDYNNF TKR
carrot	BAA84763.1	RRRAV WAIYV WCRRT	LDA IEANDYDNF TKR

3.2.5 Sequence analysis

Eight to 12 clones representing the partial *psy* coding region amplified with degenerate primers were sequenced at least once in both directions using the M13 universal sequencing primers (Chapter 2.2.10). Sequencing data was analysed using the Seqman (Lasergene8) DNA analysis program, which created consensus sequences by clustering individual clone sequences into groups on the basis of an 80 – 95% minimum percentage identity. NCBI

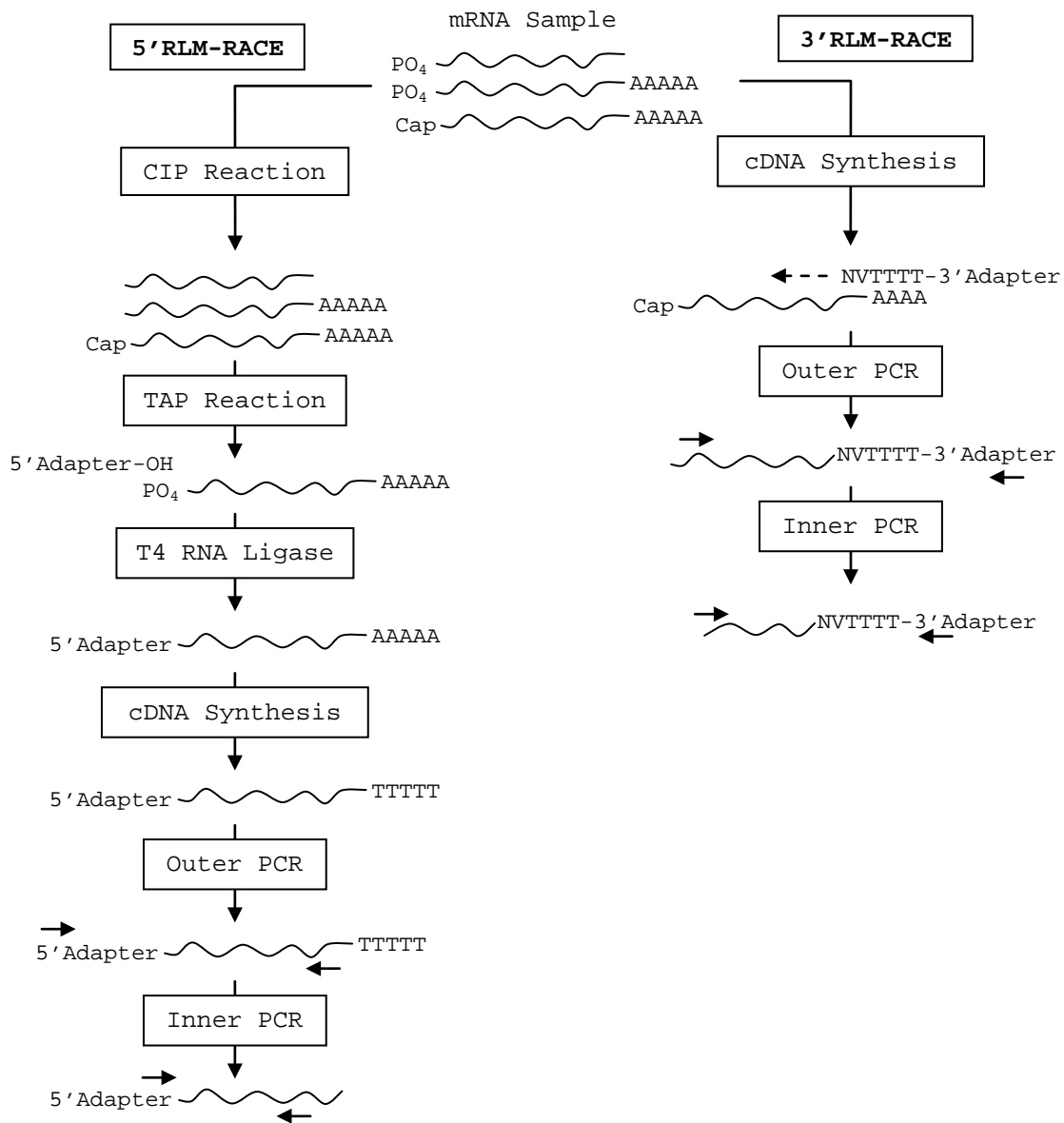
nucleotide and protein BLAST tools were used to determine the identity of the consensus sequences. Those positively identified as *psy* were further classified according to similarity with *psy* sequences from monocots such as maize and rice in GenBank. Consensus sequences not identified as *psy* were discarded. For phylogenetic analysis, partial banana *psy* consensus sequences generated by Seqman were cropped to a 600 bp region (encoding 203 amino acids). The same was done for the maize B73 *psy1* (GenBank No. AY324431) and *psy2* (GenBank No. AY325302) genes for comparison. The corresponding region of the *Dunaliella salina psy* gene (GenBank No. AY601075; 624 bp) was included as an outgroup. Clustal W2 v2.0.1.0 (Larkin *et al.*, 2007) at the European Bioinformatics Institute server (www.ebi.ac.uk) was used to produce sequence alignments and percentage identity comparisons with the default parameters. Bootstrapped phylogenetic trees were produced using Clustal X2 v2.0.6 (Larkin *et al.*, 2007).

3.2.6 Isolation of banana *psy* mRNA sequences

The FirstChoice[®] RLM-RACE kit (Ambion) was used to obtain the 5' and 3' ends of the Asupina and Cavendish *psy* transcripts from leaf and fruit mRNA. RNA Ligase Mediated Rapid Amplification of cDNA Ends (RLM-RACE) is optimised to preferentially amplify products from full length mRNA templates and this strategy is outlined in Figure 3.1a.

Templates for 5' RLM-RACE were prepared according to the manufacturer's instructions for the standard reaction. The amount of mRNA used for 5' RLM-RACE template preparation (2 to 5 μ L) was based on previous observations of the efficiency of PCR amplification using degenerate primers. The mRNA concentration could not be estimated by agarose gel electrophoresis or spectrophotometry and other methods were unavailable. The 5' RACE adapter sequence is shown in Figure 3.1b and 0.3 μ g was used in the ligation step (Figure 3.1 a). The 5' RLM-RACE adapter ligated mRNA (2 μ L) was converted into cDNA using SuperScript[®] III reverse transcriptase (RT) according to the manufacturer's instructions. The RT reaction included 100 pmol random decamers (Ambion, supplied with the RLM-RACE kit) and 40 U Protector RNase inhibitor (Roche Applied Science). SuperScript[®] III proved more efficient than the M-MLV RT provided with the RLM-RACE kit. The RT reaction was incubated at 25 °C for 5 min, followed by 50 °C for 60 min and then either used immediately or stored at -20 °C. Templates for 3' RLM-RACE were prepared from 2 μ L total mRNA using the SuperScript[®] III RT reaction described for 5' RLM-RACE adapter ligated mRNA. However, the 5' RLM-RACE adapter and random decamers were replaced by the 3' RLM-RACE adapter (Figure 3.1 b).

a)



b)

5'RLM-RACE adapter:

5'-GCUGAUGGCGAUGAAUGAACACUGCGUUUGCUGGCUUGAUGAAA-3'

3'RLM-RACE adapter:

5'-GCCGAGCACAGAATTAATACGACTCACTATAGG(T)₁₂VN-3'

Figure 3.1: Summary of 5' and 3'RLM-RACE strategies. a) Illustrates how mRNA is converted into cDNA templates used in nested PCR for 5' and 3' RLM-RACE using b) 5' and 3' adapters. Adapter primer sequences are listed in Table 3.2. Enzymes used for cDNA preparation included T4 RNA ligase, calf intestine alkaline phosphatase (CIP) and tobacco acid phosphatase (TAP).

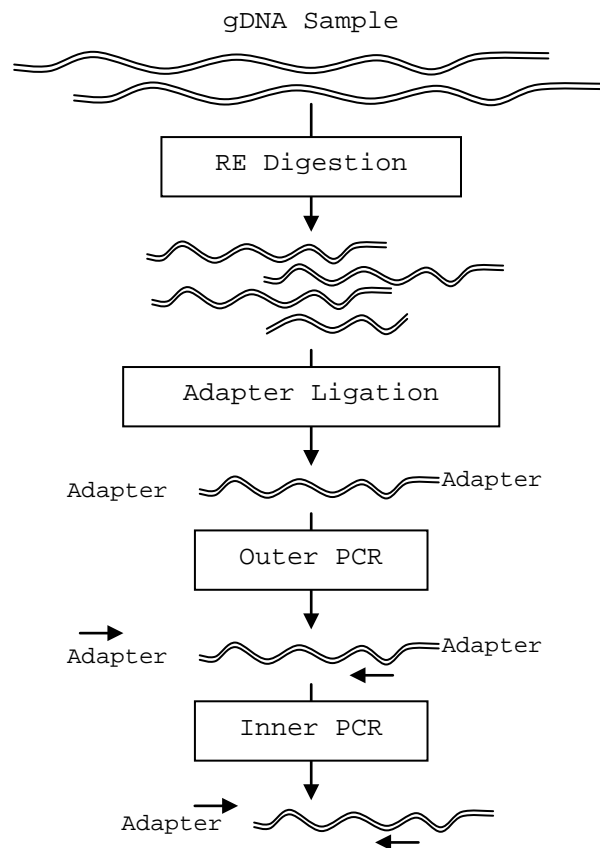
The 5' and 3' ends of *psy1* and *psy2* mRNAs were amplified from the respective cDNA templates using nested primers and the adapter primers supplied with FirstChoice[®] kit (Table 3.2), as summarised in Figure 3.1a. PCR primer pairs used to isolate the 5' regions of *psy1* mRNA were *5'Adapter-Out/psy1-5'RACE-Out-01* (outer primers) and *5'Adapter-In/psy1-5'RACE-In-01* (nested primers). The 3' ends of *psy1* mRNAs were amplified using *3'Adapter-Out/psy1-3'RACE-Out-01* (outer primers) and *3'Adapter-In/psy1-3'RACE-In-01* (nested primers). For amplification of *psy2* mRNA 5' regions, *5'Adapter-Out/psy2-5'RACE-Out-01* (outer primers) and *5'Adapter-In/psy2-5'RACE-In-01* (nested primers) were used. For amplification of *psy2* mRNA 3' ends, PCR primers *3'Adapter-Out/psy2-3'RACE-Out-01* and *3'Adapter-In/psy2-3'RACE-In-01* were used for outer and nested amplification, respectively.

Outer PCRs for both 5' and 3' RLM-RACE used 1µL cDNA template, while for inner PCRs 1 to 5 µL of the outer PCR was used, depending on template abundance. PCR amplification used Taq DNA Polymerase (Roche Applied Science) and thermal cycling conditions as described in Chapter 2.2.1 with an extension time of 2 min and annealing temperatures ranging from 55 °C to 60 °C. The PCRs were analysed on a 1% agarose gel, gel purified and cloned into pGEM-T Easy (Chapter 2.2.2 to 2.2.7). Putative clones were confirmed by *EcoRI* digestion and sequencing (Chapter 2.2.2 and 1.2.10) and analysed as per Chapter 3.2.5.

3.2.7 Isolation of partial banana *psy* sequences from gDNA

Where sequences could not be obtained using RLM-RACE, strategies were used to isolate these regions from gDNA. Genome walking libraries were constructed from Asupina and Cavendish gDNA for the isolation of coding and regulatory segments of the carotenoid biosynthesis genes (Figure 3.2a). The genome walking method was based on the GenomeWalker[™] Universal Kit (Clontech Laboratories, Inc.). Banana gDNA (0.3 to 1 µg) was digested overnight at 37 °C with selected restriction enzymes in 20 µL reactions containing 10 U restriction enzyme and corresponding 1× restriction buffer. Cavendish gDNA was digested with *EcoRI*, *EcoRV*, *NaeI*, *PvuII*, *StuI*, *StyI* and *SwaI*, while Asupina gDNA was digested with *BamHI*, *EcoRV*, *HindIII*, *PvuII* and *StuI*. Aliquots of each reaction (5 µL) were electrophoresed to verify complete digestion. Where necessary, overhanging ends were filled in by incubation with 2 U Klenow polymerase (Roche Applied Science) and 1× filling buffer (supplied with the enzyme) at 37 °C for 15 min. The remaining digest reaction (15 µL) was precipitated with 2.2 volumes of 100% ethanol for 2 hours at –20 °C.

a)



b)

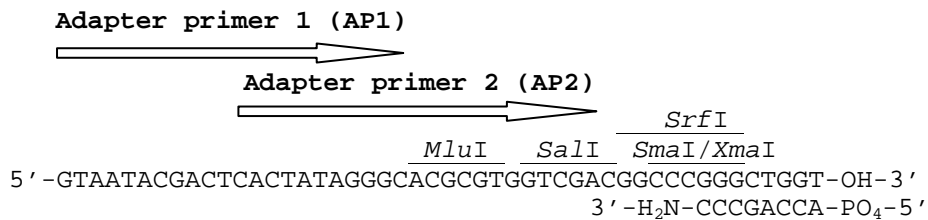


Figure 3.2: Summary of genome walking strategy a) illustrating how genomic fragments are obtained by nested PCR from genomic libraries created by ligation of the genome walking adapter to restriction enzyme digested gDNA. **b)** Structure of the genome walking adapter (adapted from GenomeWalker™ Universal Kit Manual, Clontech Laboratories, Inc.) and position of the adapter primers listed in Table 3.2.

DNA was collected by centrifugation at $10,000 \times g$ for 25 min and the pellet washed in 70% ethanol and dried under vacuum. The gDNA was resuspended in 10 mM Tris buffer (20 μ L) for 2 hours at 65 °C. The digested gDNA (10 μ L) was ligated to 5 pmol genome walking adapter (GWA, Figure 3.2b) in 20 μ L ligation reactions which also included 2 U T4 DNA ligase (Promega) and 1 \times T4 DNA ligase buffer. The reactions were incubated overnight at 16 °C before addition of 10 mM Tris (80 μ L) to create 100 μ L GWA libraries that were stored at 4 °C.

The 5' sequence of the coding region and part of the 5' UTR of the Cavendish *psy2a* gene were obtained through three stages of nested PCR with new primers designed as sequence data was generated. The first genome fragment was isolated using primer pairs *API/psy2-5'RACE-Out-01* for outer PCR followed by a nested PCR with *AP2/psy2-5'RACE-In-01*. Primer pairs *API/psy2-GW04* (outer) and *AP2/psy2-GW05* (inner) were designed to amplify the second fragment. The final Cavendish *psy2a* region was amplified with outer and inner primer pairs *API/psy2-GW06* and *AP2/psy2-GW07*, respectively. For outer PCRs, 0.5 μ L of each Cavendish genome walking library was amplified with the ExpandTM Long Template PCR system (Roche Applied Science). For nested PCR, 0.5 μ L of the outer PCR reaction was used as template. Thermal cycling conditions were as per Chapter 2.2.1 with an extension time of 2 min and annealing temperatures between 55 °C and 60 °C. PCR products were cloned and sequenced (Chapter 3.2.4), before analysis (Chapter 3.2.5).

Primer pair *Apsy2a-CR-F1/psy2-5'RACE-Out-01* was used to amplify part of the 5' end of the *psy2b* coding region from Asupina and Cavendish gDNA (0.3 to 1 μ g) using Taq DNA Polymerase (Roche Applied Science, Chapter 2.2.1) and with annealing temperature and extension times of 48 °C and 1 min, respectively. PCR products were cloned and sequenced as per Chapter 3.2.4.

3.2.8 Amplification of the complete *psy* coding region from mRNA and gDNA

Fragments representing the complete coding region of the Asupina and Cavendish *psy* genes were amplified from 1 μ L leaf mRNA (*psy1*) or fruit mRNA (*psy2a* and *psy2b*) using Titan One-Tube RT-PCR (Roche Applied Science; Chapter 2.2.1) with an annealing temperature and extension time of 50 °C and 1 min, respectively. Primer sets used included *psy1-CR-F1/Apsy1-CR-R1* [Asupina *psy1*], *psy1-CR-F1/Cpsy1-CR-R1* [Cavendish *psy1*], *Apsy2a-CR-F1/Apsy2a-CR-R1* [Asupina *psy2a*], *Cpsy2a-CR-F1/Cpsy2a-CR-R1* [Cavendish *psy2a*] and *Apsy2a-CR-F1/Cpsy2b-CR-R1* [Asupina and Cavendish *psy2b*]. The same regions, including introns, were also amplified with the same primer sets from Asupina and Cavendish gDNA

(300 to 500 ng), prepared using the QIAGEN DNeasy™ kit (Chapter 2.1.3). The Asupina *psy2a* genomic coding region was amplified using the GoTaq Green® system (Chapter 2.2.1), while all others were obtained using Expand™ Long Template PCR (Chapter 2.2.1). The annealing temperature and extension times were modified to 50 °C and 2 min, respectively. The resulting PCR products were cloned and analysed as per Chapter 3.2.6.

3.3 Results

3.3.1 Initial characterisation of banana *psy*

3.3.1.1 Isolation of partial banana *psy* sequences

Degenerate primers *psy-F01* and *psy-R01* were designed to conserved regions identified in a sequence alignment of plant PSY proteins (Table 3.3) and used to amplify a 680 bp fragment of the banana *psy* coding region. Initially, RT-PCR conditions were optimised using capsicum fruit total RNA (results not shown) as this *psy* gene was known to include the conserved primer sequences. From these results the decision was made to use mRNA as the template for isolating banana *psy* sequences, instead of total RNA, to enhance the efficiency of degenerate primer RT-PCR and to reduce the potential for gDNA contamination. The primers were used to amplify a fragment of the expected size from several banana cultivars including Asupina, Cavendish, Ladyfinger, Lakatan and Wain (Table 3.1), with represented a range of pVA content. A band of approximately 680 bp was obtained following RT-PCR from leaf or fruit mRNA of all cultivars. Figure 3.3 (band #1) shows a typical result. Smaller, faint bands (#2) were sometimes observed but were not characterised.

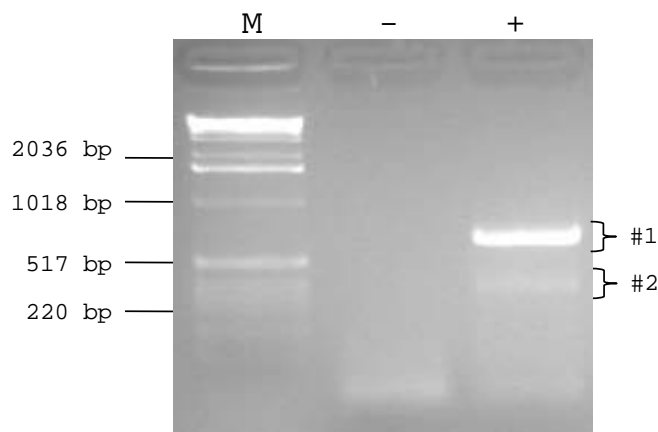


Figure 3.3: Representative agarose gel showing amplification of partial *psy* coding region using degenerate primers. (+) PCR product obtained from Cavendish leaf mRNA; (-) negative PCR control; (M) DNA Molecular weight marker X (Roche Applied Science). Samples were electrophoresed in a 2% agarose gel for 25 min. The positions of the expected 680 bp *psy* fragment (#1) and unknown RT-PCR product (#2) are indicated.

The first fragments to be cloned and sequenced were amplified from leaf mRNA of Ladyfinger (AAB). Nine sequences were confirmed to be *psy* based on BLASTn analysis. Of these, five were similar to *psy1* sequences from plants such as daffodil (79%) and rice (78%)

and were tentatively called *psy1*, while two clones were similar to *psy2* sequences such as rice *psy2* (78%) and maize *psy2* (76%) and were tentatively called *psy2* (Table 3.4). Translation of these sequences confirmed that they contained an uninterrupted coding region. The remaining two clones, although identified as *psy1*, each included a single putative intron of 79 and 97 bp, respectively, which appeared to interrupt the coding region at the same relative position. The nucleotide sequences of the nine clones were then used to generate *psy1* and *psy2* consensus sequences, which were approximately 75% identical to each other.

Eight clones were isolated following RT-PCR from leaf mRNA of the diploid cultivar Lakatan (AA) and of these, four represented a single *psy1* consensus and four represented a single *psy2* consensus sequence (Table 3.4). A total of 17 clones were obtained following RT-PCR with *psy* degenerate primers from mRNA isolated from fruit and leaf of the triploid cultivar Cavendish (AAA; Table 3.4). Of the seven clones obtained from leaf, three were identified as *psy1* and four as *psy2*, while all 10 clones from Cavendish fruit mRNA corresponded to *psy2*. Interestingly, there were two different sequence subgroups within the *psy2* clones from both leaf and fruit which were subsequently called *psy2a* (most abundant) and *psy2b* (Table 3.4). The *psy2a* and *psy2b* consensus sequences were 85% identical. One other Cavendish *psy* clone obtained from leaf mRNA, was identified as *psy2* based on BLASTn analysis, but did not closely match either *psy2a* or *psy2b*. This sequence, called *psy2c*, was 80% identical to *psy2b* and 87% identical to both *psy1* and *psy2a*. Further analysis suggested that *psy2c* was a chimera whose 5' and 3' halves were *psy1* and *psy2a*, respectively.

Asupina and Wain cultivars both have Fe'i genotypes. A total of 19 clones were obtained from Asupina leaf (6 clones) and fruit (13 clones) mRNA. Of the clones isolated from leaf mRNA, one sequence was identified as *psy1* and the other five as *psy2*. One of the *psy2* clones had a putative 92 bp intron at a position closer to the 3' end than previously identified in the Ladyfinger clones. All 13 clones isolated from fruit mRNA were *psy2* and represented a single consensus. Only leaf tissue of the Wain banana cultivar was available. Eleven clones were obtained, six corresponding to *psy1* and five to *psy2*. However, two of the *psy1* clones contained a 79 bp intron located at the same relative position as those found in Ladyfinger *psy1* clones.

Cavendish was the only banana cultivar from which more than one variant of the *psy2* gene was identified by degenerate primer RT-PCR. Overall, the region of the *psy1* and *psy2* coding region represented in these clones for the five cultivars were approximately 75% identical. These relationships were further investigated using phylogenetic analysis.

Table 3.4: Partial *psy* clones obtained using degenerate primer RT-PCR. Summary of the number of *psy1* and *psy2* RT-PCR clones obtained from each banana cultivar and tissue. Tissues that were not available (NA) or not tested (NT) by RT-PCR are also indicated.

Cultivar	Gene	Tissue Source of Degenerate Primer RT-PCR clones		
		Leaf	Fruit	Total
<i>Asupina</i>	<i>psy1</i>	1	0	1
<i>Asupina</i>	<i>psy2</i>	5	13	18
<i>Cavendish</i>	<i>psy1</i>	3	0	3
<i>Cavendish</i>	<i>psy2a</i>	2	7	9
<i>Cavendish</i>	<i>psy2b</i>	1	3	4
<i>Cavendish</i>	<i>psy2c</i>	1	0	1
<i>Ladyfinger</i>	<i>psy1</i>	7	NT ^a	7
<i>Ladyfinger</i>	<i>psy2</i>	2	NT ^a	2
<i>Lakatan</i>	<i>psy1</i>	4	NA	4
<i>Lakatan</i>	<i>psy2</i>	4	NA	4
<i>Wain</i>	<i>psy1</i>	6	NA	6
<i>Wain</i>	<i>psy2</i>	5	NA	5

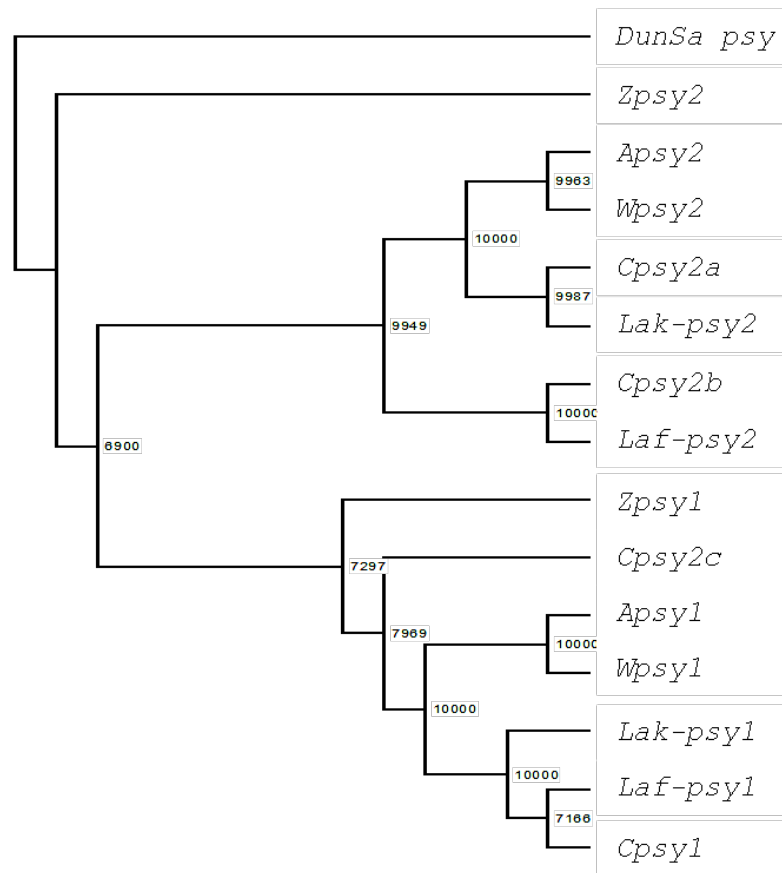
^a as fruit was not available for some cultivars. *Asupina* and *Cavendish* were selected as representative high and low pVA varieties, respectively, for fruit analysis. Therefore *Ladyfinger* fruit was not included in the study.

3.3.1.2 Phylogenetic analysis of partial banana *psy* sequences

Phylogenetic analysis was used to investigate the relationships between the partial banana *psy1* and *psy2* sequences from different cultivars and to assess the significance of factors such as genotype. Equivalent regions of maize *psy1* and *psy2* were included for comparison of the banana sequences to other monocots and *psy* from *Dunaliella salina*, a green algae, was included as an outgroup (Figure 3.4).

The *psy1* and *psy2* sequences diverged early from a single main branch, when compared to *D. salina psy*. The main *psy1* clade included all five banana cultivars and was further divided into two major subgroups. One subgroup included *Asupina* and *Wain psy1* (both Fe'i-genomes), which were 99% identical. The second *psy1* clade included sequences from the *Cavendish*, *Ladyfinger* and *Lakatan* banana varieties, all of which have the A-genome,

a)



b)

Gene	#	1	2	3	4	5	6	7	8	9	10	11	12	13	14	15
<i>Apsy1</i>	1	■	74	97	74	74	86	99	74	98	74	97	74	77	74	68
<i>Apsy2</i>	2	74	■	74	98	85	86	73	99	75	97	74	84	73	76	64
<i>Cpsy1</i>	3	97	74	■	74	74	87	96	74	99	74	99	74	77	74	67
<i>Cpsy2a</i>	4	74	98	74	■	85	87	73	97	74	99	74	84	72	75	64
<i>Cpsy2b</i>	5	74	85	74	85	■	80	73	84	74	84	74	98	73	76	59
<i>Cpsy2c</i>	6	86	86	87	87	80	■	85	86	87	87	87	79	75	74	66
<i>Wpsy1</i>	7	99	73	96	73	73	85	■	73	97	73	97	73	76	73	68
<i>Wpsy2</i>	8	74	99	74	97	84	86	73	■	75	97	74	84	73	75	64
<i>Lak-psy1</i>	9	98	75	99	74	74	87	97	75	■	74	99	74	77	74	68
<i>Lak-psy2</i>	10	74	97	74	99	84	87	73	97	74	■	74	84	72	74	64
<i>Laf-psy1</i>	11	97	74	99	74	74	87	97	74	99	74	■	74	77	74	67
<i>Laf-psy2</i>	12	74	84	74	84	98	79	73	84	74	84	74	■	73	76	60
<i>Zpsy1</i>	13	77	73	77	72	73	75	76	73	77	72	77	73	■	72	65
<i>Zpsy2</i>	14	74	76	74	75	76	74	73	75	74	74	74	76	72	■	64
<i>DunSa-psy</i>	15	68	64	67	64	59	66	68	64	68	64	67	60	65	64	■

Figure 3.4: Phylogenetic analysis of the banana *psy* partial coding region. a) Neighbour Joining tree illustrating the relationships between the nucleotide sequences of the various *psy1* and *psy2* sequences. b) Percentage identity matrix comparing levels of nucleotide sequence similarity. The numbers (#) correspond to each of the 15 partial sequences in the analysis, Asupina *psy1* (*Apsy1*) and *psy2* (*Apsy2*); Cavendish *psy1* (*Cpsy1*), *psy2a* (*Cpsy2a*), *psy2b* (*Cpsy2b*) and *psy2c* (*Cpsy2c*); Ladyfinger *psy1* (*Laf-psy1*) and *psy2* (*Laf-psy2*); Lakatan *psy1* (*Lak-psy1*) and *psy2* (*Lak-psy2*); Wain *psy1* (*Wpsy1*) and *psy2* (*Wpsy2*); maize *psy1* (*Zpsy1*) and *psy2* (*Zpsy2*); *D. salina psy* (*DunSa-psy*). The tree was bootstrapped to 10,000 trials and the values are shown at each node of the rectangular cladogram.

although Ladyfinger also has a B-genome component. These sequences were also 99% identical, although the Cavendish and Ladyfinger *psy1* sequences grouped together with Lakatan *psy1* on a separate branch. All banana *psy1* sequences were between 96% and 98% identical. Interestingly, Cavendish *psy2c* formed a separate branch adjacent to the banana *psy1* clade, with 85 to 87% similarity with these genes. The banana *psy1* sequences were only 76 to 77% identical to maize *psy1*, which was in a separate clade.

The relationships between the six banana *psy2* sequences were more complex than those seen for the *psy1* group, and were divided into three clades (Figure 3.4a). The *psy2* sequences from the Fe'i-type Asupina and Wain cultivars grouped together with 99% identity. The Cavendish *psy2a* and Lakatan *psy2* sequences paired in an adjacent group with 99% identity. The close relationship between these four sequences suggests that they are equivalent to *psy2a*. Interestingly, the Cavendish *psy2b* and Ladyfinger *psy2* sequences grouped together in a separate clade with 98% identity. This suggests that *psy2b* transcripts are expressed, at least in related cultivars. Maize *psy2* was in a separate clade from all the other banana *psy1* and *psy2* sequences, sharing 74 to 76% sequence identity with the banana *psy2* sequences and only 67 to 68% identity with the banana *psy1* sequences.

Within the Cavendish *psy* gene family, *psy1* was 74% identical to both *psy2a* and *psy2b*, while *psy2a* and *psy2b* were 85% identical to each other. Comparatively, Cavendish *psy2c* was 87% identical to both *psy1* and *psy2a* but was only 80% compared to *psy2b*. The similarity between the *psy1* and *psy2* sequences of the Asupina, Lakatan, Ladyfinger and Wain cultivars ranged between 73 and 75%. The maize *psy1* and *psy2* sequence were 72% identical.

3.3.2 Isolation of complete *psy* mRNA sequences

Asupina and Cavendish were selected as representative high and low pVA cultivars, respectively, for isolation of the complete *psy1* and *psy2* mRNA sequences and subsequent comparison of enzyme activity. This choice was based on availability of both leaf and fruit tissue for analysis (Table 3.1). The remaining 5' and 3' sequences of the coding region and the respective 5' and 3' UTRs were obtained by RLM-RACE using specific primers derived from the partial *psy* sequences. Primers were designed to ensure that there was significant overlap between new sequences and existing partial sequences so that they could be verified as belonging to the same gene. The 5' RLM-RACE nested gene-specific primers were designed to amplify RT-PCR products with a 218 bp overlap with the 5' end of the degenerate primer clones. Similarly, 3' RLM-RACE primers were designed to produce PCR

products with an overlap of 167 bp with the 3' end of degenerate primer clones. Following analysis of the 5' and 3' RLM-RACE sequences, the complete coding region for each of the Asupina and Cavendish *psy* mRNAs was isolated using RT-PCR with specific primers.

3.3.2.1 Isolation of *psy1* mRNA sequences

Leaf was selected as the target tissue for isolation of the complete *psy1* transcript as this was the source of all partial *psy1* clones obtained earlier (Table 3.3). RLM-RACE to amplify the 5' end of the *psy1* transcript from Cavendish leaf cDNA gave a single product of approximately 1000 bp. Five putative clones of this fragment were selected and the inserts sequenced. The fragments were either 1020 or 1050 bp and the sequences formed a single *psy1* consensus, which on further analysis suggested the presence of two transcription start sites. RLM-RACE to amplify the 3' end of the *psy1* transcript produced a broad product of approximately 400 to 500 bp, from which a total of 17 clones of varying lengths were obtained. All clones appeared to be polyadenylated as they ended in strings of at least eight adenosine nucleotides terminated by the 3' RLM-RACE adapter sequence. Of these, 12 clones overlapped with the partial *psy1* sequences but varied in length with one clone each of 328, 407 and 457 bp, three clones of 420 bp and six clones of 475 bp. This sequence group also included another two clones that appeared to have a single 74 bp intron in the 3' coding region and a 3' UTR that was 50 bp longer than those found in the other *psy1* 3' RACE clones. These clones were 597 bp in length, making them the longest of the Cavendish *psy* 3' RACE clones. These results suggest the existence of at least six polyadenylation sites in *psy1*. One of the clones was 451 bp and appeared to be a *psy2* clone as it was homologous to the 3' end of the Cavendish *psy2b* partial coding region and will be discussed later.

Collectively, the Cavendish *psy1* RLM-RACE data, in combination with the partial sequences, suggest a maximum putative transcript size of 1854 bp with transcription initiation and polyadenylation possible at two and six sites, respectively (Figure. 3.5b), corresponding to a 5' UTR of either 255 or 322 bp and a 3' UTR ranging from 110 to 239 bp. The putative Cavendish *psy1* coding region is 1293 bp, encoding a polypeptide of 430 amino acids. A fragment representing the complete coding region was amplified from leaf mRNA using coding region-specific primers, yielding a product of approximately 1300 bp. Five clones were selected and sequenced and four of these were identical to the putative *psy1* coding region. One of these four clones, *Cpsy1* coding region clone Q4, was selected for functional analysis (Chapter 4). The remaining clone had the same putative 74 bp intron found in the longest *psy1* 3' RLM-RACE clone.

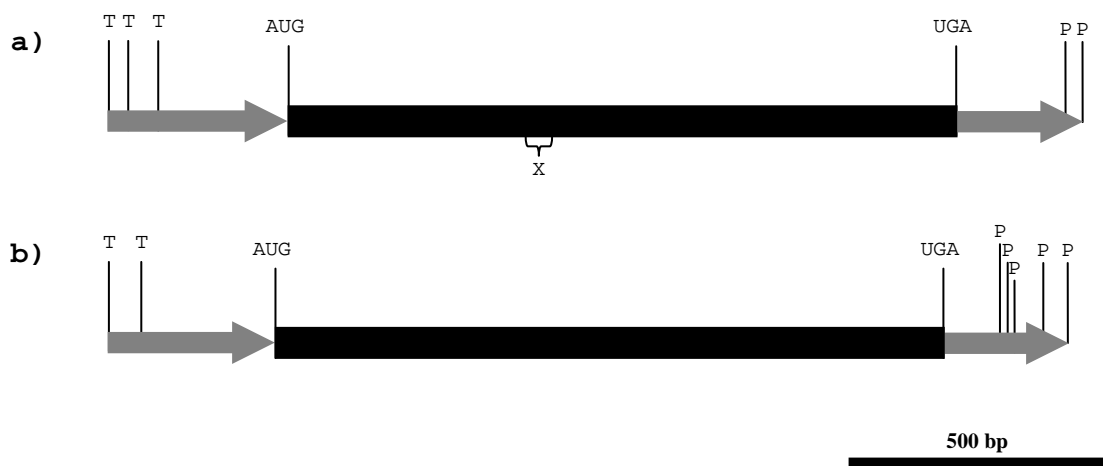


Figure 3.5: Putative structure of *psyI* mRNA of the **a)** Asupina and **b)** Cavendish banana varieties showing the coding region (black rectangle) marked with the start (AUG) and stop (UGA) codons. Putative transcription initiation (T) and polyadenylation (P) sites are marked on the 5' and 3' UTRs (grey arrows), respectively. The position of a 51 bp deletion observed in one of the Asupina *psyI* clones is marked (X).

One pair of Cavendish leaf 3' RLM-RACE clones was distinct from the other sequences, although BLASTn analysis suggested that they were *psyI*. These sequences, subsequently called *psyX*, did not match the *psyI* partial sequence consensus and could not be grouped into existing *psy* categories. This pair of sequences was 542 and 582 bp and identical to each other except that the longer clone had a putative 40 bp intron located in the 3' coding region at the same relative position as other *psyI* 3' RACE intron-bearing clones. Alignment of the *psyX* 3' RACE clones with the Cavendish *psyI* 3' RACE clone with an intron found these sequences to be 48% identical. However, translation of these clones revealed that the stop codon was missing from the expected position compared to *psyI* and a premature stop codon was found 4 bp after the putative intron.

A single product (~1000 bp), representing the 5' UTR and partial coding region of *psyI*, was obtained following 5' RLM-RACE from Asupina leaf cDNA. Five clones were sequenced and products of three different sizes were obtained (850 bp, 920 bp and 950 bp). The clones formed a single consensus that differed at the 5' terminus, suggesting multiple transcription start sites, giving putative 5' UTRs of 250 bp, 307 bp and 348 bp. Following 3' RLM-RACE, two clones were sequenced and found to be approximately 490 bp and 520 bp. As with the Cavendish 3'UTR clones, these sequences were polyadenylated. This suggests that Asupina *psyI* has at least two polyadenylation sites, producing transcripts with 3' UTRs of 210 and 243 bp. The combined 5' and 3' RACE data indicated that Asupina *psyI* mRNA transcripts may be up to 1890 bp (Figure 3.5a). Amplification of the complete Asupina *psyI* coding region with specific primers produced a single band of approximately 1300 bp.

Sequence analysis of three clones confirmed that the coding region was 1293 bp long, as previously found in Cavendish *psy1*. *Apsy1* coding region clone 13 was selected for functional analysis (Chapter 4). Interestingly, the coding region of a fourth clone was only 1242 bp due to a nucleotide sequence deletion from position 464 to 514 in the coding region (Figure 3.5a). The sequence following the deletion was still in frame and capable of producing a polypeptide of 413 amino acids, suggesting that this could be an Asupina *psy1* isoform.

3.3.2.2 Isolation of *psy2* coding regions

Fruit tissue was chosen for cloning and sequencing of the complete Asupina *psy2* transcript as all partial *psy2* clones were obtained from this tissue. All primers used to isolate the 5' and 3' ends of the Asupina and Cavendish *psy2* mRNAs were also capable of amplifying *psy2b* due to the high sequence similarity between the Cavendish *psy2a* and *psy2b* partial sequences. However, amplification of the complete coding region of each *psy* sequence used gene-specific primers.

Asupina *psy2a*: Amplification of the 5' end of Asupina *psy2* mRNA by RLM-RACE gave a single product of ~1000 bp. Two clones were sequenced and both were found to be 876 bp, which indicated that the 5' UTR was 276 bp. 3' RLM-RACE produced a broad band of 400 to 500 bp from Asupina fruit and six clones were selected for analysis. Five clones overlapped with the Asupina partial *psy2* coding region consensus; two clones were 305 bp and 342 bp, while three clones were 365 bp in length. This suggests that Asupina *psy2* has at least three polyadenylation sites and a 3'UTR of 30, 67 or 90 bp. Interestingly, the sixth clone corresponded to *psy2b* and is discussed later. This was the first indication that Fe'i-genome cultivars also expressed *psy2b* transcripts. Consequently, all *psy2* sequences were subsequently designated *psy2a* or *psy2b*, depending on their phylogenetic relationship to the Cavendish *psy2* sequences. Overall, it appeared that Asupina *psy2a* had a maximum transcript length of 1551 bp, with one transcription start site and three polyadenylation sites (Figure 3.6a). The Asupina *psy2a* coding region was 1185 bp, encoding a polypeptide of 394 amino acids. Using gene-specific primers, a product representing the full Asupina *psy2a* coding region was amplified. Five clones were analysed and all matched the expected consensus. *Apsy2a* coding region clone 2 was selected for functional analysis (Chapter 4).

Cavendish *psy2a*: Ripe fruit mRNA was used to isolate the complete Cavendish *psy2a* transcript, as a significant number of partial *psy2* clones had been obtained from this tissue. The position of the primers used for 5' RLM-RACE and results from Asupina *psy2a*,

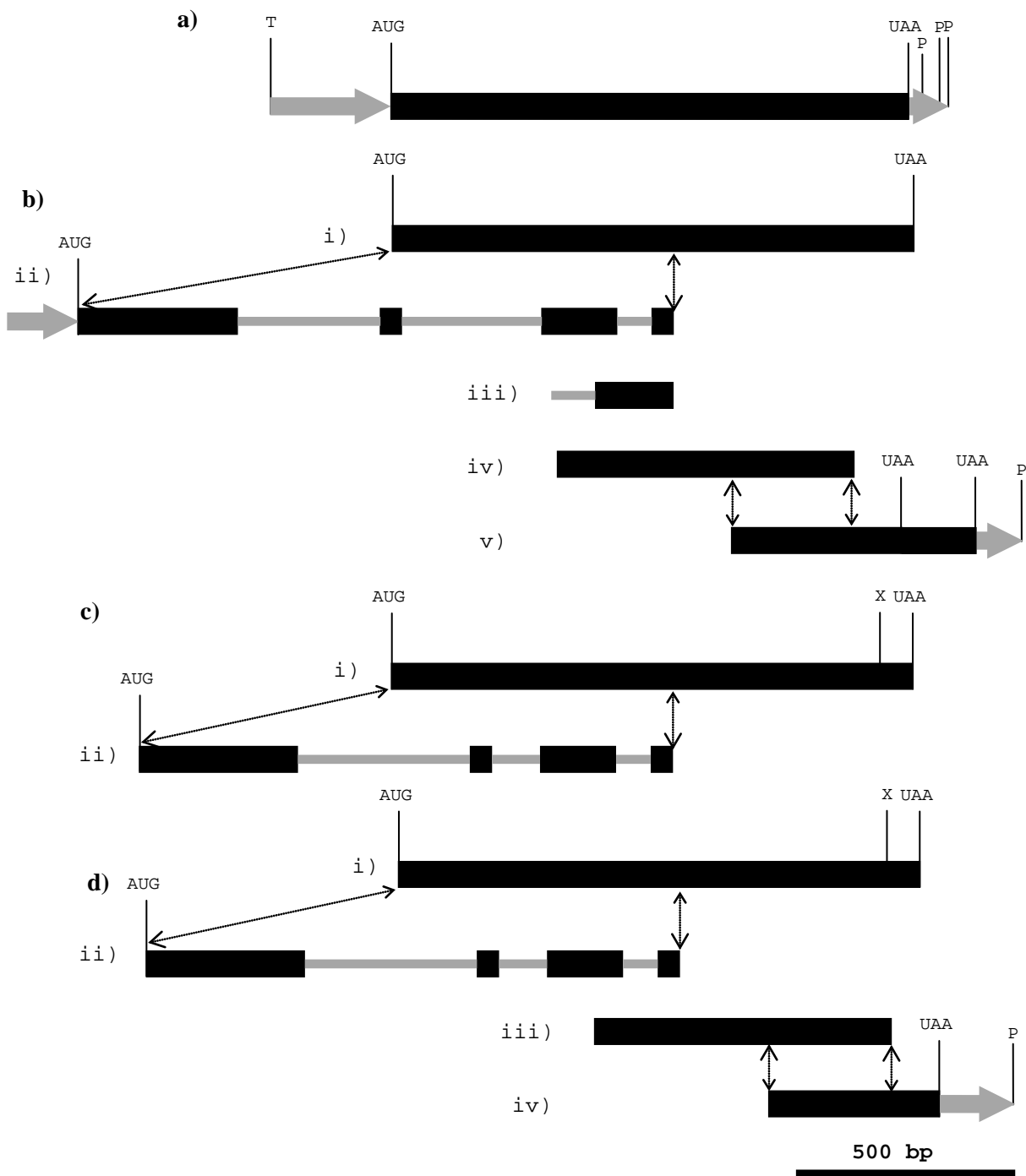


Figure 3.6: Summary of *psy2a* and *psy2b* sequences isolated from *Asupina* and *Cavendish* showing a) the putative *Apsy2a* mRNA transcript and b) the isolation process of *Cpsy2a* representing i) the complete coding region, ii) 5' genomic region obtained by genome walking, iii) 5'RLM-RACE fragment, iv) original partial coding region obtained by degenerate primer RT-PCR, and v) 3'RLM-RACE clone. c) Isolation of *Apsy2b* fragments including i) the complete coding region and ii) the 5' genomic region obtained by standard PCR. d) Isolation of *Cpsy2b* showing i) the complete coding region, ii) the 5' genomic region, iii) partial coding region and iv) 3'RLM-RACE. The position of the start (AUG) and stop (UAA or UGA) codons on the coding region (black rectangle) are shown. Putative transcription initiation (T) and polyadenylation (P) sites are marked on the 5' and 3' UTRs (grey arrows), respectively, and the positions of introns (thin grey lines) are indicated on the genomic sequences. The position of premature polyadenylation (X) in *Cavendish psy2b* clones [d i)] is also indicated. Overlapping sequences are denoted by dotted arrows as observed between b i) and ii) for example.

suggested that a 1000 bp product would be obtained from Cavendish mRNA, representing a 280 bp 5' UTR and 720 bp of the coding region. However, a product of approximately 300 bp was consistently amplified (Figure 3.7; band #2) despite extensive modification of cDNA synthesis and PCR amplification conditions. Cloning and sequencing of this product confirmed that it was 234 bp and, when compared to Asupina *psy2a*, consisted of 94 bp that matched the Cavendish *psy2a* coding region preceded by 140 bp of what appeared to be intron sequence (Figure 3.6b iii).

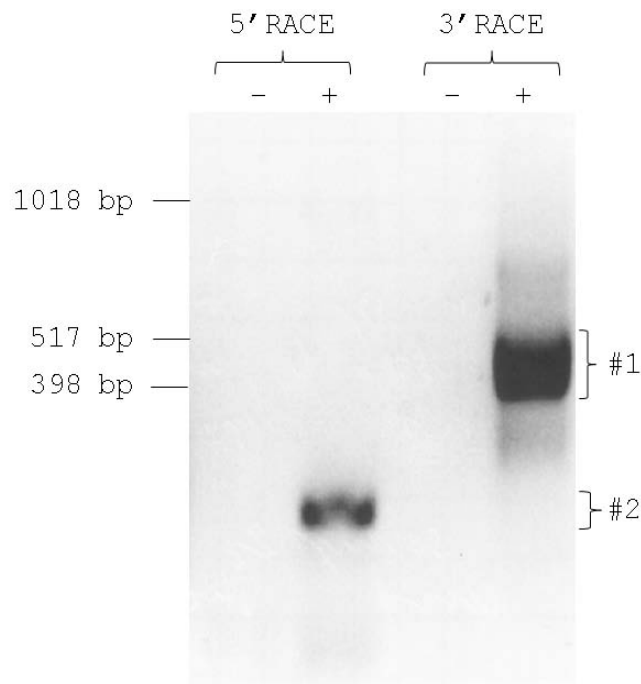


Figure 3.7: Agarose gel electrophoresis of *psy2a* 5' and 3' RLM-RACE products from Cavendish fruit mRNA (+) compared to negative controls (-) imaged in reverse contrast. The positions of the 5' (#2) and 3' (#1) RACE bands are marked.

Amplification of the Cavendish *psy2a* 5' coding region was also attempted using a forward primer designed to the start of the Asupina *psy2a* coding region (*Apsy2a-CR-F1*) in combination with *psy2-5'RACE-Out01*, an outer 5' RLM-RACE primer capable of amplifying both Asupina and Cavendish *psy2*. The aim was to take advantage of the high conservation among the *psy2* sequences; however, no Cavendish *psy2a* products were amplified. Consequently, genome walking was used to obtain the 5' region of the Cavendish *psy2a* coding region in three stages of nested PCR. The first stage gave a 1100 bp band from which six clones were analysed. The second and third stages each produced bands of approximately 300 bp, from which three and two clones were analysed, respectively. Together, the sequence of these 11 clones overlapped to produce a 1600 bp consensus consisting of a 246 bp upstream sequence similar to the Asupina *psy2a* 5' UTR, as well as

the first three exons (367, 51 and 173bp) and three introns (328, 320 and 79 bp) of the Cavendish *psy2a* coding region (Figure 3.6b ii). This sequence was confirmed to be Cavendish *psy2a* as the last 45 bp, which appeared to be the start of the fourth exon, was identical to existing Cavendish *psy2a* partial sequence data.

RLM-RACE to amplify the 3' end of the Cavendish *psy2a* transcript produced a band of approximately 400 to 500 bp (Figure 3.7; band #1) similar to that obtained for *psy1* and Asupina *psy2a*. Of the eight clones obtained, seven were *psy2b* and will be considered later. The eighth clone was approximately 640 bp and represented 362 bp of the 3' *psy2a* coding region and a 278 bp 3' UTR (Figure 3.8a). The Cavendish *psy2a* sequence was compared with the longest Asupina *psy2a* 3' RACE clone and it was found that the last 107 bp of the Cavendish *psy2a* clone was 97% identical to the Asupina *psy2a* 3' UTR. Interestingly, the first 172 bp of the Cavendish *psy2a* 3' UTR appeared to be a duplication of the 3' end of the coding region (Figure 3.8a). The true size of the Cavendish *psy2a* mRNA transcript could not be estimated due to the failure of 5' and 3' RLM-RACE, although comparison of the 5' upstream sequence obtained by genome walking with the Asupina *psy2a* 5' UTR suggests that this region may be of similar size in both genes. As the major aim of this work was to clone the full coding region, no further 5' and 3' RLM-RACE was undertaken for Cavendish *psy2a*. The complete Cavendish *psy2a* coding region was amplified from fruit mRNA using primers based on existing 5' genome walking and 3' RLM-RACE sequence and a fragment of ~1200 bp was obtained. Of the five clones analysed, clones 1 to 3 had inserts of 1194 bp, encoding a polypeptide of 397 amino acids, similar in size to Asupina *psy2a*. Clone 4 was 1160 bp, encoding a truncated protein of 115 amino acids, due to a 34 bp deletion that resulted in a frame shift. The fifth clone was 1102 bp, encoding a truncated polypeptide of 256 amino acids due to a 92 bp deletion that caused a frame shift. These clones may represent abnormal transcripts as neither sequence was predicted to produce a functional protein. *Cpsy2a* coding region clone 1 was selected for functional analysis (Chapter 4).

Asupina and Cavendish *psy2b*: Asupina or Cavendish *psy2b* clones were not obtained from 5' RLM-RACE of either cultivar despite the capacity for these primers to amplify both *psy2a* and *psy2b*. However, the 5' coding region of these genes was obtained from gDNA using the *Apsy2a-CR-F1* and *psy2-5'RACE-Out01* primers, producing a band of ~1200 bp. Clones from Asupina (one clone) and Cavendish (three clones) were sequenced and this region was shown to be similar in structure to that of Cavendish *psy2a*, consisting of the first 3 exons (364, 51 and 173 bp) and 3 introns (390, 110 and 78 bp) of the Asupina and Cavendish *psy2b* coding region. The final 40 to 60 bp of the partial fourth exon was very similar to existing Cavendish *psy2b* partial sequence data (Figure 3.6c ii & d ii). The only *psy2b* cDNA clone

a)

aacatactcagggatggttgagaggactccaggagggggagagtgtaccttctcaagat
 N I L R D V G E D S R R G R V Y L P Q D
gaactggcccacgctggtctgtcagatgatgacgtcttcgaagggaggggtgacagacaaa
 E L A H A G L S D D D V F E G R V T D K
tggcggaccttcatgaaggggtcaaattacgcgagcgaggatggtcttcgacgagggccgag
 W R T F M K G Q I T R A R M F F D E A E
aagggcataatatgagctgaactcagccagcagatggccgggttttggttcggttgctgctg
 K G I Y E L N S A S R W P V L A S L L L
tatcggcagattctggatgccattgaggcaaacgactacaacaacttcaccaagcgtgca
 Y R Q I L D A I E A N D Y N N F T K R A
tacgtagggaaagcaagaaactggcttcggttacccatagcatatgccaaggcagtaatt
 Y V G K A K K L A S L P I A Y A K A V I
gtaggcccgctcaaaatttgcaggaacactataagtataatcggttgctgctgtaccggcag
 V G P S K F A G T L - V - S L L L Y R Q
attttgatgccattgaagcaaatgactacagcaacttcaccaagcgtgcatacgtaggg
 I L D A I E A N D Y S N F T K R A Y V G
aaagcaagaaactggcttcggttacccatagcatatgccaaggcagtaattgtaggccg
 K A K K L A S L P I A Y A K A V I V G P
tcaaaatttgcaggaacactataagtataatcttcatttgcttctcattgcaatcgcca
 S K F A G T L - V -
 aatgtaagtttaagttgattcggttctctcactcgggggcttatatatttggtaacttca
 taatttgttac

b)

<i>Cpsy2b-3'</i>	AATGGAGGAGCTTCATGAAGGGACAGATTAGGCGAGCCAGGATGTTCTTTGAGG-AGGCT
<i>Cpsy2b-T</i>	AATGGAGGAGCTTCATGAAGGGACAGATTAGGCGAGCCAGGATGTTCTTTGAGG-AGGCT
<i>Apsy2b-T</i>	AATGGAGGAGCTTCATGAAGGGACAGATTAGGCGAGCCAGGATGTTCTTTGGGGGAGGCT ***** *****
<i>Cpsy2b-3'</i>	GAGAAGGGCATATACGAGCTGAATTCAGCTAGCAGATGGCCGGTTTTGGCTTCTCTGCTG
<i>Cpsy2b-T</i>	GAGAAGGGCATATACGAGCTGAATTCAGCTAGCAGATGGCCGGTTTTGGCTTCTCTGCTG
<i>Apsy2b-T</i>	GAGAAGGGCATATACGAGCTGAATTCAGCTAGCAGATGGCCGGTTTTGGCTTCTCTGCTG ***** *****
<i>Cpsy2b-3'</i>	CTATATCGATAGATCCTT-GACGCCATCGAAGAAAATGACTACAACAACCTTCACGAGGCG
<i>Cpsy2b-T</i>	CTATATCGACAGATCCTT-GACGCCATCGAAGCAAATGACTACAACAACCTTCACAAGGCG
<i>Apsy2b-T</i>	CTATATCGACAGATCCTTTGACGCCATCGAAGCAAATGACTACAACAACCTTCACAGGCGT *****#*****^***** * * * * *
<i>Cpsy2b-3'</i>	TGCATATGTAGGAAAAGCAAAGAACTGGCTTCATTGCCCATAGCATATACCAGGGCAGG
<i>Cpsy2b-T</i>	TGCATATGTAGGAATAGC-----
<i>Apsy2b-T</i>	TGCATATGTAGGATAC----- *****
<i>Cpsy2b-3'</i>	TCTGGGCCCTTCTAGGTTTACAGGAGCAACAAGGACATAA TGTTCACTTCCTCTCTGTAC
<i>Cpsy2b-3'</i>	TCTCTGCACAAAATCATAACCACTGTATCTGTAGTACCTTTGACAGTGTATATAAGAA
<i>Cpsy2b-3'</i>	GGTGTATGTGATTTGCATTAGATGTACTGAAATGATAGTAACTTCAATGATTTGGAGAA
<i>Cpsy2b-3'</i>	GAAGAGAGTAAAAGATAATGATATTTGTGCGCC

Figure 3.8: Analysis of *psy2* 3'RLM-RACE clones. Translated sequence of the a) Cavendish *psy2a* 3'RACE clone starting at nt position 808 from the start of the coding region. The coding region duplication (bold) inserted into the 3' UTR (underlined) and the positions of stop codons (grey highlight) are shown. b) Sequence alignment of Cavendish *psy2b* 3' coding region clone (*Cpsy2b-3'*) from leaf mRNA against truncated Asupina (*Apsy2b-T*) and Cavendish (*Cpsy2b-T*) 3' RACE clones from fruit mRNA. The alignment starts at nt position 923 from the start of the Asupina and Cavendish *psy2b* coding region. Positions of conserved nucleotides (*) and insertions in *Apsy2b-T* sequence (^) compared to the Cavendish *psy2b* clones are marked. The position of a C/T mutation (#) in *Cpsy2b-3'* compared to the *Cpsy2b* coding region consensus is also marked.

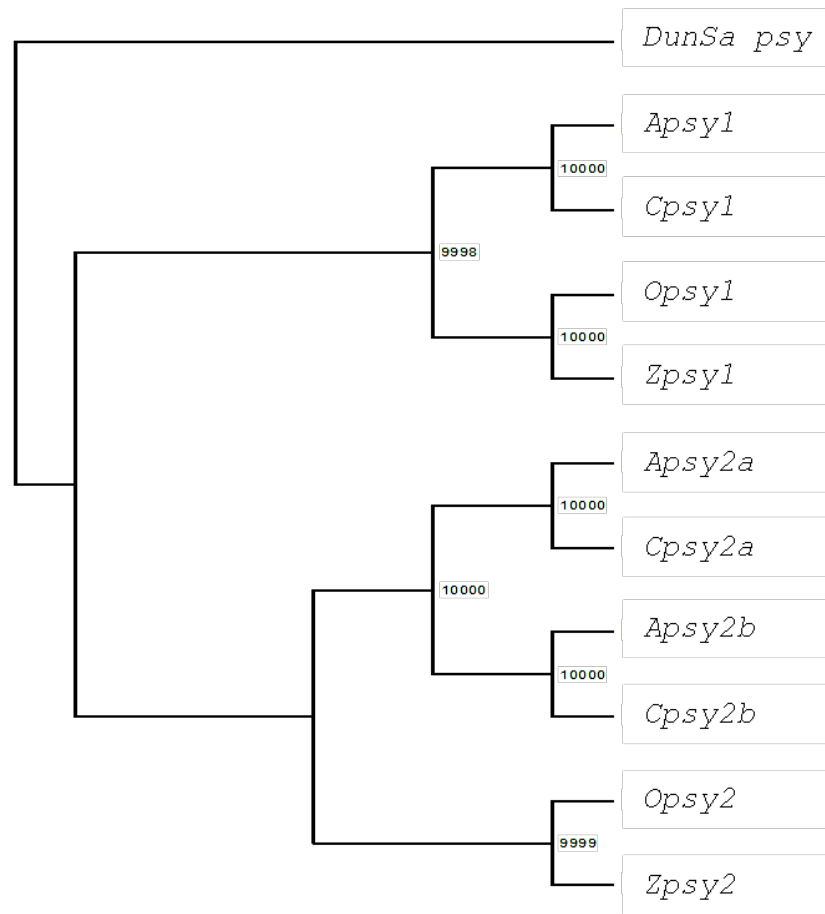
without a truncated 3' UTR was obtained from Cavendish leaf tissue as a by-product of *psy1* 3'RLM-RACE, and was 450 bp with a 172 bp 3' UTR (Chapter 3.3.2.1). Translation of this sequence suggested that the Cavendish PSY2B protein would be prematurely truncated by an internal TAG stop codon (Figure 3.8b). However, the corresponding codon in the *psy2b* partial sequence consensus was CAG, suggesting that the C/T substitution in the 3'RACE clone could be a PCR amplification error. Seven further clones were obtained from Cavendish fruit tissue, but were only 320 bp long and polyadenylated prematurely just after the region of overlap with the partial *psy2b* coding region (Figure 3.6d i & Figure 3.8b). The translated protein was uninterrupted until the point at which the sequences were truncated. One Asupina 3'RACE clone corresponding to *psy2b* was 316 bp long and truncated at the same position as the Cavendish *psy2b* clones but appeared to have multiple stop codons (Figure 3.8b). The full mRNA transcript lengths of Asupina or Cavendish *psy2b* could not be predicted as sufficient 5' or 3' RLM-RACE data was not available. Nevertheless, the complete coding region of *psy2b* was isolated from fruit mRNA of both Asupina and Cavendish using the primers *Apsy2a-CR-F1* (used to obtain the *psy2b* 5' coding region from gDNA), and *Cpsy2b-CR-R1* (designed from the end of the Cavendish *psy2b* coding region of the full length 3'RACE clone). This confirmed that the *psy2b* coding region was 1194 bp, encoding a polypeptide of 397 amino acids. No other sequence variants were detected from the five clones sequenced from Asupina and Cavendish *psy2b*.

In summary, although complete mRNA sequence information was only deduced for Asupina *psy1*, Cavendish *psy1* and Asupina *psy2a*, clones of the complete coding region of *psy1*, *psy2a* and *psy2b* from both varieties was obtained. The relationship between these sequences was investigated by phylogenetic analysis.

3.3.3 Phylogenetic analysis of complete banana *psy* coding regions

The sequences of the complete *psy1*, *psy2a* and *psy2b* coding regions from Asupina and Cavendish were compared to those of rice and maize *psy1* and *psy2* (Figure 3.9). Phylogenetic analysis showed that the *psy1* and *psy2* sequence groups diverged at the first branch of the tree. The *psy1* group further divided with Asupina and Cavendish *psy1* (97% identical) forming one clade and maize and rice *psy1* forming a second clade (81% identical). Maize and rice *psy2* (79% identical) diverged from the banana *psy2* sequences, while the *psy2a* and *psy2b* sequences also diverged into two pairs of sequences. The Asupina and Cavendish *psy2a* sequences were 97% identical, while surprisingly, the respective *psy2b* sequences were 100% identical. The Asupina and Cavendish *psy1* coding regions were approximately 60% identical to their respective *psy2a* and *psy2b* sequences, and in both

a)



b)

Abbreviation	#	1	2	3	4	5	6	7	8	9	10	11
<i>Apsy1</i>	1	■	60	60	97	59	60	61	57	62	59	46
<i>APsy2a</i>	2	60	■	83	62	97	83	61	63	61	65	49
<i>APsy2b</i>	3	60	83	■	59	83	100	60	67	59	63	46
<i>CPsy1</i>	4	97	62	59	■	59	59	60	57	63	56	46
<i>CPsy2a</i>	5	59	97	83	59	■	83	61	62	60	65	49
<i>CPsy2b</i>	6	60	83	100	59	83	■	60	67	59	63	46
<i>Opsy1</i>	7	61	61	60	60	61	60	■	51	81	62	49
<i>Opsy2</i>	8	57	63	67	57	62	67	51	■	59	79	52
<i>Zpsy1</i>	9	62	61	59	63	60	59	81	59	■	61	50
<i>Zpsy2</i>	10	59	65	63	56	65	63	62	79	61	■	48
<i>DunSa_PSY</i>	11	46	49	46	46	49	46	49	52	50	48	■

Figure 3.9: Phylogenetic analysis of the coding regions of Asupina and Cavendish *psy* genes compared to rice and maize. The numbers (#) correspond to each of the sequences in the alignment, which were Asupina *psy1* (*Apsy1*), *psy2a* (*Apsy2a*) and *psy2b* (*Apsy2b*); Cavendish *psy1* (*Cpsy1*), *psy2a* (*Cpsy2a*) and *psy2b* (*Cpsy2b*); rice *psy1* (*Opsy1*) and *psy2* (*Opsy2*); maize *psy1* (*Zpsy1*) and *psy2* (*Zpsy2*); *D. salina psy* (*DunSa_psy*). The tree was bootstrapped to 10,000 trials and bootstrapping values are shown at each node of the rectangular cladogram.

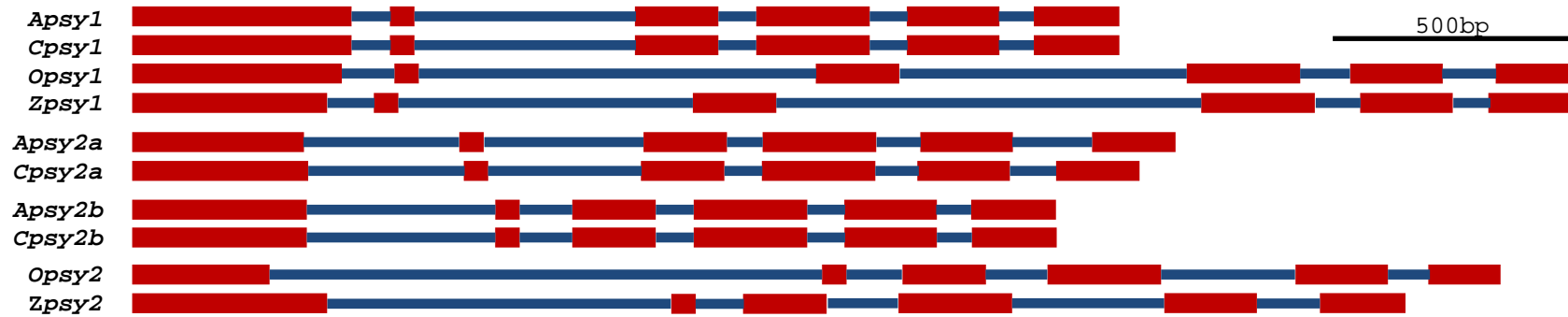
Asupina and Cavendish the *psy2a* coding regions were 83% identical to *psy2b*. This was similar to maize and rice where the *psy1* and *psy2* coding regions were 61% and 51% identical, respectively. Overall, phylogenetic analysis confirmed that the Asupina and Cavendish *psy* gene families contained three known distinct gene family members: *psy1*, *psy2a* and *psy2b*.

3.3.4 Analysis of Asupina and Cavendish *psy* gene structure

The genomic sequences representing the Asupina and Cavendish *psy1* and *psy2* coding regions were isolated (Figure 3.10) due to the presence of putative introns in RT-PCR clones and to enable comparison of banana *psy* gene structure to those of maize and rice. PCR amplification from gDNA, using the same primers used to amplify the coding regions from mRNA (Chapter 3.3.2), gave strong 2 Kb *psy* products. Alignment of the *psy* coding regions amplified from mRNA with their corresponding genomic sequences confirmed that the cDNAs were identical to the exons in the gDNA sequences. The sole exception was Cavendish *psy2b*, where the genomic sequence was only 96% identical to its respective cDNA coding region identified earlier (Chapter 3.3.2.2.). The Cavendish *psy2b* cDNA was 99% identical to the Asupina *psy2b* gDNA sequence. Although this suggests an error in amplification of the full Cavendish *psy2b* coding region from mRNA, the partial Cavendish *psy2b* sequence was identical to the full length coding region which was amplified from a separate mRNA extract.

The structure of all banana, maize and rice *psy* genes was highly conserved and each genomic coding region had six exons separated by five introns (Figure 3.10a). The size of exons 2, 3, 4 and 5 was identical across all *psy* genes, including rice and maize, and were 51, 173, 236 and 193bp, respectively. In contrast, exons 1 and 6 were variable in length (Figure 3.10b). Exon 1 ranged in size from 286 bp (rice *psy2*) to 457 bp (banana *psy1*), while exon 6 varied in length from 150 bp (maize and rice *psy2*) to 183 bp (banana *psy1*). Exon lengths were identical for corresponding Asupina and Cavendish *psy* genes with the exception of *psy2a*, where the Cavendish exon 1 was 9 bp longer than its Asupina counterpart. In contrast, introns were more variable in size (Figure 3.10 a & b). In banana, Cavendish *psy1* intron 2 was the largest (466 bp) and Asupina *psy1* intron 5 the smallest (73 bp). Generally, each intron within *psy1*, *psy2a* or *psy2b*, was similar in size in both Asupina and Cavendish. The exception was *psy2a* intron 5, which was 166 bp in Asupina and only 97 bp in Cavendish. However, introns differed considerably in size between different *psy* genes. For example, Cavendish *psy1* intron 1 was 81 bp, compared to 326 bp and 394 bp for Cavendish *psy2a* and *psy2b*, respectively. Generally, the maize and rice *psy* introns were larger than those of

a)



b)

Gene	Exon						Intron					Total		
	1	2	3	4	5	6	1	2	3	4	5	CR	intron	gDNA
<i>Apsy1</i>	457	51	173	236	193	183	81	461	79	79	73	1293	773	2066
<i>Apsy2a</i>	358	51	173	236	193	174	324	332	75	92	166	1185	989	2174
<i>Apsy2b</i>	364	51	173	236	193	177	392	110	78	124	111	1194	815	2009
<i>Cpsy1</i>	457	51	173	236	193	183	81	466	79	80	74	1293	780	2073
<i>Cpsy2a</i>	367	51	173	236	193	174	326	320	79	91	97	1194	913	2107
<i>Cpsy2b</i>	364	51	173	236	193	177	394	110	78	122	105	1194	809	2003
<i>Opsy1</i>	436	51	173	236	193	174	109	828	597	104	113	1263	1751	3014
<i>Opsy2</i>	286	51	173	236	193	150	1150	115	129	279	87	1089	1760	2849
<i>Zpsy1</i>	406	51	173	236	193	174	98	613	885	94	77	1233	1767	3000
<i>Zpsy2</i>	406	51	173	236	193	150	716	100	146	317	131	1209	1410	2619

Figure 3.10: Analysis of genomic sequence of Asupina and Cavendish *psy* genes. a) Diagrammatic representation of the structure of the genomic sequences corresponding to the coding region (CR) of Asupina and Cavendish *psy1*, *psy2a* and *psy2b* compared to that of maize and rice *psy1* and *psy2* showing the positions of the exons (red rectangles) and introns (blue lines). b) Table showing the sizes of the six exons and five introns of the coding region of the *psy* genomic sequences of Asupina, Cavendish, rice and maize. Abbreviations for the banana, maize and rice *psy* genomic sequences were as given in Figure 3.10.

Asupina and Cavendish, ranging in size from 77 bp to 1150 bp.

3.3.5 Further analysis of *psy* coding region variants

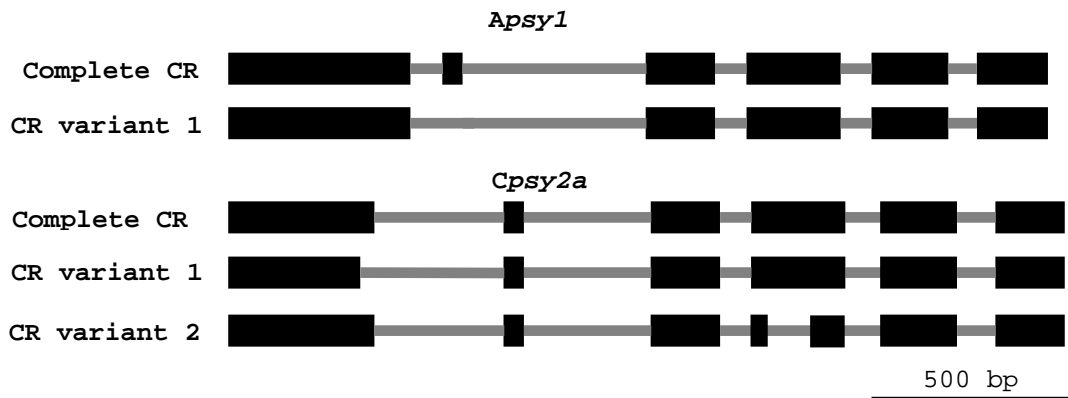
The coding region variants of Asupina *psy1* (Chapter 3.3.2.1) and Cavendish *psy2a* (Chapter 3.3.2.2) were compared to the respective gDNA sequences (Figure 3.11a). The Asupina *psy1* variant lacked 51 bp corresponding to exon 2 and was predicted to produce a smaller, possibly functional version of PSY1. Analysis of the gDNA confirmed that the intron and exon boundaries of exons 1 and 3 which flanked the missing exon were normal suggesting that exon 2 was spliced out with introns 1 and 2. Cavendish *psy2a* variant 1 (1160 bp) and variant 2 (1102 bp) lacked 34 bp from the 3' end of exon 1 and 92 bp from the middle of exon 4, respectively. Consequently, these *psy2a* transcript variants are unlikely to produce functional proteins. Variant 1 appeared to stem from misprocessing of the donor splice site (GT) of intron 1, causing the loss of the 3' end of exon 1, in conjunction with the normal processing of the acceptor splice site of intron 1 (AG; Figure 3.11b). The 92 bp fragment missing from exon 4 of variant 2 was bordered by putative donor (GT) and acceptor (AG) sequences that were apparently not recognised in variant 1 or the full length coding region (Figure 3.11b).

Using the available gene structure data, the chimeric Cavendish *psy2c* clone (Chapter 3.3.1.1) was compared with the genomic sequences of *psy1* and *psy2a* to determine how much of each of these genes it contained (Figure 3.12). The *psy2c* partial sequence consisted of 147 bp of exon 3, all of exons 4 and 5, and the first 24 bp of exon 6 (Figure 3.12a). The 5' and 3' regions of the *psy2c* sequence were derived from *psy1* and *psy2a*, respectively. The transition in the sequence occurred in exon 4 such that the first 164 bp was *psy1* while the next 62 bp was *psy2a* (Figure 3.12a & b). Although analysis of the partial coding regions showed that *psy2c*, as a whole, exhibited 87% sequence identity with both *psy1* and *psy2a*, the region of this clone represented by exon 4 was 93% and 85% identical to *psy1* and *psy2a*, respectively.

3.4 Discussion

Phytoene synthase occupies an important role in carotenoid biosynthesis and therefore may also play a role in mediating pVA levels in banana cultivars. In this study, sequences of the banana *psy* genes and putative PSY proteins were determined for the first time and as reported in other monocots, were confirmed to exist in banana as part of a gene family. The gDNA and corresponding mRNA sequences from representative high and low pVA bananas were analysed to look for a correlation with differential carotenoid accumulation.

a)



b)

i) CR variant 1

Genomic `ctactcgatgcgggcgtaacgagcggtgcgggcaggtctgcccagatgccaagactttc`

Complete CR `ctactcgatgcgggcgtaacgagcggtgcgggcaggtctgcccagatgccaagactttc`

CR variant 1 `ctactcgatgcgggcgtaacgagcggtgcgggcag-----`

CR variant 2 `ctactcgatgcgggcgtaacgagcggtgcgggcaggtctgcccagatgccaagactttc`

Genomic `tacttgggt`

Complete CR `tacttgg`

CR variant 1 `-----`

CR variant 2 `tacttgg`

ii) CR variant 2

Genomic `agccattcaaggacatgatagaaggaatgagaatggacctgcccgaatcgaggtacaaga`

Complete CR `ccattcaaggacatgatagaaggaatgagaatggacctgcccgaatcgaggtacaaga`

CR variant 1 `ccattcaaggacatgatagaaggaatgagaatggacctgcccgaatcgaggtacaaga`

CR variant 2 `ccattcaaggacatgatagaaggaatgagaatggacctgcccgaatcgag-----`

Genomic `atctcgacgaactctatctctactgctactatgtcgcccagcgggtggggctcatgagtg`

Complete CR `atctcgacgaactctatctctactgctactatgtcgcccagcgggtggggctcatgagtg`

CR variant 1 `atctcgacgaactctatctctactgctactatgtcgcccagcgggtggggctcatgagtg`

CR variant 2 `-----`

Genomic `tgccggtgatgggaattgccccagactcgaaggcctcagccgagagcgtctacagcgcag`

Complete CR `tgccggtgatgggaattgccccagactcgaaggcctcagccgagagcgtctacagcgcag`

CR variant 1 `tgccggtgatgggaattgccccagactcgaaggcctcagccgagagcgtctacagcgcag`

CR variant 2 `-----actcgaaggcctcagccgagagcgtctacagcgcag`

Genomic `cattagctcttggcatcgcggaatcaactcaccaacataactcagggatgtcggagagggt`

Complete CR `cattagctcttggcatcgcggaatcaactcaccaacataactcagggatgtcggagagga`

CR variant 1 `cattagctcttggcatcgcggaatcaactcaccaacataactcagggatgtcggagagga`

CR variant 2 `cattagctcttggcatcgcggaatcaactcaccaacataactcagggatgtcggagagga`

Figure 3.11: Analysis of coding region variants of Asupina *psy1* and Cavendish *psy2a*. a) Diagram showing the exon (black rectangles) and intron (grey lines) structure of the coding region (CR) variants of Asupina *psy1* (*Apsy1*) and Cavendish *psy2a* (*Cpsy2a*) compared to the genomic sequence of the complete coding region. b) Analysis of splicing of *Cpsy2a* coding region variant 1 and 2 compared to the complete coding region and genomic sequence showing i) the end of exon 1 and ii) exon 4. The donor (gt) and acceptor (ag) splice sites are highlighted in grey, while the position of the cryptic splice sites (↓) and removed exon sequences (-) are marked.

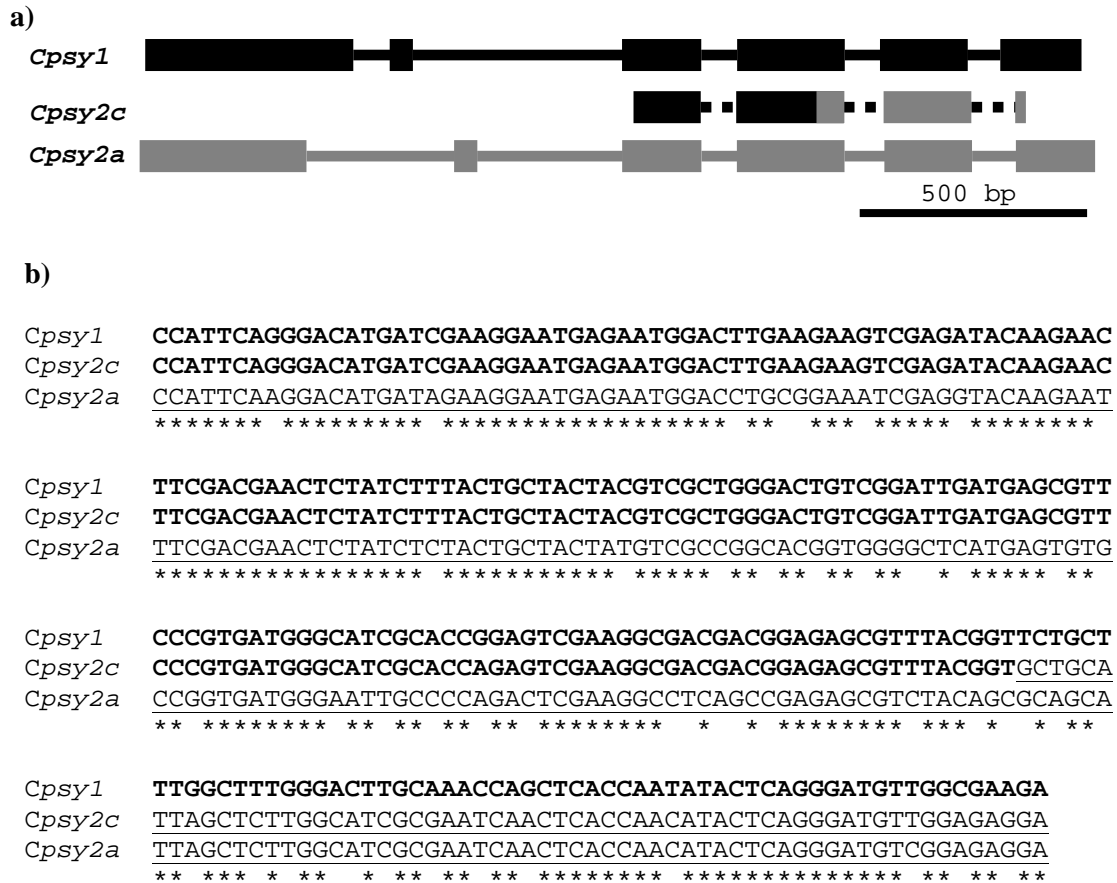


Figure 3.12: Analysis of Cavendish *psy2c* partial sequence structure. a) Diagram showing the sequence composition of the Cavendish *psy2c* (*Cpsy2c*) partial coding region compared to *psy1* (*Cpsy1*) and *psy2a* (*Cpsy2a*). The exons (rectangles) and introns (solid lines) of *Cpsy1* are marked in black while those of *Cpsy2a* are marked in grey. No introns were identified in *Cpsy2c*, however, the predicted position of introns in this sequence are denoted by black dotted lines. b) Sequence alignment of exon 4 to show the transition from *Cpsy1* sequence (bold text) to *Cpsy2a* (underlined text) in the corresponding sequence of *Cpsy2c*. Nucleotides shared between these three sequences are marked under the alignment (*).

Initially, partial *psy* sequences were obtained from the mRNA of five banana cultivars, with different carotenoid levels and genetic backgrounds, using degenerate primer RT-PCR. Phylogenetic analysis of these sequences demonstrated the existence of a *psy* gene family in banana consisting of one *psy1* and at least one *psy2* gene. Although multiple *psy2* genes were isolated only from Cavendish (*psy2a*, *psy2b* and *psy2c*), the apparent absence of these genes in other cultivars could be due to the low number of clones obtained for some cultivars or the limited availability of fruit, as *psy2* appeared more predominant in this tissue. Following initial studies with multiple cultivars, Asupina and Cavendish were selected as representative high and low pVA cultivars, respectively. This choice was made to simplify the isolation and comparison of the complete *psy* sequences, and both leaf and fruit tissue from both cultivars was available for analysis. The presence of multiple *psy2* genes in other banana genomes was confirmed with the subsequent isolation of the complete coding regions of *psy1*, *psy2a*

and *psy2b* from mRNA and gDNA of both Asupina (Fe'i genome) and Cavendish (A genome). Phylogenetic analysis of these sequences supported the relationships observed from analysis of the partial coding regions and confirmed that *psy2b* was a distinct gene. The identification of a *psy* gene family in banana is consistent with existing knowledge of other plants where the number of identified *psy* genes varies from one in *Arabidopsis* (Li *et al.*, 2008a) to four in yellow gentian (Zhu *et al.*, 2002; GenBank Nos. E15680-83). This has also been shown in algae where some species had two *psy* genes, while others had only one (Tran *et al.*, 2009).

Phylogenetic segregation of *psy* sequences, in both partial and full sequence studies, appears to be based initially on potential gene function (*psy1* or *psy2*), while the individual clades reflect the genomic origin (A, B and Fe'i). Additionally, the grouping of the *psy* genes did not appear to correlate with fruit pVA content (Figure 3.4). Based on the number of clones obtained from different tissues (Table 3.3), *psy1* appears to be primarily expressed in leaf, possibly involved in the production of secondary photosynthesis pigments in chloroplasts, as no clones were detected in Asupina or Cavendish fruit tissue using degenerate primers. In contrast, *psy2* was isolated from both leaf and fruit tissues with degenerate primers, suggesting that this gene is more widely expressed, and based on the number of clones obtained, *psy2a* appears more highly expressed than *psy2b*. The *psy2a* and *psy2b* genes may be divergent enough to have different roles in carotenoid metabolism. Interestingly, *psy1* expression in maize was linked to carotenoid production in the endosperm, while *psy2* mRNA was only detected in leaf (Gallagher *et al.*, 2004). Comparatively, tomato *psy1* expression was observed in chromoplast-bearing tissue, such as fruit and petals, while *psy2* was expressed in various tissues (Giorio *et al.*, 2008). It has been postulated that the gene duplication observed in the *psy* genes could facilitate tissue-specific regulation of carotenoid synthesis, enabling differential regulation of carotenoid expression in non-photosynthetic organs without adverse impact on carotenoid homeostasis in photosynthetic tissue (Gallagher *et al.*, 2004). This would effectively shield the photosynthetic machinery from changes in carotenoid metabolism that occur during the development of flower, seed and fruit, thereby preventing photosensitivity (Busch *et al.*, 2002) and allowing photosynthetic carotenoids to be used as secondary metabolites (Gallagher *et al.*, 2004). However, before any conclusions can be drawn as to the function of these genes in banana tissues, further work is required to confirm the expression level of *psy1* and *psy2* in Asupina and Cavendish tissues.

Evidence of multiple transcription start and polyadenylation sites was observed in the putative mRNA sequences of *psy1* (Asupina and Cavendish) and Asupina *psy2a*, indicating that transcripts of variable length may exist *in vivo*. The RLM-RACE method used to isolate

the 5' and 3' ends of the Asupina and Cavendish *psy* mRNAs is designed to amplify from mRNAs that have intact 7-methylguanosine caps at their 5' termini. Therefore, the putative multiple transcription start sites are unlikely to be artefacts due to amplification from degraded mRNAs or the RLM-RACE method itself. The *psy1* transcripts exhibited the most variation in 3' UTR length and appeared to be longer than those of *psy2a*. The discovery of polyadenylation at different sites in banana *psy* transcripts is consistent with maize, where 3' RACE detected six polyadenylation sites in *psy1* (GenBank No. ZMU32636). Transcripts with multiple polyadenylation sites are common in plants (Dean *et al.*, 1986; Montoliu *et al.*, 1990; Lupold *et al.*, 1999; Kaleikau *et al.*, 1992; Loke *et al.*, 2005). Interestingly, recent *in silico* genomic analysis in rice found that over 60% of the genes analysed had multiple polyadenylation sites (Shen *et al.*, 2008). Comparison of the number of putative transcription start sites also indicated that *psy1* was more variable in 5' UTR length than *psy2a*, potentially resulting in structural changes that could influence gene expression. Secondary structure in the 5' UTR may also influence gene expression although this has not been previously studied in *psy*. However, in tomato, the 5' UTR of *lat52* gene was involved in regulating expression of this gene during pollen development (Bate *et al.*, 1996), while secondary structure in the 5' UTR of the *psbA* gene affected mRNA stability and translational efficiency (Zou *et al.*, 2003).

Variability in 5' and 3' UTR length may indicate that *psy1* has more diverse roles than *psy2a*, as transcripts of this gene may come in a range of sizes that are regulated differently. The length of the 3' UTR has been reported to affect mRNA stability by altering secondary structure (Kaleikau *et al.*, 1992), which is also thought to be affected by the sequence of putative polyadenylation signals (Loke *et al.*, 2005). Structural differences may significantly affect *psy* gene function and regulation. For example, heterogeneous *psy1* transcripts with variable half lives may allow constant *psy1* mRNA levels that may facilitate rapid turnover of photosynthetic pigments in leaf. In contrast, carotenoid biosynthesis is highly regulated during fruit development (Chapter 1.3.3). Therefore *psy2a* expression may be coordinated primarily with banana fruit ripening and this may be reflected in lower variability in mRNA length.

The complete mRNA sequence was only obtained for Asupina and Cavendish *psy1* and Asupina *psy2a*, despite the successful isolation of the *psy1*, *psy2a* and *psy2b* coding regions from both cultivars. Failure to obtain the full *psy2a* transcript from Cavendish and the *psy2b* transcripts from Asupina and Cavendish may be of significance as it may indicate abnormal regulation of mRNA at the transcriptional or post-transcriptional level. The only Cavendish *psy2a* clone obtained through 5' RACE was smaller than expected and included part of an

intron. Although this could be a genomic fragment amplified from degraded gDNA contaminating the cDNA sample, this same fragment was amplified consistently over several attempts and no product of the expected size was ever observed. This suggests that functional Cavendish *psy2a* transcripts may be in very low abundance in fruit tissue due to poor expression or mRNA degradation. The 5' RLM-RACE template preparation process may also dilute complete transcripts below the detection threshold of nested PCR. It is also possible that the mRNA was simply purified from fruit where peak *psy2a* expression may not have occurred or may have already passed. The amplification of only one Cavendish *psy2a* 3' RACE clone supports the hypothesis that this gene is in low abundance in fruit, as template dilution is not expected to be as significant in 3' RLM-RACE. The duplication of part of the coding region in the 3' UTR of this clone raises the possibility that a genomic rearrangement may exist in at least one of the *psy2a* alleles in Cavendish.

Interestingly, all of the *psy2b* 3' RACE clones obtained from Cavendish fruit were truncated through premature polyadenylation, a process previously shown to down-regulate expression of transgenic *B.t* toxin in tobacco (Diehn *et al.*, 1998). The regulatory function of prematurely polyadenylated transcripts is also seen in the down-regulation of *Arabidopsis* flowering time control protein (FCA) expression during flower development (Amasino, 2003). Premature polyadenylation could reduce the level of functional transcripts, negatively affecting pVA accumulation during fruit development. This may be significant in Cavendish, where both *psy2a* and *psy2b* appear to suffer abnormal post-transcriptional processing. The Asupina *psy2b* truncated clone had a premature stop codon prior to the polyadenylation site, raising the possibility that nonsense-mediated mRNA decay (NMD) may be involved, where premature termination codons trigger the polyadenylation and subsequent degradation of truncated transcripts. This can be triggered by long 3' UTRs or introns in this region and is thought to be a natural regulatory mechanism of *Arabidopsis* wild-type genes (Kertész *et al.*, 2006). However, comparison of truncated *psy2b* 3' RACE clones with the Cavendish *psy2b* 3' RACE clone revealed that they terminate in an adenosine rich region similar to putative polyadenylation motifs (Dean *et al.*, 1986; Loke *et al.*, 2005). Therefore, the observed premature polyadenylation in these clones may be due to artefacts caused by preferential amplification of sequences from cDNA where the 3' RLM-RACE adapter misprimed onto this A-rich region of the *psy2b* coding region rather than the poly (A) tail.

Cavendish is triploid, with three copies of the A genome, and is thought to be an interspecific hybrid from diploid parents (Heslop-Harrison and Schwarzacher, 2007). As previously mentioned, Asupina is also thought to be triploid with a genotype of ATT, containing both A and Fe'i genomes, based on flow cytometry analysis and molecular

characterisation (Sharrock and Frison, 1998). The Asupina and Cavendish *psy* gene family members identified in this study were each assumed to exist as a single copy per genome. This was supported by comparison of the NCBI rice genome sequence where single copies of *psy1*, *psy2* and *psy3* were located on chromosomes 6 (GenBank No. NC_008399.1), 12 (GenBank No. NC_008405.1) and 9 (GenBank No. NC_008402.1), respectively. Additionally, the phylogenetic grouping (Figure 3.9) and level of percentage similarity between *psy1*, *psy2a* and *psy2b* in both Asupina and Cavendish, appears support this hypothesis. Therefore, the banana *psy* genes were each expected to reside at different loci and have three alleles per locus. The sequences isolated so far suggest that, in both Asupina and Cavendish, there is little variation at the *psy1* locus and that all alleles are intact in the genome. This is also the case for Asupina *psy2a*. However, isolation of truncated *psy2a* 5' and 3' RLM-RACE fragments (Figure 3.7) from Cavendish mRNA may indicate that expression of one or more alleles of these genes may be impaired. Other banana cultivars possessing the A genome, such as Lakatan (AA), exhibit higher fruit pVA levels (Table 1.2), suggesting that the presence of the A genome alone is not a sufficient explanation for the low pVA content of Cavendish fruit. Therefore, the Cavendish *psy2a* gene may have lost function over time through mutations. Polyploidy has been linked to genome instability (Bennetzen, 2007), which can induce genomic rearrangements, or chromosomal insertions and deletions that may be responsible for Cavendish *psy2a* alleles that express truncated or otherwise defective mRNAs.

The Cavendish *psy2c* partial sequence, a chimera of *psy1* and *psy2a*, was only found once and could be due to alternate trans-splicing of pre-mRNAs from these two genes, a process thought to expand proteome diversity by producing novel proteins with unique functions (Horiuchi and Aigaki, 2006). For example, the pre-mRNAs of the mitochondrial NADH dehydrogenase subunit genes (*nad1*, *nad2*, and *nad5*) in flowering plants require trans-splicing for their mature transcripts to be functional (Bonen, 1993). However, there is no intron at the junction between the two genes, suggesting that other mechanisms such as genomic rearrangements may be responsible. Alternatively, *psy2c* may exist only as a gene fragment (Bennetzen, 2007), a feature that is common in plant genomes. Therefore, further characterisation using methods such as genome walking is needed to determine whether *psy2c* exists in the genome or is a post-transcriptional artefact.

Interestingly, the discovery of two *psyX* 3'RACE clones may suggest that there are more members of the banana *psy* gene family. However, the presence of premature stop codons may indicate that these clones are derived from a pseudogene, which could prove interesting as these have not been reported in the *psy* gene family (Gallagher et al., 2004) but have been

identified in other gene families such as the *Arabidopsis* flavonol synthase (Owens et al., 2008) and Scots Pine phytochrome (Garcia-Gil, 2008) genes. The current set of *psy* sequences isolated from Asupina and Cavendish may not represent all alleles of *psy1*, *psy2a* and *psy2b*. Further investigation of the ploidy of the Fe'i genome and the copy number of the *psy* genes in Asupina and Cavendish using approaches such as southern hybridisation or real-time PCR will be useful. Ultimately, release of the complete the banana genome sequence would provide the greatest insight into its structure and organisation. Such work is currently being undertaken by the Global Musa Genomics Consortium (Lescot *et al.*, 2008).

Analysis of genomic clones confirmed that the three members of the *psy* gene family isolated from Asupina and Cavendish mRNA (*psy1*, *psy2a* and *psy2b*) were present in the genome. Interestingly, the isolated Asupina and Cavendish *psy2b* genomic sequences confirmed the legitimacy of both genes despite the unexpected high similarity between their cDNA sequences. Consequently, more Cavendish *psy2b* clones need to be obtained from mRNA to verify the sequence. The difference between the Cavendish *psy2b* cDNA and genomic coding regions may be a result of contamination with Asupina sequences or may indicate the existence of multiple gene copies or allelic variation. This study also showed that the genomic organisation of the coding region exons of Asupina and Cavendish *psy* genes is consistent with that of related monocots such as maize, rice, sorghum (Li *et al.*, 2008a) and wheat (He *et al.*, 2008), suggesting that these may be indicative of the genomic structure of banana *psy* genes as a whole. The differences in the conservation of intron size and gene structure between the banana (Asupina and Cavendish) *psy* family members and those of maize and rice probably represents species-specific differences. The highly conserved central coding region of *psy* represented by exons 2 to 5 is likely to contain critical domains relating to catalytic functions such as substrate specificity, while more variable exons corresponding to exons 1 and 6 may serve secondary functions that may be specific to each gene.

The gDNA sequences suggest that the difficulties encountered in obtaining complete Cavendish *psy2a* mRNA sequence were not due to genomic aberrations, such as insertion of transposable elements or deletions in the 5' or 3' region of the coding region, but may be caused by other factors such as mRNA processing or stability. As the sequences flanking the banana *psy* coding region were not available at this stage, the presence of features such as introns or genomic aberrations in the 5' or 3' UTRs was unknown. Although the isolation of more clones may be required to confirm the gDNA sequences obtained, particularly in the introns, the number of clones was sufficient to determine the gene structure corresponding to the Asupina and Cavendish *psy* coding regions. Interestingly, the partial clones which included introns are likely to be due to incomplete mRNA processing rather than to gDNA

contamination as the genomic *psy* coding regions have three introns in the region amplified by the degenerate primers, while all of the intron bearing clones obtained from mRNA had only one intron.

Multiple variant clones of the Asupina *psy1* and Cavendish *psy2a* coding regions were also obtained from cDNA, and comparison with the respective genomic sequences suggested that they were a result of alternate or cryptic splicing. Exon 2 of the Asupina *psy1* variant was completely excised, leaving an otherwise complete coding region that could encode a functional protein. However, Cavendish *psy2a* pre-mRNA may be processed into two isoforms that do not appear to produce functional PSY proteins. Alternate splicing is common in plants (Wang and Brendel, 2006; Reddy, 2007) and has recently been reported for *psy1* in wheat (Howitt *et al.*, 2009), and is discussed further in Chapter 5. High levels of non-functional *psy2a* transcripts in Cavendish fruit, compared to the Asupina *psy2a* which appears normal, may result in lower enzyme activity in Cavendish fruit. This could in turn explain the difference in the pVA content of the fruit of these two banana cultivars.

Due to time constraints, isolation of the complete *psy* sequences from these cultivars took priority over further analysis of partial clones. The number of clones used to derive some consensus sequences for analysis was low or occasionally was based on only a single clone, as in the case of Cavendish *psy2c*. Also, the number of tissue types analysed was limited as fruit tissue was available for only Asupina and Cavendish. To improve the detection of *psy* gene family members in banana, the range of tissues from which mRNA is isolated could be expanded to include other tissues such as roots and flowers. The *psy* mRNAs for which clones were difficult to obtain may have low expression levels in the tissues that were targeted. The primary aim of this chapter was to determine whether the difference in carotenoid accumulation between high and low pVA banana varieties could be attributed to differences in the *psy* genes at the level of mRNA or gDNA. This study found that the *psy* genes in banana exist as a gene family, consistent with existing knowledge in the literature for other *psy* genes. Bioinformatic analysis indicated that all complete *psy* sequences from both Asupina and Cavendish may encode functional proteins. Whether this is true and whether these enzymes differ in activity is unknown. The difficulties in obtaining complete mRNAs for *psy2b* transcripts and Cavendish *psy2a*, and the identification of non-functional variants of the latter, suggest that the *psy2* expression may be impaired in Cavendish. Intriguingly, partial sequence data for *psy2c* and *psyX* suggest that the banana *psy* gene family may yet be larger. This study also gave an insight into the tissue specificity of *psy* gene expression in leaf and fruit, suggesting that *psy1* was predominantly found in leaf while *psy2* was expressed mainly in fruit despite being obtained from both tissues.

Chapter 4: Characterisation of phytoene synthase enzymes

4.1 Introduction

Phytoene synthase (EC 2.5.1.32) occupies an important position in the biosynthesis of isoprenoids and produces phytoene from the head-to-head condensation of two GGPP molecules via the intermediate, PPPP. Studies in capsicum and tomato have demonstrated a requirement for Mn^{2+} (Dogbo *et al.*, 1988; Fraser *et al.*, 2000) and ATP (Fraser *et al.*, 2000) as cofactors in this reaction, while in daffodil, Mg^{2+} enhanced the activity of PSY in the presence of Mn^{2+} (Schledz *et al.*, 1996). PSY exists in both soluble and tightly membrane bound forms, and PSY function requires galactolipids as cofactors (Schledz *et al.*, 1996; Fraser *et al.*, 2000). PSY has a prenyltransferase catalytic domain similar to enzymes involved in squalene biosynthesis (Cunningham and Gantt, 1998). This domain is part of the trans-isoprenyl diphosphate synthases head-to-head (1'-1) condensation reaction (Trans_IPPS_HH) family (NCBI CDD No. cd00683). PSY is thought to interact with plastid membranes as well as other enzymes in carotenoid biosynthetic complexes (Cunningham and Gantt, 1998), and characterisation of purified PSY from capsicum chromoplasts indicates that it functions as a monomer (Dogbo *et al.*, 1988). Interestingly, it appears that cleavage of the signal peptide is required for PSY activity as N-terminal truncated versions were found to be significantly more active than the full length polypeptide (Misawa *et al.*, 1994; Schledz *et al.*, 1996).

The activity of the PSY enzyme has been analysed in a number of ways. PSY proteins purified from capsicum chromoplasts (Dogbo *et al.*, 1988) and tomato chloroplasts (Fraser *et al.*, 2000), were assayed using *in vitro* phytoene synthesis from radiolabelled substrates to characterise the kinetic properties of these enzymes. A similar approach was used to determine the activity of daffodil PSY protein from chromoplast extracts and recombinant PSY protein produced in insect cells (Schledz *et al.*, 1996). The activity of PSY proteins has also been analysed through functional complementation in prokaryotic systems containing components of the carotenoid biosynthetic pathway (Cunningham and Gantt, 1998). Mutants of the photosynthetic bacterium *Rhodobacter capsulatus* were used to determine the enzymatic activity of tomato PSY1 and PSY2 and the accumulated carotenoids were extracted for analysis (Bartley *et al.*, 1992; Bartley and Scolnik, 1993). The entire carotenoid biosynthetic pathway has also been integrated into *E. coli* strains which have been used to test the function of a number of PSY proteins from a range of organisms including prokaryotes such as *Erwinia uredovora* (Neudert *et al.*, 1998) and *Erwinia herbicola* (Iwata-

Reuyl *et al.*, 2003), and plants such as tomato (Misawa *et al.*, 1994), *Gentiana lutea* (Zhu *et al.*, 2002), and rice (Li *et al.*, 2008a).

Recently, the relative activity of PSY from several sources was compared in transgenic maize callus in a study aimed at improving the nutritional benefit of golden rice (Paine *et al.*, 2005). Activity was estimated based on the total carotenoid content in individual transformed calli as well as the proportion of calli with high carotenoid content. The maize (B73), tomato, capsicum and rice PSY1 proteins were the most active of the seven tested. The gene encoding B73PSY1 (ZPSY1) was subsequently transformed into rice, resulting in Golden Rice 2, which produced lines yielding as much as 37 µg/g total carotenoid levels in the endosperm, 23 fold higher than levels previously reported (Ye *et al.*, 2000). The use of a callus-based expression system provides a simple method for the simultaneous analysis of a number of PSY proteins. The aim of the work reported in this chapter was to test the hypothesis that PSY enzymatic activity was responsible for differences between the fruit pVA content of Asupina and Cavendish cultivars. Therefore, PSY protein sequences from these cultivars were analysed to investigate whether any significant differences exist in their sequence or structure. The enzymatic activity of these proteins was also compared by measuring their effects on carotenoid accumulation in rice callus.

4.2 Materials and methods

4.2.1 Bioinformatic analysis of banana PSY protein sequences

The banana PSY protein sequences were translated from the Asupina and Cavendish *psy* coding region consensus sequences (*psy1*, *psy2a* and *psy2b*), while maize *psy1* (*Zpsy1*) was included as a reference. The Cavendish *psy2b* genomic sequence was translated because the mRNA-derived coding region was identical to that of Asupina *psy2b* (Chapter 3.3.5.1). The primary structure of these proteins was analysed using ScanProsite (de Castro *et al.*, 2006), on the ExPASy proteomics server, to search the PROSITE database for conserved motifs (Hulo *et al.*, 2008). PSY primary structure was also compared using The CD Search tool (Marchler-Bauer and Bryant, 2004), on the NCBI website to search the CDD (Marchler-Bauer *et al.*, 2009). From these results, an alignment of the banana PSY sequences was constructed to highlight conserved amino acids identified by CDD and PROSITE.

Secondary structure was analysed using SSpro v4.5 (Pollastri *et al.*, 2002, <http://scratch.proteomics.ics.uci.edu/>), which was rated best performing prediction software by the EVA (continuous automatic EVALuation of protein structure prediction servers) benchmarking method (Eyrich *et al.*, 2001). Secondary structure regions were then highlighted on a multiple sequence alignment produced using the Clustal W2 program

(Larkin *et al.*, 2007) v2.0.1.0 provided by the European Bioinformatics Institute (EBI) (www.ebi.ac.uk) using default parameters. The predicted secondary structures were then superimposed onto this alignment for visualisation.

The Protein Homology/analogy Recognition Engine (PHYRE) server v0.2 (Kelley and Sternberg, 2009) was used to predict the tertiary structures of the PSY protein query sequences because analysis using the first approach mode of the SWISS-MODEL server (Arnold *et al.*, 2006) failed to generate any results. PHYRE returned several tertiary structure predictions based on several of the isoprenoid biosynthetic enzymes. These structures were viewed using SPDBV (Swiss PDB deep view) v4.0 (Kaplan and Littlejohn, 2001), which also enabled modelling of the GGPP substrate within the PSY protein structure. This was achieved by superimposing the APSY1 protein with the human squalene synthase (SQS) protein complexed to GGPP (RSCB PDB No. 2q80), before merging the GGPP and PSY molecules into one layer.

4.2.2 Cloning of *psy* coding regions into binary vectors

The coding region clones were originally in the *pGEM-T Easy* vector and included *Bam*HI and *Xba*I restriction sites at their 5' and 3' ends as a result of primers used to amplify them (Table 3.2). The clones: Asupina *psy1* (clone 13), Asupina *psy2a* (clone 2), Cavendish *psy1* (clone P4) and Cavendish *psy2a* (clone 1) were selected for subcloning into the *pCAMBIA-1302* binary vector backbone (GenBank No. AF234298.1), obtained as an *E. coli* stab culture from Dr Harjeet Khanna (QUT). The intermediate cloning vectors, *pGEM-4Z-nos-GUS-nos* and *pGEM-4Z-ubi-gus-nos* was obtained from Dr Jason Geijskes (QUT).

Asupina and Cavendish *psy1* and *psy2a* coding region binary vectors were constructed in three main steps summarised in Figure 4.1a. The first step facilitated attachment of the *nopaline synthase (nos)* terminator to the 3' end of the *psy* coding region. The *psy* coding region fragment was excised from the *pGEM-T Easy* vector by *Bam*HI/*Xba*I double digestion and ligated into the *pGEM-4Z-nos-GUS-nos* cloning vector backbone to replace the *gus* coding region which was controlled by the *nos* promoter and *nos* terminator, forming *pGEM-4Z-nos-psy-nos* (Figure 4.1a i). The maize ubiquitin (*ubi*) promoter was subsequently attached to the 5' end of the *psy* coding region fragment. The *psy-nos* fragment was excised from *pGEM-4Z-nos-psy-nos* with *Bam*HI/*Eco*RI, and ligated into *pGEM-4Z-ubi-gus-nos* to replace the *gus-nos* cassette, forming the vector *pGEM-4Z-ubi-psy-nos* (Figure 4.1a ii). This step was carried out because the *ubi* promoter has four internal *Xba*I restriction sites, preventing a more direct approach. The third step involved subcloning the *ubi-psy-nos*

expression cassette from the *pGEM-4Z* vector backbone into the *pCAMBIA-1302* vector (Figure 4.1a iii). The cassette was excised from the *pGEM-4Z* vector by *HindIII/EcoRI* double digestion and ligated into the *HindIII/EcoRI* linearised *pCAMBIA-1302* backbone, to form *pCAMBIA-1302-ubi-psy-nos* (Figure 4.1b). This was possible because the *ubi* promoter available at QUT lacks an active *EcoRI* site. The maize B73 *psy1* coding region (positive control) was available in another binary vector, *pBIN-ubi-b73-nos*, obtained from Dr Jason Geijskes (QUT) as purified pDNA. The *ubi-b73-nos* cassette was excised from the *pBIN* vector by *HindIII/EcoRI* double digestion and ligated into the *HindIII/EcoRI* linearised *pCAMBIA-1302* backbone. Completed vectors were sequenced using universal forward and reverse sequencing primers (Chapter 2.2.10) and *ubi-intron-F01* (5'-GATTTTTTTAGCCCTGCCTTC-3'), a forward primer designed to check restriction site integrity at the 3' end of the *ubi* promoter. Products from restriction digestions (carried out as per Chapter 2.2.2) were separated at each cloning stage using agarose gel electrophoresis and gel purified before the selected fragments were ligated together (Chapter 2.2.2 to 2.2.5). Ligation reactions were transformed into *E. coli* and selected on LB containing 100 µg/mL kanamycin (Chapter 2.2.6). Colonies containing putative clones were grown overnight and the plasmids recovered by alkaline lysis miniprep (Chapter 2.2.7 to 2.2.8). The *pCAMBIA-1302 psy* vector DNA was purified from *E. coli* using the UltraClean™ 6 Minute Mini Plasmid Prep Kit™ (Mobio Laboratories inc., Chapter 2.2.6), prior to transformation into *Agrobacterium*.

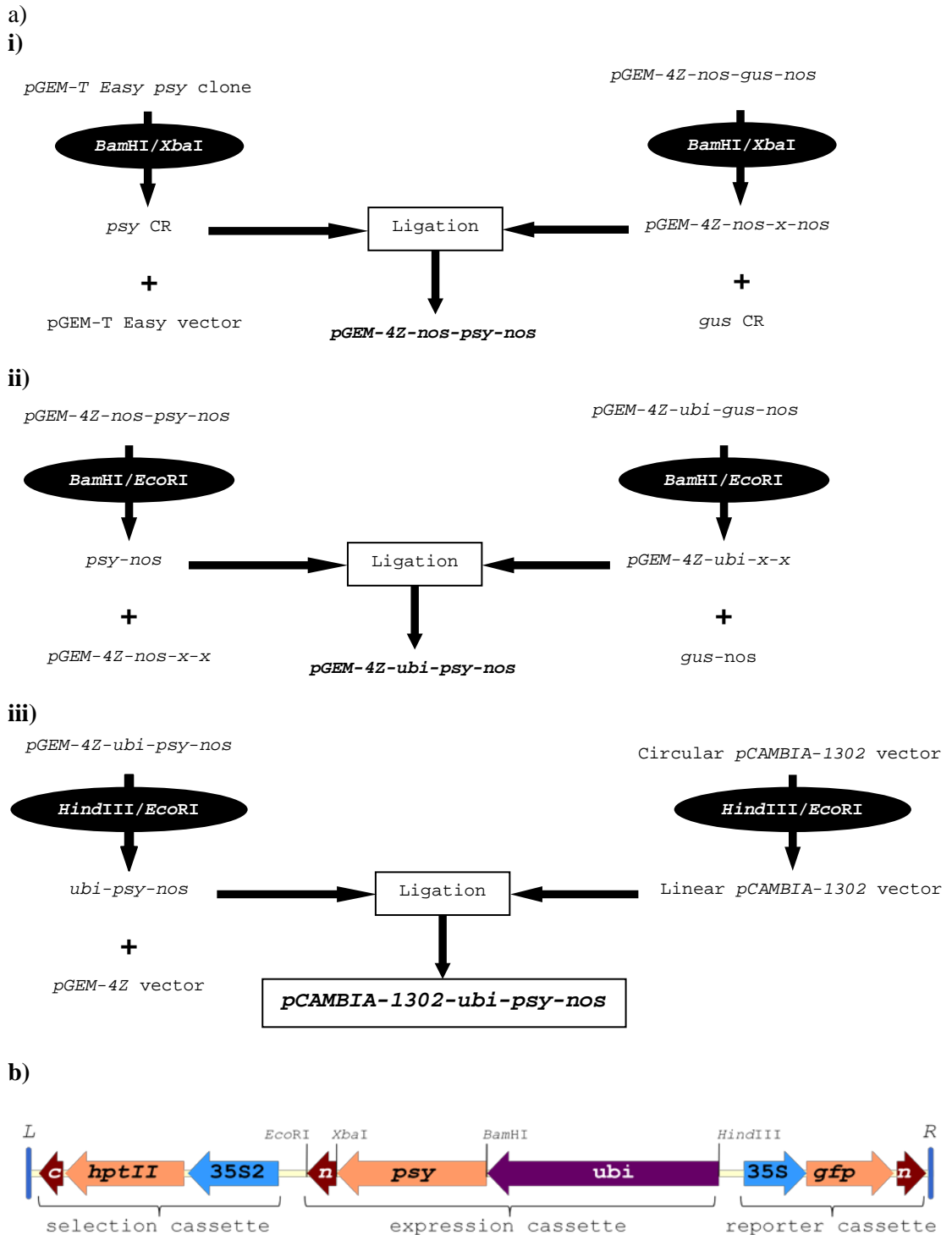


Figure 4.1: Construction of *psy* coding region binary vectors showing a) overview of steps used to subclone the banana *psy* coding regions into the *pCAMBIA-1302* binary vector: **i)** addition of nopaline synthase (*nos*) terminator (n) to *psy* coding region (CR), **ii)** addition of ubiquitin (*ubi*) promoter to *psy* coding region/*nos* terminator fragment to make a *ubi-psy-nos* expression cassette in pGEM-4Z and **iii)** insertion of *psy* expression cassette into *pCAMBIA-1302*. **b)** *pCAMBIA-1302* binary vector between the left (L) and right (R) T-DNA borders including the *psy*, hygromycin (*hptII*) selection and *gfp* reporter gene expression cassettes and including critical restriction sites. The position of sequence elements removed by restriction digestion is denoted as (x). The CaMV35S single (35S) and duplicated (35S2) promoters, and CaMV35S terminator (c) are marked.

4.2.3 Functional analysis of *psy* genes in rice

4.2.3.1 Callus induction and maintenance

Rice callus was selected as the model system for the comparison of Asupina and Cavendish PSY enzyme activity. Callus was induced from germinating rice seeds (*Oryza sativa L. ssp. japonica* cv. *Nipponbare*) essentially as previously described (CAMBIA, 2009b). Approximately 900 seeds were manually de-husked before incubation in three volumes of 70% ethanol for 1 min. Seeds were washed five times in mqH₂O and sterilised in a solution containing 4.0% hypochlorite (w/v) with one drop of Tween-20 and rotated on a suspension mixer (Ratek) at room temperature for 30 min at 30 rpm. Seeds were washed at least six times in sterile mqH₂O (until of the smell of bleach dissipated), blotted dry and plated at ~20 seeds per plate onto 2N6 media (Chapter 2.3) before germination in the dark at 25 °C for four weeks. Callus pieces, ~2.5 mm in size, were removed from the germinating seeds, transferred to fresh 2N6 media and multiplied for four weeks. Callus was maintained on 2N6 media with subculturing every four weeks.

4.2.3.2 Transformation of *Agrobacterium* with binary vectors

pCAMBIA-1302 and *pCAMBIA-1302-ubi-psy-nos* binary vectors containing maize *psy1*, and Asupina and Cavendish *psy1* and *psy2a* coding regions were transformed into *Agrobacterium tumefaciens* (AGL1 strain), using a modified protocol based on a previous method (Dower *et al.*, 1988). pDNA (~1 µg) was mixed with 50 µL electrocompetent AGL1 cells (kindly supplied by Don Catchpoole, QUT), transferred to an electroporation cuvette (Cell Projects; 0.2 cm electrode gap) and electroporated at 2800 V. The cells were mixed with SOC media (950 µL, Chapter 2.3) and incubated at 28 °C for 2 hr at 195 rpm. Transformed cells (50 µL) were plated onto solid LB media (Chapter 2.3) supplemented with 25 µg/mL rifampicin and 50 µg/mL kanamycin and incubated at 28 °C for 48 to 72 hr. Transformed colonies were inoculated into 5 mL LB liquid media (Chapter 2.3) containing 25 µg/mL rifampicin and 50 µg/mL kanamycin and incubated at 28 °C for 72 hr. Cultures were then streaked onto YM solid media (Chapter 2.3) containing the same antibiotic selection and grown at 28 °C for 72 hr. The transformed cells on YM solid media were stored at 4 °C and subcultured weekly onto fresh media. The *pART-TEST7* binary vector containing the *gfp* reporter gene, and used as a control vector, was obtained as an *Agrobacterium* (AGL1 strain) liquid culture (kindly supplied by Jennifer Kleidon, QUT) and was maintained on YM solid media containing 100 µg/mL spectinomycin.

4.2.3.3 Preparation of *Agrobacterium* for transformation of rice callus

A single *Agrobacterium* colony containing the plasmid of interest was inoculated in LB liquid media (5 mL), containing 100 µg/mL spectinomycin or 50 µg/mL kanamycin for *pART-TEST7* and *pCAMBIA-1302* vectors, respectively. Cultures were incubated at 28 °C for 72 hr at 195 rpm, before addition of further LB liquid media (20 mL) and incubation at 28 °C overnight at 195 rpm. Two overnight *Agrobacterium* cultures were prepared per pDNA treatment and bacterial concentration measured at OD₆₀₀.

4.2.3.4 Transformation of rice callus

Three methods for the *Agrobacterium*-mediated transformation of rice callus were investigated: (i) the transformation protocol according to CAMBIA (CAMBIA, 2009b), (ii) the centrifugation assisted *Agrobacterium*-mediated transformation (CAAT) method (Khanna *et al.*, 2004), and (iii) a modified version of the CAAT protocol that used media from the CAMBIA protocol. Proliferation and selection controls included untransformed rice callus grown on media with or without antibiotic selection.

(i) CAMBIA method

Overnight *Agrobacterium* cultures were pelleted by centrifugation at 3880 × g for 1 min at room temperature. The bacteria were resuspended in AAM media (Chapter 2.3) containing 100 µM acetosyringone to an OD₆₀₀ of 1.0 and incubated for 3 hr at room temperature with gentle shaking. Thirty rice calli (~2.5 mm in size), were mixed with *Agrobacterium* suspension (10 mL). Callus for the untransformed negative control was mixed with AAM media without *Agrobacterium*. This mixture was swirled vigorously then incubated for 40 min at room temperature. The callus was blotted dry on sterile paper towel and transferred to Petri dishes containing 2N6-AS (2N6 media with 100 µM acetosyringone) media. The calli were then co-cultivated with the *Agrobacterium* for 3 days at 25 °C in the dark.

(ii) CAAT method

Overnight *Agrobacterium* cultures were pelleted by centrifugation at 3880 × g for 10 min at room temperature. The bacteria were then resuspended in BRM media (Chapter 2.3) containing 100 µM acetosyringone to an OD₆₀₀ of 0.7 and incubated for 3 hr at room temperature with gentle shaking. Thirty subcultured calli (~2.5 mm in size) were mixed with 10 mL preheated 2N6 media and incubated for 5 min at 45 °C before removal of 2N6 media and addition of BRM media (10 mL) containing *Agrobacterium*. Untransformed control calli were mixed with BRM media lacking *Agrobacterium*. Pluronic F68 (0.02% v/v final concentration) was added to the calli, which were centrifuged at 670 × g for 10 min and

incubated at room temperature for 30 min. The BRM media was removed from the calli, which were blotted dry and co-cultivated with the *Agrobacterium* on CCM media (Chapter 2.3) for 3 days at 25 °C in the dark.

(iii) Rice heat shock method

The rice heat shock-assisted *Agrobacterium*-mediated protocol was essentially the same as the CAAT protocol with the following modifications. Firstly, the *Agrobacterium* cultures were pelleted by centrifugation at $3880 \times g$ for 1 min and resuspended in AAM media as per the CAMBIA protocol. Secondly, the calli were left to sit at room temperature for 40 min after centrifugation at $670 \times g$ for 10 min. Finally, the calli were blotted dry and left to co-cultivate on 2N6-AS media as per the CAMBIA protocol. This experiment was carried out to assess whether the CAAT method could be successfully modified to replace its more complex media with those used in the CAMBIA protocol.

Callus washing, selection and visual analysis of rice callus

After co-cultivation, calli were agitated in 25 mL timentin wash solution (200 µg/mL timentin in sterile mqH₂O) before incubation for 30 min at room temperature. The calli were washed in 25 mL timentin wash solution five times (until the solution was clear) and blotted dry on sterile filter paper. Calli were maintained in the dark at 25 °C on 2N6-TG40 (2N6 media supplemented with 200 µg/mL timentin and 40 µg/mL geneticin) and subcultured every two to four weeks for selection of *pART-TEST7* transformants. Cells transformed with *pCAMBIA-1302*-based vectors were initially incubated for two weeks in the dark at 25 °C in 2N6-TH25 (2N6 media supplemented with 200 µg/mL timentin and 25 µg/mL hygromycin) to assist cell recovery. Thereafter, callus was maintained in the dark at 25 °C on 2N6-TH50 media (2N6 supplemented with 200 µg/mL timentin and 50 µg/mL hygromycin) with subculturing every two to four weeks. Untransformed calli were grown with and without antibiotic selection to assess selection effectiveness and proliferative capacity, respectively. Calli were assessed for carotenoid accumulation and GFP expression two, four and six weeks post transformation and photographed using the SZ-CTV stereo microscope (Olympus) with CAMEDIA C-5060 camera (Olympus).

4.2.4 Analysis of carotenoid accumulation in rice callus

Carotenogenic callus (300 to 400 mg) was collected and freeze dried overnight in a Flexi-Dry MP freeze drying system (FTS Systems). The dried callus was weighed and ground with a 2 mm stainless steel bead in a Mini-Beadbeater-8 (Biospec Products) for 1 min at medium speed. Total carotenoids were extracted three times from the ground callus using acetone (2

mL, HPLC grade) and the supernatants collected at $3880 \times g$ for 5 min at room temperature under low light conditions to prevent carotenoid degradation. The acetone supernatants were pooled before addition of 2 mL 2:1 v/v petroleum ether 40-60 °C fraction (PE): diethyl ether (DE) [PE:DE, HPLC grade] and 1% w/v NaCl to a final volume of 14 mL, before extraction of carotenoids at $3880 \times g$ for 5 min at room temperature. The upper organic phase (1 mL) was collected and a further 1 mL PE:DE (2:1 v/v) was added to the acetone supernatants before another 1 mL of the organic phase was extracted. Extracted carotenoids were dried under vacuum and resuspended in 2 mL chloroform. For simplicity, total carotenoid content was assumed to be entirely β -carotene (measured at 465 nm) as carotenoid accumulation would be due to PSY activity. Samples were compared against a β -carotene (Sigma-Aldrich) standard curve measured at 465 nm and carotenoid concentration ($\mu\text{g/g}$ dry weight) was calculated. Results were graphed and analysed statistically in Excel 2007 (Microsoft) and SPSS v16 (SPSS Inc.), respectively.

4.3 Results

4.3.1 PSY protein sequence analysis

4.3.1.1 Primary sequence analysis

The primary amino acid sequences of three Asupina and three Cavendish PSY proteins were analysed for putative differences that could affect enzyme activity and possibly explain the variation in pVA accumulation in these cultivars. Maize B73 PSY1 (ZPSY1) was included for comparison.

Analysis of the PSY protein sequences against the CDD confirmed that they had the Trans-IPPS-HH domain required for isoprenoid synthesis (Figure 4.2). This domain contains the PSY active site and the amino acids that interact with the GGDP substrate and cation cofactor. Two aspartic acid rich motifs (ARMs, Figure 4.2), each five residues long, were predicted to serve the dual role of substrate and cofactor binding. However, the aspartic acid residues in both ARMs were also predicted to form part of the substrate binding pocket and active site (catalytic residues). The active site and substrate binding pocket also share many amino acids. ScanProsite analysis identified two motifs within the Trans_IPP-HH domain of the banana and maize PSY sequences called squalene/phytoene synthase signatures 1 and 2 (SQS-PSY1 and SQS-PSY2), which comprised 16 and 26 amino acids, respectively (Figure 4.2). The conserved SQS-PSY signatures formed by the alignment of the six banana PSY sequences and ZPSY1 were referred to as the local consensus (Figure 4.2). SQS-PSY1 was completely conserved in all banana PSY sequences and ZPSY1, while SQS-PSY2 was not as highly conserved as SQS-PSY1.

```

1      11      21      31      41
APSY2B  ERCGEVCAEYAKNFYLGTLMLTPERRRAIWAIDVWCRRTDELVDGPNASH
CPSY2B  ERCGEVCAEYAKTFYLGTLMLTPERRRAIWAIVVWCRRTDELVDGPNASH
APSY2A  ERCGEVCAEYAKTFYLGTLMLTPERRRAIWAIVVWCRRTDELVDGPNASH
CPSY2A  ERCGEVCAEYAKTFYLGTLMLTPERRRAIWAIVVWCRRTDELVDGPNASH
APSY1   DRCGEVCAEYAKTFYLGTLMLTPERRRAIWAIVVWCRRTDELVDGPNASQ
CPSY1   DRCGEVCAEYAKTFYLGTLMLTPERRRAIWAIVVWCRRTDELVDGPNASQ
ZPSY1   DRCGEICEEYAKTFYLGTLMLTEERRRAIWAIVVWCRRTDELVDGPNANY
Lid     .....YAKTF.....
Catalytic .....F.....Y.....D...D.....
Pocket   .....K.F.....Y...R..D...D.....
ARM1    .....DELVD.....

51      61      71      81      91
APSY2B  MTPPTALDRWQNRLEDLFNCRPYDLYDAALSDTVSKFPVDIQPFKAMVDGM
CPSY2B  MTPPTALDRWQNRLEDLFNDRPYDMYDAALSDTVSKFPVDIQPFKDMIDGM
APSY2A  ITPTALDRWSNRLEDLFAGRPYDMYDAALSDTVSKFPVDMQPFKDMVEGM
CPSY2A  ITPTALDRWSNRLEDLFAGRPYDMYDAALSDTASNFVDMQPFKDMIEGM
APSY1   ITPTALDRWESRLEDVDFAGRPYDMLDAALSDTVSKYPVDIQPFKDMIEGM
CPSY1   ITPTALDRWESRLEDVDFAGRPYDMLDAALSDTVSKYPVDIQPFKDMIEGM
ZPSY1   ITPTALDRWEKRLEDLFTGRPYDMLDAALSDTISRFPIDIQPFKDMIEGM

101     111     121     131     141
APSY2B  RMDLWKSRYNNFDELYLYCYVAGTVGLMSVPVMGIAPDSKASTESVYNA
CPSY2B  RMDLWKSRYNNFDELYLYCYVAGTVGLMSVPVMGIAPDSKASTESVYNA
APSY2A  RMDLWKSRYKNFDELYLYCYVAGTVGLMSVPVMGIAPDSKASAESVYGA
CPSY2A  RMDLWKSRYKNFDELYLYCYVAGTVGLMSVPVMGIAPDSKASAESVYSA
APSY1   RMDLWKSRYKNFDELYLYCYVAGTVGLMSVPVMGIAPESKATTESVYGA
CPSY1   RMDLWKSRYKNFDELYLYCYVAGTVGLMSVPVMGIAPESKATTESVYGS
ZPSY1   RSDLWKTRYNNFDELYMYCYVAGTVGLMSVPVMGIATESKATTESVYSA
Catalytic .....Y.....V...S.....
Pocket   .....Y...A...G.....
SQS-PSY1 .....YCYVAGTVGLmSvpV.....

151     161     171     181     191
APSY2B  ALALGIANQLTNILRDVGEDARRGRIYLPQDELAQAGLSDDDDIFKGRVTD
CPSY2B  ALALGIANQLTNILRDVGEDARRGRIYLPQDELAQAGLSDDDDVFEGRVTD
APSY2A  ALALGIANQLTNILRDVGEDSRRGRVYLPQDELAQAGLSDDDDVFEGRVTD
CPSY2A  ALALGIANQLTNILRDVGEDSRRGRVYLPQDELAHAGLSDDDDVFEGRVTD
APSY1   ALALGLANQLTNILRDVGEDARRGRIYLPQDELAQAGISDEDIFDGKVTE
CPSY1   ALALGLANQLTNILRDVGEDARRGRIYLPQDELAQAGLSDEDIFGGKVTE
ZPSY1   ALALGIANQLTNILRDVGEDARRGRIYLPQDELAQAGLSDEDIFKGVVTN
Catalytic .....N.....RD...D....R.....
Pocket   ...G..N.....RD..ED....R.....
ARM2    .....DVGED.....
SQS-PSY2 ...LGianQltNIlRDVgeDarrgRiYlP.....

201     211     221     231     241
APSY2B  KWRSFMKGQIRARMFFEEAEKGIYELNSASRWPVLASLLLYRQILDAIE
CPSY2B  KWRSFMKGQIRARMFFEEAEKGIHELNSASRWPVLASLLLYRQILDAIE
APSY2A  KWRTFMKGQITRARMFFDEAEKGIYELNSASRWPVLASLLLYRQILDAIE
CPSY2A  KWRTFMKGQITRARMFFDEAEKGIYELNSASRWPVLASLLLYRQILDAIE
APSY1   KWRSFMKNQIKRARMFFQQAEEAGVTELNRASRWPVWASLQLYRQILDEIE
CPSY1   KWRSFMKNQIKRARMFFQQAEEAGVTELNRASRWPVWASLQLYRQILDEIE
ZPSY1   RWRNFMKROIKRARMFFEEAERGVELSQASRWPVWASLLLYRQILDEIE
Catalytic .....WP...S.....
Pocket   .....WP.....

251     261
APSY2B  ANDYNNFTRRAYVGIKAKLA
CPSY2B  ANDYNNFTRRAYVGKAKKLA
APSY2A  ANDYNNFTKRAYVGKAKKLA
CPSY2A  ANDYNNFTKRAYVGKAKKLA
APSY1   ANDYNNFTKRAYVSKAKKLL
CPSY1   ANDYNNFTKRAYVSKAKKLL
ZPSY1   ANDYNNFTKRAYVGKAKKLL
Lid     .....RAYV.....

```

Figure 4.2: Primary structure of banana PSY proteins. Sequence alignment showing the location of the functional residues in the Trans-IPPS-HH domain predicted by the Conserved Domain Database (CDD) that constitute the active site lid (Lid), catalytic residues (Catalytic), GGPP binding pocket (Pocket) and substrate/Mg²⁺ binding sites (ARM1 and ARM2; which are also the aspartic acid rich regions) in their respective positions below the alignment. The squalene/phytoene synthase signatures 1 and 2 (SQS-PSY1 and SQS-PSY2) were included for comparison. Partially conserved amino acids are highlighted in grey. The Trans-IPPS-HH domain is represented by residues at different positions in the: APSY1 (137 to 406), CPSY1 (137 to 406), APSY2A (104 to 373), CPSY2A (107 to 376), PSY2B (106 to 375) and ZPSY1 (120 to 389) proteins. Upper and lower case letters in SQS-PSY1 and SQS-PSY2 represent amino acids that are critical and non critical, respectively, according to the respective Prosite consensus sequences.

Comparison of the residues characterised using CDD with the SQS-PSY motifs showed that SQS-PSY1 contained three residues of the active site and substrate binding pocket. Comparatively, SQS-PSY2 accounted for approximately 39% of the substrate binding pocket residues and 33% of the catalytic residues. Interestingly, several conserved residues in the SQS-PSY motifs (designated by capital letters in Figure 4.2 local consensus) were not assigned a function by CDD (Figure 4.2). All but two of the functional residues in the motifs identified by CDD were completely conserved across the analysed banana and maize sequences. These differences, which both occurred in APSY2B, were in the fourth residue of the first active site lid motif (T118N) and at the tyrosine residue that appears to be involved in both catalytic activity and substrate binding, respectively (Y135D, Figure 4.2). Many amino acids other than the functional residues were not conserved, and some differences were unique to specific PSYs. However, there were numerous examples where limited conservation was observed in a manner similar to that previously observed upon analysis of the SQS-PSY2 motif. In these cases one group of proteins shared a particular residue at a given position while the other group of sequences shared a different residue at the same position; this was also observed for pairs of neighbouring amino acids. For example, the glutamic acid residue at position 191 (Figure 4.2) in the PSY1 proteins was an aspartic acid residue in the PSY2A and PSY2B at this location. This residue was located in a region with several aspartic acid residues, 11 amino acids C-terminal to SQS-PSY2 whose residues were DED and DDD in the PSY1 and PSY2 proteins, respectively (Figure 4.2). In total, 35 residues were conserved in this manner.

4.3.1.2 Secondary and tertiary sequence analysis

Secondary structure of the PSY protein was examined for putative structural differences that could affect enzyme function in light of the primary structure analysis. The banana and maize PSYs consisted primarily of α -helices and coiled regions with a small number of residues in extended configuration (Figure 4.3a). Fifteen predicted α -helices were conserved in all the banana PSY proteins and ZPSY1 within a region of approximately 320 amino acids. Generally, the lengths of these helices were well conserved across these proteins, especially towards the C-terminus where the functional domain is located (Figure 4.3a). Predicted lengths of conserved α -helices range from two (Helix 13) to approximately 30 amino acids (Helix 9), and some were separated by only one or two residues. However, the lengths of some of the conserved helices did vary between the PSY proteins. The most notable was Helix 1, which was approximately 20 amino acids in all PSYs except CPSY2A where it was 28 amino acids long. This was predicted to be due to a tandem repeat of 3

a)

Exon 1

Helix #	n1	n2	n3	
APSY2B	MSGIVVVVSP-----KESIR-----CSLLNQFIEVKRRSWRRSSVA-----			37
CPSY2B-gDNA	MSGIVVVVSP-----KESIR-----CSLLNQFIEVKRRSWRRSSVE-----			37
APSY2A	MSGIVVVVATP-----KEASR-----SSGFNQFVGVTRRWRSSSAG-----			37
CPSY2A	MSGVVVVVVSP-----KETS-----SSGFQFAGVKRRWRSSSAG-----			37
APSY1	MACLLLRMTAPADIPSGLSAEAVREGDHLPRKAFPPRNNRNLRSRKRRLWSLRSPHADSK			60
CPSY1	MACLLLRMTAPADIPAGLGSAEATREGDRFPKRAFPRNNRNLRSRKRRLWSLRSPHADSK			60
ZPSY1	MATILVRAASP-----GLSAADSIHQGTLCSTLL-KTKRPAARRWMPCSLLGLHP---			51
	*: : : * :	:	:	* *

Helix #	n4	n5	n6	c1	###
APSY2B	WSFSRPAPASG--HSPVASLVVTPP---RTSEELVYEVVLRQAALVGETKRRKP-ATVQ				90
CPSY2B-gDNA	WTCRSRPAPSSG--HSVSASLVVTPP---RTSEELVYEVVLRQAALVGETRKRKP-TAVR				90
APSY2A	WSCARSASTAR--RSVSASLVVTPP---RSSEELVDVLRQAALVGDARRK---AVE				88
CPSY2A	WSCARSASTAR--RSVSASLVVTPP---RSSEALVDVLRQAALVGEARRKRAVEAVE				91
APSY1	YASLRFDPESGRNPLVSSLLTSTAGEVAVSSEQKVYNVVLKQAALV--KQPRSSTAPD				118
CPSY1	YASLRFDPESGMNPLVSSLLTSTAGEVAVSAEQKVYNVVLKQAALV--KQPRSSTALD				118
ZPSY1	WEAGRPS-----AVYSSLAVNPAGEAVVSSQKVYDVLKQAALL--KRQLR-TPVLD				102
	: * .	: : **	:	: * ** : * : * : * : * : * : * : * : * : * : *	: : *

Exon 2

Helix #	c2	c3	c4
APSY2B	LPP---VPLRGDLLYEAYERCGEVCAEYAKNFYLGTLTLLMTPERRRAIWAIVWCRRTDE		146
CPSY2B-gDNA	LPQ---VPLRGDLLYEAYERCGEVCAEYAKTFYLGTLTLLMTPERRRAIWAIVWCRRTDE		146
APSY2A	APP---APLRGDLDAAYERCGEVCAEYAKTFYLGTLTLLMTPERRRAIWAIVWCRRTDE		144
CPSY2A	APP---APLRGDLDAAYERCGEVCAEYAKTFYLGTLTLLMTPERRRAIWAIVWCRRTDE		147
APSY1	VKP-DTVIPGSVGLLKEAYDRCGEVCAEYAKTFYLGTLTLLMTPERRRAIWAIVWCRRTDE		177
CPSY1	VKP-DTVIPGSVGLLKEAYDRCGEVCAEYAKTFYLGTLTLLMTPERRRAIWAIVWCRRTDE		177
ZPSY1	ARPQDMDMPRNG--LKEAYDRCGEICEEYAKTFYLGTLTLLMTEERRRAIWAIVWCRRTDE		160
	*	* ** : * : * * : * : * : * : * : * : * : * : * : * : * : * : * : * : *	

Exon 3

Helix #	c5	c6	c7
APSY2B	LVDGPNASHMTPALDRWQNRLEDLFNGRFPYDLYDAALSDTVSKFPVDIQPFKAMVDGMR		206
CPSY2B-gDNA	LVDGPNASHMTPALDRWQNRLEDLFNDRFPYDLYDAALSDTVSKFPVDIQPFKDMIDGMR		206
APSY2A	LVDGPNASHITPTALDRWNRLEDLFAGRPYDLYDAALSDTVSKFPVDMQPFKDMVEGMR		204
CPSY2A	LVDGPNASHITPTALDRWNRLEDLFAGRPYDLYDAALSDTASNFPVDMQPFKDMIEGMR		207
APSY1	LVDGPNASQITPTALDRWESRLEDVFAGRPYDMLDAALSDTVSKYPVDIQPFKDMIEGMR		237
CPSY1	LVDGPNASQITPTALDRWESRLEDVFAGRPYDMLDAALSDTVSKYPVDIQPFKDMIEGMR		237
ZPSY1	LVDGPNANYITPTALDRWEKRLLEDLFTGRPYDMLDAALSDTISRFPIDIQPFKDMIEGMR		220
	*****	: ***** . * : * * : * : * : * : * : * : * : * : * : * : * : * : * : * : *	

Exon 4

Helix #	c8	c9
APSY2B	MDLWKSRYNNFDELYLYCYVAGTVGLMSVPVVGIAIPDSKASTESVYNAALALGIANQLT	266
CPSY2B-gDNA	MDLWKSRYNNFDELYLYCYVAGTVGLMSVPVVGIAIPDSKASTESVYNAALALGIANQLT	266
APSY2A	MDLRKSRYKNFDELYLYCYVAGTVGLMSVPVVGIAIPDSKASAESVYGAALALGIANQLT	264
CPSY2A	MDLRKSRYKNFDELYLYCYVAGTVGLMSVPVVGIAIPDSKASAESVYSAALALGIANQLT	267
APSY1	MDLKKRYKNFDELYLYCYVAGTVGLMSVPVVGIAIPESKATTESVYGAALALGIANQLT	297
CPSY1	MDLKKRYKNFDELYLYCYVAGTVGLMSVPVVGIAIPESKATTESVYGSALALGIANQLT	297
ZPSY1	SDLRKTRYNNFDELYMYCYVAGTVGLMSVPVVGIAIPESKATTESVYSAALALGIANQLT	280
	** * : *	

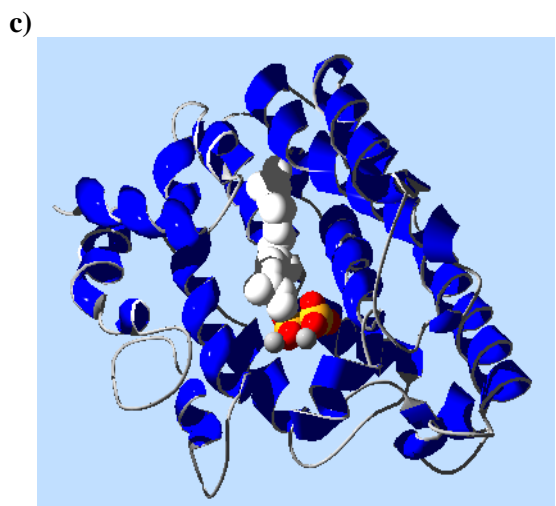
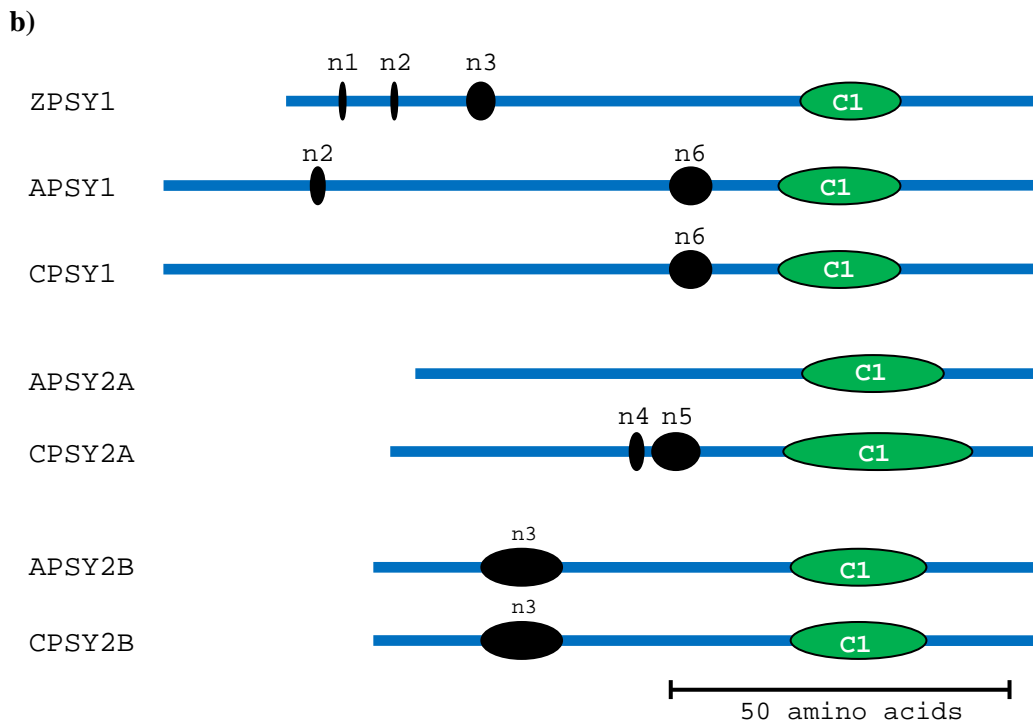
Exon 5

Helix #	c10	c11	c12
APSY2B	NILRDVGEDARRGRITVLPQDELAQAGLSDDDFKGRVTDKWRFSFMKGQIRRRARMFEEAE		326
CPSY2B-gDNA	NILRDVGEDARRGRITVLPQDELAQAGLSDDDFKGRVTDKWRFSFMKGQIRRRARMFEEAE		326
APSY2A	NILRDVGEDSRRGRVYLPQDELAQAGLSDDDFEGRVTDKWRTFMKGQITRRARMFDEAE		324
CPSY2A	NILRDVGEDSRRGRVYLPQDELAHAGLSDDDFEGRVTDKWRTFMKGQITRRARMFDEAE		327
APSY1	NILRDVGEDARRGRITVLPQDELAQAGISDEDIFDGKVTWKWRFSFMKNQIKRRARMFQOAE		357
CPSY1	NILRDVGEDARRGRITVLPQDELAQAGLSDEDIFGGKVTWKWRFSFMKNQIKRRARMLFQOAE		357
ZPSY1	NILRDVGEDARRGRITVLPQDELAQAGLSDEDIFKGVVTRWRNRFMKRQIKRRARMFEEAE		340
	*****	: ***** : * : * : * : * : * : * : * : * : * : * : * : * : * : * : * : * : *	

Exon 6

Helix #	c13	c14	c15
APSY2B	KGIYELNSASRWVFLASLLLYRQILDAIEANDYNNFTRRAYVGIKAKKLASLPAYARALR		386
CPSY2B-gDNA	KGIHELNSASRWVFLASLLLYRQILDAIEANDYNNFTRRAYVGIKAKKLASLPAYARALR		386
APSY2A	KGIYELNSASRWVFLASLLLYRQILDAIEANDYNNFTRRAYVGIKAKKLASLPAYAKAVI		384
CPSY2A	KGIYELNSASRWVFLASLLLYRQILDAIEANDYNNFTRRAYVGIKAKKLASLPAYAKAVI		387
APSY1	AGVTELNRSASRWVWASLQLYRQILDEIEANDYNNFTRRAYVSKAKKLLALPVAYGRSLI		417
CPSY1	AGVTELNRSASRWVWASLQLYRQILDEIEANDYNNFTRRAYVSKAKKLLALPVAYGKSLI		417
ZPSY1	RGVTELSQASRWVWASLLLYRQILDEIEANDYNNFTRRAYVGIKAKKLLALPVAYGKSLI		400
	* : * . *****	*** ***** ***** : * : * : * : * : * : * : * : * : * : * : * : * : * : * : * : *	

Helix #	n7
APSY2B	-GPSRFTGART- 397
CPSY2B-gDNA	-GPSRFTGART- 397
APSY2A	VGPSRFAGTL--- 394
CPSY2A	VGPSRFAGTL--- 397
APSY1	SPSSLSQSSLAKT 430
CPSY1	SPSSLSQSNLAKT 430
ZPSY1	LPCSLRNGQT--- 410
	* .



d)

protein	e-value	ratio
ZPSY1	4.85E ⁻²⁷	3.83
APSY1	2.63E ⁻²⁶	20.78
APSY2A	1.26E ⁻²⁷	1.00
APSY2B	2.25E ⁻²⁶	17.80
CPSY1	3.39E ⁻²⁶	26.80
CPSY2A	1.34E ⁻²⁷	1.06
CPSY2B	2.66E ⁻²⁷	2.10

Figure 4.3: Analysis of secondary and tertiary structure of banana PSY proteins. **a)** Alignment of Asupina and Cavendish PSY proteins and maize ZPSY1 with secondary structure prediction using SSpro v4.5 that predicts the structure of amino acids as either coiled (plain text), α -helical (grey highlighting) or extended conformation (white text highlighted in black). The α -helices are numbered above the alignment as conserved (numbers c1 to c15) or non-conserved (numbers n1 to n7). The exons encoding the different parts of PSY are labelled with the locations of exons 2, 4 and 6 indicated by boxes. **b)** Scale diagram of the putative PSY signal peptide region showing the relative positions of the six predicted non-conserved α -helices (n1 to n6, black shapes) and conserved α -helix 1 (c1, green shape) along the PSY sequence (blue line). **c)** Predicted tertiary structure of APSY1 is shown as an example to illustrate the organisation of α -helices (blue ribbons) and loop regions (grey strands) and the expected orientation of the GGPP substrate (white hydrocarbon chain with yellow and red phosphate group) and Mn^{2+} atoms (grey spheres). **d)** Table of e-values from the tertiary structure prediction and their ratio compared to APSY2A, which was the most similar to the human SQS template structure (RSCB PDB No. 1ezf). Note, that 100% modelling precision for all tertiary structures was estimated for all PSY proteins studied.

amino acids, AVE, at the C-terminal end of the helix (Figure 4.3a). Interestingly, APSY2A had a single AVE repeat, which was not present in any of the PSY1 or PSY2B proteins. At the N- and C-termini of this conserved region the secondary structure was primarily composed of coiled regions. However, non-conserved α -helical structures were found in some PSY proteins, labelled n1 to n6, which were located in the putative signal peptide (Figure 4.4b). The most notable were helices n3 to n6. Helix n3 was 16 amino acids from the N-terminus of APSY3B and CPSY2B and was 11 to 12 residues long. ZPSY1 also had a helix (Helix n3) which was only 4 amino acids long. Helices n4 (3 amino acids) and n5 (7 amino acids) were in the N-terminus of CPSY2A, 40 amino acids from the start of the protein and were separated by a single amino acid. Interestingly, these were absent from APSY2A. The α -helix at position n6 was 6 and 7 amino acids long in Asupina and CPSY1, respectively. These predicted differences in the structures of the putative signal peptide region of the banana PSYs (Figure 4.3b) may influence their activity. The putative non-conserved α -helices at the C-terminus were very close to the end of APSY1, CPSY2A and ZPSY1 in a position labelled n7 and consisted of one or two amino acids.

Tertiary structure was initially examined by homology modelling of the PSY primary sequences using the first approach method on the SWISS-MODEL server. However, using this method no suitable tertiary structure was identified. Subsequently, tertiary structure analysis was performed using PHYRE fold recognition server (Figure 4.3c). The template for the predicted tertiary structure was the human SQS α -chain (RSCB PDB No. 1ezf), which was approximately 280 amino acids long and represented approximately 88% of the conserved α -helical region. This template was the only significant match for all the banana PSY proteins and ZPSY1 (Figure 4.3d), returning the highest predicted protein threading precision (100%) and lowest e-values, ranging from $1.26E^{-27}$ (APSY2A) to $3.39E^{-26}$ (CPSY1). An e-value ratio was calculated to provide a comparison of the predicted PSY tertiary structures relative to APSY2A, which was most similar to the human SQS template structure. These ratios were used to gauge the level of overall structural variation among banana PSYs, and suggested that the tertiary structures of CPSY2A, CPSY2B and ZPSY1 were most related to Asupina PSY2A as their e-value ratios were between 1.1 and 3.8 fold higher. In contrast, the structures of APSY2B, Asupina PSY1 and CPSY1 were least similar to APSY2A as their e-values were between 17.8 and 26.7 fold higher. Orientation of the GGPP substrate, based on comparison with the PDB structure of substrate-bound human SQS (RSCB PDB No. 2Q80), suggested that it was positioned in the protein with the charged phosphate group closest to the surface and the hydrocarbon chain in the protein core (Figure 4.3c). Despite the many differences observed at the levels of primary, secondary and tertiary

structure, none of these variations appeared to conclusively relate to the differences in pVA accumulation between the Asupina and Cavendish PSYs.

4.3.2 Functional analysis of banana PSYs

Rice callus was used as a model system, to compare the relative ability of the banana PSY proteins to synthesise carotenoids, as banana embryogenic cells were not available at the time. The binary vector, *pCAMBIA-1302*, encoding the hygromycin phosphotransferase II (HPTII) selectable marker and *gfp* reporter gene, was selected as the base vector for *Agrobacterium*-mediated transformation as hygromycin selection has been used successfully for rice transformation (Hiei *et al.*, 1994). It was also rationalised that the presence of the *gfp* reporter gene, in addition to the *psy* genes, would facilitate monitoring of the transformation process. Asupina and Cavendish *psy1* and *psy2a* coding regions were selected for analysis and subcloned into *pCAMBIA-1302*, as they were the major *psy* sequences obtained using degenerate primers from leaf and fruit, respectively (Chapter 3).

4.3.2.1 Rice callus induction and optimisation of transformation

Rice seeds were successfully germinated and produced callus over a four week period (Figure 4.4a). Although some seeds produced complex root structures with no usable callus (Figure 4.4a i), most seeds responded by producing a simple root structure in addition to callus tissue, which budded off the seeds in place of the shoots and was friable and white in colour (Figure 4.4a ii). Callus was excised from the germinating seeds and multiplied in preparation for transformation (Figure 4.4a iii).

Rice transformation was being undertaken by other researchers at QUT; however, several different procedures were being used. Therefore, the first experiment compared three available *Agrobacterium*-mediated transformation methods to determine the most efficient protocol: i) the rice transformation protocol according to CAMBIA, ii) the centrifugation assisted *Agrobacterium*-mediated transformation (CAAT) method, and iii) a modified version of the CAAT protocol that used media from the CAMBIA protocol. The *pART-TEST7* binary vector, encoding the sGFP (S65T) protein regulated by the CaMV 35S promoter and catalase intron, was used to test transformation efficiency as it had previously been used at QUT and was known to be functional in rice callus. Four replicate plates of callus (~30 individual calli per plate) were transformed separately with *pART-TEST7* for each of the three transformation methods. One plate of ~30 untransformed calli was included in each experiment as proliferation (no antibiotic selection) and selection controls. This experiment showed qualitatively that the CAAT method was the most efficient method for

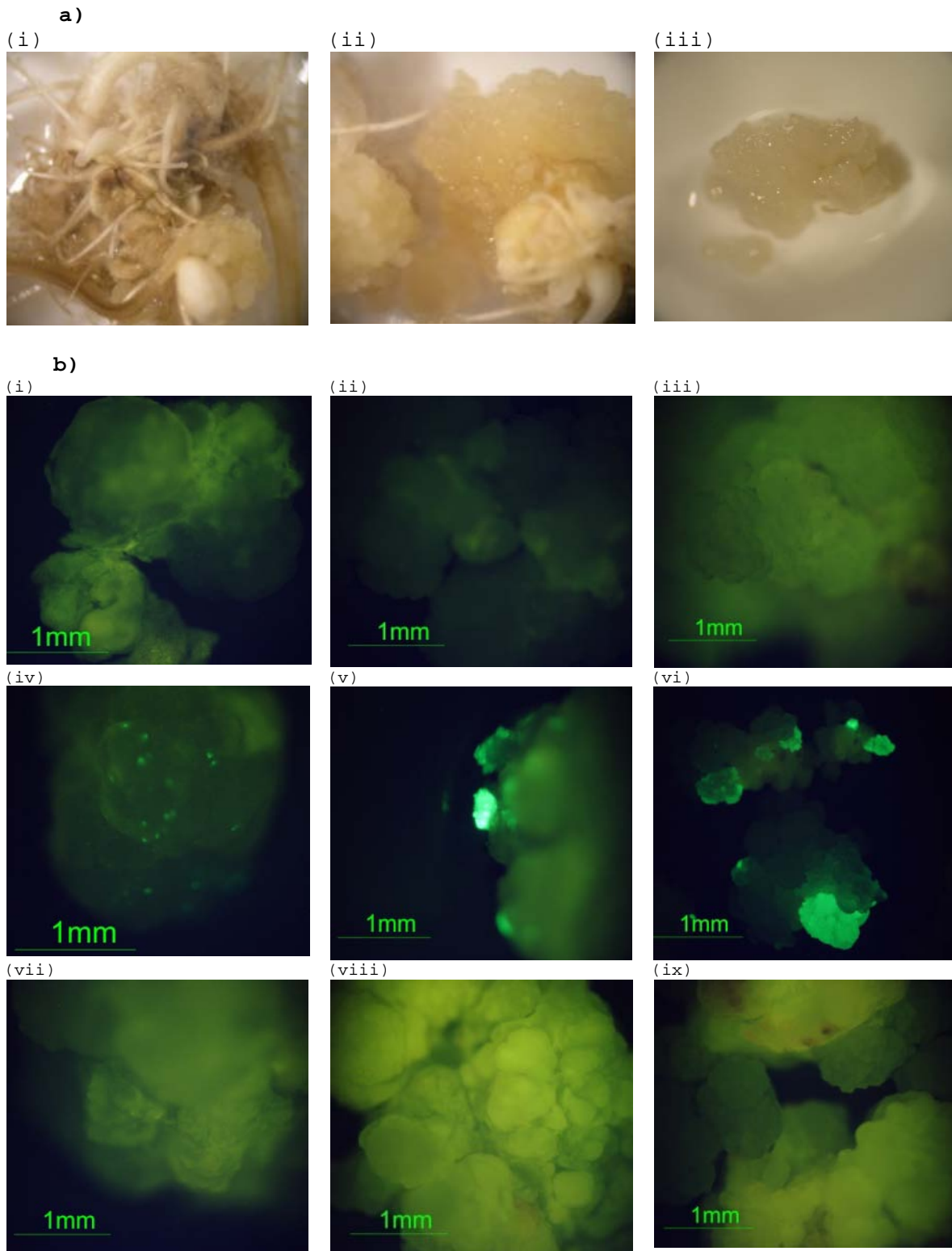


Figure 4.4: Testing of GFP reporter genes in rice callus. a) Induced rice callus after 4 weeks showing seeds with (i) complex root structure, (ii) callus and simple roots structure (iii) callus transferred from seeds. **b)** Comparison of GFP expressed by *pART-TEST7* and *pCAMBIA-1302* binary vectors which have different versions of the *gfp* reporter gene. Untransformed rice callus after (i) 3 days, (ii) 7 days and (iii) 2 weeks on selection as a negative control. Rice callus transformed with sGFP encoded by *pART-TEST7* was monitored for transient expression after 3 days (iv) and stable expression after 7 days (v) and 2 weeks (vi) and compared to callus transformed with mGFP5 encoded by *pCAMBIA-1302* after 3 days (vii), 7 days (viii) and 2 weeks (ix).

rice callus transformation, producing higher numbers of transiently transformed cells than the other two methods after three days and more stably transformed callus after two weeks (results not shown). This method was used for all further transformation experiments.

The relative transformation efficiencies of the *pART-TEST7* (sGFP reporter gene) and *pCAMBIA-1302* (mGFP5 reporter gene) vectors in rice callus were compared before undertaking experiments with *psy* constructs. *Agrobacterium* cultures containing these vectors were each used to transform four separate batches of callus (~30 calli) that were grown on separate selection plates. Two replicate plates of untransformed calli (~30) were included as proliferation and selection controls respectively. Callus exhibited some autofluorescence (Figure 4.4b i), however, transient expression was seen in *pART-TEST7* transformed callus after three days as bright foci (Figure 4.4b iv) which were not present in the untransformed callus control (Figure 4.4b i). After further selection (1-2 weeks), stable GFP expression was seen in large clumps of callus (Figure 4.5b v & vi) compared to the untransformed tissue (Figure 4.4b ii & iii). In contrast, *pCAMBIA-1302* gave no visible transient or stable GFP expression after more than two weeks of culture (Fig 4.4b, vii-ix), although clumps of regenerating callus were apparent. It was subsequently determined that the GFP version encoded by *pCAMBIA-1302* (mGFP5) expresses poorly in rice (CAMBIA, 2009a). As there was insufficient time to change the reporter gene in the *pCAMBIA-1302*-based *psy* constructs, they were used directly for rice transformation.

4.3.2.2 Comparison of banana *psy* genes in rice

The Asupina and Cavendish *psy1* and *psy2a* coding regions were selected for transformation into rice callus because they appeared to be the predominant *psy* genes in leaf and fruit respectively. The *psy2b* coding regions were not tested due to the high similarity between the Asupina and Cavendish *psy2b* sequences, and the latter differed from its genomic sequence (Chapter 3).

A pilot study was undertaken with selected *psy* constructs to confirm the ability of rice callus to accumulate carotenoids in the absence of other carotenoid biosynthetic genes. Four batches of callus were transformed with the *pCAMBIA-1302* base vector (included as a negative control), maize *psy1*, and the Asupina *psy1* and *psy2a* vectors. Untransformed controls (two replicates) were also included. The hygromycin selection regime successfully inhibited the proliferation of untransformed rice callus, which appeared necrotic and was considered dead after six weeks on selection (results not shown). Callus appearing to arise from different transformation events was grown separately as “callus lines” during selection,

such that all multiplying tissue could be traced to the original transformation event. Evidence of carotenoid expression was first seen four weeks post transformation as a change in colour of the transformed callus. Calli transformed with the *psy* constructs exhibited a range of colours from creamy white, similar to the negative control, to pale yellow to dark orange (Figure 4.5). The colour became more obvious six weeks post transformation as the transformed calli began to proliferate on selection. This range of colours was seen in transformations with all the *psy* constructs, although the proportion of each colour varied between treatments. Rice callus transformed with *Zpsy1* appeared to exhibit more orange clumps of calli compared to plates of callus transformed with *Apsy1* and *Apsy2a*.

Consequently, a large scale rice transformation experiment was carried out to compare the carotenoid accumulation of Asupina and Cavendish PSYs. Rice callus was transformed with *pCAMBIA-1302* alone (negative control) or containing the banana *Apsy1*, *Apsy2a*, *Cpsy1* and *Cpsy2a*, or maize *Zpsy1* (positive control) sequences; untransformed rice callus was also included as a control for multiplication and selection. The number of batches of calli transformed for each *psy* construct and untransformed controls, and the segregation of “callus lines” was as per the pilot study. Hygromycin selection efficacy was consistent with that observed in the pilot experiment (Figure 4.6 ii). Carotenoid accumulation, seen as a range of colours from creamy white, light yellow to dark orange, was observed in all the *psy* treatments while no accumulation was seen in the *pCAMBIA-1302* vector or untransformed controls (Figure 4.6). As previously observed in the pilot experiment, maize *Zpsy1* plates appeared to have larger amounts of orange callus than banana *psy* plates. However, although not as prolific, all banana *psy* treatments had some dark orange callus. Often, very dark orange callus did not multiply well, as evidenced by very small, dark clumps of callus (results not shown). Many of the proliferating clumps of callus had mixtures of colour, ranging from white to yellow and orange (Figure 4.6 viii).

Quantitative analysis of carotenoid accumulation was undertaken to confirm that visual observations (colour) correlated with actual carotenoid accumulation. Rice callus was multiplied for 22 weeks post transformation and carotenogenic callus clumps were selected by colour and photographed, before total carotenoids were extracted and quantified by spectrophotometry. Callus (300 to 400 mg wet weight) was harvested from each line according to colour, and tissue from different lines were analysed separately, allowing observation of the variation arising from different transformation events. The correlation between callus colour and β -carotene content was first investigated using transformed *Zpsy1* lines (Figure 4.7). Untransformed calli and *pCAMBIA-1302* negative control calli (line 4A-

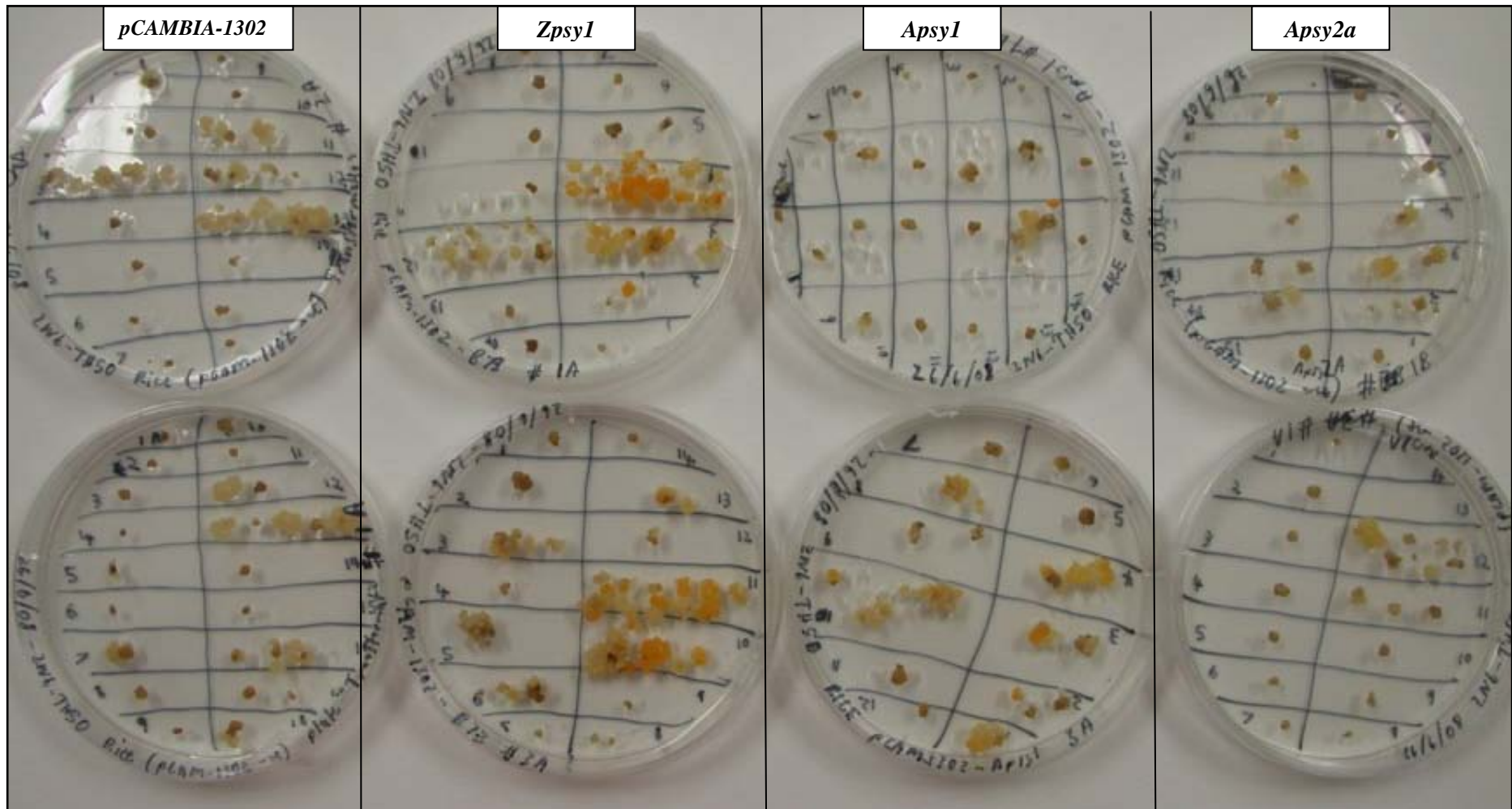


Figure 4.5: Pilot experiment to confirm carotenoid accumulation in transgenic rice callus. Plates of rice callus transformed with *pCAMBIA-1302* (negative control), maize *Zpsy1* (positive control), *Apsy1* and *Apsy2a* coding regions were photographed 6 weeks post transformation [4× magnification].

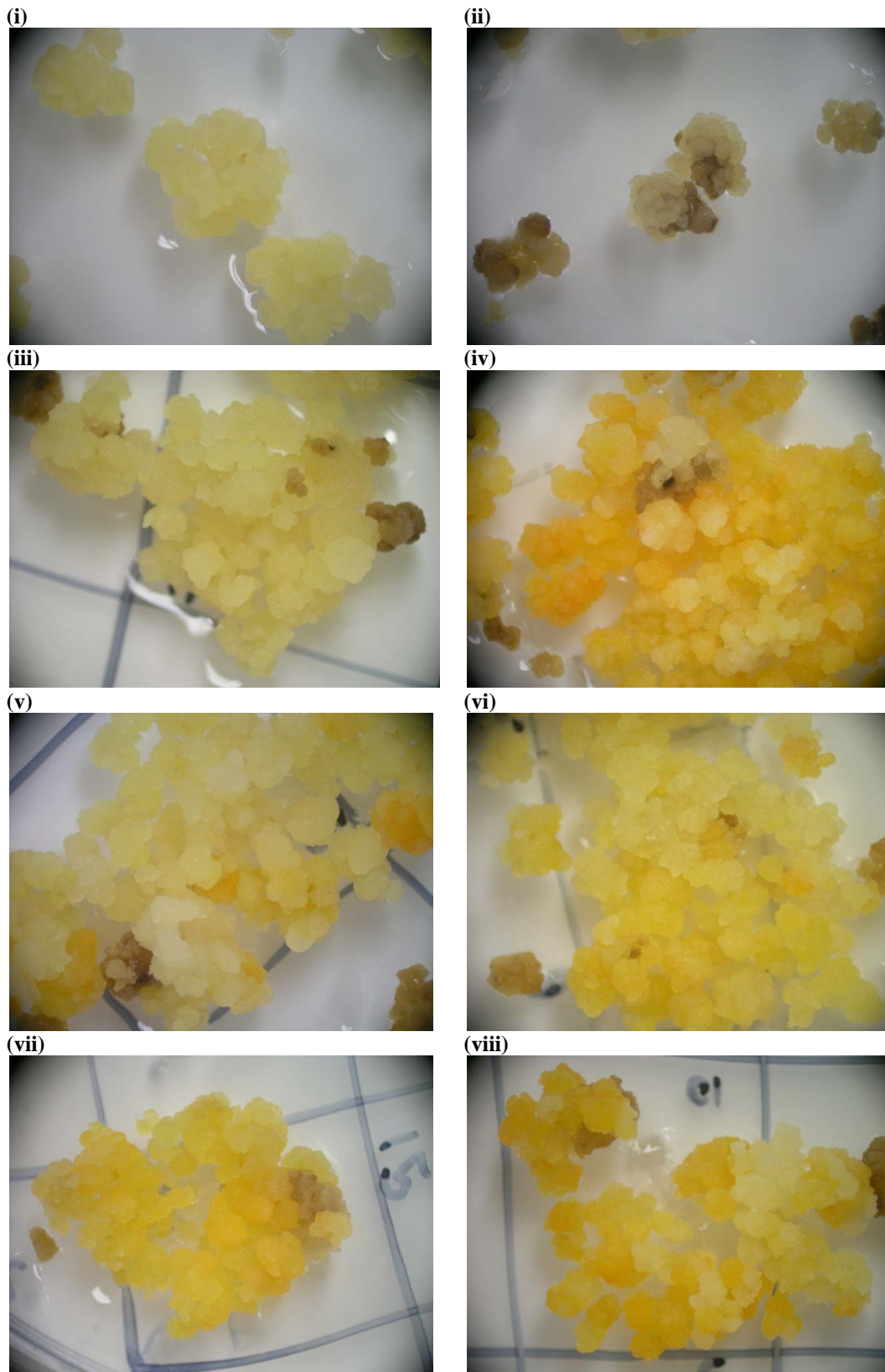


Figure 4.6: Carotenoid accumulation in rice callus transformed with different *psy* coding region constructs. Each panel is a close-up [8× magnification] of selected calli clumps containing the darkest orange callus visible at 7 weeks post transformation. (i) Untransformed callus without selection; (ii) Untransformed callus on selection; (iii) *pCAMBIA-1302* vector (negative transformation control); (iv) maize *Zpsy1* (positive control); (v) *Apsy1*; (vi) *Apsy2a*; (vii) *Cpsy1*; (viii) *Cpsy2a*.

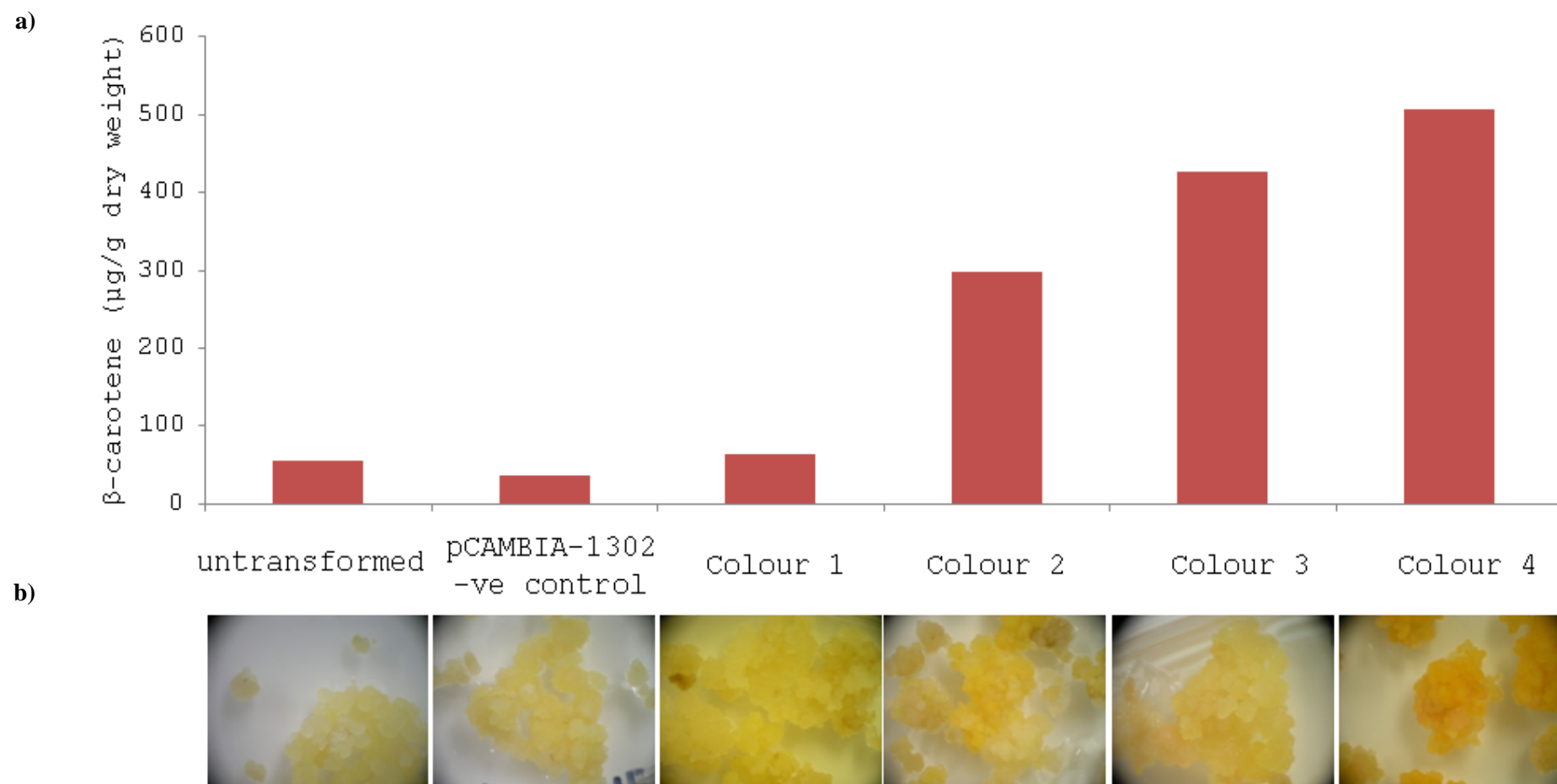


Figure 4.7: Total carotenoids in *Zpsy1* transformed rice calli. β -carotene content **a)** of different coloured clumps of rice callus **b)** transformed with *Zpsy1* including untransformed and *pCAMBIA-1302* vector only negative controls. Callus lines of each sample are labelled under the respective photographs [8 \times magnification].

11) were creamy white in colour (Figure 4.7b) and had β -carotene levels of 54.7 $\mu\text{g/g}$ dry weight and 35.9 $\mu\text{g/g}$ dry weight, respectively (Figure 4.7a). Representative *Zpsy1* rice calli were harvested according to three different colour groups: pale yellow, yellow and orange (Figure 4.7b). The β -carotene content of *Zpsy1* lines ranged from 64 $\mu\text{g/g}$ dry weight (pale yellow callus; line 2A-41) to 507 $\mu\text{g/g}$ dry weight (orange callus; line 2A-13) [Figure 4.7a], confirming a positive correlation between callus colour and carotenoid content.

To investigate carotenoid accumulation in lines transformed with banana *psy* coding regions, the average carotenoid content of three lines each of the most visibly carotenogenic calli transformed with *Zpsy1*, and Asupina and Cavendish *psy1* and *psy2a* was analysed (Figure 4.8). The average β -carotene content of the untransformed callus and *pCAMBIA-1302* negative control lines was significantly lower than *psy* lines at 22.3 $\mu\text{g/g}$ and 37.1 $\mu\text{g/g}$ dry weight, respectively. The average β -carotene content of the *Zpsy1* callus was the lowest of the *psy* genes at 455.7 $\mu\text{g/g}$ dry weight, while the banana *psy* callus was 511.8 $\mu\text{g/g}$, 567.5 $\mu\text{g/g}$, 682.0 $\mu\text{g/g}$ and 793.6 $\mu\text{g/g}$ dry weight for *Apsy1*, *Cpsy2a*, *Cpsy1* and *Apsy2a*, respectively. There was considerable variation within the three samples for each *psy* transformation, which is seen by the large standard deviation in most *psy* treatments. However, all *psy* transformed lines were at least 10 fold higher than the untransformed or vector only negative controls. The highest individual value was 957.3 $\mu\text{g/g}$ dry weight for one *Apsy2a* line which was 1.8 fold higher than the highest *Zpsy1* line. Statistical analysis confirmed that the β -carotene levels in callus transformed with *Apsy2a* and *Zpsy1* differed significantly, however, neither treatment differed significantly from the β -carotene levels of the other PSYs. These results confirm that, at least in rice, the banana PSYs have the potential to mediate carotenoid accumulation to levels higher than maize *psy1*. Moreover, Cavendish PSY1 and PSY2A appeared capable of synthesising carotenoids to similar levels as the Asupina PSYs.

4.4 Discussion

In this study, the efficacy of the cloned banana *psy1* and *psy2a* coding regions was confirmed as they all mediated an increase in carotenoid content in transgenic rice callus to a level comparable to the previously characterised maize B73 *psy1* coding region.

Analysis of the primary structure of the complete banana PSY proteins confirmed that the catalytic domain was the Trans-IPPS-HH domain linked to isoprenoid biosynthesis, all the predicted critical residues were intact, and sequence differences did not affect important structural motifs (Figure 4.2). Interestingly, the 7th amino acid before the first ARM of APSY2B is aspartic acid instead of tyrosine, which is in the other banana PSY proteins, and

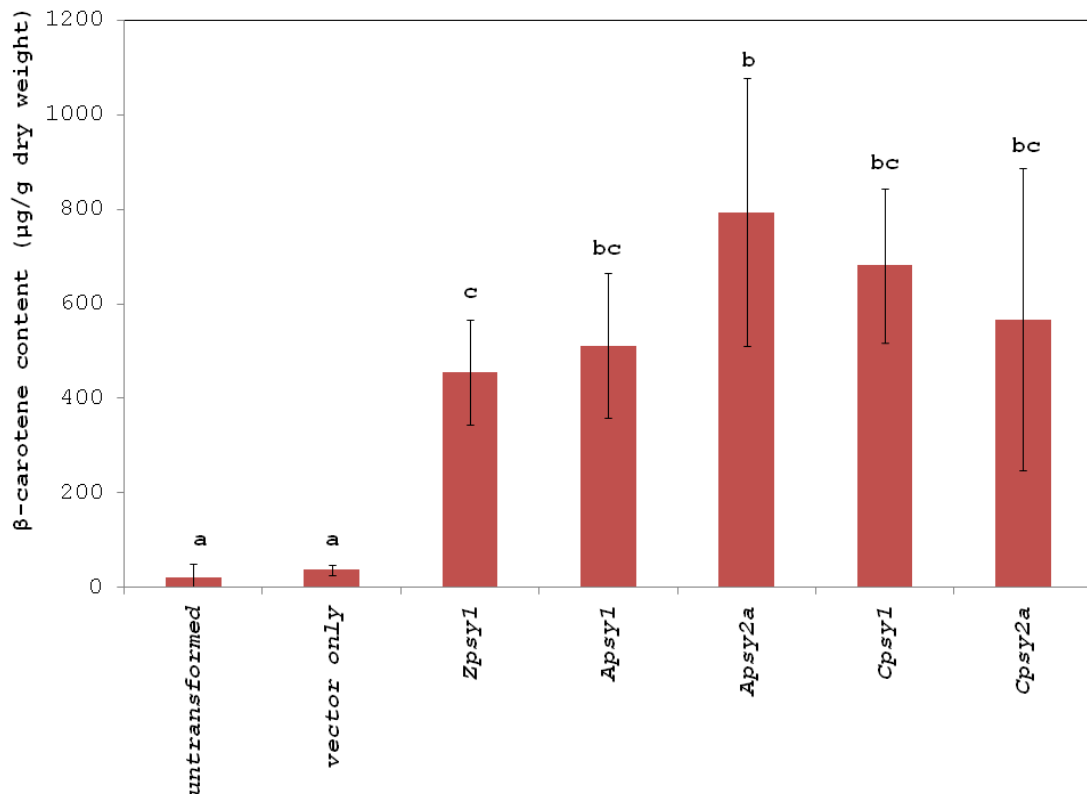


Figure 4.8: Carotenoid accumulation in rice calli transformed with different *psy* genes: Graph of the carotenoid content of the three most visually carotenogenic calli from each of the experimental treatments including untransformed and vector only controls. Standard deviation between the three replicates is indicated by black error bars above each average (red bars). One-way ANOVA with least significant difference post-hoc analysis was used to determine the statistical significance of β -carotene content with a 95% confidence level. Letters above each bar (a, b and c) in the graph indicate treatments where β -carotene levels were not statistically different.

is predicted to form the substrate binding pocket. In prenyltransferases, this region is known as the chain length determination region (CLD) and the 2nd, 4th and 5th amino acids before the first ARM are known to affect prenyltransferase product length in farnesyl diphosphate synthase (FPS) and GGPS (Ohnuma *et al.*, 1997). The hydrophobicity and steric properties of these residues are thought to define the depth of the substrate binding pocket (Ohnuma *et al.*, 1996; Wang and Ohnuma, 1999). However, the 5th residue before the first ARM is tryptophan (Figure 4.2), whose bulky aromatic side chain would be expected to restrict the size of the GGPP binding pocket (Tarshis *et al.*, 1996), suggesting that all banana PSY have the same binding pocket depth. The 4th residue in the active site lid (arginine) of APSY2B also differed from the consensus (tyrosine), suggesting that this protein may have a different substrate binding efficiency. However, all other functional residues were identical. Therefore, all PSYs are expected to be capable of producing phytoene.

Apart from the two mutations in the CLD region of APSY2B, the catalytic residues were identical in all of the banana PSY proteins and ZPSY1. Interestingly, primary structure analysis predicted that several amino acids may carry out multiple functions, indicating that these residues may be more highly conserved than others. However, differences in amino acids not involved in catalytic function may still influence enzyme function by altering overall protein structure and changing interactions between adjacent regions. The banana PSY proteins were all predicted to consist predominantly of α -helices and coiled loop regions (Figure 4.3c), consistent with the structures of other prenyltransferases (Wang and Ohnuma, 1999) and the fact that PSY is a soluble protein (Dogbo *et al.*, 1988). Interestingly, two potentially significant structural differences were found between Asupina and Cavendish PSY2A (Figure 4.3a & b). Firstly, conserved Helix 1 is longer in CPSY2A due to two consecutive AVE tripeptides at the C-terminal end of this structure while APSY2A has only one. In addition, the amino acids prior to Helix 1 form non-conserved helices (helices n4 and n5) in Cavendish but not Asupina despite the fact that the residues are the same. The additional AVE motif could be responsible for the presence of both structural differences in Cavendish PSY2A due to interactions between adjacent residues. These structural differences are located in the large N-terminal plastid targeting signal peptide that must be cleaved in order for the mature PSY protein to be fully functional (Misawa *et al.*, 1994). This could potentially reduce carotenoid biosynthesis in Cavendish fruit by interfering with PSY2A signal peptide cleavage or plastid targeting. The AVE motif itself may be part of the signal peptide cleavage site, therefore the change in sequence alone may be sufficient to disrupt signal peptide cleavage.

Tertiary structure prediction only compared the catalytic domains of the banana PSYs; therefore potential differences in the putative signal peptides could not be further examined. Interestingly, PSY was predicted to have a tertiary structure similar to SQS (Tansey and Shechter, 2000), and the SQS-PSY motifs conserved between these two enzymes are thought to participate in reaction catalysis. These similarities may shed light on some aspects of the function of PSY. SQS plays a pivotal role in the synthesis of sterols such as cholesterol, and its activity is thought to direct the use of farnesyl diphosphate in the manufacture of both sterol and non-sterol isoprenoids (Tansey and Shechter, 2000). This is similar to the role played by PSY in irreversibly directing GGPP, which is a precursor for other compounds such as tocopherols and chlorophylls, towards to synthesis of carotenoids (Cunningham and Gantt, 1998). The similarities between these proteins may shed light on the putative function of the banana PSY C-terminus, which could be responsible for anchoring PSY to the plastid membranes where its hydrophobic products would accumulate (Cunningham and Gantt, 1998). The nature of this attachment would have to facilitate both the acquisition of water

soluble GGPP substrate and cofactors, as well as the delivery of phytoene to plastid membranes. Such a mechanism has been proposed for the function of the endoplasmic reticulum-associated mammalian SQS enzymes (Tansey and Shechter, 2000).

Analysis of the potential functional impacts of sequence differences in the banana PSY proteins was tempered by the fact that secondary and tertiary structure predictions are approximations and may not therefore be fully representative. For example, the SSpro secondary structure prediction program only has a structure prediction accuracy of 78% although it performs well against other programs (Pollastri *et al.*, 2002). Additionally, although the tertiary structure of many isoprenoid biosynthetic enzymes has been elucidated (Liang *et al.*, 2002), no such information exists for PSY, as evidenced by the failure of homology modelling to associate the non-catalytic N- and C-terminal domains of the banana PSY enzymes with any existing structures. It is therefore difficult to verify the putative functions of these regions and deduce the possible implications of any sequence or structural differences therein. Completely accurate prediction of secondary and tertiary structures from primary sequence data is unlikely as a number of factors are not accounted for including: pH and other environmental variables; the dynamic nature of proteins and the formation of quaternary structures; the existence proteins that do not fold automatically and limitations in prediction methodologies (Pollastri *et al.*, 2002). In addition, predicted secondary or tertiary structures may not account for any post-translational effects such as glycosylation that may influence protein structure. In the case of PSY2B, the sequence of the first 20 amino acids corresponds to APSY2A due to the primers used to amplify the complete coding region (Chapter 3). Consequently, the activity of the banana PSYs was confirmed directly in rice callus as their actual structures may differ significantly from predictions in Figures 4.2 & 4.3.

Rice transformation was optimised through induction of rice callus and selection of the CAAT method as the best transformation method using GFP reporter gene analysis. This enabled subsequent transformation of expression constructs containing Asupina and Cavendish *psy1* and *psy2a* coding regions. All banana PSY proteins were functional in transgenic callus and appeared capable of producing much higher levels of carotenoids than the negative controls despite significant variability between individual replicates. In previous studies (Ye *et al.*, 2000), PSY expression in rice endosperm relied on co-expression of additional enzymes in the carotenoid biosynthesis pathway and *E. uredovora crtI* was used as had both ZDS and PDS activity. However, like the maize callus used to compare *psy* genes for production of Golden Rice 2 (Paine *et al.*, 2005), the callus induced in this study should express the full carotenoid biosynthesis pathway as it is derived from the rice embryo.

Based on initial visual observations, little difference was observed in levels of carotenoid accumulation between banana PSYs, with callus colours ranging from cream to dark orange (Figure 4.6 and 4.7). Although not significantly higher than other banana PSYs, APSY2A produced callus with the highest carotenoid levels (Figure 4.8). However, it is uncertain whether this difference alone would sufficiently explain the observed differences between pVA content of Asupina and Cavendish fruit as CPSY2A is clearly functional. As this experiment was undertaken in rice callus, it is also possible that the relative activity of these enzymes will differ in banana.

Interestingly, when assayed quantitatively, ZPSY1 appeared to be the least active of the enzymes tested, having the lowest average carotenoid accumulation and significantly lower than APSY2A. This control was expected to have higher activity than the banana PSY proteins as it was the most active enzyme in maize callus (Paine *et al.*, 2005), and because rice is more closely related to maize than to banana. Additionally, there appeared to be a greater proportion of orange callus in experiments transformed with ZPSY1. A similar result was seen in maize callus (Paine *et al.*, 2005) transformed with rice PSY1, which had only half the level of relative carotenoid accumulation compared to ZPSY1, yet 70% of calli transformed with rice *psy* had carotenoid levels at least five times higher than baseline levels, while for ZPSY1 this was only 60%. The more active PSYs, giving high levels of carotenoid accumulation, might inhibit callus multiplication. A few banana *psy* lines were observed which had dark orange callus, suggesting very high expression. These calli were small and tended to proliferate more slowly than those with lower carotenoid levels suggesting that high carotenoid levels have a negative effect on callus growth. This is supported by studies in cauliflower where lines homozygous for the *Or* gene had high carotenoid accumulation but were very small (Li *et al.*, 2001). The effect was less obvious in heterozygous *Or* lines. This may be due to GGPP depletion within the callus cells, which was thought to be have caused phenotypic abnormalities in tomato as phytohormone production was suppressed (Fray *et al.*, 1995). Similar phenotypic abnormalities were observed in tobacco when either *psy1* or *psy2* was overexpressed (Busch *et al.*, 2002). Although these limitations were overcome in tomato using a fruit-specific promoter (Fraser *et al.*, 2002), this was not possible for the callus-based assay as the tissue is undifferentiated. The reduced proliferative capacity of highly carotenogenic lines may also mean that the relative activity of some enzymes such as CPSY2A or APSY1 was under-reported as their best performing lines produced too little callus for quantitative analysis. Because 200 mg was the minimum wet weight for feasible carotenoid extraction, lines were selected for quantitative analysis based on the amount of available tissue as well as carotenoid content. This meant that there was insufficient material from some highly carotenogenic lines to be analysed. This challenge

may be solved by increasing the number of replicates during transformation in order to increase the frequency of highly carotenogenic lines for analysis or allowing more time for callus to proliferate. This would also provide more conclusive results by allowing more lines to be tested, thus reducing the variability observed in the results.

Previous work in maize (Paine *et al.*, 2005), the only other work that used callus tissue to compare PSY activity, assessed the activity of various PSYs based on the level of carotenoid accumulation and on the proportion of highly carotenogenic clumps of individual callus. In the present study, callus was segregated into lines based on the origin from a single callus “mother” clump representing the original transformation. However, sections of some clumps were different colours suggesting multiple transformation events. This made it impossible to determine the proportions of transformants for each of the banana *psy* sequences represented by the different colour levels. Nevertheless, the present study was able to verify that PSY1 and PSY2A from both Asupina and Cavendish were capable of producing pVA carotenoids. Analysis of carotenoid accumulation in rice callus proved to be a simple model for testing PSY enzyme function compared to radiolabelled biochemical assays (Dogbo *et al.*, 1988; Fraser *et al.*, 2000; Schledz *et al.*, 1996) due to the nature of the reagents and detection systems required. Bacterial systems such as *E. coli* for functional complementation studies were not available. Interestingly, despite the poor GFP expression, PSY proved to be an excellent alternative reporter gene as carotenoid accumulation was visible. Rice callus provided a simple model for assessing the carotenogenic potential of a given *psy* coding region, but does not directly measure enzyme activity. Consequently, as the intrinsic activity of each enzyme was not measured biochemically, subtle differences in enzyme function could not be determined. Comparison of PSY enzyme activity in rice would also be limited by restrictions in plastid storage capacity, size and number, as well as GGPP substrate restrictions that may negatively affect callus growth.

Transgene copy number and site of integration into the rice genome were not expected to bias the results as *Agrobacterium*-mediated transformation is known to produce transformants with lower copy number and fewer genetic aberrations than microprojectile bombardment. However, it is still possible that these factors may contribute to the variation in carotenoid content observed. All the transformations were conducted on the same day under the same experimental conditions in order to further limit variation. Further, some variability may be attributed to the nature of rice callus, which is probably a mixture of different embryonic cell types and morphologies observed during callus maintenance ranged from soft friable callus to harder tissue. Therefore, differences in the properties of these cells such as transformability, water content and proliferative capacity could contribute to the

variation in carotenoid content observed between the various callus lines. However, the trends in carotenoid accumulation observed in Figure 4.6 were unchanged when wet weight measurements were used instead of dry weight (results not shown). Therefore variation in cellular water content did not appear to have an impact on the results.

The work reported in this Chapter tested the hypothesis that differences in the activity of the PSY proteins in Asupina and Cavendish may be responsible for the difference in their respective fruit pVA content. Bioinformatic analysis of PSY structure yielded differences that were largely inconclusive, although differences in PSY2A signal peptide structure may yet prove important. The Asupina and Cavendish *psy1* and *psy2a* coding regions were expressed in rice callus for *in vivo* analysis of enzyme function and all sequences were capable of producing active enzymes that catalysed visually observable and quantifiable levels of carotenoid accumulation. These enzymes appeared to possess similar levels of maximal activity based on β -carotene accumulation measurements. Cumulatively, these results indicated that factors other than PSY enzyme activity may be responsible for differences in the fruit pVA content of Asupina and Cavendish.

Chapter 5: Characterisation of factors affecting phytoene synthase expression

5.1 Introduction

Carotenoids are synthesised by plants and have numerous functions such as photosynthesis in leaves, colouration of fruits and flowers (Cunningham and Gantt, 1998), and precursors for abscisic acid synthesis in organs such seeds, leaf and vascular tissue (Nambara and Marion-Poll, 2005). This requires carotenoids to be synthesised at different times, in different amounts in the various tissue through regulation of the enzymes in the carotenoid biosynthetic and degradation pathways.

Tissue-specific regulation of PSY activity has been observed in a number of plants (Bartley and Scolnik, 1993; Clotault *et al.*, 2008; Gallagher *et al.*, 2004). The tomato *psy* genes function in both leaf and fruit (Bartley and Scolnik, 1993), with *psy1* predominantly associated with chromoplast bearing tissue (fruit and petals) and *psy2* more widely expressed (Giorio *et al.*, 2008). Semi-quantitative RT-PCR analysis of *psy* transcripts in maize varieties with yellow (high carotenoid) or white (low carotenoid) endosperm implicated *psy1* in endosperm carotenoid accumulation (Gallagher *et al.*, 2004). Expression of *psy1* was higher than *psy2* in yellow endosperm maize, while only *psy2* was expressed in white endosperm maize. The *psy* expression in rice endosperm was identical to that of white endosperm maize. Comparison of two apricot varieties with yellow (high carotenoid) and white (low carotenoid) fruit indicated that ethylene production influenced *psy* expression during fruit development (Marty *et al.*, 2005). Initial studies in banana (Chapter 3) suggest that *psy1* is predominantly expressed in leaf and *psy2* in fruit. However, this was based on the frequency of obtaining particular clones and a more robust analysis is required to confirm this and to correlate expression of these genes with differences in carotenoid accumulation in fruit.

Gene expression in plants is regulated by mRNA stability (Abler and Green, 1996), methylation of DNA and histone proteins (Vaillant and Paszkowski, 2007), and promoter activity. Promoters play the most significant role in regulating tissue specificity and transcript abundance through the specific interactions of DNA sequence motifs (Higo *et al.*, 1999; Sawant *et al.*, 2005) or secondary structures (Yamagishi *et al.*, 2008) with transcription factors. The promoter regions of the maize (Palaisa *et al.*, 2003) and *Arabidopsis* (Welsch *et al.*, 2003) *psy* genes have been studied. In maize, an *Ins2*

transposable element in the promoter of the *yl* gene that encodes PSY1, was predominantly associated with lines that had high carotenoid accumulation, suggesting that this phenotype was due to enhanced promoter activity (Palaisa *et al.*, 2003). The *Arabidopsis psy* promoter is the best characterised *psy* promoter, and characterisation of this promoter identified DNA regulatory motifs activated by different light conditions (Welsch *et al.*, 2003). Response to light was controlled by two adjacent G-box-like elements, approximately 200 bp upstream from the transcription start site. However, constitutive expression was linked to a pair of ATCTA motifs located approximately 840 bp upstream from the transcription start site. This motif was thought to coordinate the expression of genes involved in photosynthesis, as well as carotenoid and tocopherol metabolism. Interestingly, during photomorphogenesis in *Arabidopsis thaliana*, *psy* expression and enzymatic activity was also shown to be regulated by light through the activity of phytochromes, and increased carotenoid content was seen only under light conditions conducive to chlorophyll biosynthesis (von Lintig *et al.*, 1997).

The work reported in this chapter investigated the hypothesis that differences in the regulation of *psy* expression were responsible for determining pVA accumulation in banana fruit. Consequently, the promoters of the *psy1* and *psy2a* genes from Asupina and Cavendish were isolated and their activity characterised using transient GUS expression in green fruit tissue. In addition, semi-quantitative RT-PCR was used to further investigate relative levels of *psy1* and *psy2a* mRNA transcripts in leaf and fruit of Asupina and Cavendish bananas.

5.2 Materials and methods

5.2.1 Oligonucleotide primers

PCR primers were sourced as previously described (Chapter 3.2.3) and their sequences are listed in Table 5.1.

5.2.2 *psy* promoter isolation

The putative promoter regions of Asupina and Cavendish *psy1* and *psy2* were obtained using the genome walking strategy (Chapter 3.2.7). Overlapping DNA fragments ranging between 2600 and 3500 bp were obtained through consecutive rounds of nested PCR using adapter-specific primers *AP1* and *AP2* (Table 3.2) in combination with promoter-specific primers (Table 5.1) designed from previously characterised *psy* sequences (Chapter 3). The genome walking strategy for promoter isolation is outlined in Figure 5.1.

The promoter regions of Asupina and Cavendish *psy1* were amplified using primer pairs *AP1/psy1pr-GW01* and *AP2/psy1pr-GW02* for outer and inner PCR, respectively. Two

Table 5.1: PCR primers used in banana *psy* promoter isolation and semi-quantitative PCR

Primer name	Sequence (5'-3')	Orientation ^a	Target sequence	Restriction site ^b
<i>psy1pr-GW01</i>	TAATCCACTGAGAAGGTGGAATCC	Reverse	<i>psy1</i> 5' UTR	none
<i>psy1pr-GW02</i>	CAAAGGCGATCCTCCTTTCTGTG	Reverse	<i>psy1</i> 5' UTR	none
<i>psy2apr-GW01</i>	GGGAAGAAGCACGACGGTCGTCG	Reverse	<i>psy2a</i> 5' UTR	none
<i>psy2apr-GW02</i>	CAGGCGTCCACTTGGTTGGCGCCGC	Reverse	<i>psy2a</i> 5' UTR	none
<i>Apsy2apr-GW01</i>	TTGAGGTGAAACGCAGAAGCGTC	Reverse	Asupina <i>psy2a</i> 5' promoter region	none
<i>Apsy2apr-GW02</i>	CTCATTTCATTGCCATTGTGTCAAAC	Reverse	Asupina <i>psy2a</i> 5' promoter region	none
<i>Cpsy2apr-GW01</i>	ACCGAAGAATCAATTTAGGTCCAAC	Reverse	Cavendish <i>psy2a</i> 5' promoter region	none
<i>Cpsy2apr-GW02</i>	AATGTTTCATGTTTGTGTCATAATCTGTGG	Reverse	Cavendish <i>psy2a</i> 5' promoter region	none
<i>psy2b_5utr-R1</i>	GCTCCGCTCTTTCACCTCT	Reverse	<i>psy2B</i> 5' coding region	none
<i>Apsy1_pr-F1</i>	ggtaccGTTACATTCTTAATGAGAGGTATT	Forward	Asupina <i>psy1</i> promoter region	KpnI
<i>Cpsy1_pr-F1</i>	ggtaccGTCACATAGTTGAATGAGATGC	Forward	Cavendish <i>psy1</i> promoter region	KpnI
<i>psy1_pr-R1</i>	ccatggGAAGCAAGAGCAAGATCGTATAAC	Reverse	<i>psy1</i> 5' UTR	NcoI
<i>Apsy2a_pr-F1</i>	ggtaccGCAATAATGACCTGGTGACATA	Forward	Asupina <i>psy2a</i> promoter region	KpnI
<i>Cpsy2a_pr-F1</i>	ggtaccGCAATAATGACAGGGTGATGATA	Forward	Cavendish <i>psy2a</i> promoter region	KpnI
<i>psy2a_pr-R1</i>	ccatggCTGCTTAGTTTCGTCTTCCG	Reverse	<i>psy2a</i> 5' UTR	NcoI
<i>qActin1-F1</i>	TGGCTGACACTGACGACATTC	Forward	Musa acuminata <i>actin1</i> coding region	none
<i>qActin1-R1</i>	CAACAATACTTGGGAAAACGG	Reverse	Musa acuminata <i>actin1</i> coding region	none
<i>psy1_qPCR-F1</i>	GCCTGTTGCTACGGATGATTGC	Forward	<i>psy1</i> 5' coding region	none
<i>psy1_qPCR-R1</i>	ACTCCATCTTCGCCTCTTCCTC	Reverse	<i>psy1</i> 5' coding region	none
<i>Apsy2a_qPCR-F1</i>	CAAGTGGACGCCTGTCTCGG	Forward	Asupina <i>psy2a</i> 5' UTR	none
<i>Cpsy2a_qPCR-F1</i>	CAAGTGGATGCCTGTCTCGG	Forward	Cavendish <i>psy2a</i> 5' UTR	none
<i>psy2a-qPCR-R1</i>	CGCTGCTTAGTTTCGTCTTCCG	Reverse	<i>psy2a</i> 5' UTR	none
<i>psy2int-qPCR-RVS</i>	CAGCAACGAAGCCAAAACC	Reverse	exon 6 of <i>psy2a</i> and <i>psy2b</i>	none

^(a) orientation with respect to mRNA sequence

^(b) presence of restriction sites (indicated in the primer sequence in lowercase)

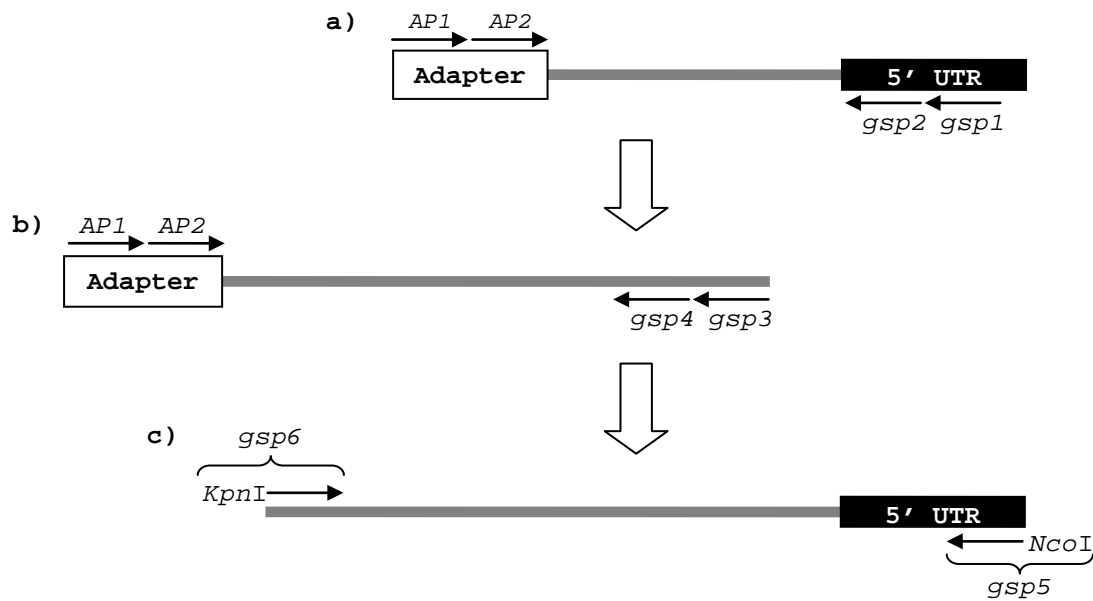


Figure 5.1: Strategy for the isolation of *psy* promoter sequences from restriction digested Asupina and Cavendish gDNA libraries. Genome walking nested PCRs (Chapter 5.2.2) with adapter primers (*AP1* and *AP2*) designed to the genome walking adapter (white rectangle) and gene-specific (*gsp1* to *gsp4*) designed to **a)** the 5' UTR (black rectangle) and **b)** the upstream regulatory region (grey line) were used to obtain overlapping promoter fragments. **c)** Consensus sequence information from these fragments was used to design primers *gsp5* and *gsp6* to the *psy* promoter regions and 5' UTRs respectively (Chapter 5.2.3), enabling amplification of *psy1* and *psy2a* promoters as single fragments with 5' *KpnI* and 3' *NcoI* restriction sites for cloning and construction of vectors for microprojectile bombardment.

rounds of nested PCR were required to obtain the *psy2a* promoter regions of Asupina and Cavendish. The outer and inner primers for the first round were *AP1/psy2apr-GW01* and *AP2/psy2apr-GW02*, respectively. The remaining *psy2a* promoter sequence was amplified with the *AP1/Apsy2apr-GW01* (Asupina) or *AP1/Cpsy2apr-GW01* (Cavendish) outer PCR and *AP2/Apsy2apr-GW02* (Asupina) or *AP2/Cpsy2apr-GW02* (Cavendish) inner PCR primer combinations. The *AP1/psy2-GW06* and *AP2/psy2b_5utr-R1* outer and inner PCR primer pairs, respectively, were used in attempts to amplify the Asupina and Cavendish *psy2b* promoter regions. PCR products were amplified from the genome walking libraries and analysed as described previously (Chapter 3.2.7).

5.2.3 Cloning of *psy* promoters into *pGEM-4Z* vectors

Consensus sequence information for the Asupina and Cavendish *psy1* and *psy2a* promoter regions was used to generate contiguous full length PCR products (Figure 5.1c), including the 5' UTR and upstream regulatory regions, that were cloned into *pGEM-4Z* vectors containing the GUS reporter gene (Figure 5.2). The *psy1* fragments were amplified using the *Apsy1pr-F1/psy1pr-R1* (Asupina) and *Cpsy1pr-F1/psy1pr-R1* (Cavendish) primer pairs. The

primer sets for *psy2a* fragment amplification were *Apsy2apr-F1/psy2apr-R1* (Asupina) and *Cpsy2apr-F1/psy2apr-R1* (Cavendish). The Expand Long Template PCR system (Chapter 2.2.1) was used to amplify promoter fragments from 1 µg gDNA with an extension time of 2 min and annealing temperatures between 55 °C to 60 °C. PCR fragments were cloned into pGEM-T Easy and sequenced as previously described (Chapter 2.2.2-10).

Primers for amplification of Asupina and Cavendish *psy* promoters included *KpnI* and *NcoI* restriction sites to facilitate subcloning in front of the GUS coding region, which had an *NcoI* site in the start codon (Figure 5.2). The *psy* promoters were excised from the *pGEM-T Easy* vector and the *nos* promoter from the *pGEM-4Z*-based GUS expression vector (*pGEM-4Z-nos-gus-nos*) by double digestion with *KpnI/NcoI* (Chapter 2.2.2). Digests were separated by agarose gel electrophoresis (Chapter 2.2.3), and *psy* promoter fragments and *pGEM-4Z-X-gus-nos* vector backbone fragments were gel purified (Chapter 2.2.4). Gel purified vector/insert fragments were ligated together (Chapter 2.2.5) to form the *psy* promoter expression vectors (*pGEM-4Z-psy-gus-nos*). Ligation reactions were transformed into *E. coli* and putative clones selected and sequenced as described previously (Chapter 2.2.6-10). The following clones were purified in high concentration for microprojectile bombardment using a Geno Pure Plasmid Midi Kit (Chapter 2.2.8): *pGEM-4z-Apsy1pr-gus-nos*, *pGEM-4z-Apsy2apr-gus-nos*, *pGEM-4z-Cpsy1pr-gus-nos*, *pGEM-4z-Cpsy2apr1-gus-nos*, *pGEM-4z-Cpsy2apr2-gus-nos*, and *pGEM-4z-Cpsy2apr3-gus-nos*. The *Musa acuminata 1-aminocyclopropane-1-carboxylate oxidase* promoter (*acopr*) and Maize *ubiquitin* promoter with intron (*ubipr*), kindly supplied by Dr Jason Geijskes (QUT), were included as fruit-specific and constitutive positive controls, respectively.

5.2.4 Bioinformatic analysis of promoter sequences

Consensus promoter sequences were compiled from the sequence trace files of overlapping genome walking fragments of the respective *psy* promoter regions. Separate consensus sequences were also compiled for the individual promoter clones in *pGEM-4Z* listed in Chapter 5.2.3 above. Sequence alignment and analysis were as described in Chapter 3.2.5. Phylogenetic analysis, multiple sequence alignment and percentage identity comparisons were performed using the Clustal W2 program (Larkin *et al.*, 2007) v2.0.1.0 provided by the European Bioinformatics Institute (www.ebi.ac.uk) using the default parameters. For secondary structure analysis, the repeat sequence adjacent to the *psy2a* transcription start site and 10 bp flanking this region from each of the Asupina and Cavendish *psy2a* promoter clones were submitted to the Quickfold program interface (based on the Unafold program; Markham and Zuker, 2008), on the DINAMelt server (Markham and Zuker, 2005) using default settings.

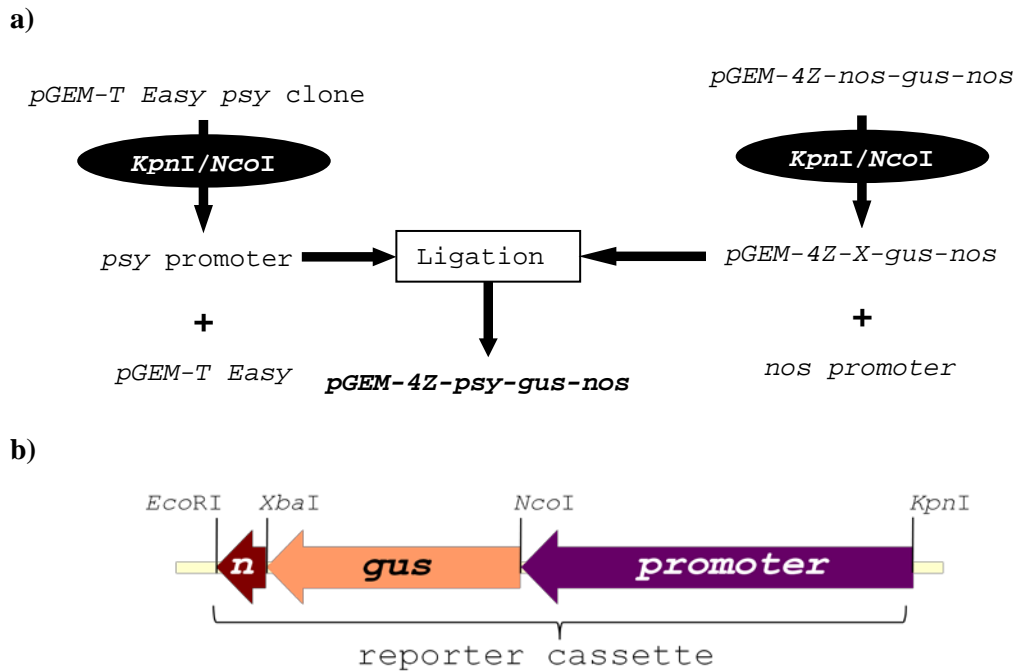


Figure 5.2: Strategy for generation of *psy* promoter constructs in pGEM-4Z showing a) cloning of *psy* promoters into *pGEM-4Z* to make the GUS reporter cassette containing b) the Asupina or Cavendish *psy* promoter, *gus* coding region interrupted by a catalase intron and *nos* terminator (*n*). This diagram also represents the structure of the *Musa acuminata 1-aminocyclopropane-1-carboxylate oxidase (aco)* and maize *ubiquitin (ubi)* promoter driven GUS reporter cassettes.

5.2.5 Preparation of banana tissue for microprojectile bombardment

5.2.5.1 Banana embryogenic cell suspensions

Banana embryogenic cell suspensions (ECS), kindly supplied by Jennifer Kleidon (QUT), were maintained in 250 mL flasks containing 50 mL BL media (Chapter 2.3) and subcultured every 10 days. Typically, one flask of banana ECS was required to prepare one plate of cells for microprojectile bombardment. Banana ECS were prepared for transformation as described previously (Becker and Dale, 2004). Four days after subculture, the cell suspensions were plated out onto sterile filter paper discs (Whatman) placed onto BL solid media (BL liquid media solidified with 0.25% phytigel, Sigma-Aldrich) and incubated at 25 °C for 3 days prior to microprojectile bombardment.

5.2.5.2 Banana fruit tissue

The outer surface of the banana flesh was chosen as the target tissue for microprojectile bombardment as it could be obtained routinely as an undamaged surface. Each banana was peeled such that only part of the surface of the flesh was exposed, enabling the surface layer to be removed without damage as the unpeeled tissue would be protected from injury. To excise tissue sections, a scalpel was used to make parallel longitudinal incisions approximately 2 to 3 cm apart and then a further incision was made approximately 1 to 2 mm

under the surface at one end of the fruit, connecting both parallel incisions. This was continued under the entire length of the fruit, essentially peeling the intact outer surface of the flesh from the inner layers. The surface was then cut into sections approximately 3 to 4 cm in length. The exact dimensions of the fruit sections were dependent on the size and malleability of the fruit being sampled. For microprojectile bombardment, two fruit sections were placed in Petri dishes onto filter paper moistened with 1 mL BL media without phytohormones.

5.2.6 Microprojectile bombardment of *psy* promoter GUS constructs

5.2.6.1 Microprojectile bombardment procedure

Microprojectile bombardment was carried out as previously described (Becker and Dale, 2004). Gold particles (1 μm), prepared for microprojectile bombardment as described by Becker and Dale (2004), were kindly supplied by Jennifer Kleidon (QUT). Samples were placed 7.5 cm from the point of particle discharge, and were transformed using 550 kPa helium pressure in a chamber at -84 kPa vacuum.

5.2.6.2 Histochemical GUS staining

Plates of banana ECS were incubated for 48 hr at 25 °C in the dark following microprojectile bombardment. The filter paper carrying the disc of embryogenic cells was cut out from the media using a scalpel blade and transferred to a well in a plastic 6 well plate. Cells were washed into the well with 1 mL GUS histochemical stain (1mM X-gluc, 50 mM Na_2HPO_4 , pH 7.0). The wash step was repeated with a further 1 mL GUS stain solution and the cells incubated for 10 min at room temperature on an orbital shaker at 90 rpm to dislodge remaining cells from the filter paper. The paper was rinsed with an additional 1 mL GUS histochemical stain before being discarded. Cells were incubated undisturbed overnight at 37 °C before the GUS stain was carefully removed and replaced with 1 mL 100% ethanol. For photography, the cells in ethanol were transferred to smaller wells to increase cell density, allowed to settle under gravity and the ethanol completely removed. Cells were photographed at 8 \times and 16 \times magnification under an SZ-CTV stereo microscope (Olympus) using a CAMEDIA C-5060 digital camera (Olympus) under full zoom using the portrait setting under controlled lighting conditions.

Transformed fruit sections were incubated for either 24 or 72 hr at 25 °C in the dark to facilitate transient GUS reporter expression. Prior to histochemical staining, the fruit sections were photographed under a measuring grid of 0.25 cm² squares to enable determination of sample surface area for subsequent analysis. The fruit tissue was sealed into plastic pouches

containing 4 to 6 mL of GUS histochemical stain per treatment to optimise staining efficiency. Fruit tissue was incubated overnight at 37 °C and then transferred to Petri dishes for photography at 2.68× magnification as described above for embryogenic cells. Transient GUS expression for each treatment was estimated by counting the total number of individual blue-staining foci visible in the photographs regardless of intensity. Total surface area of each treatment was estimated to the nearest 0.0625 cm² and promoter activity estimated as GUS foci per cm². Excel 2007 (Microsoft) and SPSS v16 (SPSS Inc.) were used for visualisation and statistical analysis of results, respectively.

5.2.6.3 Fluorimetric analysis of GUS activity

Bombarded banana embryogenic cells (three replicates per treatment) and untransformed control tissue (two replicates) were incubated for 48 hr at 25 °C in the dark. Cells were scraped off the filter paper disc and mixed with 400 µL GUS extraction buffer (1 M Na₂HPO₄, 50 mM NaPO₄, 10 mM EDTA; 0.1% v/v Triton X-100, 0.1% w/v N-lauroylsarcosine sodium salt, 0.7 µL/mL β-mercaptoethanol, pH 7.0). The cells were lysed by sonication at 14 W for 30 sec on ice using a Misonix 3000 sonicator. Samples were centrifuged at 10,000 × g for 5 min at room temperature and supernatants stored overnight at –80 °C. For analysis, the samples were clarified by centrifugation at 10,000 × g for 25 min at 4 °C. Total protein was measured against a BSA (PIERCE) standard curve using a Bradford assay (Bio-Rad). A 200 µL aliquot of 1× Bradford Assay Reagent was mixed with 10 µL protein extract, incubated for 5 min at room temperature and the absorbance measured at 595 nm. GUS activity of 100 µg soluble protein was determined using a fluorimetric (MUG) assay (Jefferson *et al.*, 1987) with 1 mM MUG substrate (Fluka Chemicals) in 200 µL GUS extraction buffer at 37 °C for 1 hr. Reactions were terminated by addition of 1 mL GUS stop buffer (0.2 M Na₂CO₃) and the fluorescence of 200 µL aliquots were measured in a LS50B luminescence spectrometer (Perkin Elmer) at excitation and emission wavelengths of 365 and 455 nm respectively. GUS activity was recorded as pmol MU/µg protein/min, and results were visualised and analysed statistically in Excel 2007 (Microsoft) and SPSS v16 (SPSS Inc.), respectively.

5.2.7 Analysis of Asupina and Cavendish banana fruit ripening

5.2.7.1 Plant materials

Green Asupina and Cavendish fruit was simultaneously ripened over a 12 day period to assess carotenoid accumulation during fruit maturation. Ungassed (not ethylene treated) green fruit was obtained from the QDPI Banana Germplasm collection at South Johnston (North Queensland) courtesy of Jeff Daniells (QDPI) and came in two sizes: i) large, mature

fruit from the top of the bunch which were fully formed but unripened, and ii) small, immature fruit from the bottom of the bunch whose ridges were more pronounced than in large fruit. Due to the limited number of fruit that could be shipped, six Asupina fruit (each size) and five Cavendish fruit (each size) were used for the trial.

5.2.7.2 Ripening trial

Fruit were ripened in an enclosed box (30 × 21.5 × 22.5 cm) containing additional fruit as ripening agents (a ripe apple, tomato, and banana and an unripe tomato) at room temperature (25 °C) in a plant tissue culture room to limit fluctuations in environmental conditions. Small and large fruit from each cultivar were sampled separately. Fruit were photographed; the mass and length recorded, and observations made of fruit characteristics. Transverse sections of fruit flesh (1 to 2 cm thick) were stored at –80 °C for further analysis. The first large and small fruits sampled from Asupina and Cavendish were not ripened, while the remaining fruit were sampled in the same manner at 48 hr intervals. All photographs were taken under identical lighting conditions to ensure consistency for comparison between samples. The ripening agents were removed after six days as they were no longer required for further ripening.

5.2.8 Semi-quantitative RT-PCR

5.2.8.1 Preparation of mRNA

Total mRNA was obtained as described in Chapter 2.1.1-2 from Asupina mature leaf tissue, Cavendish leaf tissue, Cavendish green and ripe fruit tissue (obtained as per Chapter 3.2.1), and Asupina unripened small green fruit and ripening small fruit (sampled day 10 post ripening induction, Chapter 5.2.7.2). Contaminating gDNA was removed from total mRNA using the Turbo-DNAfree™ (Ambion) system in reactions consisting of 40 µL total mRNA, 1× Turbo DNase buffer, 2 U Turbo DNase, 40 U Protector RNase Inhibitor (Roche Applied Science) and mqH₂O to 50 µL. The reactions were then incubated for 30 min at 37 °C before the addition of 5 µL DNase Inactivation reagent, incubated for 2 min at room temperature with periodic mixing and centrifuged at 10,000 × g for 2 min at room temperature. Integrity of mRNA was confirmed by RT-PCR of part of the banana *actin1* coding region using the Titan™ One Tube RT-PCR system (Roche Applied Science) as per Chapter 2.2.1 from 1 µL mRNA with annealing temperature and extension time of 60 °C and 30 sec, respectively. The *actin1* control primers, *actin1-qPCR-F1* and *actin1-qPCR-R1* (Table 5.1), were designed from *Musa acuminata actin1* mRNA (GenBank #: AF246288). Total mRNA concentration was measured using the Quant-it™ RiboGreen RNA assay kit (Invitrogen) as per the manufacturer's instructions for the 96 well plate format. The mRNA samples were

diluted to 3 ng/ μ L in mqH₂O (DEPC-treated), and the concentration was confirmed using the Quant-it™ RiboGreen kit (Invitrogen).

5.2.8.2 RT-PCR analysis

The mRNA levels of *psy1*, *psy2a* and *actin1* in the leaf, green fruit and ripe fruit of Asupina and Cavendish bananas were measured semi-quantitatively by RT-PCR using primers listed in Table 5.1. Asupina and Cavendish *psy1* were analysed using the *psy1_qPCR-F1/psy1_qPCR-R1* primer pair. The *Apsy2a_qPCR-F1/psy2a_qPCR-R1* (Asupina) and *Cpsy2a_qPCR-F1/psy2a_qPCR-R1* (Cavendish) primer sets were used to amplify *psy2a* templates. The *psy2-3'RACE-In-01/psy2-qPCR-RVS* and *actin1-qPCR-F1/actin1-qPCR-R1* control primer pairs were designed to amplify regions of *psy2* and *actin1*, respectively, that include introns for the detection of gDNA contamination.

The Titan™ One Tube RT-PCR system (Roche Applied Science, Chapter 2.2.1) was used to amplify templates from 3 ng mRNA using these primers with the annealing temperature and extension time modified to 60 °C and 30 sec, respectively. The semi-quantitative PCRs were repeated for consistency. The *actin1* and *psy2* control primers were used to detect gDNA contamination from 3 pg mRNA using the GoTaq Green® (Promega) PCR system as per Chapter 2.2.1 with annealing temperature and extension time of 60 °C and 30 sec, respectively. RT-PCRs (12.5 μ L) was electrophoresed on a 2% TAE agarose gel for 40 min (Chapter 2.2.3) against 500 ng GeneRuler™ 50 bp DNA Ladder (Fermentas). GeneTools v3.07 software was used for densitometry of RT-PCR product band intensity based on the 500 bp reference band (75 ng DNA) and results analysed in Excel 2007 (Microsoft).

5.3 Results

5.3.1 PSY promoter isolation and analysis

5.3.1.1 Promoter isolation

The genome regions approximately 2500 to 3000 bp upstream of the Asupina and Cavendish *psy1* and *psy2a* genes, containing their respective putative promoters, were isolated using genome walking PCR. Overlapping fragments were used to generate consensus sequences representing each promoter region, which were then amplified as single fragments that also included the native 5' UTR. The promoter fragments for each gene and cultivar were cloned and sequenced and a representative clone of each was selected for further analysis. The *psy1* promoter clones from Asupina (*Apsy1pr*) and Cavendish (*Cpsy1pr*) cultivars contained fragments of approximately 2700 bp. The Asupina *psy2a* promoter (*Apsy2apr*) clone contained an insert of approximately 2300 bp. However, during isolation of the Cavendish

psy2a promoter, three clones (*Cpsy2apr1*, *Cpsy2apr2* and *Cpsy2apr3*) containing slightly different sequences were identified. *Cpsy2apr1* was approximately 2300 bp, while *Cpsy2apr2* and *Cpsy2apr3* were approximately 2400 bp. The activity of all three *psy2a* promoter clones was subsequently investigated. The Asupina and Cavendish *psy2b* promoter regions could not be isolated using the same genome walking strategy. This was possibly due to technical limitations such as PCR amplification efficiency or target template quality.

5.3.1.2 Promoter analysis

The overall structure of the *psy1* and *psy2a* genes from Asupina and Cavendish was investigated by comparing their promoter sequences with available mRNA and gDNA data obtained in Chapter 3.

Comparison of the genomic 5' UTR sequences of Asupina and Cavendish *psy1* with their corresponding mRNA sequences showed that the *psy1* 5' UTR was divided into 3 exons that were interrupted by two introns (Figure 5.3). The first exon was 175 bp and 143 bp in Asupina and Cavendish, respectively, while the second exon was 91 bp in both *psy1* sequences. The 3' 88 bp of the 5' UTR in combination with the first coding region exon (termed exon 1 in Chapter 3) formed exon 3. In contrast, the *psy2a* genes did not have introns in their 5' UTRs, which formed the first half of exon 1 (Figure 5.3). As 5' RACE was not able to identify the true 5' end of the Cavendish *psy2a* mRNA transcript (Chapter 3), a 282 bp 5' UTR was predicted by aligning its genomic sequence with the 276 bp Asupina *psy2a* 5' UTR. Overall, exon 1 of Asupina and Cavendish *psy2a* was 634 and 649 bp, respectively (Figure 5.3). Phylogenetic analysis of the *psy* promoters (Figure 5.4) showed that the *psy1* and *psy2a* sequences separated into distinct groups as expected. Asupina and Cavendish *psy1* sequences were 88% identical, while *Apsy2apr* was 84% identical to *Cpsy2apr1* and 86% identical to *Cpsy2apr2* and *Cpsy2apr3*. The longer Cavendish *psy2a* promoter clones were 99% identical to each other but were only approximately 94 to 95% identical to *Cpsy2apr1* (Figure 5.4b). In contrast, the promoters of different *psy* genes exhibited very low identities.

Sequence alignment of *Apsy1pr* and *Cpsy1pr* suggested that both promoters had the same structure with no notable gaps. In contrast, alignment of the Asupina and Cavendish *psy2a* promoters identified large sequence gaps in one or more sequences relative to each other (Figure 5.5). *Apsy2apr* had several large gaps compared to the Cavendish *psy2a* promoters including 23, 33, 31 and 18 bp, which occurred at nucleotide position 451, 1118, 1226 and 1295, respectively, in the *Apsy2apr* sequence (Figure 5.5a – c). The most prominent gap in

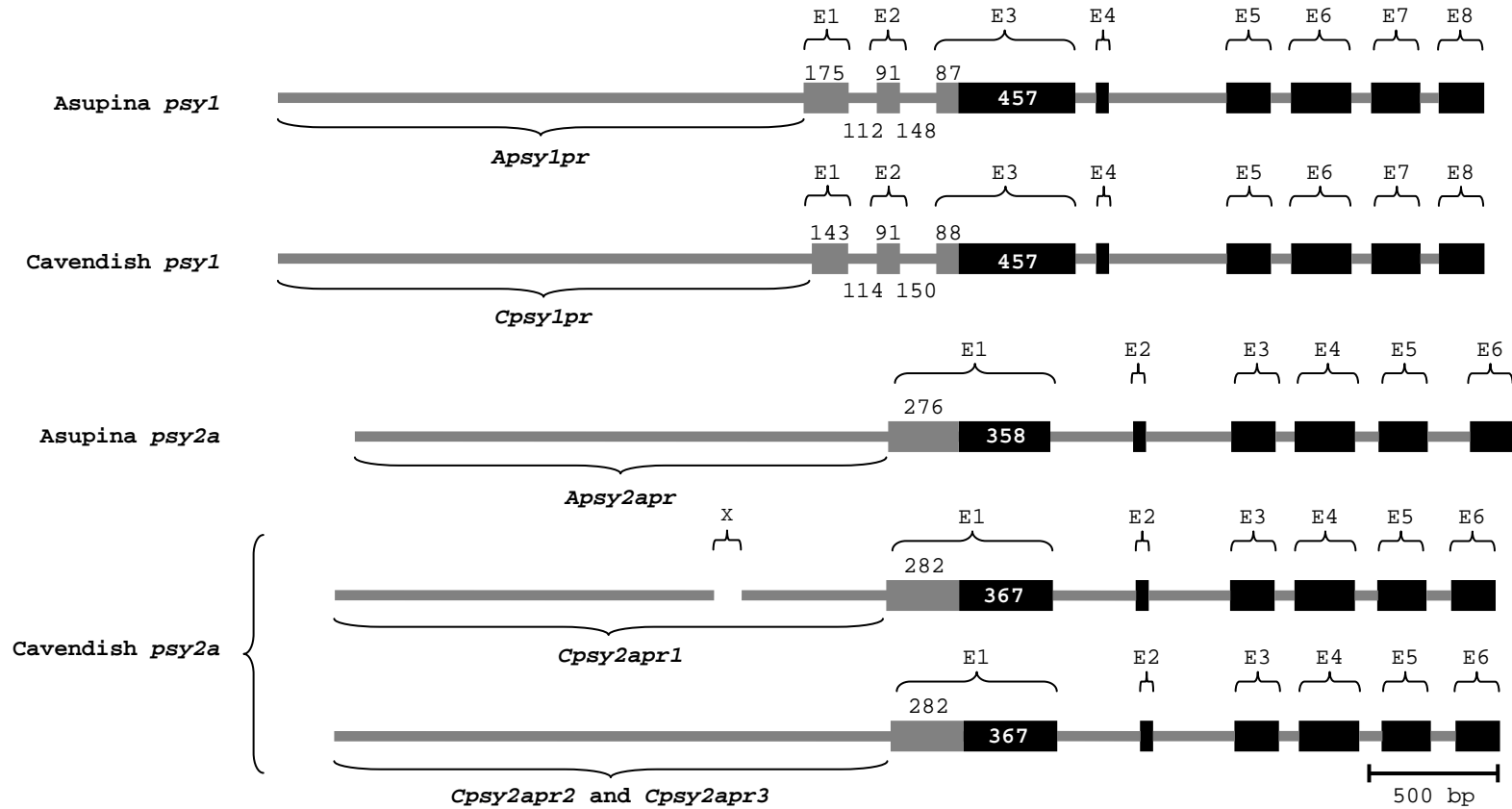
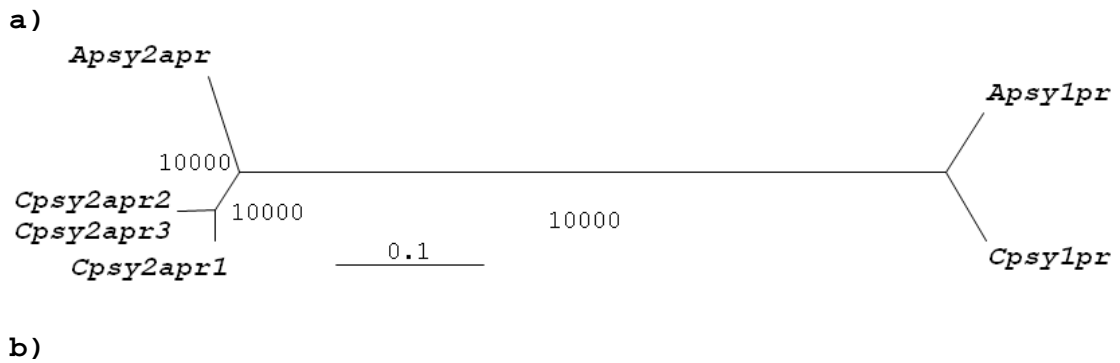


Figure 5.3: Updated *psy1* and *psy2a* genomic sequence information. Locations of the regulatory regions (grey line) of the Asupina *psy1* (*Apsy1pr*), Asupina *psy2a* (*Apsy2apr*), Cavendish *psy1* (*Cpsy1pr*), Cavendish *psy2a* (*Cpsy2apr1*, *Cpsy2apr2*, and *Cpsy2apr3*) promoters is indicated. Known exons (E) are numbered showing the position of 5' UTRs (grey rectangle) and coding regions (black rectangle), and are separated by introns (grey line). The sizes of the first exon of the coding region of each *psy* gene (white text), 5' UTR portion of exons (black text above grey rectangle) and introns in 5' UTR (black text below grey lines) are also labelled. The 107 bp internal deletion in *Cpsy2apr1* compared to *Cpsy2apr2* and *Cpsy2apr3* is also indicated (X).



Sequence A	Length (bp)	Sequence B	Length (bp)	Identity (%)
<i>Apsy1pr</i>	2672	<i>Cpsy1pr</i>	2650	88
<i>Apsy2apr</i>	2333	<i>Cpsy2apr1</i>	2292	84
<i>Apsy2apr</i>	2333	<i>Cpsy2apr2</i>	2427	86
<i>Apsy2apr</i>	2333	<i>Cpsy2apr3</i>	2415	86
<i>Cpsy2apr1</i>	2292	<i>Cpsy2apr2</i>	2427	95
<i>Cpsy2apr1</i>	2292	<i>Cpsy2apr3</i>	2415	94
<i>Cpsy2apr2</i>	2427	<i>Cpsy2apr3</i>	2415	99

Figure 5.4: Analysis of *psy* promoter sequences showing a) Bootstrapped radial tree of the Asupina *psy1* (*Apsy1pr*), Asupina *psy2a* (*Apsy2apr*), Cavendish *psy1* (*Cpsy1pr*), Cavendish *psy2a* (*Cpsy2apr1*, *Cpsy2apr2*, and *Cpsy2apr3*) promoters and b) percentage identity between promoter sequences.

Cpsy2apr1 was at nucleotide position 1478 (Figure 5.5d) with 118 bp and 107 bp deletions compared to *Apsy2apr* and the other Cavendish *psy2a* promoters, respectively. There were also two sequence gaps of 20 bp in the Cavendish *psy2a* promoters compared to *Apsy2apr* (Figure 5.5e) at nucleotide positions 1912 and 1966 in *Apsy2apr*. These gaps occur at the 3' end of the *psy2a* promoters in a region that was rich in repeat sequences and approximately 200 bp before the predicted transcription start sites. A common AG dinucleotide repeat that was 30 bp in *Apsy2apr* and 40 to 48 bp in the Cavendish *psy2a* promoters was found at the 3' end of this region (Figure 5.6). Several differences were observed upstream of the AG repeat (Figure 5.6). *Apsy2apr* had eight TA dinucleotide repeats ranging in size from (TA)₄ to (TA)₁₈ in an 82 bp region downstream of a (CA)₈ dinucleotide repeat. In contrast, *Cpsy2apr1* had a single (TA)₈ dinucleotide repeat downstream of a (CA)₁₅ dinucleotide repeat. Interestingly, there was a (TC)₉ dinucleotide repeat immediately upstream of the CA repeat. The Cavendish *psy2apr2* and *psy2apr3* promoters had TC repeats that were about 3 fold larger than that of *Cpsy2apr1*, smaller (CA)₄ repeats and lacked the TA repeat region. Upstream of the conserved AG repeat, *Cpsy2apr1* did not have a spacer sequence that separated it from the other dinucleotide repeats unlike the other Cavendish *psy2a* promoter sequences (8bp spacer) and *Apsy2apr* (26 bp spacer).

a)	<i>Cpsy2apr2</i>	ACATAGATCATGAACTGCACATGATGGCTAACGTGAAGACCAAGGAGAATTACTTCATCC	480
	<i>Cpsy2apr3</i>	ACATAGATCATGAACTGCACATGATGGCTAACGTGAAGACCAAGGAGAATTACTTCATCC	480
	<i>Cpsy2apr1</i>	GCATAGATCATGAACTGCACATGATGGCTAACGTGAAGACCAAGGAGAATTGCTTCATCC	476
	<i>Apsy2apr</i>	ACATAGATCATGAACTGCACATGATGGCTAACGTGAAGACCA-----	451

	<i>Cpsy2apr2</i>	AACCATTCTTCTTTGCTGCAGCAGCAATTGTTTTAATGGAAGCTTGCAGCGAAGCCTTA	540
	<i>Cpsy2apr3</i>	AACCATTCTTCTTTGCTGCAGCAGCAATTGTTTTAATGGAAGCTTGCAGCGAAGCCTTA	540
	<i>Cpsy2apr1</i>	AACCATTCTTCTTTGCTGCAGCAGCAATTGTTTTAATGGAAGCTTGCAGCGAAGCCTTA	536
	<i>Apsy2apr</i>	-----TTGCTTCTTTGCTGGAAGCAGCAATTGTTTTAATGGAAGCTTGCAGCGAAGCCTTA	506
		* * * * *	
		* * * * *	
	b)	<i>Cpsy2apr2</i>	TGTAGACGA-----CGAAGAATATTTGTTCATACCATATAAATTTCTCCCTCATTAAATC
<i>Cpsy2apr3</i>		TGTAGACGA-----CGAAGAATATTTGTTCATACCATATAAATTTCTCCCTCATTAAATC	1194
<i>Cpsy2apr1</i>		TATAGACGATAGGACGGAGAATATTTGTTCGTACCATATAAATTTCTCCCTCATTAAATC	1189
<i>Apsy2apr</i>		GGTAGATGATAGGACGAGATAAATTTGTT-----	1118
		* * * * *	
<i>Cpsy2apr2</i>		GGATATAAAAAGTCACTTAGAACATGATAAAACAAGTTAATTATTATTACTAAAATTAT	1254
<i>Cpsy2apr3</i>		GGATATAAAAAGTCACTTAGAACATGATAAAACAAGTTAATTATTATTACTAAAATTAT	1254
<i>Cpsy2apr1</i>		TGATAGAAAAGTCACTTAGAACACGATAAAACAAGTTAATTATTATTACTAAAATTAT	1249
<i>Apsy2apr</i>		--ATATAAAAAGTCCGTTGGAGCATGATAAATGAGATCAATTACTATTACTAAAATTAT	1176
		* * * * *	
		* * * * *	
<i>Cpsy2apr2</i>		TTCATCCTTGTCAACTACCAACTTGAGCAT--GGTTAGATCATGTCGAAAACCTCTATTTCGA	1313
<i>Cpsy2apr3</i>	TTCATCCTTGTCAACTACCAACTTGAGCAT--GGTTAGATCATGTCGAAAACCTCTATTTCGA	1313	
<i>Cpsy2apr1</i>	TTCATCCTTGTCAACTAT-----AGCATCGGATAGATTATGTCGAAAACCTCTATTTCGA	1302	
<i>Apsy2apr</i>	TTCATTCTTATCAGCTATCAATTTGAGCATCCAATAGTTAA-----CTATTTCGA	1225	
	* * * * *		
	* * * * *		
<i>Cpsy2apr2</i>	CCTTAATCTTCATGTAGGTTGACGGTTGGATGAGCGTACAATCGAGTCTACATCAGCCCC	1373	
<i>Cpsy2apr3</i>	CCTTAATCTTCATGTAGGTTGACGGTTGGATGAGCGTACAATCGAGTCTACATCAGCCCC	1373	
<i>Cpsy2apr1</i>	CCTTAATCTTCATGTAAG-----AGTGTAATCGAGTCTACATTAGCCCC	1348	
<i>Apsy2apr</i>	C-----G-----AGCATACAATTCAGTCTAC--CAA--C	1250	
	* * * * *		
	* * * * *		
c)	<i>Cpsy2apr2</i>	CAAGCAATTATTTCGAACTTCCACTCAATCACATCGAACTTCTTACGCAAACCTAAATCAA	1433
	<i>Cpsy2apr3</i>	CAAGCAATTATTTCGAACTTCCACTCAATCACATCGAACTTCTTACGCAAACCTAAATCAA	1433
	<i>Cpsy2apr1</i>	CAAGCAAGTGTTCAAGCTTCCACTCAATCACATCGGACTACTTACACAAATCTAAATCAA	1408
	<i>Apsy2apr</i>	CAAGTAAGCGTTTAGGTTTTCTTTAATCATATCGAAATTTTAC-----	1295
		* * * * *	
	<i>Cpsy2apr2</i>	ATCAGCTTATTCTATGTATCATTAATATTTATATTATGGCACATTAATATACTGACTCAT	1493
	<i>Cpsy2apr3</i>	ATCAGCTTATTCTATGTATCATTAATATTTATATTATGGCACATTAATATACTGACTCAT	1493
	<i>Cpsy2apr1</i>	ATCAGCTTGTTCAGGATCATTAATATTTATATTATCGCACATTAATATGCTGACTCAT	1468
	<i>Apsy2apr</i>	---AGTCTGTTCCAAACATCATCGATATTTATGTTATCTCACATTAATCCGTTGACTCAT	1352
		* * * * *	
		* * * * *	
	d)	<i>Cpsy2apr2</i>	AAAATCTTAAAATTTAACTCTCAAACCTGTTGTAATATCAACATC-----GACATTAA
<i>Cpsy2apr3</i>		AAAATCTTAAAATTTAACTCTCAAACCTGTTGTAATATCAACATC-----GACATTAA	1545
<i>Cpsy2apr1</i>		AAAATCTTAA-----GACATTAA	1478
<i>Apsy2apr</i>		AAAATCTTAAAATTTAACTCCCAAACCGTTATAATATCAATATCCAAACATGGACATTAA	1412

<i>Cpsy2apr2</i>		ATCGGAAGAGATGG--TTTGAATGATGACGAAGAGAGTTGCCTCCAACATCGACACA--AA	1602
<i>Cpsy2apr3</i>		ATCGGAAGAGATGG--TTTGAATGATGACGAAGAGAGTTGCCTCCAACATCGACACA--AA	1602
<i>Cpsy2apr1</i>		-----	
<i>Apsy2apr</i>		ATTGGAAGAGATGGGTTTGAATGATGACCGAGAGAGTAGCCTCCAACATTGACACATAAA	1472
<i>Cpsy2apr2</i>		TAGTTTGATACATGTAGATAGCTATCCAATCTTCTATTTCATGCATATGAAAGACCAACA	1662
<i>Cpsy2apr3</i>		TAGTTTGATACATGTAGATAGCTATCCAATCTTCTATTTCATGCATATGAAAGACCAACA	1662
<i>Cpsy2apr1</i>		-----TACATGTAGATAGCTATCCAATCTTCTATTTCATGCATCTGTAAGACCAACA	1530
<i>Apsy2apr</i>	TTGTTTGATACACGTAGA--AGCTATCCAATCTTCTATTTCATGCATCTATAAAACCAACA	1531	
	* * * * *		
	* * * * *		
e)	<i>Cpsy2apr2</i>	CT	2055
	<i>Cpsy2apr3</i>	CT	2055
	<i>Cpsy2apr1</i>	CTCTCTCTCTCACACACACACACAC-----ACACACACACACACA	1924
	<i>Apsy2apr</i>	CACACACATATATATGTATATATATGTGTATAAATATATATGTGTATATATATATACACA	1946
		* * * *	
	<i>Cpsy2apr2</i>	CTCTCTC--CACACACATAT-----CATTCAGAGAGAGAGAGAGAGAG	2094
	<i>Cpsy2apr3</i>	CTCTC--CACACACATAT-----CATTCAGAGAGAGAGAGAGAGAG	2092
	<i>Cpsy2apr1</i>	TATAT-----ATATATATAT-----AGAGAGAGAGAGAGAGAGAG	1959
	<i>Apsy2apr</i>	TATATATACATATATATATGTGTATATATGGGTTTGACACAATGGCAATGAATGAGAG	2006
		* * * * *	
		* * * * *	
	<i>Cpsy2apr2</i>	AGAGAGAGAGAGAGAGAGAGAGAAAGAGACAGATGCTGATGGGTTTCACCTCAAATTTGTTCT	2154
<i>Cpsy2apr3</i>	AGAGAGAGAGAGAGAGAGAGAGAAAGAGACAGATGCTGATGGGTTTCACCTCAAATTTGTTCT	2152	
<i>Cpsy2apr1</i>	AGAGAGAGAGAGAGAGAGAGAGAGAGACAGATGCTGATGGGTTTCACCTCAAATTTGTTCT	2019	
<i>Apsy2apr</i>	AGAGAGAGAGAGAGAGAGAGAGAGAGAGAGCCGACGCTTCTGCGTTTTCACCTCAAATTTGTTG	2066	

	* * * * *		

Figure 5.5: Alignment of selected regions of *psy2a* promoters showing sequence gaps found in each promoter. The location of each region a) to e) from the first nucleotide of the cloned promoter sequence is indicated by numbers on the right hand side of each line. Gaps in the sequence alignment (dashes highlighted in grey) and conserved residues (* below each line) are also highlighted.

Apsy2apr
TTATGCAGATCACACACACACACACATATATATGTATATATATGTGTATAAAATATATATGTGTATATA
TATATACACATATATATACATATATATATGTGTGTATATAATGGTTTGACACAATGGCAATGAATGAGAGAGA
GAGAGAGAGAGAGAGAGAGAGAGGCCGACGCTT

Cpsy2apr1
TTTATGCAGATCTCTCTCTCTCTCTCTCTCACACACACACACACACACACACACACACACATATATATAT
ATATATAGACAGATGCTG

Cpsy2apr2
TTTATGCAGATCC
CACACATATCATTGAAAGAGACAGATGCTG

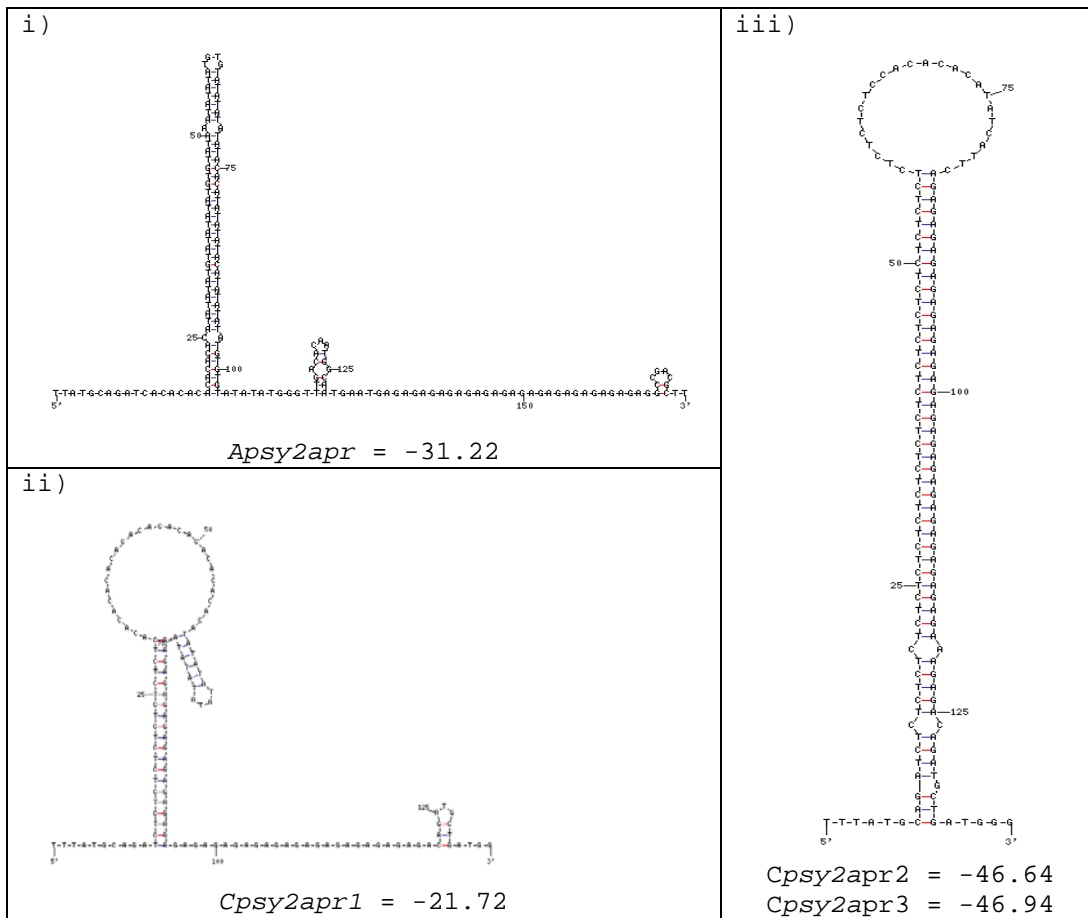
Cpsy2apr3
TTTATGCAGATCCACA
CACATATCATTGAAAGAGACAGATGCTG

Figure 5.6: Repeat sequence analysis of *psy2a* promoters of Asupina and Cavendish showing the position of identified dinucleotide repeats in each promoter: TA (text underlined with dots), CA (italicised text), TC (bold text) and AG (white text with black background). Spacer nucleotides preceding the AG dinucleotide repeat (small capital letters) and the 10 nucleotides flanking the repeat region (plain capital letters) are also shown.

The presence of adjacent TC and AG dinucleotide repeats in this region raised the possibility that it may form secondary structure in the Asupina and Cavendish *psy2a* promoters. The most stable structures identified during analysis of this region for DNA secondary structure elements are shown in (Figure 5.7a). The main loop of *Apsy2apr* had a 39 bp long stem region that terminated in a small loop consisting of 4 bp. Approximately 11 bp downstream of the main *Apsy2apr* loop, before the conserved AG repeat, was a smaller secondary loop structure. The main feature of this region in *Cpsy2apr1* was a structure with a stem of 18 bp and a 33 bp main loop. Interestingly, at the 3' end of the main loop was a smaller 14 bp structure with a 6 bp loop region, and no other structures were observed prior to the AG repeat region. *Cpsy2apr2* and *Cpsy2apr3* were predicted to form the largest secondary structure which consisted of stem and loop regions of 104 bp and 27 bp, respectively. Analysis of the properties of all the predicted DNA secondary structures (Figure 5.7a) showed that the loops of the longer Cavendish *psy2a* promoters (*Cpsy2apr2* and *Cpsy2apr3*) were the most stable, followed by those of *Apsy2apr* and *Cpsy2apr1*. The more stable loops tended to have higher predicted melting temperatures. Interestingly, the *Cpsy2apr1* secondary structure had only one predicted form while *Apsy2apr* and the other Cavendish *psy2a* promoters had 3 and 4 forms respectively. The region in which the predicted DNA secondary structures occurred was approximately 50 bp upstream of the transcription start site of the Asupina and Cavendish *psy2a* promoters (Figure 5.7b).

As differences in promoter sequence composition, such as the gaps in the *psy2a* promoters, could affect the presence of regulatory elements, the Asupina and Cavendish *psy1* and *psy2a*

a)



b)



Figure 5.7: Secondary structure analysis of repeat region in the *psy2a* promoters of *Asupina* and *Cavendish*. a) Predicted secondary structures of the repeat regions of: (i) *Apsy2apr*, (ii) *Cpsy2apr1*, (iii) *Cpsy2apr2* and *Cpsy2apr3* with the free energies ΔG , measured in kcal/mol) of the most stable predicted structures. b) Representation of the 3' end of the *psy2a* promoters marking the location of the predicted secondary structures (loop), 5' UTR region, and 5' coding region (CR) with the positions of the transcription start site (tx start) and start codon (ATG) shown.

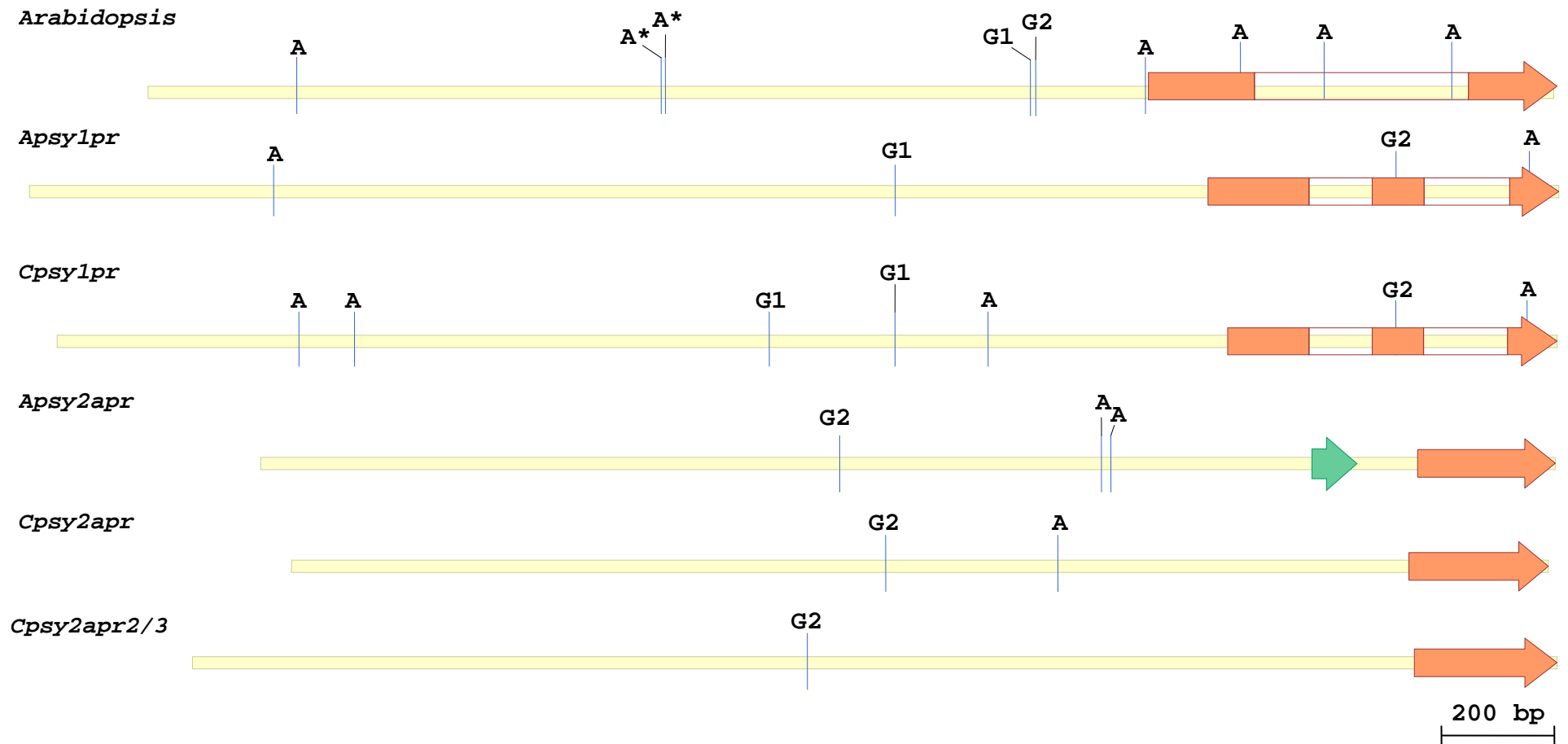


Figure 5.8: Identification of putative DNA regulatory motifs in banana *psy* promoters compared to those previously identified in the *Arabidopsis thaliana* *psy* promoter (Welsch *et al.*, 2003). The position of A (ATCTA), G1 (CACGAG) and G2 (CTCGAG) motifs in the 5' UTR (orange arrow) and untranscribed regions (yellow line) of the promoters is shown. The two ATCTA motifs previously characterised in *Arabidopsis* are marked with an asterisk (A*).

promoter sequences were further analysed to look for the ATCTA (basal promoter activity), G1 and G2 (red light responsive) regulatory motifs previously identified in the *Arabidopsis thaliana psy* promoter (Figure 5.8). The untranscribed regulatory region upstream of the 5' UTR of *Apsy1pr* had single putative ATCTA (position 427) and G1 (position 1512) motifs, while the *Cpsy1pr* regulatory region had three putative ATCTA motifs (positions 427, 526 and 1645) and two putative G1 motifs (positions 1258 and 1480). There were no G2 motifs in the untranscribed region of the *psy1* promoters but there was a single putative G2 motif and ATCTA motif in the 5' UTR of both *Apsy1pr* and *Cpsy1pr*.

There were no G1 motifs found in any *psy2a* promoter sequences. *Apsy2apr*, *Cpsy2apr1*, *Cpsy2apr2* and *Cpsy2apr3* each had one G2 motif at positions 1044, 1084, 1094 and 1094, respectively, in the untranscribed regulatory region. Interestingly, while there were two ATCTA motifs in *Apsy2apr* (positions 1516 and 1533) and one in *Cpsy2apr1* (position 1398), there were no ATCTA motifs identified in *Cpsy2apr2* and *Cpsy2apr3*. Additionally, no putative regulatory motifs were found in any of the *psy2a* 5' UTRs. Generally, the putative ATCTA motifs in the *psy1* promoters were located 5' of the putative G1 motifs, but were 3' of the putative G2 motif found in the *psy2a* promoters. However, one predicted ATCTA motif in *Cpsy1pr* was 3' of both putative G1 sequences. Differences in the presence and location of these putative regulatory elements may reflect differences in the activity of the Asupina and Cavendish *psy1* and *psy2a* promoters that could influence pVA accumulation by modifying gene expression.

5.3.2 Comparison of promoter activity

The activity of the Asupina and Cavendish *psy1* and *psy2a* promoters was compared by subcloning these regions into the *pGEM-4Z*-based expression vector to facilitate GUS expression in banana (Cavendish Williams) ECS and Cavendish green and ripe fruit tissue. The promoter regions investigated included *Apsy1pr*, *Apsy2a-pr*, *Cpsy1pr* and the three variants of the Cavendish *psy2a* promoter (*Cpsy2apr1*, *Cpsy2apr2*, and *Cpsy2apr3*) identified during promoter isolation. The ACC oxidase and ubiquitin promoter regions, *acopr* and *ubipr*, were included as fruit-specific and constitutive positive control promoters, respectively. Untransformed tissue was included as a negative control.

5.3.2.1 Microprojectile bombardment of banana ECS

Each of the six *psy* promoter constructs and two controls were bombarded onto four plates of banana ECS, before histochemical staining for qualitative analysis of GUS expression to estimate promoter activity. Transient expression of GUS under the control of *Apsy1pr*,

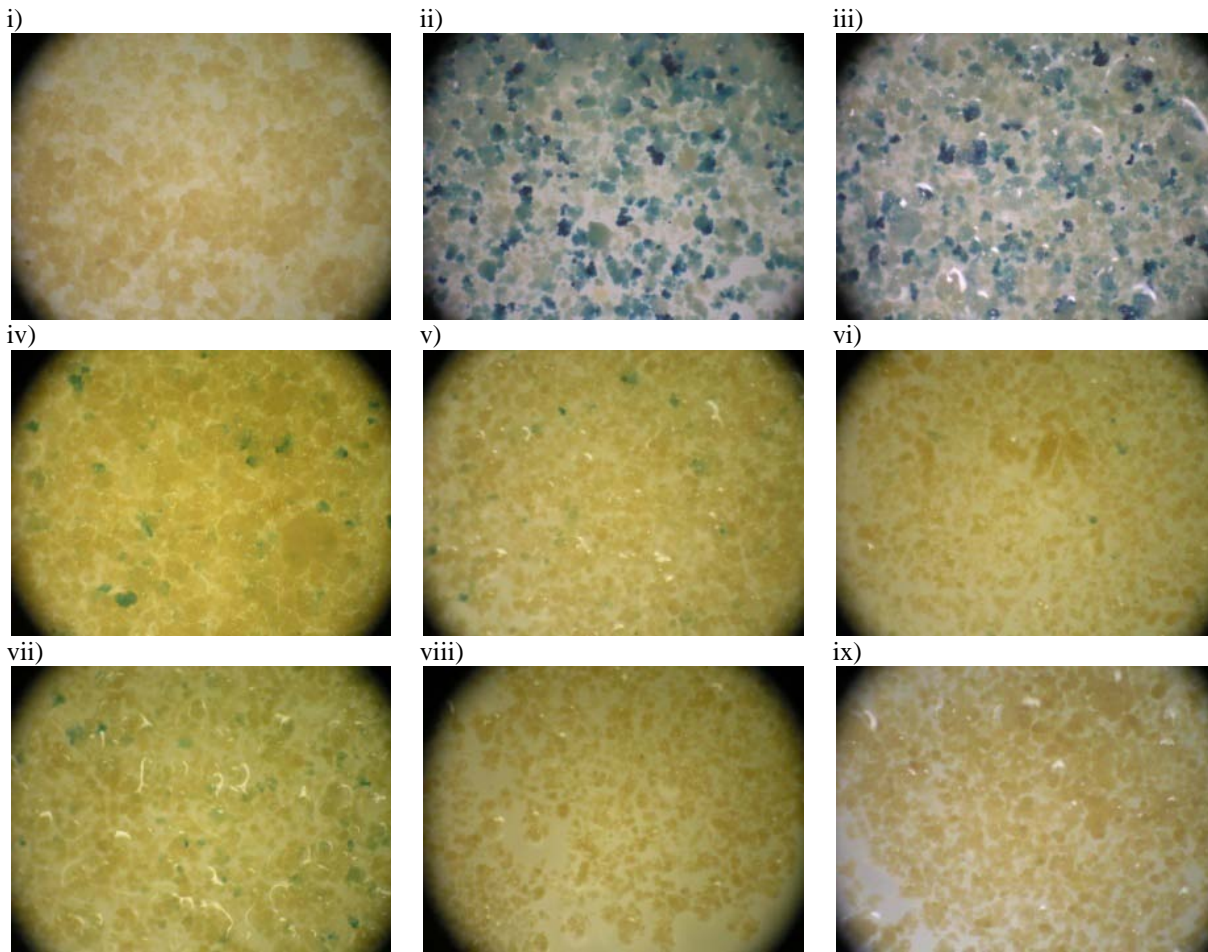
Cpsy1pr and *Cpsy2apr1* appeared to be similar based on visual analysis of the numbers transformed cells (blue foci) at 16× magnification while *Apsy2apr* yielded fewer foci and ECS transformed with the *Cpsy2apr2* and *Cpsy2apr3* constructs were identical to the unshot control (no visible foci, results not shown). The control promoters *acopr* and *ubipr* appeared to direct significantly higher transient GUS expression than the banana *psy* promoter constructs as greater numbers of foci were observed (results not shown). This experiment was repeated and one replicate of each treatment was stained histochemically (Figure 5.9a). The results were consistent with those observed in the first experiment. The remaining three replicates were assayed using a fluorimetric MUG assay (Figure 5.9b & c) to quantitatively compare the differences in Asupina and Cavendish promoter activity in ECS. GUS expression directed by *ubipr* and *acopr* was significantly higher than both the unshot ECS and banana promoters (Figure 5.9b). Closer comparison of banana *psy* promoter activities (Figure 5.9c), without the two positive controls, showed that *Cpsy2apr1* was the most active of the *psy* promoters followed by *Apsy1pr*, *Apsy2apr* and *Cpsy1pr* which were 6.5 fold, 3.7 fold, 2.7 fold and 1.5 fold higher than the unshot control, respectively. ECS transformed with GUS vectors driven by *Cpsy2apr2* and *Cpsy2apr3* showed no visible GUS foci (Figure 5.9a), and their GUS expression was consistent with that of the unshot control (Figure 5.9c). There was considerable variability within sample replicates and only *Cpsy2apr1* differed significantly from other promoters, with the exception of *Apsy1pr*, which was also not statistically different from the unshot controls. The high level of variation seen between *Cpsy2apr1* replicates was confirmed not to be due to the MUG assays and must have arisen during bombardment. The experiment could not be repeated due to limited availability of ECS.

5.3.2.2 Microprojectile bombardment of banana fruit

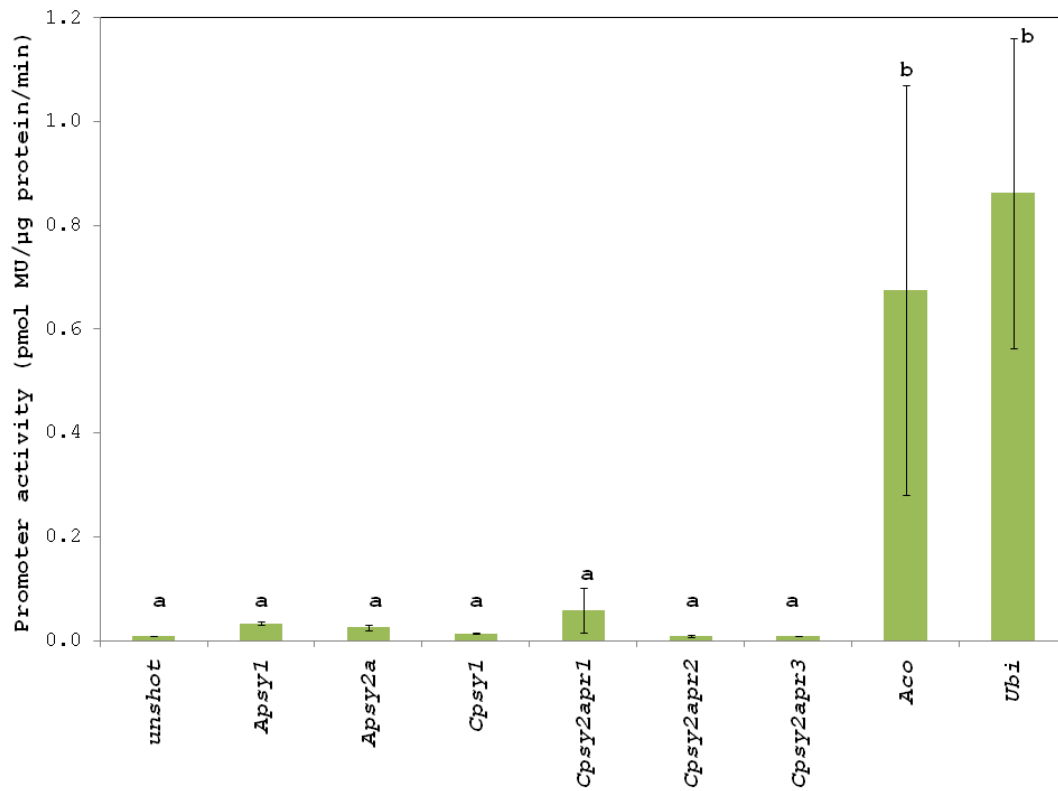
Having observed differences in the activity of the Asupina and Cavendish *psy* promoters in banana ECS, these promoters were then tested transiently in banana leaf and fruit tissue for comparison in a more representative gene expression background to better reflect their potential impact on carotenoid biosynthesis.

Promoter activity was initially examined in tissue cultured leaf of Asupina and Cavendish (two leaves per treatment). Each banana *psy* and control promoter was bombarded into leaf tissue of both cultivars (four replicates) and histochemically stained after 24 hr incubation post-bombardment. Only a handful of faint GUS foci were observed across all treatments (results not shown). The experiment was repeated once with similar results, particularly for the *acopr* and *ubipr* positive controls (results not shown), indicating the need for further

a)



b)



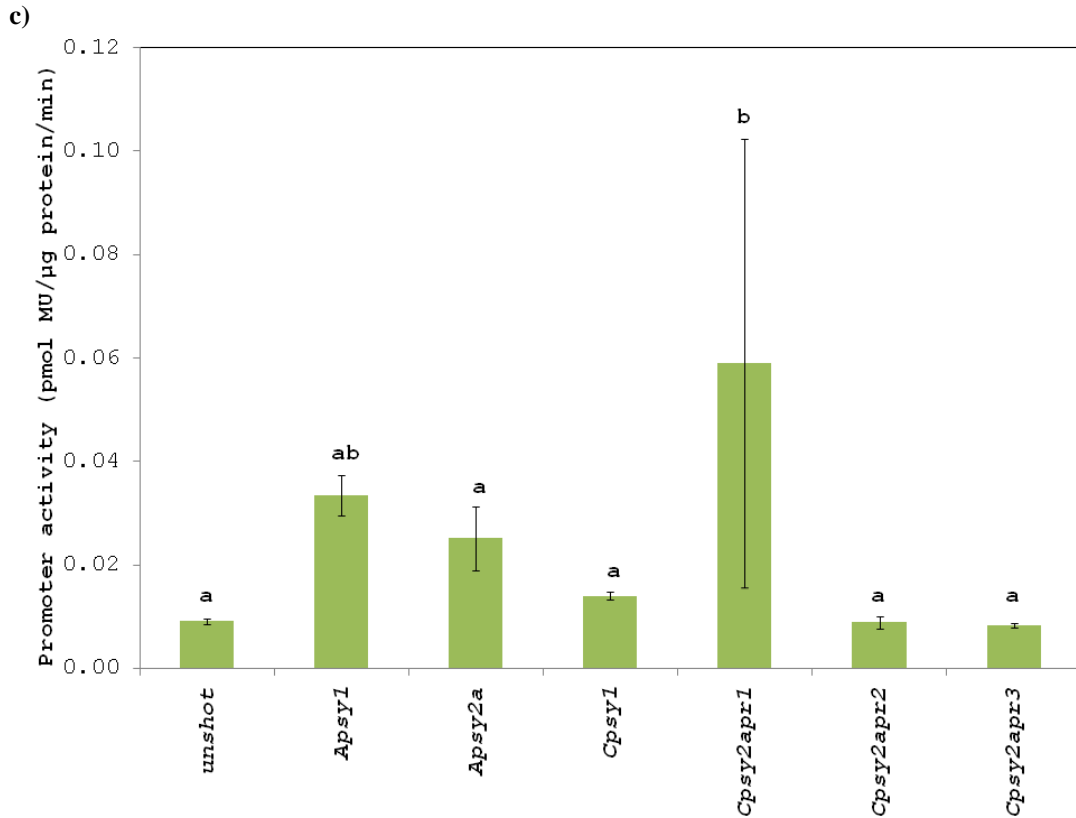


Figure 5.9: Analysis of banana *psy* promoter activity in banana ECS (24hr post bombardment). **a)** Histochemical assays of GUS reporter gene activity controlled by banana *psy* and control promoters. Representative photographs showing i) unshot cells and cells transformed with ii) *aco*, iii) *ubi*, iv) *Apsy1pr*, v) *Cpsy1pr*, vi) *Apsy2apr*, vii) *Cpsy2apr1*, viii) *Cpsy2apr2* and ix) *Cpsy2apr3* promoter constructs (16× magnification). Quantitative fluorimetric analysis (MUG assay) of banana *psy* promoter activity compared to the unshot negative control and the *acopr* and *ubipr* positive control promoters **b)** or the negative control only **c)** (to better demonstrate differences in *psy* promoter activity). Three replicates were averaged per fluorescence measurement (green columns) except the unshot control (two replicates). The error bars on each column represent standard deviation (not calculated for unshot samples due to the number of replicates). One-way ANOVA with least significant difference post-hoc analysis was used to determine the statistical significance of promoter activity in **b)** and **c)** with a 95% confidence level. Letters above each bar (a and b) in the graphs were used to group treatments with promoter activity levels that were not statistically different. Statistical analysis in **c)** omitted the *acopr* and *ubipr* positive controls.

optimisation. However, analysis of promoter activity in leaf tissue was discontinued due to unavailability of leaf tissue for further experiments and insufficient time. All subsequent promoter analysis was undertaken in fruit tissue.

Initially, the Asupina and Cavendish *psy* and control promoter constructs were bombarded into ripe Cavendish fruit tissue purchased from a supermarket. This fruit was at an advanced stage of ripening characterised by completely yellow peel colour and ripened flesh (but was not overripe). Due to difficulties in obtaining fruit slices of consistent mass and surface area, and the fact that microprojectile bombardment would only transform surface tissue, meaning that GUS expression would not be detectable in fruit lysates that would consist mainly of untransformed cells, fluorimetric analysis was not considered reliable for comparison of GUS expression in fruit. Therefore, all bombarded fruit replicates were histochemically stained to assess GUS activity. Histochemical staining after 24 hr incubation gave no visible signs of expression for any of the banana *psy* promoter constructs in addition to inconsistent results for *acopr* and *ubipr* control promoters, which did not show expression in some replicates (results not shown). This was hypothesised to be due to the condition of the fruit, therefore, ethylene-treated green fruit obtained from a supermarket and exhibiting a completely green peel colour and firm flesh texture, were subsequently used. GUS expression driven by *ubipr* was lower than expected and yielded far fewer foci than *acopr* (Figure 5.10a), which was almost four fold more active (Figure 5.10b). Generally, the banana *psy* promoters were identical to the unshot control (Figure 5.10a), and only one of the four *Cpsy2apr1* replicates displayed any visible GUS expression (four GUS foci). This was visible only under high magnification using a stereo microscope and was comparatively lower than *acopr* (Figure 5.10a iv & v). Statistical analysis (Figure 5.10b) showed that the activities of *acopr* and *ubipr* differed significantly from those of the banana *psy* promoters, but not from each other. The apparent statistical similarity between the activities of the unshot (two replicates) and *ubipr* (four replicates) controls was due to software limitations in the handling of the number of replicates rather than equivalence of the activities of the two treatments. In summary, the results suggested that the banana promoters were not active to detectable levels in ethylene-treated green fruit as all were comparable to unshot tissue (Figure 10b). However, low expression of the constitutive *ubipr* promoter indicated that the experiment required further optimisation such as a longer incubation time post transformation to enhance GUS accumulation.

On the strength of the previous results, a larger experiment was carried out on green fruit tissue that had not been ethylene treated, and obtained directly from a banana grower. The number of replicates was doubled to eight so that GUS staining could be tested at both 24

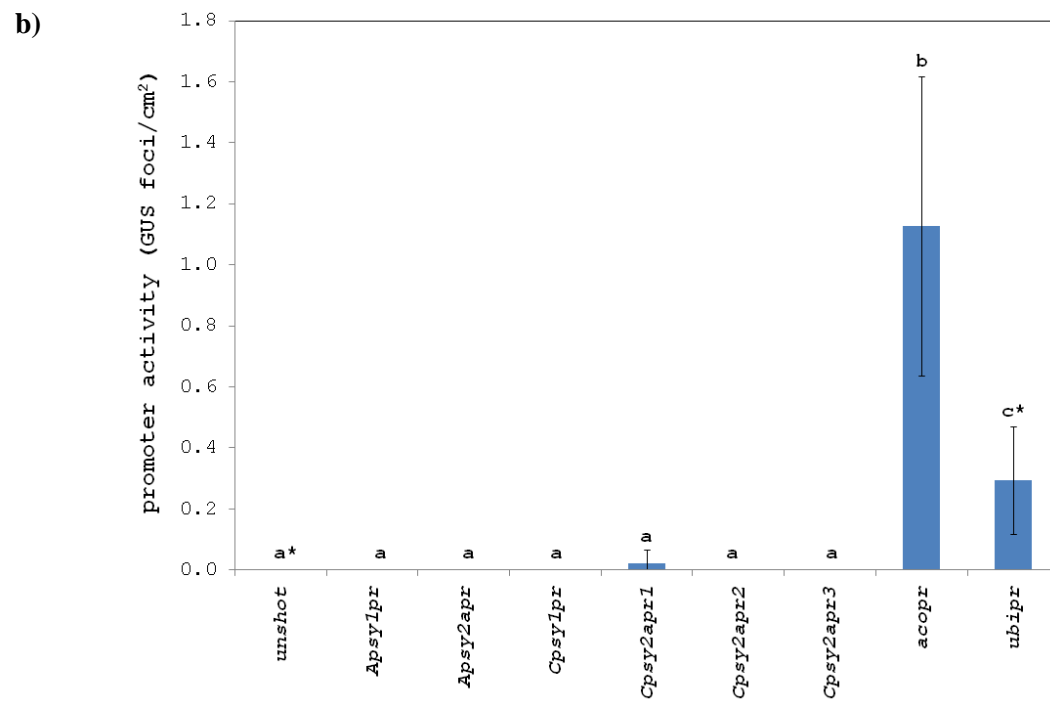
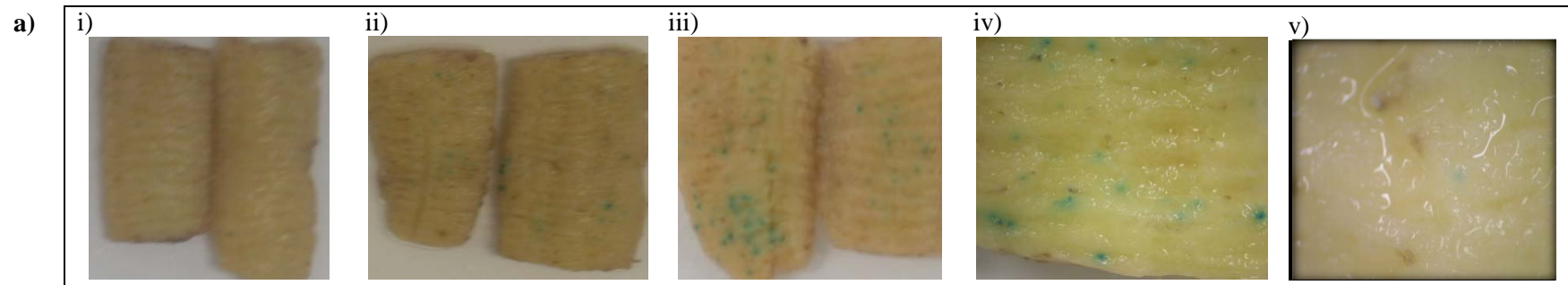
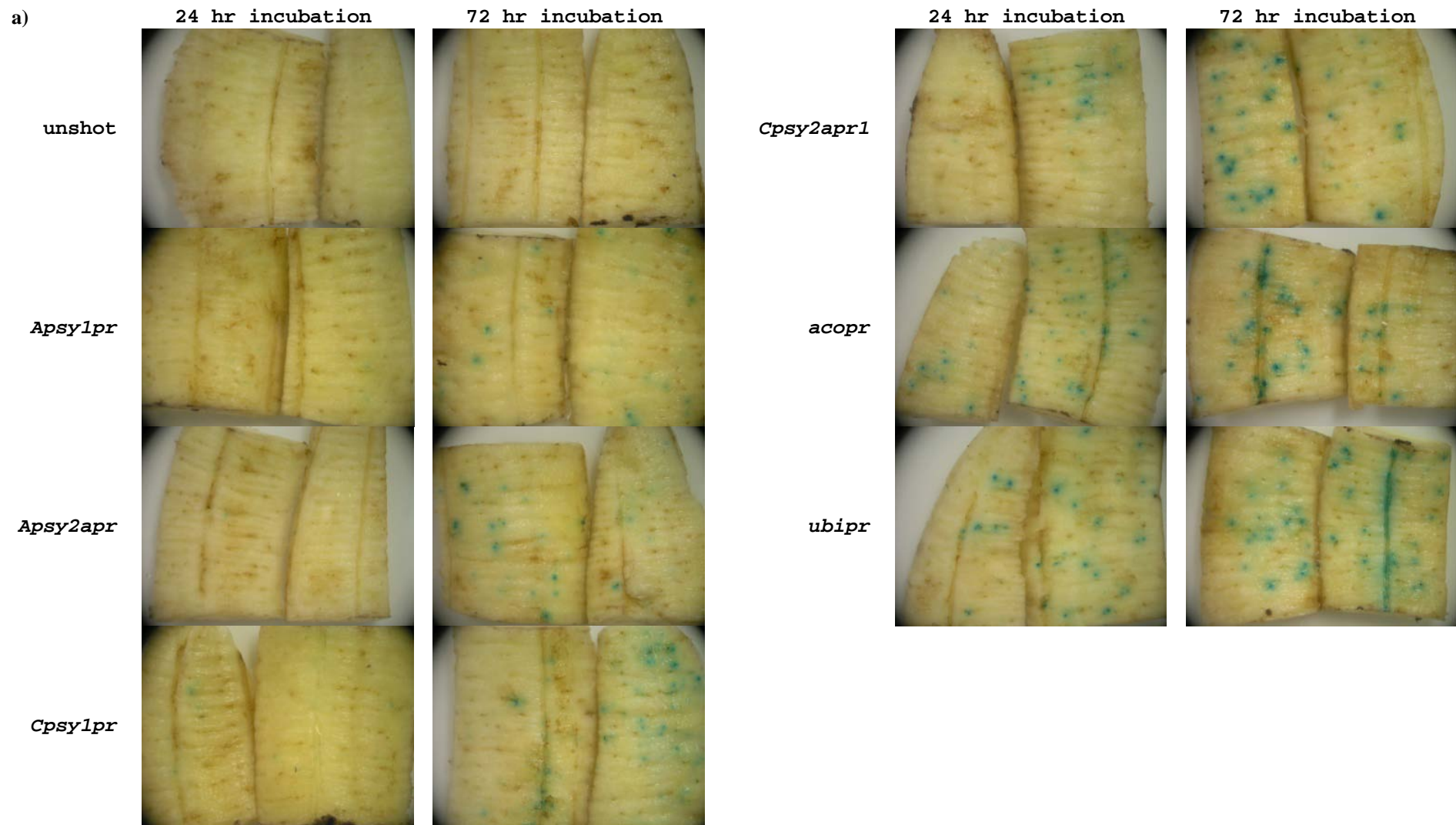


Figure 5.10: Analysis of *psy* promoter activity in gassed green fruit (24 hr post bombardment) showing a) unshot tissue i), tissue bombarded with ii) *ubipr* and iii) *acopr* at 2.68 \times magnification, and iv) *acopr* and v) *Cpsy2apr1* at 16 \times magnification. b) Semi-quantitative analysis of promoter activity measuring average GUS expression (four replicates), with standard deviation represented as error bars on each column. No standard deviation was calculated for the unshot control (two replicates). Statistical significance of promoter activity was calculated with 95% confidence using a one-way ANOVA and least significant difference post-hoc analysis. Promoters whose activities were not statistically different were grouped using the same letter (a, b or c), located above each bar. The unshot (a*) and *ubipr* (c*) groups were not determined to be statistically significant by SPSS v16 due to the difference in the number of replicates in the unshot control (two) compared to *psy* the promoter treatments (four), which affected the way that SPSS processed the data.

and 72 hr post bombardment (four replicates each). After 24 hr, tissue transformed with *acopr* and *ubipr* GUS expression vectors appeared to have similar numbers of foci (Figure 5.11a) although closer analysis suggested that the activity of *ubipr* was 30% higher than *acopr* (Figure 5.11b). Histochemical staining of fruit bombarded with *Apsy1pr*, *Apsy2apr* and *Cpsy1pr* GUS vectors produced very few foci, and *Cpsy2apr1* transformants yielded more foci that were clearly visible (Figure 5.11a). Semi-quantitative analysis showed that *Cpsy2apr1* was twice as active as *Apsy1pr* and *Cpsy1pr*, whose levels were similar, and over 3.5 fold more active than *Apsy2apr* (Figure 5.11b). *Cpsy2apr2* and *Cpsy2apr3* showed no visible GUS staining and were identical to the unshot control (results not shown). Only the activities of positive control promoters (*acopr* and *ubipr*) were statistically significant from unshot tissue after 24hr incubation (Figure 11b), although *Cpsy2apr1* was also statistically similar to *acopr*. In comparison, after 72 hr incubation post bombardment distinct GUS foci were obvious in all treatments (Figure 5.11a) except *Cpsy2apr2* and *Cpsy2apr3*, which were identical to the unshot control (results not shown). The activity of *ubipr* was almost double that of *acopr* (Figure 5.11b). *Cpsy1pr* was approximately 2.5 fold more active than *Apsy1pr* and *Apsy2apr*, which had similar activity (Figure 5.11b). *Cpsy2apr1* appeared to have more prominent foci than *Cpsy1pr* (Figure 5.11a) but was only 85% as active based on number of foci (Figure 5.11b).

Incubation for 72 hr compared to 24 hr gave improved results for all the promoters tested with the greatest difference seen in *Apsy2apr* and *Cpsy1pr* which were 10 and 15 fold higher, respectively (Figure 5.11b). Generally, the Cavendish *psy* promoters performed better than those of Asupina and both *psy1* and *psy2a* appear capable of similar levels of expression in fruit. However, as was seen in the transformation of banana ECS, *Cpsy2apr1* was the only Cavendish *psy2a* promoter that showed any activity. Neither *Cpsy2apr2* nor *Cpsy2apr3* were active even after 72 hr incubation. There was high variation in promoter activity between replicates of each treatment, and the only promoters driving GUS expression that were statistically significant from unshot tissue after 72 hr were *Cpsy1pr*, *Cpsy2apr1* and the positive controls (*acopr* and *ubipr*). However, the activities of these promoters were equivalent to *Apsy1pr* and *Apsy2apr*, whose activities were not statistically significant from unshot tissue. These results suggested that there was no significant difference between the Asupina and Cavendish *psy* promoter activities. To investigate the impact of promoter activity in the context of other variables that affect gene expression, the transcript levels of *psy1* and *psy2a* were analysed semi-quantitatively.



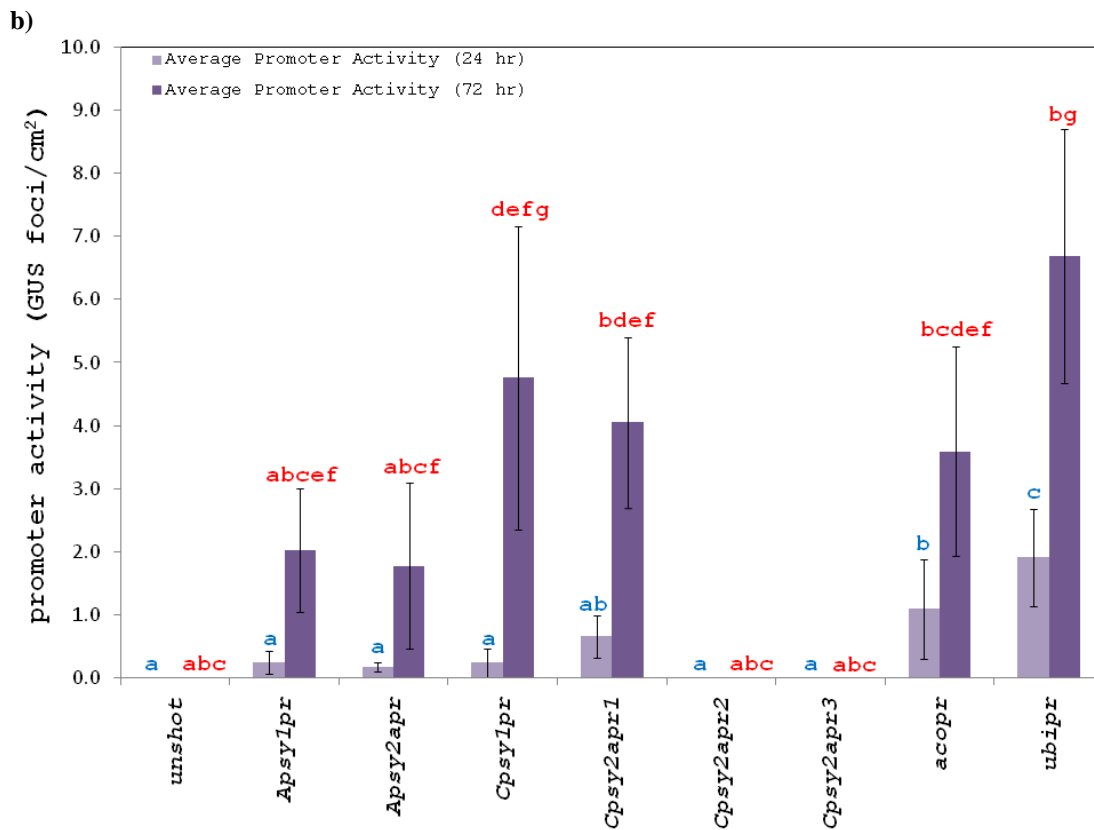


Figure 5.11: Analysis of *psy* promoter activity in ungasped green fruit after 24 and 72 hr incubation post transformation. a) Photographs showing GUS activity of representative samples of each *psy* promoter and control treatment [8× magnification]. **b)** Graph comparing average promoter activity of each treatment (4 replicates) in **a)** with standard deviations represented by error bars on the respective column. Statistical significance of promoter activity was calculated separately for 24 and 72 hr treatments, with 95% confidence using a one-way ANOVA and least significant difference post-hoc analysis. Promoters whose activities were not statistically different were grouped using the same letter (a to f) located above each bar in bold blue (24 hr) or red (72 hr) text, respectively.

5.3.3 Analysis of mRNA transcript abundance

5.3.3.1 Ripening trial

Samples of Asupina and Cavendish fruit flesh were required at different stages of ripening to compare changes in pVA accumulation (Figure 5.12) and as a source of material from which mRNA would be extracted for semi-quantitative comparison of *psy1* and *psy2a* transcript levels.

Green fruit from both cultivars was simultaneously ripened over a 12 day period with sampling every two days. These fruit were classified into two sizes, large and small, depending on their position on the banana bunch which correlated with the level of maturity. During the ripening trial, observations were made regarding the morphological characteristics of the fruit at each sampling point. On day 0 (prior to ripening induction) the peel of both Asupina and Cavendish fruit samples was completely green and difficult to remove. When an incision was made into the skin of the Asupina fruit during the removal of the peel, a viscous and sticky purple sap was observed oozing out of the incision in significant quantity (Figure 5.12, day 0 panel). However, incision of Cavendish fruit produced a sap that was initially colourless before darkening on exposure to air and was much less viscous and less sticky than the Asupina sap (not shown). Comparatively, the sap exuded by the Asupina fruit did not darken. The fruit flesh of both the Cavendish and Asupina specimens was starchy and firm in texture and creamy white in colour. Characteristics of the fruit that was sampled are summarised in Table 5.2. By day 6 it was clear that Cavendish fruit was not likely to ripen as the peel and flesh colour of the fruit remained unchanged and it began to desiccate. Consequently, sampling of Cavendish fruit was discontinued. Ripening of the Asupina fruit was continued and is documented in Figure 5.12. On the final day of the ripening trial, Day 10, the peel of the Asupina fruit sampled at this stage was completely yellow, although the ridges of the small fruit retained small green streaks.

The slow development of colour during ripening suggesting that pVA accumulation is gradual in Asupina. At Day 10 the Asupina fruit was still not completely ripe compared to previously obtained samples (Chapter 3.2.1, results not shown), which had a distinct orange flesh colour. Unfortunately, additional fruit was not available. Overall, the large and small fruit samples of Asupina shared the same ripening progression despite differing stages of maturity as indicated by size and position on the bunch. As the Cavendish fruit failed to fully ripen, unripened small fruit (day 0) and ripe fruit (purchased from a supermarket) were the only available tissue samples from this cultivar. Therefore, samples of unripened small fruit (day 0) and the most ripe small fruit available (day 10) from Asupina (Figure 5.12) were





































Day 0	Small fruit			
	Large fruit			
Day 2	Small fruit			
	Large fruit			
Day 4	Small fruit			
	Large fruit			
Day 6	Small fruit			
	Large fruit			
Day 8	Small fruit			
	Large fruit			
Day 10	Small fruit			
	Large fruit			

Figure 5.12: Ripening of Asupina green fruit. a) Photographs showing changes in outer peel and flesh colour during the ripening of large and small fruit.

Table 5.2: Analysis of the ripening of Asupina and Cavendish green fruit

Date	Source	type	day	Outer Peel colour	Mass (g)	Length (cm)
22/11/2007	Asupina	large	0	Fully green	180.2	16
22/11/2007	Asupina	Small	0	Fully green	133.1	15
22/11/2007	Cavendish	large	0	Fully green	287.9	23
22/11/2007	Cavendish	Small	0	Fully green	195.5	17
24/11/2007	Asupina	large	2	Green, yellowing slightly	186.0	16
24/11/2007	Asupina	Small	2	Green, yellowing slightly	124.1	13
24/11/2007	Cavendish	large	2	Green, lighter than day 0	264.5	21
24/11/2007	Cavendish	Small	2	Green, lighter than day 0	183.0	17
26/11/2007	Asupina	large	4	Light green	164.8	15.5
26/11/2007	Asupina	Small	4	Light green	117.2	13.5
26/11/2007	Cavendish	large	4	Light green	229.0	20.0
26/11/2007	Cavendish	Small	4	Light green	192.3	17.5
28/11/2007	Asupina	large	6	Green with yellow sections	166.2	15
28/11/2007	Asupina	Small	6	Green with yellow sections	112.4	13
28/11/2007	Cavendish*	large	6	Fruit not sampled	N/A	N/A
28/11/2007	Cavendish*	Small	6	Fruit not sampled	N/A	N/A
30/11/2007	Asupina	large	8	Yellow with green patches	151.9	14.5
30/11/2007	Asupina	Small	8	Yellow with green patches	119.4	13.5
02/12/2007	Asupina	large	10	Yellow	146.2	15
02/12/2007	Asupina	Small	10	Yellow with green ridges	133.7	13

*Ripening of Cavendish fruit was terminated at day 6 and no samples were taken (N/A) as the fruit failed to ripen and began to desiccate.

selected for semi-quantitative comparison of *psy* mRNA levels at similar developmental stages. Total mRNA was isolated from these Asupina and Cavendish fruit samples in addition to leaf tissue from these cultivars.

5.3.3.2 Semi-quantitative PCR

The expression of *psy1* and *psy2a* mRNA was examined in leaf, green fruit and ripe fruit tissue of Asupina and Cavendish using semi-quantitative RT-PCR (semi-qRT-PCR) to determine their relative abundance in these tissues and potential tissue specificity. Half of each mRNA sample was DNase-treated to remove gDNA, while the remaining mRNA aliquot was stored untreated. Template quality of the DNase-treated mRNA was investigated by RT-PCR using primers to amplify a fragment of the 5' sequence of the *actin1* coding region, chosen as the housekeeping gene. In preliminary experiments, RT-PCR with *actin1* primers amplified a band of approximately 110 bp as expected in all extracts, confirming that the mRNA template was undegraded (results not shown).

To confirm the absence of intron-bearing sequences indicative of gDNA contamination and without gDNA sequence data for *actin1*, control primers (*psy2-3'* gDNA) were designed to amplify across *psy2* intron 5 (Chapter 3.3.4). These primers were designed to amplify both *psy2a* and *psy2b* from Asupina and Cavendish and were expected to amplify products of 254 bp from mRNA. However, from gDNA, the primers were expected to amplify bands of 512 and 442 bp from Asupina and Cavendish *psy2a* templates, respectively, and bands of 489 and 481 bp from Asupina and Cavendish *psy2b* templates, respectively. These primers repeatedly amplified RT-PCR products corresponding to fragments expected from both gDNA and mRNA, indicating gDNA contamination (results not shown). This was also supported by the presence of larger than expected products (~220 bp) in some samples amplified by the *actin1* primers (results not shown), suggesting that the actin primers actually amplify across an intron (~100 bp) present in banana *actin1* gDNA. Unexpectedly, these results did not change despite additional DNase-treatment of the mRNA samples. To further investigate this problem with gDNA contamination, *actin1* and *psy2-3'* gDNA control primers were tested on the DNase-treated mRNA samples using GoTaq Green[®] which lacks reverse transcriptase activity. This was compared with amplification using the standard RT-PCR protocol and included Cavendish gDNA as a positive control (Figure 5.13a & b). The *psy1* and *psy2a* primers, designed for semi-qRT-PCR to amplify the 5' coding region and 5' UTR, respectively, were also tested (Figure 5.13 c & d). While products were amplified from the gDNA positive control template using both GoTaq Green[®] PCR (Figure 5.13 a – d i) and RT-PCR (Figure 5.13 a – d ii), no fragments were amplified

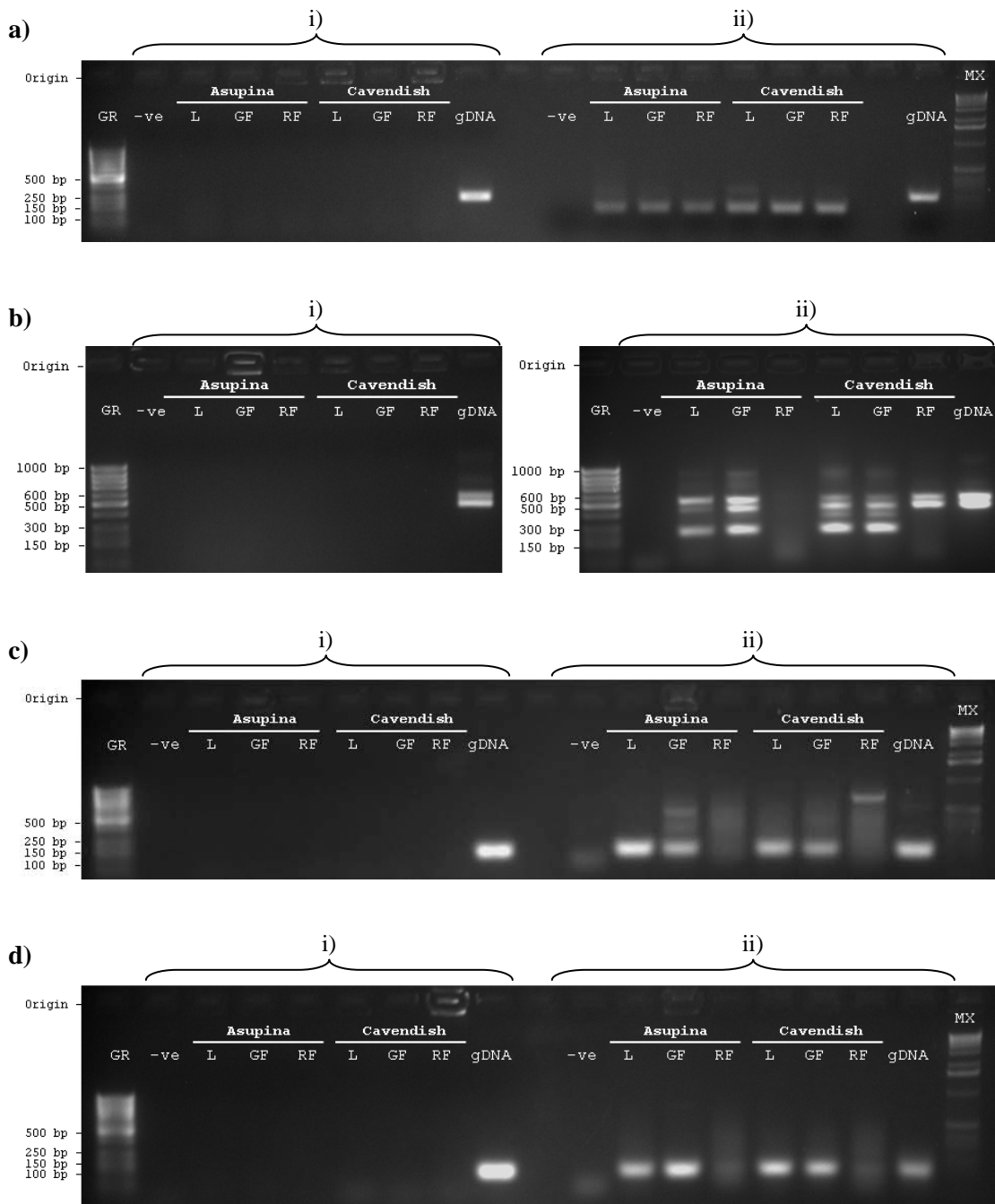


Figure 5.13: Analysis of Asupina and Cavendish mRNA using i) GoTaq PCR and ii) RT-PCR followed by electrophoresis on 2% agarose gels. Primers **a)** *actin1* 5' coding region, **b)** *psy2* 3' coding region, **c)** *psy1* 5' coding region and **d)** *psy2a* 5' UTR were tested on mRNA template from Asupina and Cavendish leaf (L), green fruit (GF) and ripe fruit (RF). Cavendish gDNA (gDNA) was used as a positive control. Lanes containing the GeneRuler™ 50 bp ladder (GR, Fermentas) and Marker X (MX, Roche Applied Science) molecular weight markers are indicated, as is the position of the wells (origin) in each gel.

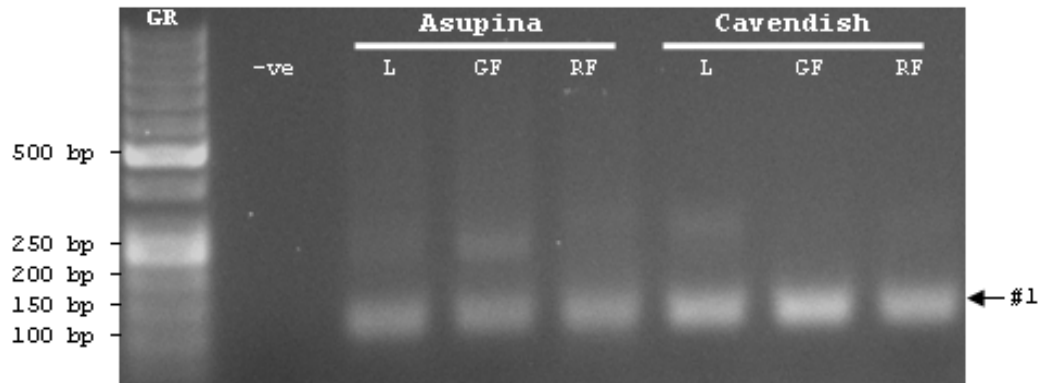
with any of the primers from mRNA samples or negative controls using GoTaq Green[®] PCR. This indicated that mRNA extracts were not contaminated with gDNA. Importantly, *actin1* RT-PCR products were observed in all mRNA samples but not negative controls (Figure 5.13 a ii), confirming that the mRNA template was undegraded.

RT-PCR using the *psy*-specific primers produced amplicons of the sizes expected from mRNA templates in all tissues except ripe fruit (Figure 5.13 b – d ii), suggesting an absence of *psy*-specific RNA in this tissue. Surprisingly, the *psy2*-3' gDNA control primers also produced amplicons larger than the size predicted for mRNA, but consistent with those from the gDNA control, in leaf and green fruit samples from both Asupina and Cavendish (Figure 5.13 b ii). As these bands were not amplified in GoTaq Green[®] PCR and were similar to those previously seen after several treatments with DNase, they appeared to represent amplicons from unprocessed *psy2* mRNA (where at least intron 5 was not processed). Interestingly, these products were also amplified in significant amounts from Cavendish ripe fruit mRNA but not from Asupina. Larger bands (~220 bp), consistent with the size of the gDNA positive control, were also observed in some lanes following RT-PCR with *actin1* primers (Figure 5.13 a ii). An additional product (~ 400 bp) was amplified from Cavendish leaf and green fruit mRNA and was not consistent with sizes expected from processed or unprocessed transcripts (Figure 5.13 d ii). Additionally, larger bands that did not correspond to processed mRNA were also amplified with *psy1* 5' gDNA primers, from Asupina green fruit and Cavendish ripe fruit (Figure 5.13 c ii). These bands appeared to be non-specific amplification because the *psy1* primers do not amplify across introns (identified in Chapter 3.3.4). No larger bands were observed from RT-PCR using *psy2a* 5' UTR primers (Figure 5.13 d ii).

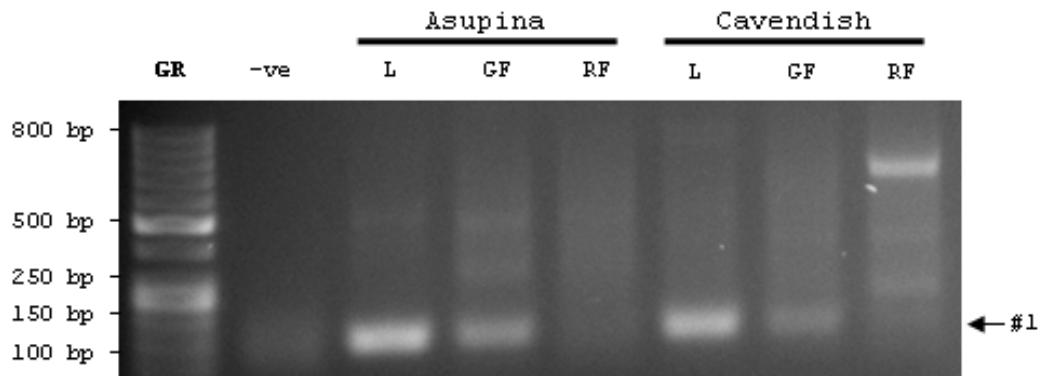
Semi-qRT-PCR templates were prepared by DNase-treatment of the second mRNA aliquots before quantitation and normalising of mRNA concentration to approximately 3 ng/μL. Relative expression of different *psy* transcripts could not be measured using earlier templates because the mRNA concentrations were expected to be variable, despite the use of similar amounts of starting tissue for mRNA extraction. The quality of this template and absence of gDNA were confirmed by RT-PCR and GoTaq PCR, respectively, using *actin1* primers (results not shown), and results were identical to those in Figure 5.13a. The *actin1*, *psy1*, *psy2a* and *psy2*-3' gDNA primer sets were used in semi-qRT-PCR using equivalent amounts of mRNA (~3ng) and repeated once for confirmation (Figure 5.14). Generally, RT-PCR amplicons were consistent with previous results. However, several putatively non-specific bands were also noted in some tissues amplified using *psy2a* 5' UTR primers (Figure 5.14a iii) and from Cavendish ripe fruit using *psy2*-3' gDNA primers (Figure 5.14a iv). Only bands

a)

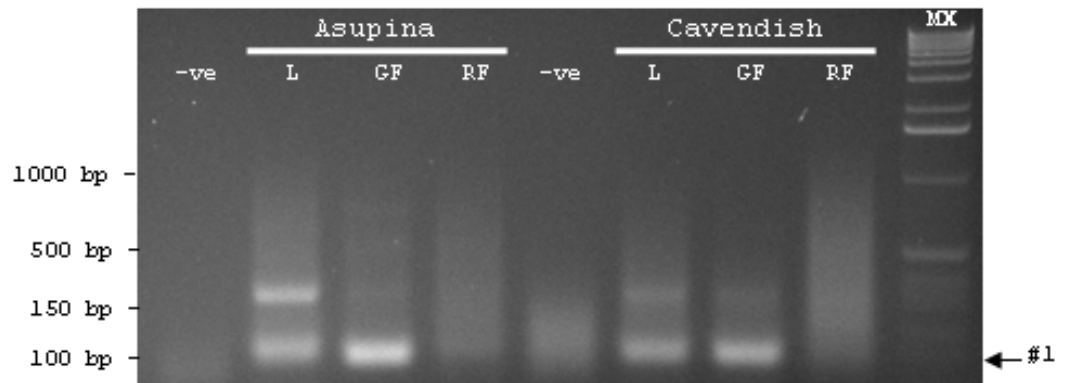
i)



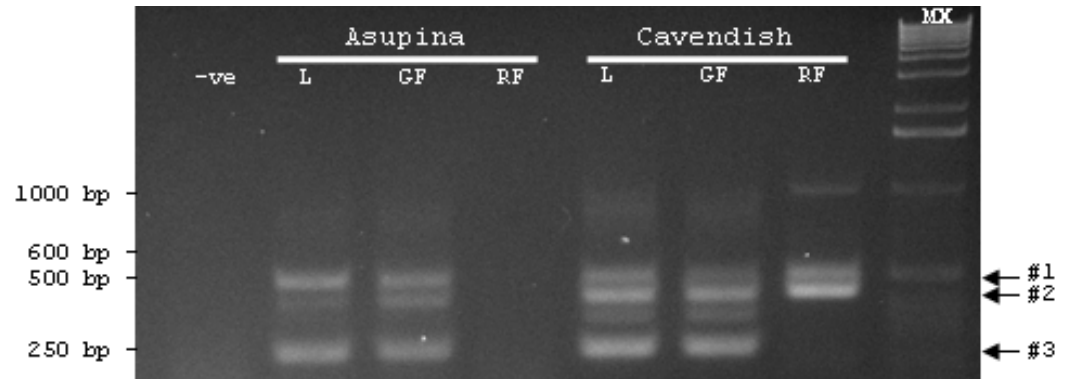
ii)



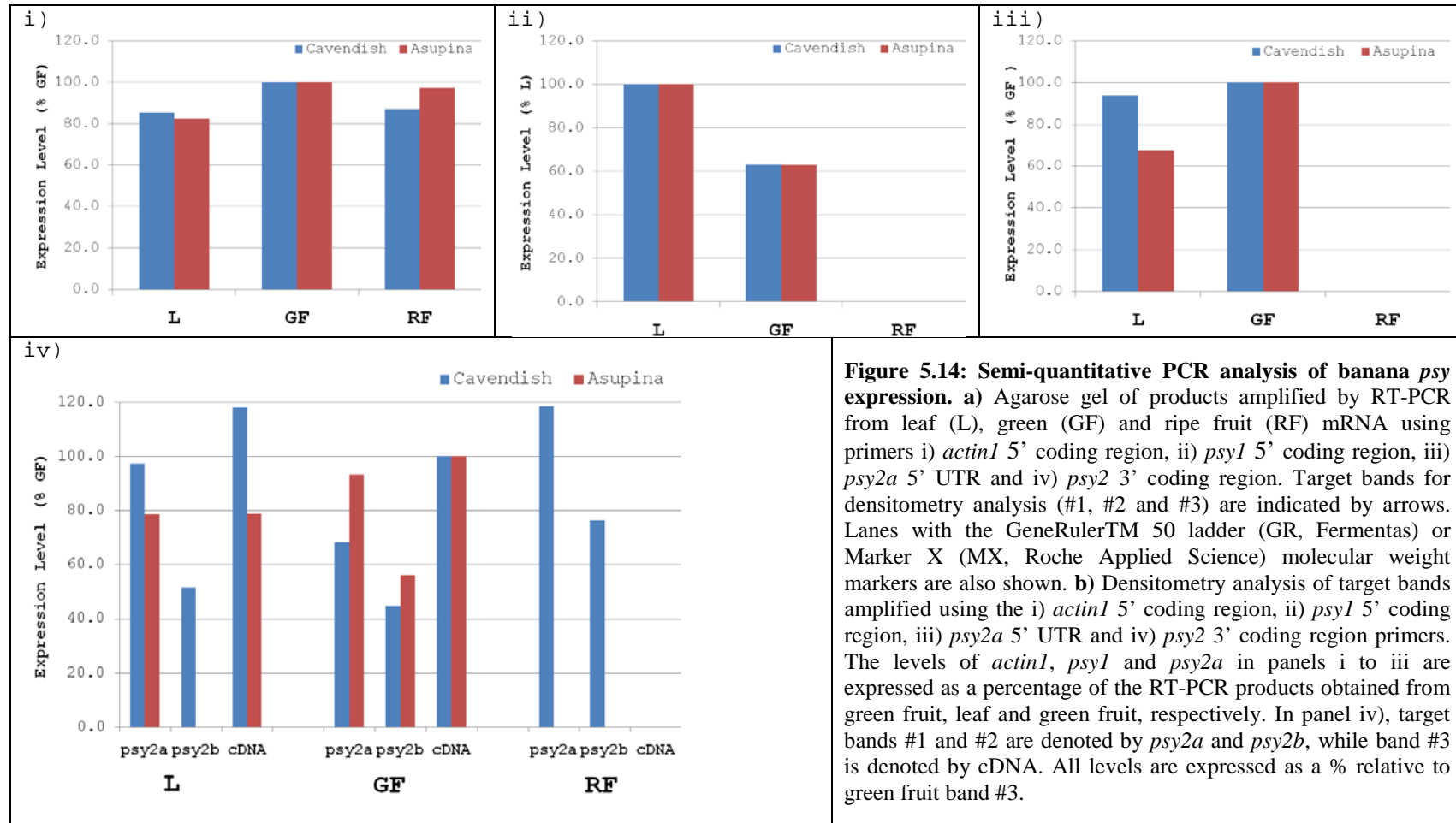
iii)



iv)



b)



of the expected sizes (target bands) corresponding to amplicons from processed and where expected, unprocessed mRNA, were quantitated by densitometry. As expected, the *actin1* target band (#1) was of similar intensity in all tissues tested (Figure 5.14a i) and this was supported by densitometry analysis (Figure 5.14b i). The relative intensity of the *psy1* target band (#1) was 40% higher in leaf mRNA from both cultivars than in green fruit, and was absent in ripe fruit (Figure 5.14a & b ii). The *psy2a* target band (#1) appeared more prominent in green fruit mRNA of both cultivars than in leaf mRNA (Figure 5.14a iii). The Asupina *psy2a* target band was approximately 30% higher in green fruit than leaf mRNA, while the Cavendish *psy2a* target band intensity was marginally higher in green fruit (Figure 5.14b iii).

The *psy2a/psy2b* target band expected from amplification of processed mRNA using *psy2*-3' gDNA control primers (Figure 5.14a iv; #3), was observed at similar intensities in both Asupina and Cavendish leaf and green fruit samples, but was absent from ripe fruit of both cultivars. The target band putatively representing *psy2a* with intron 5 (Asupina band #1 and Cavendish band #2) was more intense than the equivalent band putatively representing *psy2b* (Asupina band #1 and Cavendish band #2). No *psy2* bands of any kind were observed in Asupina ripe fruit, and no processed *psy2* mRNA band (#3) was amplified from Cavendish ripe fruit. However, both *psy2a* and *psy2b* unprocessed mRNA bands (#1 and #2) were observed in Cavendish ripe fruit, and were more intense than those observed in leaf and green fruit. The relative expression determined by densitometry supported these observations (Figure 5.14b iv).

5.4 Discussion

Preliminary studies in Chapter 3 suggested that there were differences in tissue specificity of the *psy* genes, such that *psy1* and *psy2* were predominantly leaf and fruit associated, respectively. In this chapter, the relative abundance of these transcripts in leaf, green fruit and ripe fruit was further investigated. The *psy1* and *psy2a* promoters were also isolated, and their relative activity tested in banana fruit. Bioinformatic analysis of these promoters revealed sequence differences that may be linked to *psy* promoter activity. Interestingly, there was evidence of alternative intron splicing in banana and some differences in *psy2* intron processing in ripe fruit of Cavendish compared to Asupina, which could potentially influence pVA accumulation.

Single promoter sequences were identified for each of the Asupina and Cavendish *psy1* and *psy2a* genes with the exception of the Cavendish *psy2a* promoter, for which three variants of different sizes were found. Efforts to isolate the *psy2b* promoters from these cultivars were

unsuccessful although several attempts were made using genome walking PCR with different primer combinations. Failure to obtain these promoters was surprising due to the high sequence similarity between *psy2a* and *psy2b*. Consequently, parameters such as primer design or preparation of genome walking DNA library templates may need further optimisation. The *psy1* and *psy2a* gene structures proposed in Chapter 3 were revised to include the promoter sequences, showing that the Asupina and Cavendish *psy1* 5' UTRs were divided between the first three exons, two of which were upstream of coding region exon 1 (Chapter 3). Conversely, the Asupina and Cavendish *psy2a* 5' UTRs were not interrupted by introns and formed the 5' end of exon 1. The presence of introns in the 5' UTR is common in monocots (Christensen et al., 1992; Sivamani and Qu, 2006) as well as dicots (Chung et al., 2006; Garbarino et al., 1995) and their presence has been shown to enhance gene expression. This has been demonstrated for potato *ubi7* (Garbarino et al., 1995) and rice *ubi3* (Sivamani and Qu, 2006) promoters, which directed significantly higher levels of reporter gene expression than their intronless versions. The impact of the rice *ubi3* 5' UTR intron on promoter activity was subsequently found to be tissue specific, with apparently greater effect in roots than leaf tissue (Lu et al., 2008). The introns found in the Asupina and Cavendish *psy1* 5' UTRs could also play a role in tissue-specific regulation. This could explain the high *psy1* expression in leaf and its apparent down-regulation during fruit ripening. Interestingly, the identification of G2 and ATCTA motifs in the Asupina and Cavendish *psy1* 5' UTRs may also play some related but presently unknown role in determining tissue specificity.

Transient GUS reporter gene analysis of the Asupina and Cavendish *psy1* and *psy2a* promoters demonstrated that all promoters except the Cavendish *psy2a* variants, *Cpsy2apr2* and *Cpsy2apr3*, were functional in embryogenic cells and green fruit. Cavendish promoters, *Cpsy1pr* and *Cpsy2apr1*, seemed to be the most active of the promoters tested in green fruit tissue. While *Cpsy1pr* gave similar numbers of GUS foci to *Cpsy2apr1*, the intensity of GUS staining in cells transformed with *Cpsy2apr1* appeared to be higher, suggesting this was a stronger promoter. The lower level of GUS expression seen in the Asupina promoters compared to those from Cavendish may reflect the fact that the Cavendish promoters were expressed in their native tissue. However, none of the differences in activity between the Asupina and Cavendish *psy* promoters tested were statistically significant (Figure 5.10 and 5.11). There were a number of sequence differences in the *psy1* and *psy2* promoters that may influence promoter activity and tissue specificity. One of these was the repeat region that forms a secondary structure immediately prior to the known transcription start sites of Asupina and Cavendish *psy2a*. DNA secondary structures are widely known to influence nucleic acid synthesis and gene expression, and examples of this can be seen in

bacteriophages (Gleghorn et al., 2008), bacterial plasmids, eukaryotic viruses and geminiviruses (Orozco and Hanley-Bowdoin, 1996), and eukaryotic promoters (Yamagishi et al., 2008). The function of the Asupina and Cavendish *psy2a* promoters appears to correlate with the stability of the secondary structures formed in the repeat region. The inactive Cavendish *psy2a* promoters (*Cpsy2apr2* and *Cpsy2apr3*) appeared to form the most stable structures, possibly due to the large stretches of CT dinucleotide repeat which are complementary to the long GA dinucleotide repeats in all of the *psy2a* promoters. *Apsy2apr* and *Cpsyp2apr1* had either few or no CT repeats and were shown to putatively form weaker structures. The promoter with the weakest predicted secondary structure was *Cpsyp2apr1*, which appeared to be the most active. Weaker secondary structure may result in increased transcriptional efficiency, as DNA strands would separate more easily to accommodate transcriptional machinery. Interestingly, the length of dinucleotide repeats in different alleles has been widely reported to affect promoter activity. For example, upregulation of HGMA2 promoter activity was associated with an increased number of TC repeats (Borrmann et al., 2003), while an increase in the number of CA repeats was reported to reduce activity of the *Cyr61* promoter (Wang et al., 2005).

The shape of the secondary structures in the proximal promoter region of *psy2a* may also influence its activity by affecting the binding of transcription factors that may ultimately downregulate *psy2a* mRNA levels in Cavendish or upregulate them in Asupina. The activation of the *hoxd1* promoter and repression of *hoxb9* and *hoxd8* promoters, whose gene products are transcription factors in early animal development, is regulated simultaneously in mice (Yamagishi et al., 2008). This regulation appeared to be mediated by a DNA secondary structure, in the 3' promoter region adjacent to the 5' UTR, which interacts with a putative chromatin modification protein. These structures also appeared to be conserved across different species. The presence of a hairpin structure in both Asupina and Cavendish *psy2a* promoters suggested that this structure and putative function may be conserved in all banana *psy2a* promoters. The impact of these secondary structures on *psy* expression is not currently understood as it has not been previously investigated. Interestingly, the absence of these DNA repeat sequences within 200 bp of the known *psy1* transcription start sites, may suggest that the *psy1* promoter lacks a secondary structure feature required for fruit-specific expression. The requirement for different transcription factors could explain the low activity of the Asupina promoters in Cavendish tissue.

DNA regulatory elements, previously identified in the *Arabidopsis psy* promoter, were also present in the Asupina and Cavendish *psy1* and *psy2a* promoter regions. Previous work demonstrated that the presence of the ATCTA motif determined the strength of *psy* promoter

activity in *Arabidopsis*, and that one such motif was sufficient to mediate gene expression (Welsch et al., 2003). Consequently, the absence of the ATCTA sequence from *Cpsy2apr2* and *Cpsy2apr3* may explain the lack of transient expression in both embryogenic cells and fruit tissue. Comparison of the Asupina and Cavendish *psy2a* promoters (Figure 5.15) suggested that the absence of these motifs from *Cpsy2apr2* and *Cpsy2apr3* was due to nucleotide substitutions at three positions. Segregation of the G1 and G2 motifs between the *psy1* and *psy2a* promoters of banana was consistent with the differential expression of these mRNAs in leaf and fruit, respectively. These elements are thought to mediate light-induced responses in *Arabidopsis* (Welsch et al., 2003), which have also been linked to phytochrome A activity (von Lintig et al., 1997). Light has also been shown to influence lycopene accumulation in tomato fruit without triggering ripening (Alba et al., 2000), suggesting that fruit-specific phytochromes were able to control carotenoid accumulation independently of ethylene. Consequently, the expression of phytochrome P₄₅₀ during Cavendish fruit ripening (Pua and Lee, 2003), may be indicative of a role for light in regulating banana fruit carotenogenesis. The presence of both motifs in the *Arabidopsis psy* promoter is consistent with the presence of only one *psy* gene, which must be regulated in multiple tissues. However, other as yet unidentified DNA elements may also regulate *psy* promoter function.

<i>Cpsy2apr2</i>	TCGAACTTCTTACGCAA ACCTAAATCAA	1433	Figure 5.15: Comparison of putative ATCTA motifs in <i>psy2a</i> promoters of Asupina and Cavendish (bold text) showing the sites of conserved nucleotides (*) and putative mutations in the ATCTA sequence (#).
<i>Cpsy2apr3</i>	TCGAACTTCTTACGCAA ACCTAAATCAA	1433	
<i>Cpsy2apr1</i>	TCGGACTACTTACACAA ATCTAAATCAA	1408	
<i>Apsy2apr</i>	TCGAAATTTTTTAC-----	1295	
	*** * * **** #		
<i>Cpsy2apr2</i>	TGC ATAT GAAAGACCAACAC ACCTACTC	1671	
<i>Cpsy2apr3</i>	TGC ATAT GAAAGACCAACAC ACCTACTC	1671	
<i>Cpsy2apr1</i>	TGC ATCT GTAAGACCAACAC ACCTACTC	1539	
<i>Apsy2apr</i>	TGC ATCT TATAAAACCAACAC ATCTACTC	1540	
	*****##** ** *****##*****		

The presence of *psy1* and *psy2a* mRNA was detected in both leaf and fruit using semi-qRT-PCR. The relative expression of these transcripts was consistent with the frequency of their respective partial mRNA clones isolated from Asupina and Cavendish leaf and fruit tissue (Chapter 3). The abundance of *psy1* transcripts was highest in leaf followed by green fruit, while *psy2a* was higher in green fruit than leaf. Conversely, RT-PCR analysis of *psy* expression in maize and rice showed that *psy1* expression was responsible for leaf carotenogenesis and high endosperm carotenoid accumulation, while *psy2* was predominantly associated with photosynthetic activity in leaf (Gallagher et al., 2004). Interestingly, maize PSY1 also appears to responsible for carotenogenesis in the dark and heat stress tolerance in photosynthetic tissue (Li et al., 2008b). Leaf carotenogenesis required

both phytochrome-dependent and phytochrome-independent photoregulation of PSY2 and non-photoregulated PSY1 expression. This supports the results seen in banana as both *psy1* and *psy2a* were detected in leaf although *psy1* transcript appears to be more abundant. This could reflect the photoprotective role of PSY1 in photosynthesis in banana. Interestingly, with the exception of *psy2a* in leaf, the relative abundance of *psy1* and *psy2a* mRNA was essentially identical in Asupina and Cavendish (Figure 5.13b). The variation in leaf *psy2a* may be because the Cavendish leaf material used in the present study was sourced from tissue culture, while Asupina leaf tissue was obtained from mature plants. The semi-qRT-PCR analysis was repeated once to verify consistency. However, this variation may also be due to the semi-quantitative nature of the RT-PCR assay used in this study, which is less sensitive than real-time PCR. The expression of *psy2a* mRNA in Cavendish leaf and green fruit, suggests that the *Cpsy2apr1* may be sufficient to compensate for the lack of function of *Cpsy2apr2* and *Cpsy2apr3*. Given that Cavendish is triploid, these three promoter variants could control the expression of three *psy2a* alleles at a single locus in a dominant fashion. However, multiple *psy2a* loci may exist, in which case *Cpsy2apr1* could represent the functional locus, while *Cpsy2apr2* and *Cpsy2apr3* may represent inactive genes.

Fragments corresponding to the sizes expected for processed and unprocessed *psy2a* and *psy2b* were amplified using primers designed to span intron 5, and may result from normal or abnormal *psy2* mRNA processing. This conclusion was supported by extensive experiments that confirmed the absence of gDNA contamination in the mRNA samples analysed. The level of unprocessed *psy2a* mRNA appeared higher than that of *psy2b* tissues in both Asupina and Cavendish, adding further to the hypothesis that *psy2a* is the predominant gene involved in fruit pVA accumulation. Mature transcripts of *psy2* were detected in both leaf and green fruit of Asupina and Cavendish but were not detected in ripe fruit of either cultivar, consistent with previous data (Chapter 3). The Asupina *psy2a* and *psy2b* unprocessed mRNA was present with processed *psy2* transcripts in leaf and green fruit, but were both absent from ripe fruit, suggesting that unprocessed transcripts were a normal part of the regulation of these genes in fruit. Interestingly, although mature *psy2* transcripts were not detected in Cavendish ripe fruit, unprocessed *psy2a* and *psy2b* mRNA was still present. This may be due to the expression of abnormal unprocessed or partially processed transcripts that are truncated at their 5' ends. The isolation of truncated Cavendish *psy2* 5' RLM-RACE products from fruit mRNA (Figure 3.6b iii and 3.7) may support this hypothesis. These mRNAs may be transcribed from an abnormal *psy2a* allele and may accumulate in ripe fruit, possibly due to the absence of sequences associated with normal degradation that may be located in the 5' UTR. This may explain why semi-qRT-PCR using *psy2* 3' coding region primers was successful in Cavendish ripe fruit while *psy2a* 5' UTR

primers produced no amplicons. However, other factors may be responsible for the presence of these transcripts, including aberrations in mRNA degradation mechanisms such as NMD (discussed in Chapter 3.4) in Cavendish compared to Asupina. Alternatively, the insertion of the 3' end of the coding region in the Cavendish *psy2a* 3' UTR (Figure 3.6b v and 3.8a) may somehow explain the accumulation of unprocessed *psy2a* mRNAs in Cavendish ripe fruit.

Intron processing may be another level of regulation of *psy* expression. Interestingly, intron 5 which was spanned by the *psy2* 3' coding region primers used in semi-qRT-PCR was the only one whose size was different between *Apsy2a* and *Cpsy2a* but not in *psy2b* (Chapter 3, Figure 3.10). Therefore, this difference in intron size may be somehow related to the nonsense Cavendish *psy2a* alternate splicing sequences obtained in Chapter 3 (Figure 3.11). Consequently, the proportion of Cavendish *psy2* transcripts able to produce active enzymes may be low despite apparently high mRNA levels. Therefore, carotenoid production may have to be supplemented by *psy1* expression, which may cease early in fruit ripening. Intron splicing is directed by cis-acting regulatory elements that reside in both introns and exons (Zhang et al., 2005), and are recognised by RNA binding proteins that facilitate pre-mRNA processing (Fu, 2004).

Alternate splicing is common in plants (Wang and Brendel, 2006; Reddy, 2007) and this process was investigated in *Arabidopsis* and rice using bioinformatic analysis that included approximately 34,000 and 61,000 full length transcripts from *Arabidopsis* and rice, respectively (Campbell *et al.*, 2006). A significant number of genes in *Arabidopsis* (~5,000 genes) and rice (~8,800 genes) were linked with alternate splicing, and approximately 16,000 and 37,000 alternate splicing events were observed in *Arabidopsis* and rice, respectively. Interestingly, various classes of alternative splicing events were observed, including the skipped exon and alternative donor site classes observed in Asupina *psy1* and Cavendish *psy2a* alternate splicing variants, respectively (Figure 3.11). There is evidence that alternate splicing plays a significant role in normal plant gene expression. The activity of the FCA protein involved in the regulation of *Arabidopsis* flower development is thought to be negatively self-regulated through the production of prematurely polyadenylated transcripts (Amasino, 2003). Alternative splicing has recently been linked to the function of the *psy1* gene in wheat (Howitt et al., 2009). Sequence duplication at the 3' end of exon 2 resulted in the production of non-functional alternately spliced transcripts that were expected to reduce wheat carotenoid content due to decreased levels of functional PSY1. Similarly, the production of non-functional *psy2a* transcripts in Cavendish fruit could reduce the abundance of functional transcripts, leading to low pVA content as low amounts of PSY2A would be produced. The apparently non-functional coding region variants 1 and 2 of

Cavendish *psy2a* (Figure 3.11) are examples of alternative donor site and alternative position modes of alternate splicing, respectively (Wang and Brendel, 2006). In contrast, the Asupina *psy1* coding region variant appears to be formed by exon skipping, which may result in the absence of a functional domain that could affect cellular targeting or catalytic function. Interestingly, the two introns in the banana *psy1* 5' UTR (Figure 5.3) may contribute to the variability of 5' UTR length observed in Chapter 3 through alternate splicing, which may regulate *psy1* expression through mRNA stability and turnover.

The experiments described in this chapter investigated the hypothesis that the differential pVA accumulation in Asupina and Cavendish fruit was due to factors affecting promoter activity and mRNA abundance. Promoter analysis showed that the *psy1* promoters, and at least one *psy2a* promoter from both cultivars, were functional in banana fruit. Transcript abundance of *psy2a* was highest in green fruit and decreased during ripening; reinforcing the hypothesis (Chapter 3) that fruit pVA accumulation was largely due to *psy2a* expression. However, *psy2* transcript abundance was similar between Asupina and Cavendish fruit. In contrast, high levels of *psy2a* and *psy2b* unprocessed mRNA were present in ripe fruit of Cavendish but not in Asupina. Whether the abnormalities in promoter activity or mRNA processing in Cavendish fruit play some role in *psy2a* expression remains to be determined.

Chapter 6: General discussion

Bananas are an important staple food for millions of people in developing countries where VAD is prevalent. The fruit of nutritionally important staple banana varieties is low in pVA carotenoids, although numerous banana cultivars with high pVA content have been identified. However, no studies have yet investigated the molecular mechanisms underlying this variation in banana fruit pVA content. PSY appears to play an important role in carotenoid metabolism and has been extensively characterised in a wide range of plants. This study investigated the role of this enzyme in carotenoid biosynthesis in banana fruit, testing the hypothesis that factors affecting PSY function and regulation were responsible for the differences in pVA accumulation. Overall, the *psy1* and *psy2a* mRNA and gDNA nucleotide sequences appeared to be intact (Chapter 3) and capable of producing functional PSY, as demonstrated in rice callus (Chapter 4). However, anomalies in *psy2a* transcript processing, observed in Chapters 3 and 5, may somehow contribute to the low pVA levels in Cavendish fruit. Another contributing factor may be abnormal Cavendish *psy2a* promoter activity (Chapter 5), although the active Cavendish *psy2a* promoter variant may compensate for the loss of function of the other sequences. However, the production of at least two types of non-functional Cavendish *psy2a* transcripts may lead to the translation of less PSY2A than in Asupina. The accumulation of unprocessed *psy2a* mRNA in the ripe fruit of Cavendish but not Asupina, despite sharing the same *psy1* and *psy2a* abundance profile in green and ripe fruit, may also affect PSY2A protein levels.

Results from Chapters 3 and 5 supported the hypothesis that *psy1* was mainly expressed in leaf and *psy2a* in fruit, suggesting that PSY1 and PSY2A direct carotenoid biosynthesis in chloroplasts and chromoplasts, respectively. Both *psy1* and *psy2a* transcription was detected in green fruit, suggesting that both PSY1 and PSY2A were active. However, *psy2a* mRNA levels (based on semi-qRT-PCR) appeared higher than those of *psy1* in green fruit and may indicate that PSY2A is more active than PSY in early ripening stages. No processed *psy2a* transcript was detected in semi-qRT-PCR of ripe fruit (Chapter 5), however, low levels of full-length transcript must be present since complete coding region clones were isolated from ripe fruit (Chapter 3). This may be due to differences in the maturity of ripe fruit tissue used in Chapter 3 and Chapter 5. The absence of *psy1* transcript in ripe fruit (Chapter 5) was consistent with the lack of *psy1* partial clones obtained from ripe fruit (Chapter 3). The coordination of *psy* expression and enzyme function during banana fruit ripening may be regulated during chromoplast development. This process may be similar to those involved in light-induced transformation of etioplasts into chloroplasts during photomorphogenesis in

Arabidopsis (Welsch et al., 2000), or the development of chloroplasts into chromoplasts during tomato fruit ripening (Kobayashi et al., 1990). The maturation of chromoplasts from precursor plastids may be incomplete in banana green fruit prior to ethylene induction. Recent analysis of *psy* gene expression in tomato demonstrated that *psy1* was fruit-specific while *psy2* was expressed in a broader range of tissues (Giorio et al., 2008), suggesting that these genes were equivalent to banana *psy2a* and *psy1*, respectively. During ripening, tomato *psy1* mRNA levels were higher in ripening fruit than in ripe fruit, and lowest in mature green fruit. This was consistent with the patterns of banana *psy2a* expression (Chapter 5), where ripening green fruit had higher *psy* mRNA levels than ripe fruit, suggesting that ripening banana and tomato fruit share similar coordination of PSY activity and chromoplast maturation. Therefore, *psy2a* expression may be low in very early stages of banana fruit ripening and increase during ripening as chromoplasts mature, before decreasing in ripe fruit once carotenoid accumulation is complete. Interestingly, tomato *psy2* levels appeared to increase during ripening although at much lower relative levels than *psy1*. This may be indicative of differences in *psy* gene regulation in the ripening of banana and tomato fruit or a reflection of the greater sensitivity of real-time RT-PCR (Giorio et al., 2008) compared to semi-qRT-PCR (Chapter 5).

This apparent tissue specificity may be linked to light-regulated transcription due to the presence of the putative light responsive G1 and G2 motifs in the *psy* promoters (Welsch et al., 2003). This regulation may occur through *psy1* promoter activity down-regulation and *psy2a* promoter upregulation by transcription factors that bind the G1 and G2 motifs, respectively. The relative activity of these promoters could be coordinated through the ATCTA motif, which may regulate other genes as photosynthetic enzymes are replaced by those involved in chromoplast function (Welsch et al., 2003). This is consistent with the identification of light responsive properties of the tobacco *pds* promoter (Corona et al., 1996), and the presence of the ATCTA motif in other *pds* promoters (Welsch et al., 2003). On the basis of this proposed model, pVA production could be suppressed in Cavendish due to the transcription of nonsense *psy2a* mRNAs (Chapter 3.3.6) incapable of producing a functional protein, despite adequate promoter function. This would explain why mRNA profiles are similar in both cultivars, but only Asupina has high pVA, as the proportion of viable *psy2a* transcript could be significantly lower in Cavendish than Asupina due to alternate splicing (discussed in Chapter 5). Additionally, although the Cavendish *psy2a* coding region (Chapter 3) was cloned from ripe fruit, and semi-qRT-PCR (Chapter 5) suggested that mature (processed) transcript is present in green fruit, no normal 5' or 3' RACE products were amplified from Cavendish fruit compared to Asupina.

Post-translational mechanisms may also be responsible for the levels of pVA accumulated in Cavendish and Asupina fruit as light triggers the activation of PSY during chloroplast maturation (Welsch et al., 2000). This regulation was apparently mediated by phytochromes independently of mRNA accumulation (von Lintig et al., 1997). Fruit-specific phytochromes are believed to regulate carotenogenesis in tomato independent of ethylene activity (Alba et al., 2000), and a ripening related phytochrome has been identified in Cavendish (Pua and Lee, 2003). Therefore, it is hypothesised that PSY1 and PSY2A activity during banana fruit ripening may be regulated by phytochromes independently of mRNA accumulation. Consequently, further work needs to be conducted to investigate the role of phytochrome activity and other post-translational mechanisms in the regulation of banana *psy* gene expression and enzyme activity in both high and low pVA bananas.

Further characterisation of PSY enzyme activity is also required to fill existing knowledge gaps in the proposed model above. Bioinformatic analysis (Chapter 4) raised the possibility that structural differences within the putative signal peptide may reduce CPSY2A activity compared to APSY2A. Signal peptide cleavage appears to be necessary for optimal PSY activity (Misawa et al., 1994; Schledz et al., 1996). This may be relevant to CPSY2A activity, despite proving the functionality of this enzyme in rice callus, as reduced carotenogenesis due to inefficient signal peptide cleavage may be masked by the effects of constitutive over-expression. However, this effect could be measured directly by comparing the activity of native and truncated forms of the Asupina and Cavendish PSY2A proteins. This has been done previously using *E. coli*, which may be a more appropriate model than rice callus because it appears incapable of PSY signal peptide cleavage (Misawa et al., 1994). Biochemical characterisation of intrinsic PSY enzyme activity would provide further insight into the possible effects of any differences in PSY1 and PSY2A catalytic properties on pVA accumulation. The *Apsy2a* coding region has also been transformed into Cavendish as part of the wider project at QUT, and field testing is currently underway. This experiment would examine whether the expression of a *psy* gene from a high pVA banana variety is sufficient to enhance pVA levels in Cavendish or whether other factors are involved. The activity of Asupina and Cavendish PSYs during fruit development could also be studied through biochemical analysis from tissue sampled during ripening. This has been done previously in daffodil (Schledz et al., 1996) and has the benefit of observing protein function in the native cellular environment. In addition, the use of antibodies raised against PSY would complement enzyme activity analysis by enabling the study of PSY localisation, signal peptide cleavage efficiency and protein interactions. Anti-PSY antibodies have been used to in the characterisation of PSY properties in capsicum (Dogbo et al., 1988), tomato (Misawa et al., 1994) and daffodil (Schledz et al., 1996).

Semi-quantitative RT-PCR analysis (Chapter 5) provided valuable data regarding *psy1* and *psy2a* expression in Asupina and Cavendish leaf and fruit. This method was selected because of its simplicity and its use in previous analysis of *psy* expression in maize and rice (Gallagher et al., 2004). However, real-time PCR would provide a more quantitative approach for future work due to its increased sensitivity and it has proven successful in the analysis of *psy1* and *psy2* expression in tobacco (Busch et al., 2002) and carrot (Clotault et al., 2008). The semi-quantitative comparison in Chapter 5 was also limited by the inability to ripen Cavendish green fruit and the incomplete ripening of Asupina fruit, making it impossible to undertake full a comparison of mRNA levels during all major ripening stages. In addition, semi-qRT-PCR analysis of *psy1* and *psy2a* (Figure 5.14a ii and iii) was not able to differentiate between mature mRNA and unprocessed mRNA as the primers were not designed to span introns. This was due to limitations resulting from the high sequence similarity between *psy1* and *psy2a* that restricted where differentiating primers could be designed. This could be addressed using Northern hybridisation, which may also observe alternate splicing and mRNA stability. However, high levels of sequence similarity between *psy1*, *psy2a* and *psy2b* would make the design of hybridisation probes difficult. Consequently, future analysis of *psy* transcription during ripening of Asupina and Cavendish fruit using real-time PCR should also include HPLC analysis of pVA levels at each stage to determine at which point differences in carotenoid accumulation exist. This combination of approaches was used previously in analysis of carotenoid production during carrot root development (Clotault et al., 2008).

Further characterisation of the Asupina and Cavendish *psy* promoters would also be valuable. The function of *psy* promoters was successfully demonstrated in banana embryogenic cells and ungasped green fruit, and putative DNA regulatory sequences were identified. However, the role of these motifs in promoter function could not be confirmed in the available time. Bananas are climacteric fruit, whose ripening depends upon ethylene production, which may somehow modulate *psy1* and *psy2a* promoter activity. During tomato fruit ripening, *psy* mRNA levels were shown to rise dramatically relative to immature fruit (Giuliano et al., 1993; summarised in Figure 1.8a). Tomato ripening inhibitor (*rin*) mutants with abnormal fruit ripening and poor carotenoid accumulation also had reduced *psy* mRNA levels (Kitagawa et al., 2005). This phenotype was subsequently linked to a mutation in a transcription factor that is up-regulated during ripening and controls the expression of ethylene biosynthetic genes (Kitagawa et al., 2006; Ito et al., 2008). Similarly, differences in ethylene sensitivity through mutations in the *psy2a* promoter region may be responsible for either the apparent lack of *Cpsy2apr2* and *Cpsy2apr3* activity or the function of *Apsy2apr*

and *Cpsy2apr1*. However, there is no evidence thus far of differences in *psy* transcript abundance between Asupina and Cavendish. Other phytohormones may also be involved in *psy* promoter regulation such as salicylic acid, which has been shown to delay ripening in banana (Srivastava and Dwivedi, 2000). ABA may also be involved is, as it is produced from carotenoid precursors (Schwartz et al., 2003), and may regulate its own production. In addition, ABA appears to play a role in ethylene regulation of banana fruit ripening (Jiang et al., 2000). This suggests that other cis-acting elements that mediate *psy* promoter activity in response to a number of environmental stimuli are likely to be involved in regulating *psy* activity during fruit ripening. Consequently, *Cpsy2apr2* and *Cpsy2apr3* activity may be triggered under other conditions.

Asupina and Cavendish *psy* promoter activity could be characterised in future studies using a combination of bioinformatic and experimental analysis. Databases such as AGRIS (Palaniswamy et al., 2006) and PLACE (Higo et al., 1999) contain a catalogue of cis-acting regulatory elements that have been experimentally determined in plants. This would expedite promoter characterisation as potential regulatory sequences in the *psy* promoters could be identified before confirmation using methods such as electrophoretic mobility shift assays and reporter gene assays, which have been used in the characterisation of *psy* promoter activity in *Arabidopsis* (Welsch et al., 2003). Promoter activity (Chapter 5) was measured semi-quantitatively (GUS foci per cm²) since fluorimetric MUG assays were not feasible as the mass of fruit samples for microprojectile bombardment could not be reliably standardised. However, high variability between sample replicates highlighted the limitations of the semi-quantitative approach. This could be addressed by using autofluorescent proteins, such as GFP, which can be assayed non-destructively. In addition, microprojectile bombardment of Asupina and Cavendish *psy* promoters into fruit sampled at different ripening stages would be useful to examine differences in the regulation mechanisms. This work should be repeated in Asupina fruit when available, and in stably transformed banana, as transient assays are not always an accurate measure of tissue-specificity. Stable transformation in banana would most likely be the most reliable and informative approach to promoter analysis, however, the time required to generate and screen transgenic plants and obtain mature fruit-bearing plants (~3 to 4 years) was outside the scope of the present study. Interestingly, the presence of two introns in the banana *psy1* 5' UTR may have significant implications for the activity of this gene. Future work may examine the role of these introns by expressing reporter genes using *psy1* promoter constructs that have one intron and no introns in leaf and fruit, comparing their activity against the native *psy1* promoter that has both introns. This would be similar to previous work on the tissue-specific effects of the rice *ubi3* promoter (Lu et al., 2008).

Further characterisation of the *psy* gene family is required. Currently, the genomic sequence corresponding to the 3' UTR and flanking sequences of the *psy1* and *psy2* genes have not been isolated. This data could be important in determining whether differences in the structure of the Asupina and Cavendish *psy* genes at the nucleotide level and may help to explain the differences in fruit pVA content. The role of *psy2b* gene structure and promoter activity could not be investigated in the present study as the 5' promoter and 3' flanking sequences could not be isolated. These sequences could be obtained through further optimisation of the genome walking PCR method used successfully in this study. In addition, further 5' and 3' RACE analysis of the *psy* genes from these cultivars, particularly *psy2a* and *psy2b*, will be important in order to confirm that clones obtained thus far are not artefacts. For example, the insertion of part of the coding region in the 3' UTR of the only Cavendish *psy2a* 3'RACE clone obtained in this study needs further characterisation. This could be attempted by modifying experimental conditions such as PCR amplification and using mRNA from a broader range of tissues and developmental stages as only fruit was used in the present study. The isolation of the known Asupina and Cavendish *psy* genes as single fragments using primers to 5' promoter and 3' flanking sequences and copy number analysis of these genes in both cultivars would also be valuable in determining whether all of the Cavendish *psy2a* promoters are attached to structurally intact genes. These techniques could also be used in future to confirm whether the *psy2c* and *psyX* partial sequences isolated from Cavendish (Chapter 3) are additional *psy* gene family members. These were not investigated in this study, as the focus of the study was isolation of genes to facilitate characterisation of enzyme activity and gene expression and there was no time to extend this study.

PSY is an important enzyme in carotenoid biosynthesis, however, other factors may be responsible for differences in Asupina and Cavendish fruit pVA accumulation. Downstream genes in pVA carotenoid biosynthesis (*pds*, *zds*, *lcyb*, *lcye* and *chyb*) and catabolism (*ccd1*) are known to influence carotenoid accumulation. The roles of these genes have been reviewed previously in Chapter 1. Disruptions in the function of these genes may result in either diminished carotenoid biosynthesis or excessive depletion of pVA in Cavendish (low pVA) compared to Asupina (high pVA). The genes encoding IPI (Campbell et al., 1998) and GGPS (Okada et al., 2000), which are responsible for GGPP production, have been identified as gene families of two and five members in *Arabidopsis*, respectively. IPI1 (Campbell et al., 1998), GGPS1 and GGPS3 (Okada et al., 2000) were found to be localised to plastids, and may influence carotenoid biosynthesis in banana by affecting the level of GGPP available for phytoene biosynthesis. However, the critical nature of GGPP as a substrate for multiple isoprenoid pathways (Cunningham and Gantt, 1998) and normal plant growth suggests that these enzymes may not be responsible for differences in pVA

accumulation between Asupina and Cavendish. This hypothesis is supported by the observation of dwarfism in transgenic tomato plants with PSY constitutively over-expressed. This phenotype was thought to stem from excessive GGPP depletion (Fray et al., 1995). In addition, at least one functional IPI enzyme was required in *Arabidopsis* because double IPI mutants were not viable (Campbell et al., 1998).

Several enzymes downstream of PSY in the carotenoid biosynthetic pathway (reviewed in Chapter 1.3.1) may be responsible for the differences in pVA content between Asupina and Cavendish. The sequential activity of PDS and ZDS is required to convert phytoene to lycopene (Figure 1.2b). Constitutive expression of *Erwinia crtI*, which performs the function of both *pds* and *zds* (Misawa et al., 1990), in tomato increased β -carotene levels up to three fold compared to wild type fruit (Romer et al., 2000). In addition, enhancement of pVA levels in rice endosperm required the transformation of *crtI* as well as *psy* (Paine et al., 2005). These examples illustrate the potential role of *pds* and *zds* expression on pVA content in banana fruit, which would influence lycopene production. The enzymes directly responsible for pVA biosynthesis are LCYB and LCYE, which convert lycopene into α - and β -carotene (Figure 1.2c). Both cyclases appear to be encoded by related single genes (Huguency et al., 1996; Pecker et al., 1996), and are capable of heterodimerisation (Candau et al., 1991). Over-expression of *lcyb* in tomato increased fruit β -carotene yield of 7-fold and 10-fold compared to wild type controls using chromoplast-specific *Arabidopsis lcyb* (Rosati et al., 2000) and constitutive tomato *lcyb* (D'Ambrosio et al., 2004) expression, respectively, compared to wild type fruit. Characterisation of these enzymes in *Arabidopsis* showed that LCYE was only able to add one ϵ -ionone ring to lycopene, while LCYB activity added β -ionone rings to both ends of the substrate (Cunningham et al., 1996). Consequently, *lcyb* would be an important gene to characterise in banana given its pivotal role in pVA production, coupled with its ability to significantly increase β -carotene content in transgenic plants. CHYB converts β -carotene to zeaxanthin (Figure 1.2) by addition of hydroxyl groups to both β -ionone rings (Cunningham and Gantt, 1998) and is encoded by two related genes, *chyb1* and *chyb2*, which have been identified in *Arabidopsis* (Tian and Della Penna, 2001). Silencing of CHYB expression in potato tubers increased β -carotene up to 38 fold compared to the wild type control (Diretto et al., 2007). Therefore, the increased fruit pVA content of Asupina compared to Cavendish may be due to mechanisms involved in suppressing CHYB activity. The down-regulation of carotenoid degradation in Asupina fruit or its upregulation in Cavendish fruit may also explain the respective pVA levels of these cultivars. The *ccd* gene family encodes enzymes involved in carotenoid cleavage to produce other secondary metabolites (Chapter 1.3.2) and may have specific functions in different organelles. CCD1

may regulate pVA accumulation as it is known to cleave β -carotene (Schwartz et al., 2001) and its precursor compounds, including phytoene and lycopene (Simkin et al., 2004). Maize mutants with the dominant *white cap 1* phenotype exhibited increased carotenoid degradation due to the presence of 20 copies of *ccd1* at the mutant locus (Tan et al., 2004), driving 40 fold higher levels of expression compared to wild type maize. This suggests that the activity of CCD1 may be an important regulator of banana pVA accumulation in light of its ability to cleave both pVA carotenoids and their precursors. Regulatory genes such as the *Or* gene may also influence pVA accumulation (reviewed in Chapter 1.3.3). This gene which was characterised in cauliflower and encodes a protein involved in chromoplast development (Lu et al., 2006), and which has been demonstrated to improve carotenogenesis in potato tubers (Lopez et al., 2008a).

Consequently, the roles of these genes could be investigated in Asupina and Cavendish using approaches adopted in this study to investigate the role of PSY. Quantitative analysis of mRNA levels during multiple stages of fruit development would be a potential starting point, and the *lcyb*, *pds*, *zds* and *ccd1* genes also appear to occupy key positions in carotenoid metabolism. The inclusion of other banana varieties with both high and low fruit pVA content in subsequent work may also prove crucial to research into the biofortification of bananas for increased fruit pVA content. This is because the pVA content of other cultivars may not be due to differences in the same components of carotenoid metabolism. Ultimately, availability of the complete banana genome would greatly accelerate this research by expediting the identification and characterisation of these genes through comparative genomics with fully sequenced genomes such as those of maize and rice.

In conclusion, *psy* exists as a multigene family in banana consisting of at least three members (*psy1*, *psy2a* and *psy2b*) in both high and low pVA cultivars. Comparison of the molecular characteristics of *psy* in Asupina (high pVA) and Cavendish (low pVA) demonstrated that the PSY1 and PSY2A proteins from both cultivars are functional. However, these results suggested that *psy1* and *psy2a* were predominant in leaf and fruit respectively, and that alternate splicing of *psy2a* in Cavendish during fruit ripening may reduce the levels of active PSY, ultimately resulting in fruit with lower pVA content. The present study forms a basis for further investigation into the regulation of PSY activity in high and low pVA banana cultivars and may also prove valuable in informing research aimed at increasing the pVA content of nutritionally important banana cultivars using genetic modification. This is the goal of the wider project at QUT sponsored by the Bill and Melinda Gates foundation to improve the pVA potential of the East African Highland Banana.

References:

- ABLER, M. L. & GREEN, P. J. (1996) Control of mRNA stability in higher plants. *Plant Mol Biol*, 32, 63-78.
- AERT, R., SAGI, L. & VOLCKAERT, G. (2004) Gene content and density in banana (*Musa acuminata*) as revealed by genomic sequencing of BAC clones. *Theor Appl Genet*, 109, 129-39.
- AGUAYO, V. M., KAHN, S., ISMAEL, C. & MEERSHOEK, S. (2005) Vitamin A deficiency and child mortality in Mozambique. *Public Health Nutr*, 8, 29-31.
- ALBA, R., CORDONNIER-PRATT, M. M. & PRATT, L. H. (2000) Fruit-localized phytochromes regulate lycopene accumulation independently of ethylene production in tomato. *Plant Physiol*, 123, 363-70.
- AMASINO, R. M. (2003) Flowering time: a pathway that begins at the 3' end. *Curr Biol*, 13, R670-2.
- AMAYA, D. R. (2001) Food carotenoids: analysis, composition and alterations during storage and processing of foods. IN ELMADFA, I., ANKLAM, E. & KÖNIG, J. (Eds.) *Modern aspect of nutrition: present knowledge and future perspectives*. Karger.
- AMMAR-KHODJA, P. (2000) *Bananas*, International Network for the Improvement of Banana and Plantain (INIBAP).
- ARMSTRONG, G. A. & HEARST, J. E. (1996) Carotenoids 2: genetics and molecular biology of carotenoid pigment biosynthesis. *FASEB J*, 10, 228-37.
- ARNOLD, K., BORDOLI, L., KOPP, J. & SCHWEDE, T. (2006) The SWISS-MODEL workspace: a web-based environment for protein structure homology modelling. *Bioinformatics*, 22, 195-201.
- ASIF, M. H., DHAWAN, P. & NATH, P. (2000) A simple procedure for the isolation of high quality RNA from ripening banana fruit. *Plant Mol Biol Rep*, 18, 109-15.
- ATKINSON, H. J., GRIMWOOD, S., JOHNSTON, K. & GREEN, J. (2004) Prototype demonstration of transgenic resistance to the nematode *Radopholus similis* conferred on banana by a cystatin. *Transgenic Res*, 13, 135-42.
- BARTLEY, G. E. & SCOLNIK, P. A. (1993) cDNA cloning, expression during development, and genome mapping of PSY2, a second tomato gene encoding phytoene synthase. *J Biol Chem*, 268, 25718-21.
- BARTLEY, G. E., VIITANEN, P. V., BACOT, K. O. & SCOLNIK, P. A. (1992) A tomato gene expressed during fruit ripening encodes an enzyme of the carotenoid biosynthesis pathway. *J Biol Chem*, 267, 5036-9.
- BARTOS, J., ALKHIMOVA, O., DOLEZELOVA, M., DE LANGHE, E. & DOLEZEL, J. (2005) Nuclear genome size and genomic distribution of ribosomal DNA in *Musa* and *Ensete* (Musaceae): taxonomic implications. *Cytogenet Genome Res*, 109, 50-7.
- BATE, N., SPURR, C., FOSTER, G. D. & TWELL, D. (1996) Maturation-specific translational enhancement mediated by the 5'UTR of a late pollen transcript. *Plant J*, 10, 613-23.
- BECKER, D. K. & DALE, J. L. (2004) Transformation of banana using microprojectile bombardment. IN CURTIS, I. S. (Ed.) *Transgenic Crops of the World; Essential Protocols*. Kluwer Academic Publishers.
- BENDER, D. A. (2003) *Nutritional biochemistry of the vitamins*, 2nd edition, Cambridge University Press.
- BENNETZEN, J. L. (2007) Patterns in grass genome evolution. *Curr Opin Plant Biol*, 10, 176-81.
- BONEN, L. (1993) Trans-splicing of pre-mRNA in plants, animals, and protists. *FASEB J*, 7, 40-6.
- BONK, M., HOFFMANN, B., VON LINTIG, J., SCHLEDZ, M., AL-BABILI, S., HOBEIKA, E., KLEINIG, H. & BEYER, P. (1997) Chloroplast import of four

- carotenoid biosynthetic enzymes in vitro reveals differential fates prior to membrane binding and oligomeric assembly. *Eur J Biochem*, 247, 942-50.
- BORRMANN, L., SEEBECK, B., ROGALLA, P. & BULLERDIEK, J. (2003) Human HMGA2 promoter is coregulated by a polymorphic dinucleotide (TC)-repeat. *Oncogene*, 22, 756-60.
- BOUVIER, F., SUIRE, C., MUTTERER, J. & CAMARA, B. (2003) Oxidative remodeling of chromoplast carotenoids: identification of the carotenoid dioxygenase CsCCD and CsZCD genes involved in *Crocus* secondary metabolite biogenesis. *Plant Cell*, 15, 47-62.
- BUSCH, M., SEUTER, A. & HAIN, R. (2002) Functional analysis of the early steps of carotenoid biosynthesis in tobacco. *Plant Physiol*, 128, 439-53.
- CAMBIA (2009a) pCambia vectors. [Online] 2009. Available: <http://www.cambia.org/daisy/cambia/585.html> Accessed: 19 April 2009.
- CAMBIA (2009b) Transformation protocol for rice. [Online]. Available: http://www.cambia.org/daisy/bioforge_transbacter/4214/version/default/part/AttachmentData/data/Transformation%20protocol%20for%20Rice-1.pdf Accessed: 18 March 2009.
- CAMPBELL, M., HAHN, F. M., POULTER, C. D. & LEUSTEK, T. (1998) Analysis of the isopentenyl diphosphate isomerase gene family from *Arabidopsis thaliana*. *Plant Mol Biol*, 36, 323-8.
- CAMPBELL, M. A., HAAS, B. J., HAMILTON, J. P., MOUNT, S. M. & BUELL, C. R. (2006) Comprehensive analysis of alternative splicing in rice and comparative analyses with *Arabidopsis*. *BMC Genomics*, 7, 327.
- CANDAU, R., BEJARANO, E. & CERDA-OLMEDO, E. (1991) In vivo channeling of substrates in an enzyme aggregate for beta-carotene biosynthesis. *Proc Natl Acad Sci U S A*, 88, 4936-40.
- CENCI, A., SOMMA, S., CHANTRET, N., DUBCOVSKY, J. & BLANCO, A. (2004) PCR identification of durum wheat BAC clones containing genes coding for carotenoid biosynthesis enzymes and their chromosome localization. *Genome*, 47, 911-7.
- CHAKRABARTI, A., GANAPATHI, T. R., MUKHERJEE, P. K. & BAPAT, V. A. (2003) MSI-99, a magainin analogue, imparts enhanced disease resistance in transgenic tobacco and banana. *Planta*, 216, 587-96.
- CHANDER, S., GUO, Y. Q., YANG, X. H., ZHANG, J., LU, X. Q., YAN, J. B., SONG, T. M., ROCHEFORD, T. R. & LI, J. S. (2008) Using molecular markers to identify two major loci controlling carotenoid contents in maize grain. *Theor Appl Genet*, 116, 223-33.
- CHANG, S., PURYEAR, J. & CAIRNEY, J. (1993) A simple and efficient method for isolating RNA from pine trees. *Plant Mol Biol Rep*, 11, 113-6.
- CHEN, H., NAMKUNG, M. J. & JUCHAU, M. R. (1995) Biotransformation of all-trans-retinol and all-trans-retinal to all-trans-retinoic acid in rat conceptual homogenates. *Biochem Pharmacol*, 50, 1257-64.
- CHEW, B. P. (1993) Role of carotenoids in the immune response. *J Dairy Sci*, 76, 2804-11.
- CHEW, B. P. & PARK, J. S. (2004) Carotenoid action on the immune response. *J Nutr*, 134, 257S-61S.
- CHRISTENSEN, A. H., SHARROCK, R. A. & QUAIL, P. H. (1992) Maize polyubiquitin genes: structure, thermal perturbation of expression and transcript splicing, and promoter activity following transfer to protoplasts by electroporation. *Plant Mol Biol*, 18, 675-89.
- CHUNG, B. Y., SIMONS, C., FIRTH, A. E., BROWN, C. M. & HELLENS, R. P. (2006) Effect of 5'UTR introns on gene expression in *Arabidopsis thaliana*. *BMC Genomics*, 7, 120.
- CLOTAULT, J., PELTIER, D., BERRUYER, R., THOMAS, M., BRIARD, M. & GEOFFRIAUX, E. (2008) Expression of carotenoid biosynthesis genes during carrot root development. *J Exp Bot*, 59, 3563-73.

- CORONA, V., ARACRI, B., KOSTURKOVA, G., BARTLEY, G. E., PITTO, L., GIORGETTI, L., SCOLNIK, P. A. & GIULIANO, G. (1996) Regulation of a carotenoid biosynthesis gene promoter during plant development. *Plant J*, 9, 505-12.
- CUNNINGHAM, F. X., JR., POGSON, B., SUN, Z., MCDONALD, K. A., DELLAPENNA, D. & GANTT, E. (1996) Functional analysis of the beta and epsilon lycopene cyclase enzymes of *Arabidopsis* reveals a mechanism for control of cyclic carotenoid formation. *Plant Cell*, 8, 1613-26.
- CUNNINGHAM, F. X. J. & GANTT, E. (1998) Genes and enzymes of carotenoid biosynthesis in plants. *Annu Rev Plant Physiol Plant Mol Biol*, 49, 557-83.
- CUTLER, A. J. & KROCHKO, J. E. (1999) Formation and breakdown of ABA. *Trends Plant Sci*, 4, 472-78.
- D'AMBROSIO, C., GIORIO, G., MARINO, I., MERENDINO, A., PETROZZA, A., SALFI, L., STIGLIANI, A. L. & CELLINI, F. (2004) Virtually complete conversion of lycopene into beta-carotene in fruits of tomato plants transformed with the tomato lycopene beta-cyclase (tscy-b) cDNA. *Plant Sci*, 166, 207-14.
- DANIELLS, J., JENNY, C., KARAMURA, D. & TOMEKPE, K. (2001) *Diversity in the genus Musa*, International Network for the Improvement of Banana and Plantain.
- DE CASTRO, E., SIGRIST, C. J., GATTIKER, A., BULLIARD, V., LANGENDIJK-GENEVAUX, P. S., GASTEIGER, E., BAIROCH, A. & HULO, N. (2006) ScanProsite: detection of PROSITE signature matches and ProRule-associated functional and structural residues in proteins. *Nucleic Acids Res*, 34, W362-5.
- DEAN, C., TAMAKI, S., DUNSMUIR, P., FAVREAU, M., KATAYAMA, C., DOONER, H. & BEDBROOK, J. (1986) mRNA transcripts of several plant genes are polyadenylated at multiple sites in vivo. *Nucleic Acids Res*, 14, 2229-40.
- DIEHN, S. H., CHIU, W. L., DE ROCHER, E. J. & GREEN, P. J. (1998) Premature polyadenylation at multiple sites within a *Bacillus thuringiensis* toxin gene-coding region. *Plant Physiol*, 117, 1433-43.
- DIRETTO, G., WELSCH, R., TAVAZZA, R., MOURGUES, F., PIZZICHINI, D., BEYER, P. & GIULIANO, G. (2007) Silencing of beta-carotene hydroxylase increases total carotenoid and beta-carotene levels in potato tubers. *BMC Plant Biol*, 7, 11.
- DOGBO, O., LAFERRIERE, A., D'HARLINGUE, A. & CAMARA, B. (1988) Carotenoid biosynthesis: isolation and characterization of a bifunctional enzyme catalyzing the synthesis of phytoene. *Proc Natl Acad Sci U S A*, 85, 7054-8.
- DOWER, W. J., MILLER, J. F. & RAGSDALE, C. W. (1988) High efficiency transformation of *E. coli* by high voltage electroporation. *Nucleic Acids Res*, 16, 6127-45.
- ENGLBERGER, L. (2003) Carotenoid-rich bananas in Micronesia. *Infomusa*, 12, 2-5.
- ENGLBERGER, L., AALBERSBERG, W., RAVI, P., BONNIN, E., MARKS, G. C., FITZGERALD, M. H. & ELYMORE, J. (2003a) Further analyses on Micronesian banana, taro, breadfruit and other foods for provitamin A carotenoids and minerals. *J Food Compost Anal*, 16, 219-36.
- ENGLBERGER, L., DARNTON-HILL, I., COYNE, T., FITZGERALD, M. H. & MARKS, G. C. (2003b) Carotenoid-rich bananas: a potential food source for alleviating vitamin A deficiency. *Food Nutr Bull*, 24, 303-18.
- ENGLBERGER, L., SCHIERLE, J., MARKS, G. C. & FITZGERALD, M. H. (2003c) Micronesian banana, taro, and other foods: newly recognized sources of provitamin A and other carotenoids. *J Food Compost Anal*, 16, 3-19.
- ENGLBERGER, L., WILLS, R. B., BLADES, B., DUFFICY, L., DANIELLS, J. W. & COYNE, T. (2006) Carotenoid content and flesh color of selected banana cultivars growing in Australia. *Food Nutr Bull*, 27, 281-91.
- EYRICH, V. A., MARTI-RENOM, M. A., PRZYBYLSKI, D., MADHUSUDHAN, M. S., FISER, A., PAZOS, F., VALENCIA, A., SALI, A. & ROST, B. (2001) EVA: continuous automatic evaluation of protein structure prediction servers. *Bioinformatics*, 17, 1242-3.

- FILTEAU, S. M. & TOMKINS, A. M. (1999) Promoting vitamin A status in low-income countries. *Lancet*, 353, 1458-9.
- FRASER, P. D., ROMER, S., SHIPTON, C. A., MILLS, P. B., KIANO, J. W., MISAWA, N., DRAKE, R. G., SCHUCH, W. & BRAMLEY, P. M. (2002) Evaluation of transgenic tomato plants expressing an additional phytoene synthase in a fruit-specific manner. *Proc Natl Acad Sci U S A*, 99, 1092-7.
- FRASER, P. D., SCHUCH, W. & BRAMLEY, P. M. (2000) Phytoene synthase from tomato (*Lycopersicon esculentum*) chloroplasts - partial purification and biochemical properties. *Planta*, 211, 361-9.
- FRASER, P. D., TRUESDALE, M. R., BIRD, C. R., SCHUCH, W. & BRAMLEY, P. M. (1994) Carotenoid biosynthesis during tomato fruit development (evidence for tissue-specific gene expression). *Plant Physiol*, 105, 405-13.
- FRAY, R. G., WALLACE, A., FRASER, P. D., VALERO, D., HEDDEN, P., BRAMLEY, P. M. & GRIERSON, D. (1995) Constitutive expression of a fruit phytoene synthase gene in transgenic tomatoes causes dwarfism by redirecting metabolites from the gibberellin pathway. *Plant J*, 8, 693-701.
- FU, X. D. (2004) Towards a splicing code. *Cell*, 119, 736-8.
- GALLAGHER, C. E., MATTHEWS, P. D., LI, F. & WURTZEL, E. T. (2004) Gene duplication in the carotenoid biosynthetic pathway preceded evolution of the grasses. *Plant Physiol*, 135, 1776-83.
- GARBARINO, J. E., OOSUMI, T. & BELKNAP, W. R. (1995) Isolation of a polyubiquitin promoter and its expression in transgenic potato plants. *Plant Physiol*, 109, 1371-8.
- GARCIA-GIL, M. R. (2008) Evolutionary aspects of functional and pseudogene members of the phytochrome gene family in Scots pine. *J Mol Evol*, 67, 222-32.
- GIORIO, G., STIGLIANI, A. L. & D'AMBROSIO, C. (2008) Phytoene synthase genes in tomato (*Solanum lycopersicum* L.) - new data on the structures, the deduced amino acid sequences and the expression patterns. *FEBS J*, 275, 527-35.
- GIOVANNONI, J. J. (2004) Genetic regulation of fruit development and ripening. *Plant Cell*, 16, S170-80.
- GIULIANO, G., BARTLEY, G. E. & SCOLNIK, P. A. (1993) Regulation of carotenoid biosynthesis during tomato development. *Plant Cell*, 5, 379-87.
- GLEGHORN, M. L., DAVYDOVA, E. K., ROTHMAN-DENES, L. B. & MURAKAMI, K. S. (2008) Structural basis for DNA-hairpin promoter recognition by the bacteriophage N4 virion RNA polymerase. *Mol Cell*, 32, 707-17.
- GOODING, P. S., BIRD, C. & ROBINSON, S. P. (2001) Molecular cloning and characterisation of banana fruit polyphenol oxidase. *Planta*, 213, 748-57.
- GOWEN, S. R. (1995) *Bananas and plantains*, Chapman & Hall.
- GRUSAK, M. A. (2005) Golden rice gets a boost from maize. *Nat Biotechnol*, 23, 429-30.
- HALLIWELL, B. (1997) Introduction: free radicals and human disease - trick or treat? IN THOMAS, C. E. & KALYANARAMAN, B. (Eds.) *Oxygen radicals and the disease process*. Harwood Academic.
- HARADA, H., MIKI, R., MASUSHIGE, S. & KATO, S. (1995) Gene expression of retinoic acid receptors, retinoid-X receptors, and cellular retinol-binding protein I in bone and its regulation by vitamin A. *Endocrinology*, 136, 5329-5335.
- HE, X. Y., HE, Z. H., MA, W., APPELS, R. & XIA, X. C. (2009) Allelic variants of phytoene synthase 1 (Psy1) genes in Chinese and CIMMYT wheat cultivars and development of functional markers for flour colour *Mol Breed*.
- HE, X. Y., ZHANG, Y. L., HE, Z. H., WU, Y. P., XIAO, Y. G., MA, C. X. & XIA, X. C. (2008) Characterization of phytoene synthase 1 gene (Psy1) located on common wheat chromosome 7A and development of a functional marker. *Theor Appl Genet*, 116, 213-21.
- HERMANN, S. R., HARDING, R. M. & DALE, J. L. (2001) The banana actin 1 promoter drives near-constitutive transgene expression in vegetative tissues of banana. *Plant Cell Rep*, 20, 525-30.

- HESLOP-HARRISON, J. S. & SCHWARZACHER, T. (2007) Domestication, genomics and the future for banana. *Ann Bot*, 100, 1073-84.
- HIEI, Y., OHTA, S., KOMARI, T. & KUMASHIRO, T. (1994) Efficient transformation of rice (*Oryza sativa* L.) mediated by *Agrobacterium* and sequence analysis of the boundaries of the T-DNA. *Plant J*, 6, 271-82.
- HIGO, K., UGAWA, Y., IWAMOTO, M. & KORENAGA, T. (1999) Plant cis-acting regulatory DNA elements (PLACE) database: 1999. *Nucleic Acids Res*, 27, 297-300.
- HIRSCHBERG, J. (2001) Carotenoid biosynthesis in flowering plants. *Curr Opin Plant Biol*, 4, 210-8.
- HOA, T. T., AL-BABILI, S., SCHAUB, P., POTRYKUS, I. & BEYER, P. (2003) Golden Indica and Japonica rice lines amenable to deregulation. *Plant Physiol*, 133, 161-9.
- HOLDEN, J. M., ELDRIDGE, A. L., BEECHER, G. R., MARILYN BUZZARD, I., BHAGWAT, S., DAVIS, C. S., DOUGLASS, L. W., GEBHARDT, S., HAYTOWITZ, D. & SCHAKEL, S. (1999) Carotenoid content of U.S. Foods: an update of the database. *J Food Compos Anal*, 12, 169-96.
- HORIUCHI, T. & AIGAKI, T. (2006) Alternative trans-splicing: a novel mode of pre-mRNA processing. 98, 135-40.
- HOWITT, C. A., CAVANAGH, C. R., BOWERMAN, A. F., CAZZONELLI, C., RAMPLING, L., MIMICA, J. L. & POGSON, B. J. (2009) Alternative splicing, activation of cryptic exons and amino acid substitutions in carotenoid biosynthetic genes are associated with lutein accumulation in wheat endosperm. *Funct Integr Genomics*, 9, 363-76.
- HUANG, P. L., DO, Y. Y., HUANG, F. C., THAY, T. S. & CHANG, T. W. (1997) Characterization and expression analysis of a banana gene encoding 1-aminocyclopropane-1-carboxylate oxidase. *Biochem Mol Biol Int*, 41, 941-50.
- HUGUENEY, P., BOUVIER, F., BADILLO, A., QUENNEMET, J., D'HARLINGUE, A. & CAMARA, B. (1996) Developmental and stress regulation of gene expression for plastid and cytosolic isoprenoid pathways in pepper fruits. *Plant Physiol*, 111, 619-26.
- HULO, N., BAIROCH, A., BULLIARD, V., CERUTTI, L., CUCHE, B. A., DE CASTRO, E., LACHAIZE, C., LANGENDIJK-GENEVAUX, P. S. & SIGRIST, C. J. (2008) The 20 years of PROSITE. *Nucleic Acids Res*, 36, D245-9.
- IBDAH, M., AZULAY, Y., PORTNOY, V., WASSERMAN, B., BAR, E., MEIR, A., BURGER, Y., HIRSCHBERG, J., SCHAFFER, A. A., KATZIR, N., TADMOR, Y. & LEWINSOHN, E. (2006) Functional characterization of CmCCD1, a carotenoid cleavage dioxygenase from melon. *Phytochemistry*, 67, 1579-89.
- ITO, Y., KITAGAWA, M., IHASHI, N., YABE, K., KIMBARA, J., YASUDA, J., ITO, H., INAKUMA, T., HIROI, S. & KASUMI, T. (2008) DNA-binding specificity, transcriptional activation potential, and the rin mutation effect for the tomato fruit-ripening regulator RIN. *Plant J*, 55, 212-23.
- IWATA-REUYL, D., MATH, S. K., DESAI, S. B. & POULTER, C. D. (2003) Bacterial phytoene synthase: molecular cloning, expression, and characterization of *Erwinia herbicola* phytoene synthase. *Biochemistry*, 42, 3359-65.
- JEFFERSON, R. A., KAVANAGH, T. A. & BEVAN, M. W. (1987) GUS fusions: beta-glucuronidase as a sensitive and versatile gene fusion marker in higher plants. *EMBO J*, 6, 3901-7.
- JIANG, Y., JOYCE, D. C. & MACNISH, A. J. (2000) Effect of abscisic acid on banana fruit ripening in relation to the role of ethylene. *J Plant Growth Regul*, 19, 106-11.
- KALEIKAU, E. K., ANDRE, C. P. & WALBOT, V. (1992) Structure and expression of the rice mitochondrial apocytochrome b gene (cob-1) and pseudogene (cob-2). *Curr Genet*, 22, 463-70.
- KAMATE, K., BROWN, S., DURAND, P., BUREAU, J. M., DE NAY, D. & TRINH, T. H. (2001) Nuclear DNA content and base composition in 28 taxa of *Musa*. *Genome*, 44, 622-7.

- KAPLAN, W. & LITTLEJOHN, T. G. (2001) Swiss-PDB viewer (deep view). *Brief Bioinform*, 2, 195-7.
- KATO, M., IKOMA, Y., MATSUMOTO, H., SUGIURA, M., HYODO, H. & YANO, M. (2004) Accumulation of carotenoids and expression of carotenoid biosynthetic genes during maturation in citrus fruit. *Plant Physiol*, 134, 824-37.
- KELLEY, L. A. & STERNBERG, M. J. (2009) Protein structure prediction on the web: a case study using the Phyre server. *Nat Protoc*, 4, 363-71.
- KERTÉSZ, S., KERÉNY, Z., MÉRAI, Z., BARTOS, I., PÁLFY, T., BARTA, E. & SILHAVY, D. (2006) Both introns and long 3'-UTRs operate as cis-acting elements to trigger nonsense-mediated decay in plants. *Nucleic Acids Res*, 34, 6147-57.
- KHANNA, H., BECKER, D., KLEIDON, J. & DALE, J. L. (2004) Centrifugation Assisted Agrobacterium tumefaciens-mediated transformation (CAAT) of embryogenic cell suspensions of banana (*Musa* spp. Cavendish AAA and Lady finger AAB). *Mol Breed*, 14, 239-52.
- KITAGAWA, M., ITO, H., SHIINA, T., NAKAMURA, N., INAKUMA, T., KASUMI, T., ISHIGURO, Y., YABE, K. & ITO, Y. (2005) Characterization of tomato fruit ripening and analysis of gene expression in F1 hybrids of the ripening inhibitor (*rin*) mutant. *Physiol Plant*, 123, 331-8.
- KITAGAWA, M., NAKAMURA, N., USUDA, H., SHIINA, T., ITO, H., YASUDA, J., INAKUMA, T., ISHIGURO, Y., KASUMI, T. & ITO, Y. (2006) Ethylene biosynthesis regulation in tomato fruit from the F1 hybrid of the ripening inhibitor (*rin*) mutant. *Biosci Biotechnol Biochem*, 70, 1769-72.
- KOBAYASHI, H., NGERNPRASIRTSIRI, J. & AKAZAWA, T. (1990) Transcriptional regulation and DNA methylation in plastids during transitional conversion of chloroplasts to chromoplasts. *EMBO J*, 9, 307-13.
- LANGI, P., SEMBA, R. D., MUGERWA, R. D. & WHALEN, C. C. (2003) Vitamin A deficiency and increased mortality among human immunodeficiency virus-infected adults in Uganda. *Nutr Res*, 23, 595-605.
- LARKIN, M. A., BLACKSHIELDS, G., BROWN, N. P., CHENNA, R., MCGETTIGAN, P. A., MCWILLIAM, H., VALENTIN, F., WALLACE, I. M., WILM, A., LOPEZ, R., THOMPSON, J. D., GIBSON, T. J. & HIGGINS, D. G. (2007) Clustal W and Clustal X version 2.0. *Bioinformatics*, 23, 2947-8.
- LESCOT, M., PIFFANELLI, P., CIAMPI, A. Y., RUIZ, M., BLANC, G., LEEBENS-MACK, J., DA SILVA, F. R., SANTOS, C. M., D'HONT, A., GARSMEUR, O., VILARINHOS, A. D., KANAMORI, H., MATSUMOTO, T., RONNING, C. M., CHEUNG, F., HAAS, B. J., ALTHOFF, R., ARBOGAST, T., HINE, E., PAPPAS, G. J., JR., SASAKI, T., SOUZA, M. T., JR., MILLER, R. N., GLASZMANN, J. C. & TOWN, C. D. (2008) Insights into the *Musa* genome: syntenic relationships to rice and between *Musa* species. *BMC Genomics*, 9, 58.
- LI, F., VALLABHANENI, R. & WURTZEL, E. T. (2008a) PSY3, a new member of the phytoene synthase gene family conserved in the Poaceae and regulator of abiotic stress-induced root carotenogenesis. *Plant Physiol*, 146, 1333-45.
- LI, F., VALLABHANENI, R., YU, J., ROCHEFORD, T. & WURTZEL, E. T. (2008b) The maize phytoene synthase gene family: overlapping roles for carotenogenesis in endosperm, photomorphogenesis, and thermal stress tolerance. *Plant Physiol*, 147, 1334-46.
- LI, L. & GARVIN, D. F. (2003) Molecular mapping of Or, a gene inducing beta-carotene accumulation in cauliflower (*Brassica oleracea* L. var. botrytis). *Genome*, 46, 588-94.
- LI, L., LU, S., O'HALLORAN, D. M., GARVIN, D. F. & VREBALOV, J. (2003) High-resolution genetic and physical mapping of the cauliflower high-beta-carotene gene Or (Orange). *Mol Genet Genomics*, 270, 132-8.
- LI, L., PAOLILLO, D. J., PARTHASARATHY, M. V., DIMUZIO, E. M. & GARVIN, D. F. (2001) A novel gene mutation that confers abnormal patterns of beta-carotene accumulation in cauliflower (*Brassica oleracea* var. botrytis). *Plant J*, 26, 59-67.

- LIANG, P. H., KO, T. P. & WANG, A. H. (2002) Structure, mechanism and function of prenyltransferases. *Eur J Biochem*, 269, 3339-54.
- LIU, X., SHIOMI, S., NAKATSUKA, A., KUBO, Y., NAKAMURA, R. & INABA, A. (1999) Characterization of ethylene biosynthesis associated with ripening in banana fruit. *Plant Physiol*, 121, 1257-66.
- LOKE, J. C., STAHLBERG, E. A., STRENSKI, D. G., HAAS, B. J., WOOD, P. C. & LI, Q. Q. (2005) Compilation of mRNA polyadenylation signals in *Arabidopsis* revealed a new signal element and potential secondary structures. *Plant Physiol*, 138, 1457-68.
- LOPEZ, A. B., VAN ECK, J., CONLIN, B. J., PAOLILLO, D. J., O'NEILL, J. & LI, L. (2008a) Effect of the cauliflower Or transgene on carotenoid accumulation and chromoplast formation in transgenic potato tubers. *J Exp Bot*, 59, 213-23.
- LOPEZ, A. B., YANG, Y., THANNHAUSER, T. W. & LI, L. (2008b) Phytoene desaturase is present in a large protein complex in the plastid membrane. *Physiol Plant*, 133, 190-8.
- LU, C., ZAINAL, Z., TUCKER, G. A. & LYCETT, G. W. (2001) Developmental abnormalities and reduced fruit softening in tomato plants expressing an antisense Rab11 GTPase gene. *Plant Cell*, 13, 1819-33.
- LU, J., SIVAMANI, E., AZHAKANANDAM, K., SAMADDER, P., LI, X. & QU, R. (2008) Gene expression enhancement mediated by the 5' UTR intron of the rice rubi3 gene varied remarkably among tissues in transgenic rice plants. *Mol Genet Genomics*, 279, 563-72.
- LU, S., VAN ECK, J., ZHOU, X., LOPEZ, A. B., O'HALLORAN, D. M., COSMAN, K. M., CONLIN, B. J., PAOLILLO, D. J., GARVIN, D. F., VREBALOV, J., KOCHIAN, L. V., KUPPER, H., EARLE, E. D., CAO, J. & LI, L. (2006) The cauliflower Or gene encodes a DnaJ cysteine-rich domain-containing protein that mediates high levels of beta-carotene accumulation. *Plant Cell*, 18, 3594-605.
- LUPOLD, D. S., CAOILE, A. G. & STERN, D. B. (1999) Polyadenylation occurs at multiple sites in maize mitochondrial cox2 mRNA and is independent of editing status. *Plant Cell*, 11, 1565-78.
- MALPEL, S., MENDELSON, C. & CARDOSO, W. V. (2000) Regulation of retinoic acid signaling during lung morphogenesis. *Development*, 127, 3057-67.
- MARCHLER-BAUER, A., ANDERSON, J. B., CHITSAZ, F., DERBYSHIRE, M. K., DEWEESE-SCOTT, C., FONG, J. H., GEER, L. Y., GEER, R. C., GONZALES, N. R., GWADZ, M., HE, S., HURWITZ, D. I., JACKSON, J. D., KE, Z., LANCZYCKI, C. J., LIEBERT, C. A., LIU, C., LU, F., LU, S., MARCHLER, G. H., MULLOKANDOV, M., SONG, J. S., TASNEEM, A., THANKI, N., YAMASHITA, R. A., ZHANG, D., ZHANG, N. & BRYANT, S. H. (2009) CDD: specific functional annotation with the conserved domain database. *Nucleic Acids Res*, 37, D205-10.
- MARCHLER-BAUER, A. & BRYANT, S. H. (2004) CD-Search: protein domain annotations on the fly. *Nucleic Acids Res*, 32, W327-31.
- MARIN-RODRIGUEZ, M. C., SMITH, D. L., MANNING, K., ORCHARD, J. & SEYMOUR, G. B. (2003) Pectate lyase gene expression and enzyme activity in ripening banana fruit. *Plant Mol Biol*, 51, 851-7.
- MARKHAM, N. R. & ZUKER, M. (2005) DINAMelt web server for nucleic acid melting prediction. *Nucleic Acids Res*, 33, W577-81.
- MARKHAM, N. R. & ZUKER, M. (2008) UNAFold: software for nucleic acid folding and hybridization. *Methods Mol Biol*, 453, 3-31.
- MARTY, I., BUREAU, S., SARKISSIAN, G., GOUBLE, B., AUDERGON, J. M. & ALBAGNAC, G. (2005) Ethylene regulation of carotenoid accumulation and carotenogenic gene expression in colour-contrasted apricot varieties (*Prunus armeniaca*). *J Exp Bot*, 56, 1877-86.
- MATHIEU, S., TERRIER, N., PROCUREUR, J., BIGEY, F. & GUNATA, Z. (2005) A carotenoid cleavage dioxygenase from *Vitis vinifera* L.: functional characterization

- and expression during grape berry development in relation to C13-norisoprenoid accumulation. *J Exp Bot*, 56, 2721-31.
- MISAWA, N., NAKAGAWA, M., KOBAYASHI, K., YAMANO, S., IZAWA, Y., NAKAMURA, K. & HARASHIMA, K. (1990) Elucidation of the *Erwinia uredovora* carotenoid biosynthetic pathway by functional analysis of gene products expressed in *Escherichia coli*. *J Bacteriol*, 172, 6704-12.
- MISAWA, N., TRUESDALE, M. R., SANDMANN, G., FRASER, P. D., BIRD, C., SCHUCH, W. & BRAMLEY, P. M. (1994) Expression of a tomato cDNA coding for phytoene synthase in *Escherichia coli*, phytoene formation *in vivo* and *in vitro*, and functional analysis of the various truncated gene products. *J Biochem*, 116, 980-5.
- MONTOLIU, L., RIGAU, J. & PUIGDOMENECH, P. (1990) Multiple polyadenylation sites are active in the alpha 1-tubulin gene from *Zea mays*. *FEBS Lett*, 277, 29-32.
- MOORE, S., VREBALOV, J., PAYTON, P. & GIOVANNONI, J. (2002) Use of genomics tools to isolate key ripening genes and analyse fruit maturation in tomato. *J Exp Bot*, 53, 2023-30.
- MURASHIGE, T. & SKOOG, F. (1962) A revised medium for rapid growth and bioassays with tobacco tissue cultures. *Physiol Plant*, 15, 473-97.
- NAMBARA, E. & MARION-POLL, A. (2005) Abscisic acid biosynthesis and catabolism. *Annu Rev Plant Biol*, 56, 165-85.
- NEUDERT, U., MARTINEZ-FEREZ, I. M., FRASER, P. D. & SANDMANN, G. (1998) Expression of an active phytoene synthase from *Erwinia uredovora* and biochemical properties of the enzyme. *Biochim Biophys Acta*, 1392, 51-8.
- NIH, O. O. D. S. (2006) Vitamin A and carotenoids. *Facts about dietary supplements*. National Institute of Health (NIH).
- OHNUMA, S.-I., HIROOKA, K., OHTO, C. & NISHINO, T. (1997) Conversion from archaeal geranylgeranyl diphosphate synthase to farnesyl diphosphate synthase. Two amino acids before the first aspartate-rich motif solely determine eukaryotic farnesyl diphosphate synthase activity. *J Biol Chem*, 272, 5192-8.
- OHNUMA, S., NARITA, K., NAKAZAWA, T., ISHIDA, C., TAKEUCHI, Y., OHTO, C. & NISHINO, T. (1996) A role of the amino acid residue located on the fifth position before the first aspartate-rich motif of farnesyl diphosphate synthase on determination of the final product. *J Biol Chem*, 271, 30748-54.
- OKADA, K., SAITO, T., NAKAGAWA, T., KAWAMUKAI, M. & KAMIYA, Y. (2000) Five geranylgeranyl diphosphate synthases expressed in different organs are localized into three subcellular compartments in *Arabidopsis*. *Plant Physiol*, 122, 1045-56.
- OKADA, T., ERNST, O. P., PALCZEWSKI, K. & HOFMANN, K. P. (2001) Activation of rhodopsin: new insights from structural and biochemical studies. *Trends Biochem Sci*, 26, 318-324.
- OROZCO, B. M. & HANLEY-BOWDOIN, L. (1996) A DNA structure is required for geminivirus replication origin function. *J Virol*, 70, 148-58.
- OWENS, D. K., ALERDING, A. B., CROSBY, K. C., BANDARA, A. B., WESTWOOD, J. H. & WINKEL, B. S. (2008) Functional analysis of a predicted flavonol synthase gene family in *Arabidopsis*. *Plant Physiol*, 147, 1046-61.
- PAINE, J. A., SHIPTON, C. A., CHAGGAR, S., HOWELLS, R. M., KENNEDY, M. J., VERNON, G., WRIGHT, S. Y., HINCHLIFFE, E., ADAMS, J. L., SILVERSTONE, A. L. & DRAKE, R. (2005) Improving the nutritional value of golden rice through increased pro-vitamin A content. *Nat Biotechnol*, 23, 482-7.
- PALACE, V. P., KHAPER, N., QIN, Q. & SINGAL, P. K. (1999) Antioxidant potentials of vitamin A and carotenoids and their relevance to heart disease. *Free Radic Biol Med*, 26, 746-61.
- PALAISSA, K. A., MORGANTE, M., WILLIAMS, M. & RAFALSKI, A. (2003) Contrasting effects of selection on sequence diversity and linkage disequilibrium at two phytoene synthase loci. *Plant Cell*, 15, 1795-806.

- PALANISWAMY, S. K., JAMES, S., SUN, H., LAMB, R. S., DAVULURI, R. V. & GROTEWOLD, E. (2006) AGRIS and AtRegNet. a platform to link cis-regulatory elements and transcription factors into regulatory networks. *Plant Physiol*, 140, 818-29.
- PECKER, I., GABBAY, R., CUNNINGHAM, F. X., JR. & HIRSCHBERG, J. (1996) Cloning and characterization of the cDNA for lycopene beta-cyclase from tomato reveals decrease in its expression during fruit ripening. *Plant Mol Biol*, 30, 807-19.
- PILLAY, M., TENKOUANO, A., UDE, G. & ORTIZ, R. (2004) Molecular characterization of genomes in Musa and its applications. IN JAIN, S. M. & SWENNEN, R. (Eds.) *Banana improvement: cellular, molecular biology, and induced mutations*. Science Publishers.
- POLLASTRI, G., PRZYBYLSKI, D., ROST, B. & BALDI, P. (2002) Improving the prediction of protein secondary structure in three and eight classes using recurrent neural networks and profiles. 47, 228-35.
- POZNIAK, C. J., KNOX, R. E., CLARKE, F. R. & CLARKE, J. M. (2007) Identification of QTL and association of a phytoene synthase gene with endosperm colour in durum wheat. *Theor Appl Genet*, 114, 525-37.
- PUA, E. C. & LEE, Y. C. (2003) Expression of a ripening-related cytochrome P450 cDNA in Cavendish banana (*Musa acuminata* cv. Williams). *Gene*, 305, 133-40.
- QUAIL, P. H. (2002) Phytochrome photosensory signalling networks. *Nat Rev Mol Cell Biol*, 3, 85-93.
- RAVANELLO, M. P., KE, D., ALVAREZ, J., HUANG, B. & SHEWMAKER, C. K. (2003) Coordinate expression of multiple bacterial carotenoid genes in canola leading to altered carotenoid production. *Metab Eng*, 5, 255-63.
- REDDY, A. S. (2007) Alternative splicing of pre-messenger RNAs in plants in the genomic era. *Annu Rev Plant Biol*, 58, 267-94.
- RODRIGO, M. J., MARCOS, J. F. & ZACARIAS, L. (2004) Biochemical and molecular analysis of carotenoid biosynthesis in flavedo of orange (*Citrus sinensis* L.) during fruit development and maturation. *J Agric Food Chem*, 52, 6724-31.
- ROMER, S., FRASER, P. D., KIANO, J. W., SHIPTON, C. A., MISAWA, N., SCHUCH, W. & BRAMLEY, P. M. (2000) Elevation of the provitamin A content of transgenic tomato plants. *Nat Biotechnol*, 18, 666-9.
- RONEN, G., COHEN, M., ZAMIR, D. & HIRSCHBERG, J. (1999) Regulation of carotenoid biosynthesis during tomato fruit development: expression of the gene for lycopene epsilon-cyclase is down-regulated during ripening and is elevated in the mutant Delta. *Plant J*, 17, 341-51.
- ROOS, T. C., JUGERT, F. K., MERK, H. F. & BICKERS, D. R. (1998) Retinoid metabolism in the skin. *Pharmacol Rev*, 50, 315-33.
- ROSATI, C., AQUILANI, R., DHARMAPURI, S., PALLARA, P., MARUSIC, C., TAVAZZA, R., BOUVIER, F., CAMARA, B. & GIULIANO, G. (2000) Metabolic engineering of beta-carotene and lycopene content in tomato fruit. *Plant J*, 24, 413-9.
- SAMBROOK, J. & RUSSELL, D. W. (2001) *Molecular Cloning: A Laboratory Manual*, 3rd edition, Cold Spring Harbor Laboratory Press.
- SANDMANN, G. (2001a) Carotenoid biosynthesis and biotechnological application. *Arch Biochem Biophys*, 385, 4-12.
- SANDMANN, G. (2001b) Genetic manipulation of carotenoid biosynthesis: strategies, problems and achievements. *Trends Plant Sci*, 6, 14-17.
- SANJOAQUIN, M. A. & MOLYNEUX, M. E. (2009) Malaria and vitamin A deficiency in African children: a vicious circle? *Malar J*, 8, 134.
- SAWANT, S. V., KIRAN, K., MEHROTRA, R., CHATURVEDI, C. P., ANSARI, S. A., SINGH, P., LODHI, N. & TULI, R. (2005) A variety of synergistic and antagonistic interactions mediated by cis-acting DNA motifs regulate gene expression in plant cells and modulate stability of the transcription complex formed on a basal promoter. *J Exp Bot*, 56, 2345-53.

- SCHLEDZ, M., AL BABILI, S., VON LINTIG, J., HAUBRUCK, H., RABBANI, S., KLEINIG, H. & BEYER, P. (1996) Phytoene synthase from *Narcissus pseudonarcissus*: functional expression, galactolipid requirement, topological distribution in chromoplasts and induction during flowering. *Plant J*, 10, 781-92.
- SCHOFIELD, A. & PALIYATH, G. (2005) Modulation of carotenoid biosynthesis during tomato fruit ripening through phytochrome regulation of phytoene synthase activity. *Plant Physiol and Biochem*, 43, 1052-60.
- SCHWARTZ, S. H., QIN, X. & ZEEVAART, J. A. (2001) Characterization of a novel carotenoid cleavage dioxygenase from plants. *J Biol Chem*, 276, 25208-11.
- SCHWARTZ, S. H., TAN, B. C., MCCARTY, D. R., WELCH, W. & ZEEVAART, J. A. (2003) Substrate specificity and kinetics for VP14, a carotenoid cleavage dioxygenase in the ABA biosynthetic pathway. *Biochim Biophys Acta*, 1619, 9-14.
- SCOLNIK, P. A. & BARTLEY, G. E. (1994) Nucleotide sequence of an *Arabidopsis* cDNA for phytoene synthase. *Plant Physiol*, 104, 1471-2.
- SHARROCK, S. & FRISON, E. (1998) Musa production around the world – trends, varieties and regional importance. *Networking Banana and Plantain: Annual Report 1998*, 41-6.
- SHEN, Y., JI, G., HAAS, B. J., WU, X., ZHENG, J., REESE, G. J. & LI, Q. Q. (2008) Genome level analysis of rice mRNA 3'-end processing signals and alternative polyadenylation. *Nucleic Acids Res*, 36, 3150-61.
- SIMKIN, A. J., SCHWARTZ, S. H., AULDRIDGE, M., TAYLOR, M. G. & KLEE, H. J. (2004) The tomato carotenoid cleavage dioxygenase 1 genes contribute to the formation of the flavor volatiles beta-ionone, pseudoionone, and geranylacetone. *Plant J*, 40, 882-92.
- SINHA, R. K. (2004) *Modern plant physiology*, Alpha Science.
- SIVAMANI, E. & QU, R. (2006) Expression enhancement of a rice polyubiquitin gene promoter. *Plant Mol Biol*, 60, 225-39.
- SOLOMONS, N. W. & OROZCO, M. (2003) Alleviation of vitamin A deficiency with palm fruit and its products. *Asia Pac J Clin Nutr*, 12, 373-84.
- SOMMER, A. & WEST, K. P. (1996) *Vitamin A deficiency : health, survival, and vision*, Oxford University Press.
- SRIVASTAVA, M. K. & DWIVEDI, U. N. (2000) Delayed ripening of banana fruit by salicylic acid. *Plant Sci*, 158, 87-96.
- SUIRE, C., BOUVIER, F., BACKHAUS, R. A., BEGU, D., BONNEU, M. & CAMARA, B. (2000) Cellular localization of isoprenoid biosynthetic enzymes in *Marchantia polymorpha*. Uncovering a new role of oil bodies. *Plant Physiol*, 124, 971-978.
- TAIZ, L. & ZEIGER, E. (2002) *Plant physiology*, 3rd edition, Sinauer Associates.
- TAN, B.-C., CLINE, K. & MCCARTY, D. R. (2001) Localization and targeting of the VP14 epoxy-carotenoid dioxygenase to chloroplast membranes. *Plant J*, 27, 373-382.
- TAN, B.-C., LIU, L., WU, S., LAI, J., SIMONE, A. & MCCARTY, D. (2004) The dominant white endosperm factor white cap encodes the ZmCCD1 carotenoid dioxygenase in a large multiple copy gene array. *Maize genetics conference*.
- TAN, B. C., JOSEPH, L. M., DENG, W. T., LIU, L., LI, Q. B., CLINE, K. & MCCARTY, D. R. (2003) Molecular characterization of the *Arabidopsis* 9-cis epoxycarotenoid dioxygenase gene family. *Plant J*, 35, 44-56.
- TANSEY, T. R. & SHECHTER, I. (2000) Structure and regulation of mammalian squalene synthase. *Biochim Biophys Acta*, 1529, 49-62.
- TARSHIS, L. C., PROTEAU, P. J., KELLOGG, B. A., SACCHETTINI, J. C. & POULTER, C. D. (1996) Regulation of product chain length by isoprenyl diphosphate synthases. *Proc Natl Acad Sci U S A*, 93, 15018-23.
- TATALA, S. R., KIHAMIA, C. M., KYUNGU, L. H. & SVANBERG, U. (2008) Risk factors for anaemia in schoolchildren in Tanga Region, Tanzania. *Tanzan J Health Res*, 10, 189-202.

- TAYLOR, M. & RAMSAY, G. (2005) Carotenoid biosynthesis in plant storage organs: recent advances and prospects for improving plant food quality. *Physiol Plant*, 124, 143-51.
- TIAN, L. & DELLA PENNA, D. (2001) Characterization of a second carotenoid beta-hydroxylase gene from *Arabidopsis* and its relationship to the LUT1 locus. *Plant Mol Biol*, 47, 379-88.
- TORIYAMA, K. & HINATA, K. (1985) Cell suspension and protoplast culture in rice. *Plant Sci*, 41, 179-183.
- TRAN, D., HAVEN, J., QIU, W. G. & POLLE, J. E. (2009) An update on carotenoid biosynthesis in algae: phylogenetic evidence for the existence of two classes of phytoene synthase. *Planta*, 229, 723-9.
- USDA (2008) USDA national nutrient database for standard reference, release 21. Available: http://www.ars.usda.gov/main/site_main.htm?modecode=12-35-45-00 Accessed: [19 May 2009].
- VAILLANT, I. & PASZKOWSKI, J. (2007) Role of histone and DNA methylation in gene regulation. *Curr Opin Plant Biol*, 10, 528-33.
- VALÁRIK, M., SIMKOVA, H., HRIBOVA, E., SAFAR, J., DOLEZELOVA, M. & DOLEZEL, J. (2002) Isolation, characterization and chromosome localization of repetitive DNA sequences in bananas (*Musa* spp.). *Chromosome Res*, 10, 89-100.
- VISHNEVETSKY, M., OVADIS, M. & VAINSTEIN, A. (1999) Carotenoid sequestration in plants: the role of carotenoid-associated proteins. *Trends Plant Sci*, 4, 232-235.
- VON LINTIG, J., HESSEL, S., ISKEN, A., KIEFER, C., LAMPERT, J. M., VOOLSTRA, O. & VOGT, K. (2005) Towards a better understanding of carotenoid metabolism in animals. *Biochim Biophys Acta*, 1740, 122-31.
- VON LINTIG, J., WELSCH, R., BONK, M., GIULIANO, G., BATSCHAUER, A. & KLEINIG, H. (1997) Light-dependent regulation of carotenoid biosynthesis occurs at the level of phytoene synthase expression and is mediated by phytochrome in *Sinapis alba* and *Arabidopsis thaliana* seedlings. *Plant J*, 12, 625-34.
- WANG, B. B. & BRENDDEL, V. (2006) Genomewide comparative analysis of alternative splicing in plants. *Proc Natl Acad Sci U S A*, 103, 7175-80.
- WANG, B. S., REN, J. W., OOI, L., CHONG, S. S. & LEE, C. G. L. (2005) Dinucleotide repeats negatively modulate the promoter activity of *Cyr61* and is unstable in hepatocellular carcinoma patients. *Oncogene*, 24, 3999-4008.
- WANG, K. & OHNUMA, S.-I. (1999) Chain-length determination mechanism of isoprenyl diphosphate synthases and implications for molecular evolution. *Trends Biochem Sci*, 24, 445-51.
- WELSCH, R., BEYER, P., HUGUENEY, P., KLEINIG, H. & VON LINTIG, J. (2000) Regulation and activation of phytoene synthase, a key enzyme in carotenoid biosynthesis, during photomorphogenesis. *Planta*, 211, 846-54.
- WELSCH, R., MEDINA, J., GIULIANO, G., BEYER, P. & VON LINTIG, J. (2003) Structural and functional characterization of the phytoene synthase promoter from *Arabidopsis thaliana*. *Planta*, 216, 523-34.
- WEST, C. E. (2000) Meeting requirements for vitamin A. *Nutr Rev*, 58, 341-5.
- WEST, C. E., EILANDER, A. & VAN LIESHOUT, M. (2002) Consequences of revised estimates of carotenoid bioefficacy for dietary control of vitamin A deficiency in developing countries. *J Nutr*, 132, 2920S-6S.
- WEST, K. P., JR. (2002) Extent of vitamin A deficiency among preschool children and women of reproductive age. *J Nutr*, 132, 2857S-66S.
- WONG, J. C., LAMBERT, R. J., WURTZEL, E. T. & ROCHEFORD, T. R. (2004) QTL and candidate genes phytoene synthase and zeta-carotene desaturase associated with the accumulation of carotenoids in maize. *Theor Appl Genet*, 108, 349-59.
- YAMAGISHI, T., HIROSE, S. & KONDO, T. (2008) Secondary DNA structure formation for *Hoxb9* promoter and identification of its specific binding protein. *Nucleic Acids Res*, 36, 1965-75.

- YE, X., AL-BABILI, S., KLOTI, A., ZHANG, J., LUCCA, P., BEYER, P. & POTRYKUS, I. (2000) Engineering the provitamin A (beta-carotene) biosynthetic pathway into (carotenoid-free) rice endosperm. *Science*, 287, 303-5.
- YEUM, K. J. & RUSSELL, R. M. (2002) Carotenoid bioavailability and bioconversion. *Annu Rev Nutr*, 22, 483-504.
- ZHANG, X. H., LESLIE, C. S. & CHASIN, L. A. (2005) Computational searches for splicing signals. *Methods*, 37, 292-305.
- ZHU, C., YAMAMURA, S., KOIWA, H., NISHIHARA, M. & SANDMANN, G. (2002) cDNA cloning and expression of carotenogenic genes during flower development in *Gentiana lutea*. *Plant Mol Biol*, 48, 277-85.
- ZIMMERMANN, M. B. & HURRELL, R. F. (2002) Improving iron, zinc and vitamin A nutrition through plant biotechnology. *Curr Opin Biotechnol*, 13, 142-5.
- ZOU, Z., EIBL, C. & KOOP, H. U. (2003) The stem-loop region of the tobacco psbA 5'UTR is an important determinant of mRNA stability and translation efficiency. *Mol Genet Genomics*, 269, 340-9.